Electronic Supporting Information

Probing the factors that influence the conformation of guanidinato ligand in [(η^5-C_5Me_5)M(*NN*)X] (*NN* = chelating *N*,*N*′,*N*″-tri(*o*-substituted aryl)guanidinate(1–); X = chloro, azido and triazolato)

Robin Kumar,[a] Ram Kishan,[a] Jisha Mary Thomas,[b] Chinnappan Sivasankar,[b] Natesan Thirupathi[a]*

[a]*Department of Chemistry, University of Delhi, Delhi 110 007, India.*

E-mail addresses: thirupathi_n@yahoo.com, tnat@chemistry.du.ac.in (N. Thirupathi)

[b]*Catalysis and Energy Laboratory, Department of Chemistry, Pondicherry University (A Central University), Puducherry 605014, India.*

General Considerations

Symmetrical *N*,*N*′,*N*″-triarylguanidines, $(ArNH)_2C{=}NAr$ (Ar = 2-MeC_6H_4 (**L1**); 2-$(MeO)C_6H_4$ (**L2**); 4-MeC_6H_4 (**L3**) and 2,4-$Me_2C_6H_3$ (**L4**)),[1] $[(\eta^5\text{-}C_5Me_5)MCl(\mu\text{-}Cl)]_2$ (M = Rh and Ir)[2] and complexes **5** and **6**[3] were prepared following the literature procedures. $MCl_3{\cdot}xH_2O$ (M = Rh and Ir), NaOAc, NaN_3, DMAD and DEAD were purchased from commercial vendors and used as received. The IR spectral data were obtained using KBr pellets on a Shimadzu IR435 spectrometer in the frequency range 400–4000 cm^{-1}. Time of flight mass (TOF–MS) spectra were recorded on Agilent Technologies 6530, Accurate-Mass Q-TOF LC/MS instrument using electrospray positive ion mode. ^1H, $^{13}C\{^1H\}$, and ^{19}F NMR spectra were recorded on a JEOL ECX 400 NMR spectrometer operating at 400, 100.5, and 376.5 MHz (with CF_3COOH as an external standard), respectively. VT ^1H NMR spectra of **13** were recorded in CD_2Cl_2 on a Bruker AV-500 NMR spectrometer. The chemical shifts are reported in ppm relative to tetramethylsilane or residual solvent signal. Melting points were recorded on a Buchi melting point apparatus (Model: M–560) and the reported values are uncorrected.

Caution: Sodium azide is shock sensitive and explosive, only a small amount of material should be used with care.

X-Ray Crystallography

Details of data collection, structure solution and refinement for **10**–**17**, **19**·$CHCl_3$, **20** and **21** are presented in Tables S1 and S2. Suitable crystals for X-ray diffraction were carefully selected after examination under an optical microscope and mounted on the goniometer head. The unit cell parameters and intensity data were collected on Oxford Xcalibur S diffractometer (4-circle kappa goniometer, Sapphire–3 CCD detector, omega scans, graphite monochromator, and a single wavelength Enhance X-ray source with MoKα radiation).[4] Pre-experiment, data

collection, data reduction, and absorption corrections were performed with the CrysAlisPro software suite.[5] The structures were solved and refined using the SHELX-2017 program package[6] and SHELXL-2017/1 (within the WinGX program package).[7] Non-hydrogen atoms were refined anisotropically. C−H/N−H hydrogen atoms were placed in geometrically calculated positions by using a riding model. The molecular structures were created with Olex2 program.[8]

Computational details

Fig. S4 represents the fully optimized geometry of *syn-syn*, *syn-anti*, *anti-syn* and *anti-anti* conformers of **14**, using the density functional theory (B3LYP).[9–11] Cl, N, C and H atoms were described using the 6-31G* basis set[12] and Rh was described using the LANL2DZ basis set.[13–16] The solvent correction for dichloromethane was carried out using the polarized continuum model.[17–19] The computational analysis was done using the Gaussian 09 software[20] on all four conformers of **14**.

References

1. K. Gopi, B. Rathi and N. Thirupathi, *J. Chem. Sci*., 2010, **122**, 157–167.
2. J. W. Kang, K. Moseley and P. M. Maitlis, *J. Am. Chem. Soc*., 1969, **91**, 5970–5977.
3. R. Kumar and N. Thirupathi, *RSC Adv.*, 2017, **7**, 33890–33904
4. *ENHANCE*, *Oxford Xcalibur Single Crystal Diffractometer*, version 1.171.34.40; Oxford Diffraction Ltd: Oxford, U.K., 2006.
5. *CrysAlisPro*, version 1.171.34.40; Oxford Diffraction Ltd: Oxford, U.K., 2006.
6. G. M. Sheldrick, University of Gottingen, Gottingen, Germany, 2017.
7. L. J. Farrugia, *J. Appl. Crystallogr.*, 1999, **32**, 837–838.

8. O. V. Dolomanov, L. J. Bourhis, R. J. Gildea, J. A. K. Howard and H. Puschmann, *J. Appl. Crystallogr.*, 2009, **42**, 339–341.
9. A. D. Becke, *Phys. Rev. A*, 1988, **38**, 3098–3100.
10. A. D. Becke, *J. Chem. Phys.*, 1993, **98**, 1372–1377.
11. A. D. Becke, *J. Chem. Phys.*, 1993, **98**, 5648–5652.
12. R. Krishnan, J. S. Binkley, R. Seeger and J. A. Pople, *J. Chem. Phys.*, 1980, **72**, 650–654.
13. T. H. Dunning Jr. and P. J. Hay, in *Modern Theoretical Chemistry* III, ed. H. F. Schaefer, Plenum, New York, 1976.
14. P. J. Hay and W. R. Wadt, *J. Chem. Phys.*, 1985, **82**, 270–283.
15. W. R. Wadt and P. J. Hay, *J. Chem. Phys.*, 1985, **82**, 284–298.
16. P. J. Hay and W.R. Wadt, *J. Chem. Phys.*, 1985, **82**, 299–310.
17. M. T. Cancès, B. Mennucci and J. Tomasi, *J. Chem. Phys.*, 1997, **107**, 3032–3041.
18. M. Cossi, V. Barone, B. Mennucci and J. Tomasi, *Chem. Phys. Lett.*, 1998, **286**, 253–260.
19. B. Mennucci and J. Tomasi, *J. Chem. Phys.*, 1997, **106**, 5151–5158.
20. M. J. Frisch, G. W. Trucks, H. B. Schlegel, G. E. Scuseria, M. A. Robb, J. R. Cheeseman, J. A. Montgomery Jr., T. Vreven, K. N. Kudin, J. C. Burant, J. M. Millam, S. S. Iyengar, J. Tomasi, V. Barone, B. Mennucci, M. Cossi, G. Scalmani, N. Rega, G. A. Petersson, H. Nakatsuji, M. Hada, M. Ehara, K. Toyota, R. Fukuda, J. Hasegawa, M. Ishida, T. Nakajima, Y. Honda, O. Kitao, H. Nakai, M. Klene, X. Li, J. E. Knox, H. P. Hratchian, J. B. Cross, C. Adamo, J. Jaramillo, R. Gomperts, R. E. Stratmann, O. Yazyev, A. J. Austin, R. Cammi, C. Pomelli, J. W. Ochterski, P. Y. Ayala, K. Morokuma, G. A. Voth, P. Salvador, J. J. Dannenberg, V. G. Zakrzewski, S. Dapprich, A. D. Daniels, M. C. Strain,

O. Farkas, D. K. Malick, A. D. Rabuck, K. Raghavachari, J. B. Foresman, J. V. Ortiz, Q. Cui, A. G. Baboul, S. Clifford, J. Cioslowski, B. B. Stefanov, G. Liu, A. Liashenko, P. Piskorz, I. Komaromi, R. L. Martin, D. J. Fox, T. Keith, M. A. Al- Laham, C. Y. Peng, A. Nanayakkara, M. Challacombe, P. M. W. Gill, B. Johnson, W. Chen, M. W. Wong, C. Gonzalez and J. A. Pople, Gaussian09, rev. A.02, Gaussian, Inc., Wallingford CT, 2009.

Table S1 Crystallographic Data for **10–14**

	10	**11**	**12**	**13**	**14**
Formula	$C_{32}H_{37}ClN_3O_3Rh$	$C_{32}H_{37}ClN_3Rh$	$C_{32}H_{37}ClN_3O_3Ir$	$C_{35}H_{43}ClN_3Rh$	$C_{29}H_{28}Cl_3N_6Rh$
Fw	650.00	602.00	739.29	644.08	669.83
Temperature (K)	298(2)	298(2)	298(2)	298(2)	298(2)
Wavelength (Å)	0.71073	0.71073	0.71073	0.71073	0.71073
Crystal system	Orthorhombic	Monoclinic	Monoclinic	Monoclinic	Orthorhombic
Space group	*Pbca*	*Cc*	$P2_1$	$C2/c$	$P2_12_12_1$
a (Å)	16.5855(7)	8.5148(5)	8.0190(13)	46.5307(10)	8.070(5)
b (Å)	15.6710(8)	23.9553(15)	15.4071(12)	8.6162(3)	15.118(5)
c (Å)	23.4002(12)	15.3322(9)	12.3484(18)	15.9481(3)	24.291(5)
α (deg)	90	90	90	90	90
β (deg)	90	104.954(6)	96.644(14)	93.121(2)	90
γ (deg)	90	90	90	90	90
Volume ($Å^3$)	6082.0(5)	3021.5(3)	1515.4(4)	6384.4(3)	2964(2)
Z	8	4	2	8	4
ρ_{calcd} (Mg/m^3)	1.420	1.323	1.620	1.340	1.501
μ(Mo Kα) (mm^{-1})	0.686	0.678	4.530	0.646	0.876
F(000)	2688	1248	736	2688	1360
θ range (deg)	2.91–26.37	3.23–26.37	2.88–26.36	3.02–26.37	2.82–26.37
No. of reflns collected	30869	21574	21582	45731	13534
No. of reflns used	6204	6154	6190	6521	6040
Parameters	369	435	369	361	421
R_1 [I>2σ(I)][a]	0.0356	0.0258	0.0321	0.0475	0.0425
wR_2 (all reflns)[b]	0.0763	0.0615	0.0559	0.1088	0.0833
GooF on F^2[c]	1.111	1.100	1.016	1.150	1.102
Largest diff. peak and hole, ($e·Å^{-3}$)	0.443/–0.528	0.473/–0.255	0.959/–0.468	0.817/–0.554	0.836/–0.393

[a] $R_1 = \Sigma||F_o| - |F_c||/\Sigma|F_o|$; [b] $wR_2 = \{\Sigma[w(F_o^2 - F_c^2)^2]/\Sigma[w(F_o^2)^2]\}^{1/2}$;
[c] $S = \{\Sigma[w(F_o^2 - F_c^2)^2]/(n-p)\}^{1/2}$

Table S2 Crystallographic Data for **15–17**, **19**·$CHCl_3$, **20** and **21**

	15	**16**	**17**	**19**·$CHCl_3$	**20**	**21**
Formula	$C_{29}H_{28}F_3N_6Rh$	$C_{32}H_{37}N_6Rh$	$C_{32}H_{37}N_6O_3Rh$	$C_{36}H_{35}Cl_6N_6O_4Rh$	$C_{37}H_{38}F_3N_6O_4Rh$	$C_{38}H_{43}N_6O_7Rh$
Fw	620.48	608.58	656.58	931.31	790.64	798.69
Temperature (K)	298(2)	298(2)	298(2)	298(2)	298(2)	298(2)
Wavelength (Å)	0.71073	0.71073	0.71073	0.71073	0.71073	0.71073
Crystal system	Monoclinic	Monoclinic	Triclinic	Triclinic	Monoclinic	Monoclinic
Space group	$P2_1/n$	$P2_1/n$	$P\bar{1}$	$P\bar{1}$	$P2_1/c$	$P2_1/c$
a (Å)	8.8527(8)	11.4770(4)	7.7877(2)	9.108(5)	11.5855(7)	9.2161(4)
b (Å)	20.0313(13)	21.3791(6)	10.8878(3)	15.326(7)	20.6617(11)	25.0946(9)
c (Å)	16.1061(9)	12.3167(4)	18.3953(5)	15.923(3)	15.7428(9)	16.4992(6)
α (deg)	90	90	93.177(2)	70.18(3)	90	90
β (deg)	104.206(7)	98.643(3)	100.148(2)	76.95(3)	101.585(6)	102.663(4)
γ (deg)	90	90	98.666(2)	91.43(4)	90	90
Volume ($Å^3$)	2768.8(4)	2987.80(17)	1512.43(7)	2024.2(15)	3691.7(4)	3723.0(3)
Z	4	4	2	2	4	4
ρ_{calcd} (Mg/m^3)	1.489	1.353	1.442	1.528	1.423	1.425
μ(Mo Kα) (mm^{-1})	0.666	0.602	0.608	0.864	0.525	0.516
F(000)	1264	1264	680	944	1624	1656
θ range (deg)	2.98–26.37	2.96–26.37	3.03–26.37	2.90–26.37	2.88–26.37	2.85–26.37
No. of reflns collected	22036	25774	21498	26462	35091	26698
No. of reflns used	5648	6112	6187	8256	7537	7611
Parameters	352	360	379	549	467	479
R_1 [$I>2\sigma(I)$][a]	0.0737	0.0457	0.0303	0.0685	0.0603	0.0738
wR_2 (all reflns)[b]	0.1308	0.0951	0.0804	0.1775	0.1278	0.1362
GooF on F^2[c]	1.164	1.068	1.110	1.052	1.083	1.088
Largest diff. peak and hole, ($e·Å^{-3}$)	0.648/–0.838	0.409/–0.426	0.370/–0.315	1.957/–0.928	0.437/–0.328	0.460/–0.485

[a] $R_1 = \Sigma\big|\,|F_o| - |F_c|\,\big| / \Sigma|F_o|$; [b] $wR_2 = \{\Sigma[w(F_o^2 - F_c^2)^2] / \Sigma[w(F_o^2)^2]\}^{1/2}$;
[c] $S = \{\Sigma[w(F_o^2 - F_c^2)^2] / (n-p)\}^{1/2}$

Table S3 Comparison of structural features of **10–17**, **19**·$CHCl_3$, **20** and **21**

Features	Δ_{CN} (Å)	Δ_{CN}' (Å)	∑N(coord.) (deg)	∑N(noncoord.) (deg)	N–C–N–H torsion angle (deg)	φ^a (deg)
10	0.009(4)	0.047(4)	356.7, 359.2	360.0	19.2, –165.0	17.6
11	0.000(7)	0.074(7)	354.3, 360.0	359.9	143.7, –37.8	37.1
12	0.011(12)	0.037(17)	355.5, 359.0	360.0	168.4, –16.0	14.2
13	0.009(5)	0.030(5)	351.5, 357.0	359.9	151.8, –31.5	30.0
14	0.001(8)	0.038(8)	353.7, 356.7	359.9	161.3, –22.0	20.5
15	0.014(6)	0.060(6)	343.5, 360.0	360.0	132.4, –50.1	48.9
16	0.012(5)	0.047(5)	349.9, 357.9	360.0	29.8, –153.1	28.4
17	0.008(3)	0.050(3)	352.7, 358.2	359.9	29.8, –154.2	26.4
19·$CHCl_3$	0.031(8)	0.067(8)	352.7, 357.6	360.0	31.0, –149.7	30.6
20	0.007(7)	0.060(7)	355.7, 356.1	360.0	19.6, –166.1	17.4
21	0.021(8)	0.043(8)	351.3, 359.3	359.9	24.2, –159.1	22.8

[a] φ = Dihedral angle between the HNC(Ar) plane and the chelate NCN plane

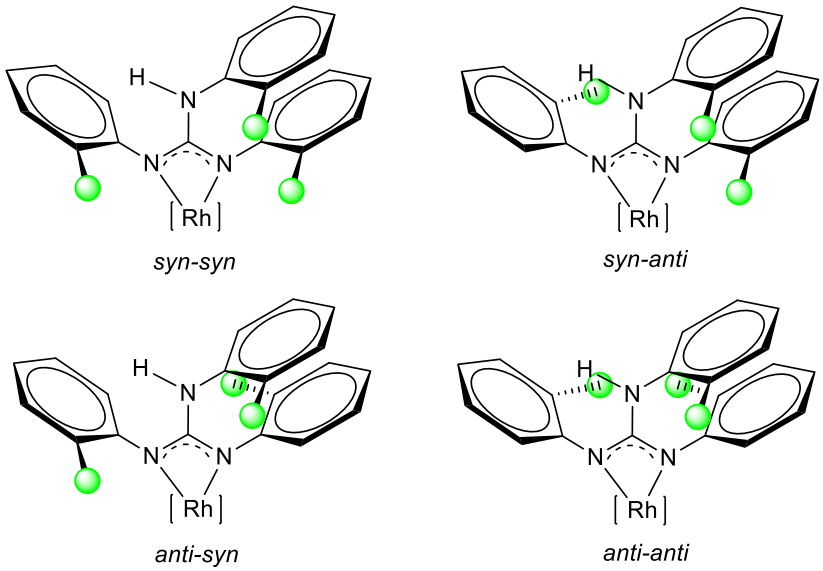

Fig. S1 Four conformers of the *o*-substituted arylguanidinato ligands in Cp*Rh(III) guanidinato complexes. ● = Cl, F, OMe, Me; [Rh] = [(η^5-Cp*)RhX] (X = Cl, N_3, $N_3C_2(R')_2$).

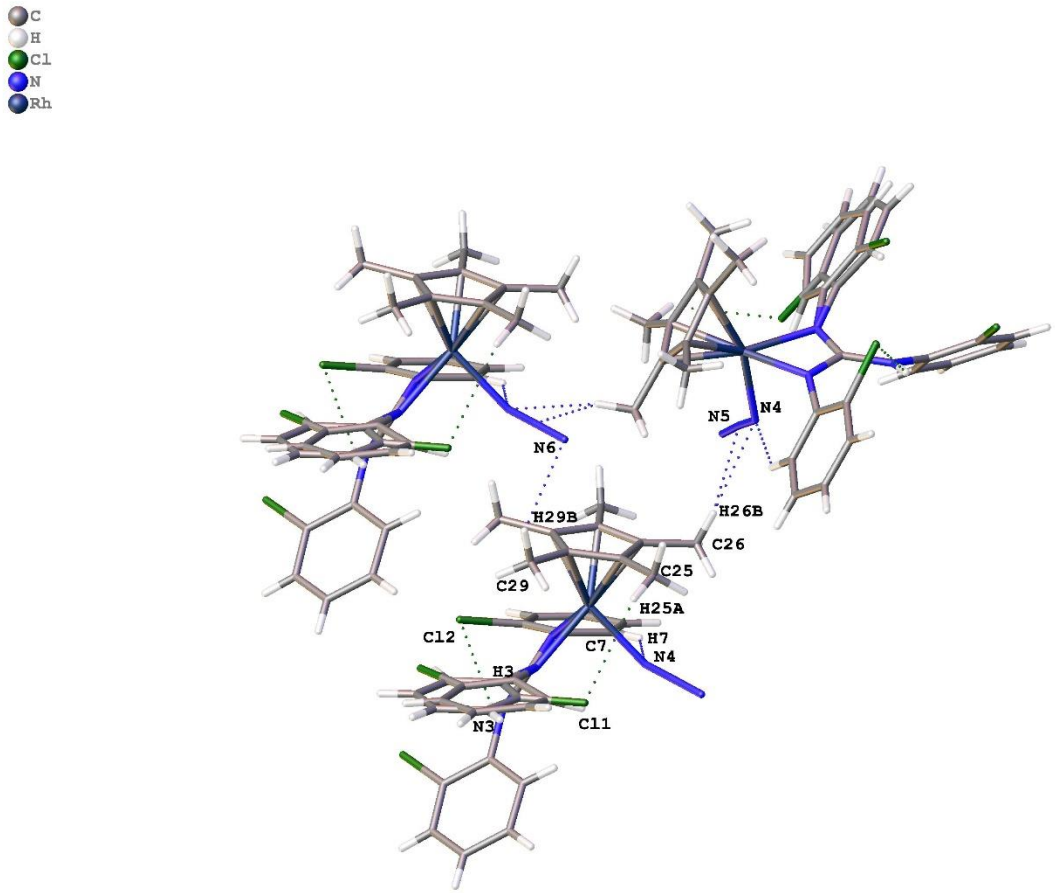

Fig. S2 Packing diagram of **14**. Hydrogen bond parameters (Å, deg): C29···N6 = 3.657(10), H29B···N6 = 2.810(7), C29–H29B···N6 = 147.6; C26···N5 = 3.425(9), H26B···N5 = 2.754(5), C26–H26B···N5 = 127.6; N3···Cl2 = 3.231(5), H3···Cl2 = 2.626(2), N3–H3···Cl2 = 128.3; C7···N4 = 3.429(8), H7···N4 = 2.709(5), C7–H7···N4 = 134.8; C26···N4 = 3.563(9), H26B···N4 = 2.688(5), C26–H26B···N4 = 151.7; C25···Cl1 = 3.766(8), H25A···Cl1 = 3.039(9), C25–H25A···Cl1 = 133.6.

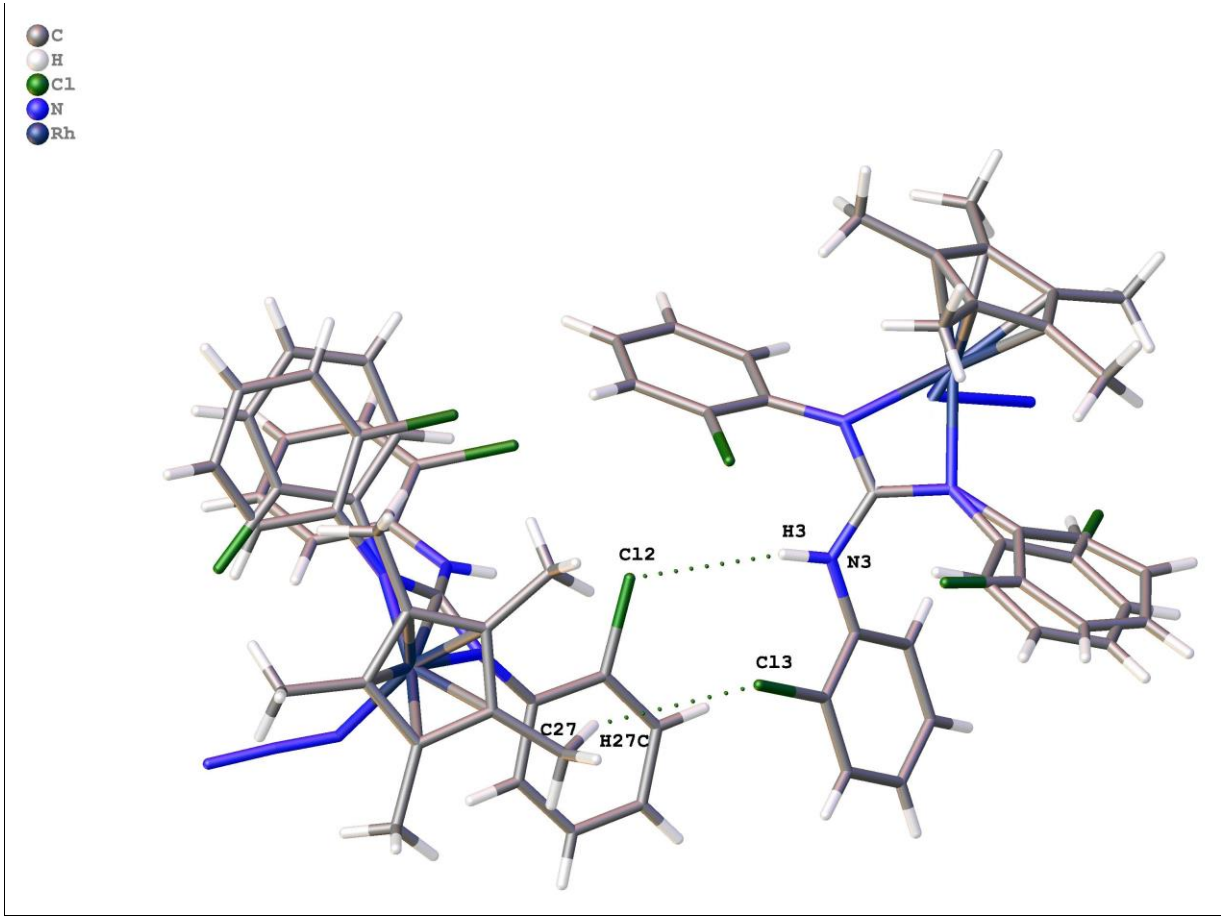

Fig. S3 Packing diagram of **14**. Hydrogen bond parameters (Å, deg): C27···Cl3 = 3.785(8), H27C···Cl3 = 3.009(2), C27–H27C···Cl3 = 138.7; C12···N3 = 3.600(5), H3···Cl2 = 2.9463(19), C12–H3···N3 = 134.3.

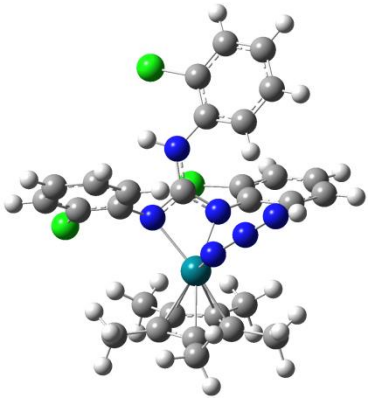

syn-syn

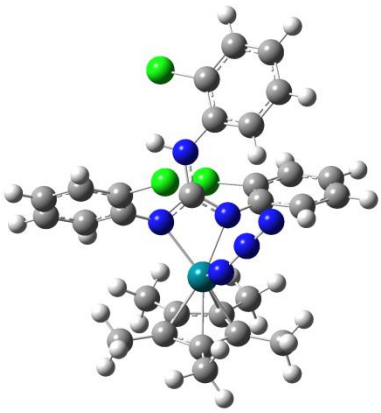

syn-anti

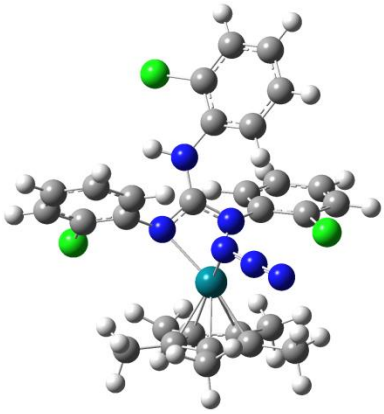

anti-syn

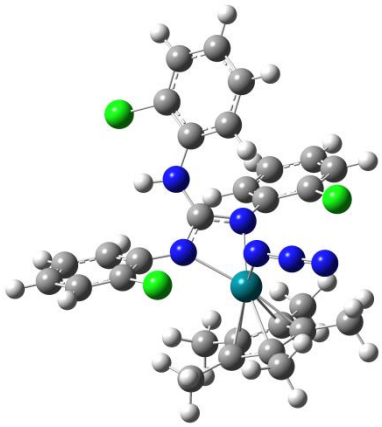

anti-anti

Fig. S4 Optimized geometry of four possible conformers of **14**.

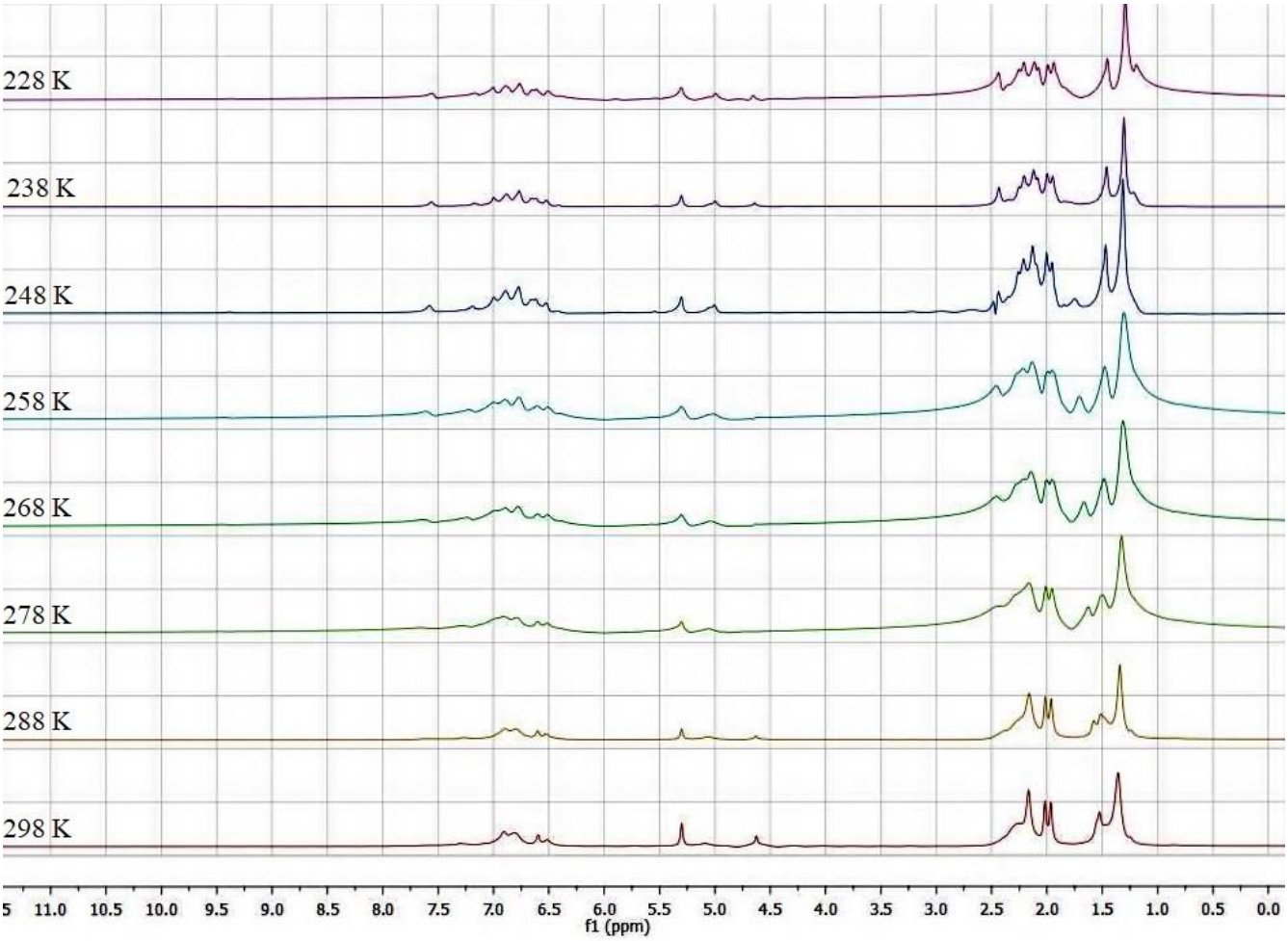

Fig. S5 VT ^{1}H NMR (500 MHz, CD_2Cl_2) stack plot of **13**.

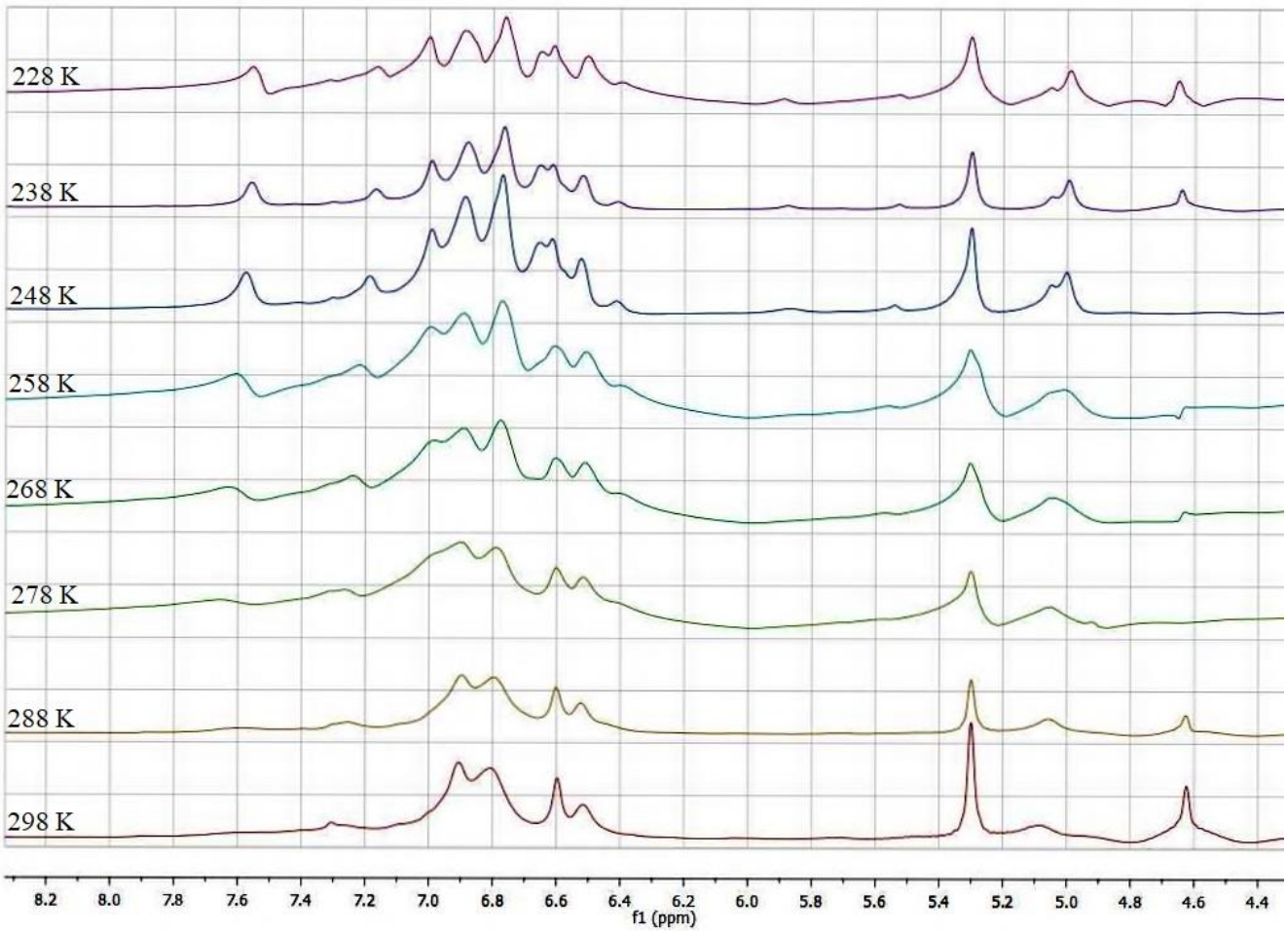

Fig. S6 VT ^{1}H NMR (500 MHz, CD_2Cl_2) stack plot of **13** illustrated for the NH and ArH protons.

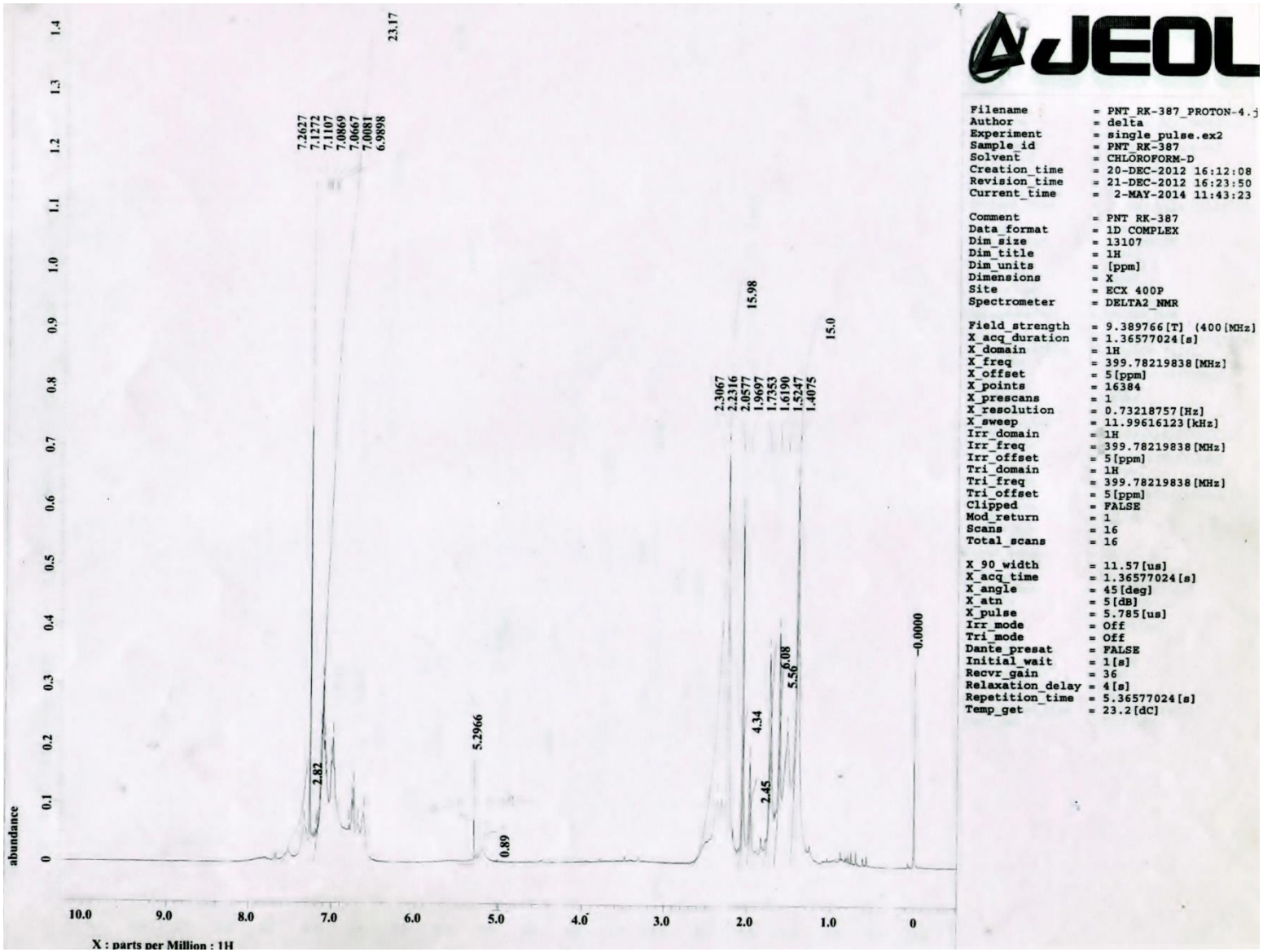

Fig. S7 ^{1}H NMR (400 MHz, $CDCl_3$) spectrum of **9** at 1.42×10^{-2} M concentration

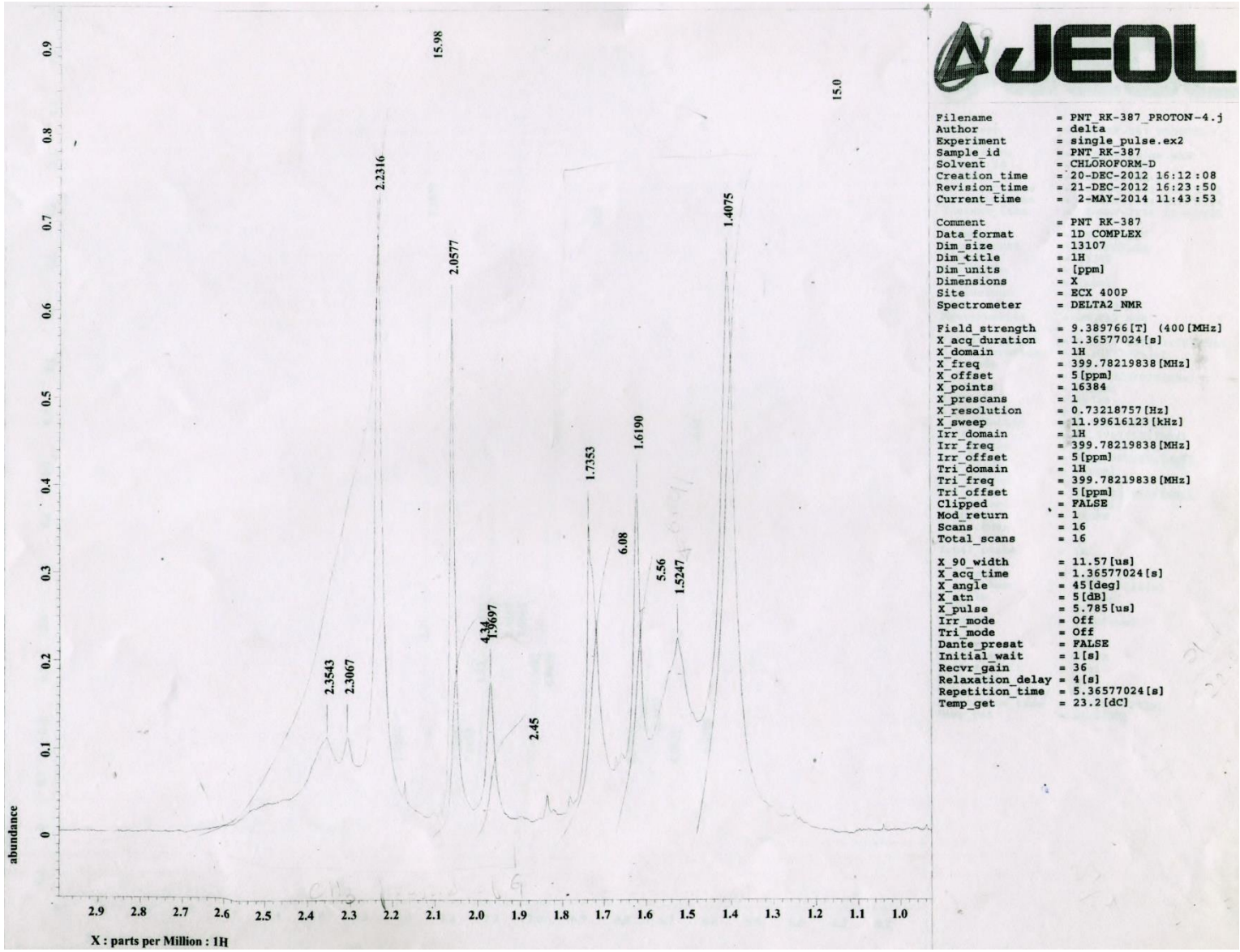

Fig. S8 ^{1}H NMR (400 MHz, $CDCl_3$) spectrum of **9** at 1.42×10^{-2} M concentration in the indicated region

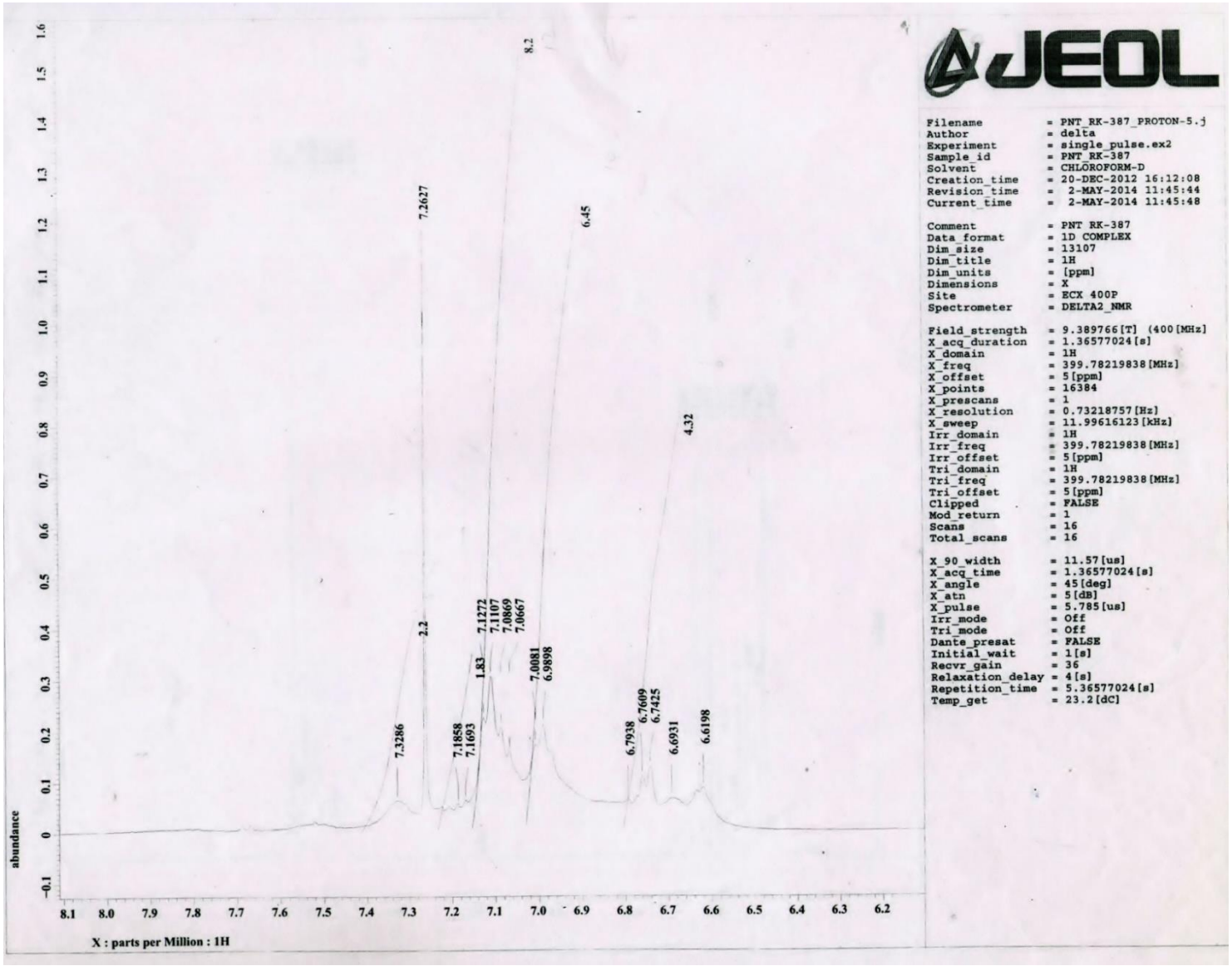

Fig. S9 ^{1}H NMR (400 MHz, $CDCl_3$) spectrum of **9** at 1.42×10^{-2} M concentration in the indicated region

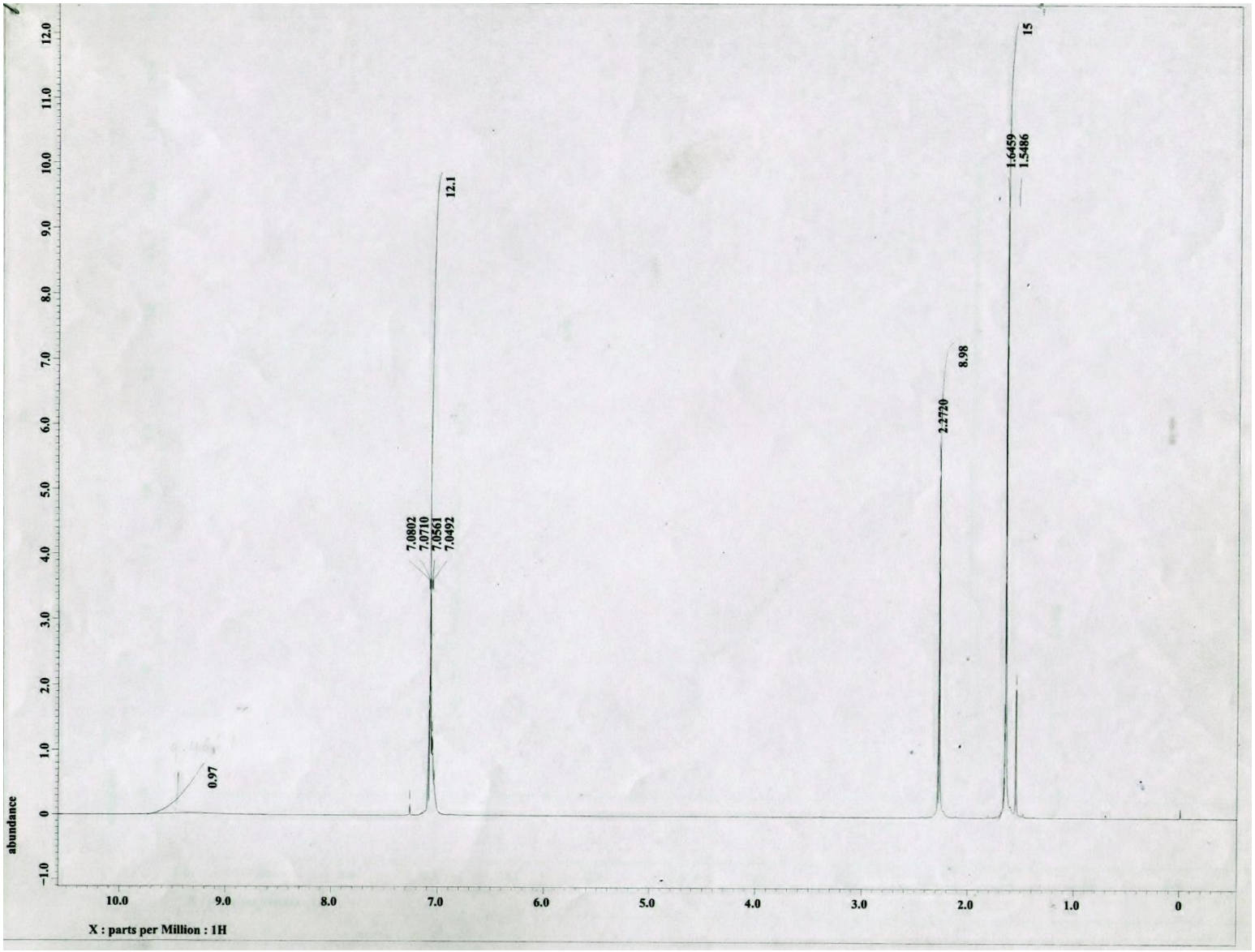

Fig. S10 ^{1}H NMR (400 MHz, $CDCl_3$) spectrum of **9** at 1.66×10^{-1} M concentration

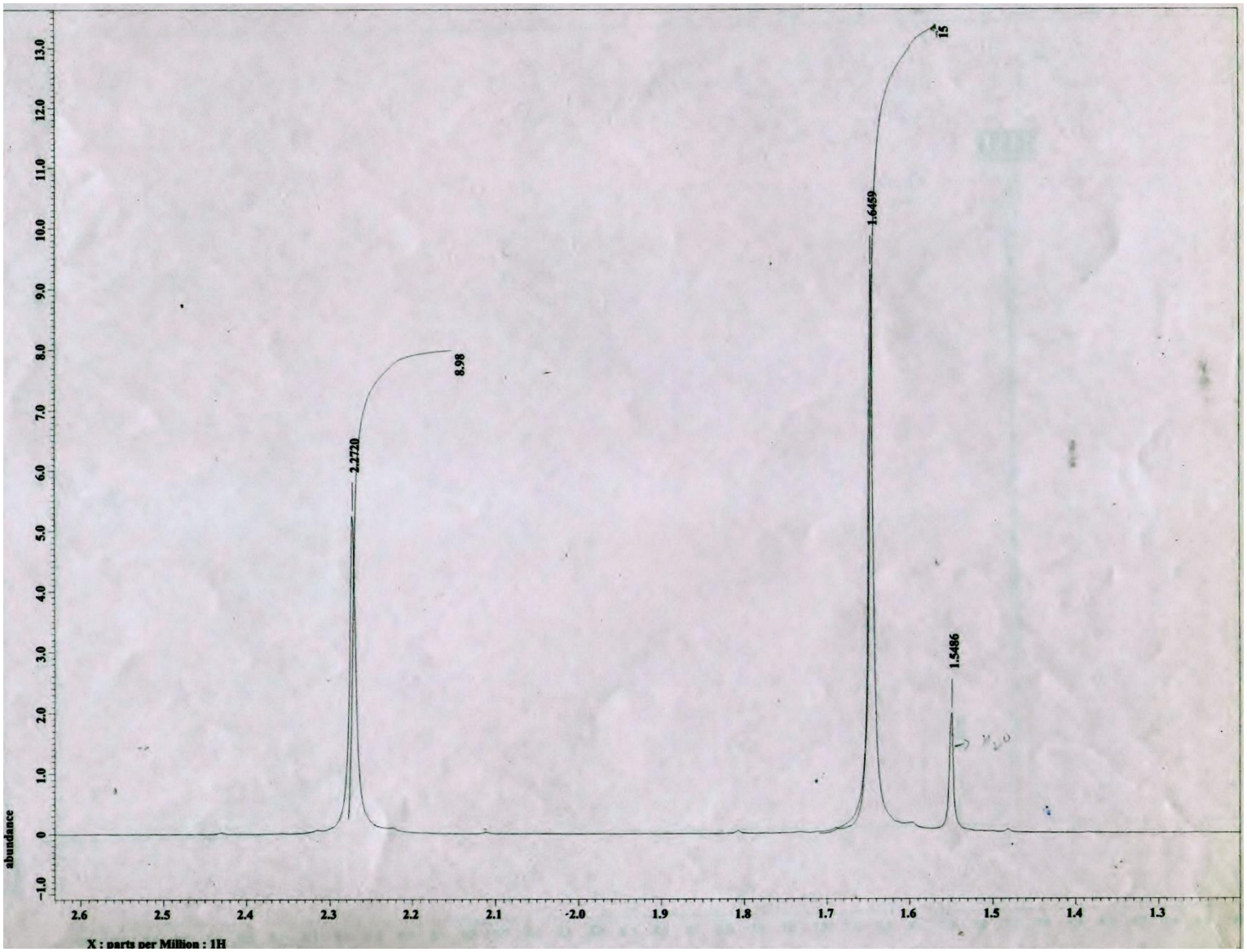

Fig. S11 ^{1}H NMR (400 MHz, $CDCl_3$) spectrum of **9** at 1.66×10^{-1} M concentration in the indicated region

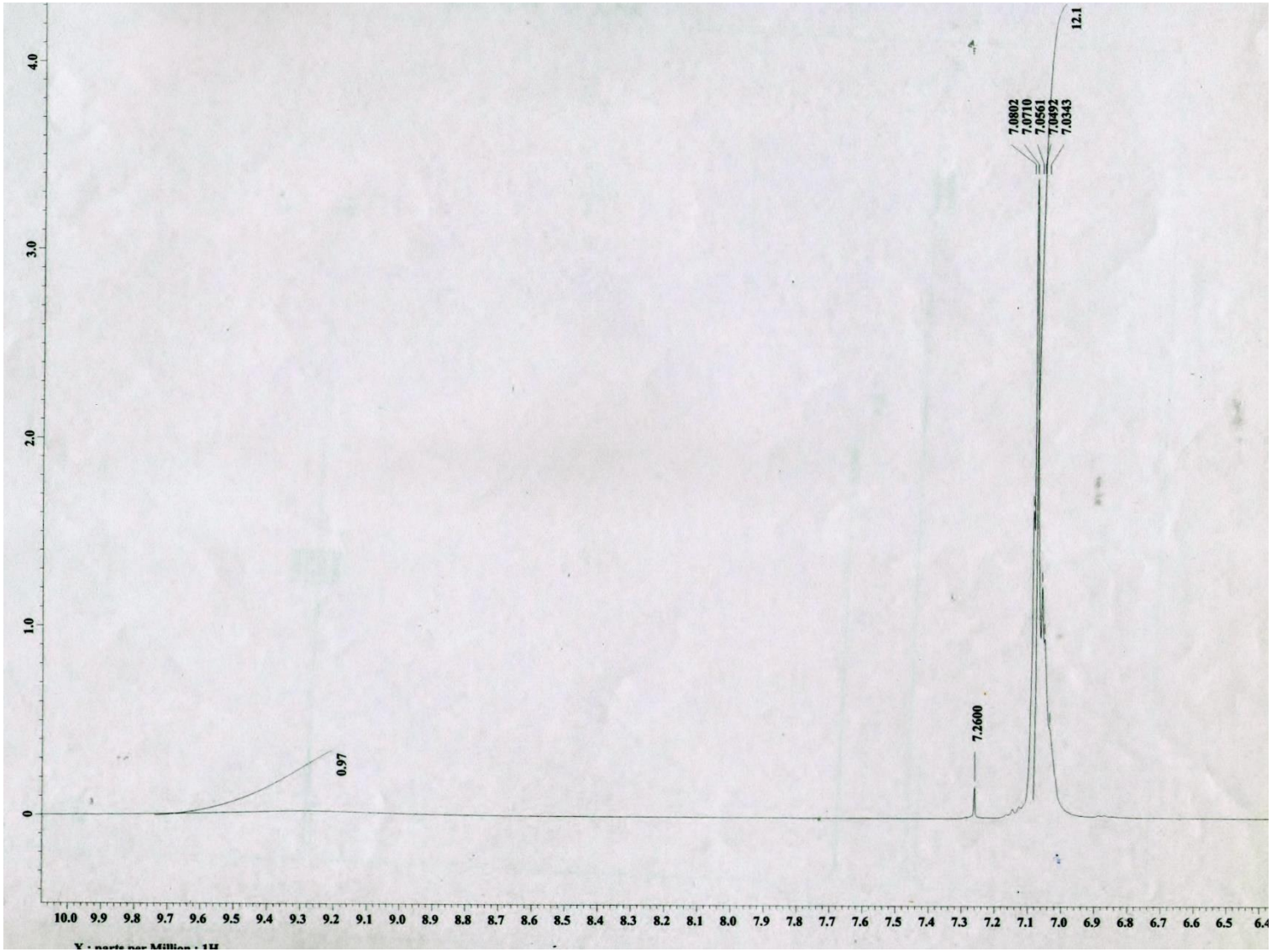

Fig. S12 ^{1}H NMR (400 MHz, $CDCl_3$) spectrum of **9** at 1.66×10^{-1} M concentration in the indicated region

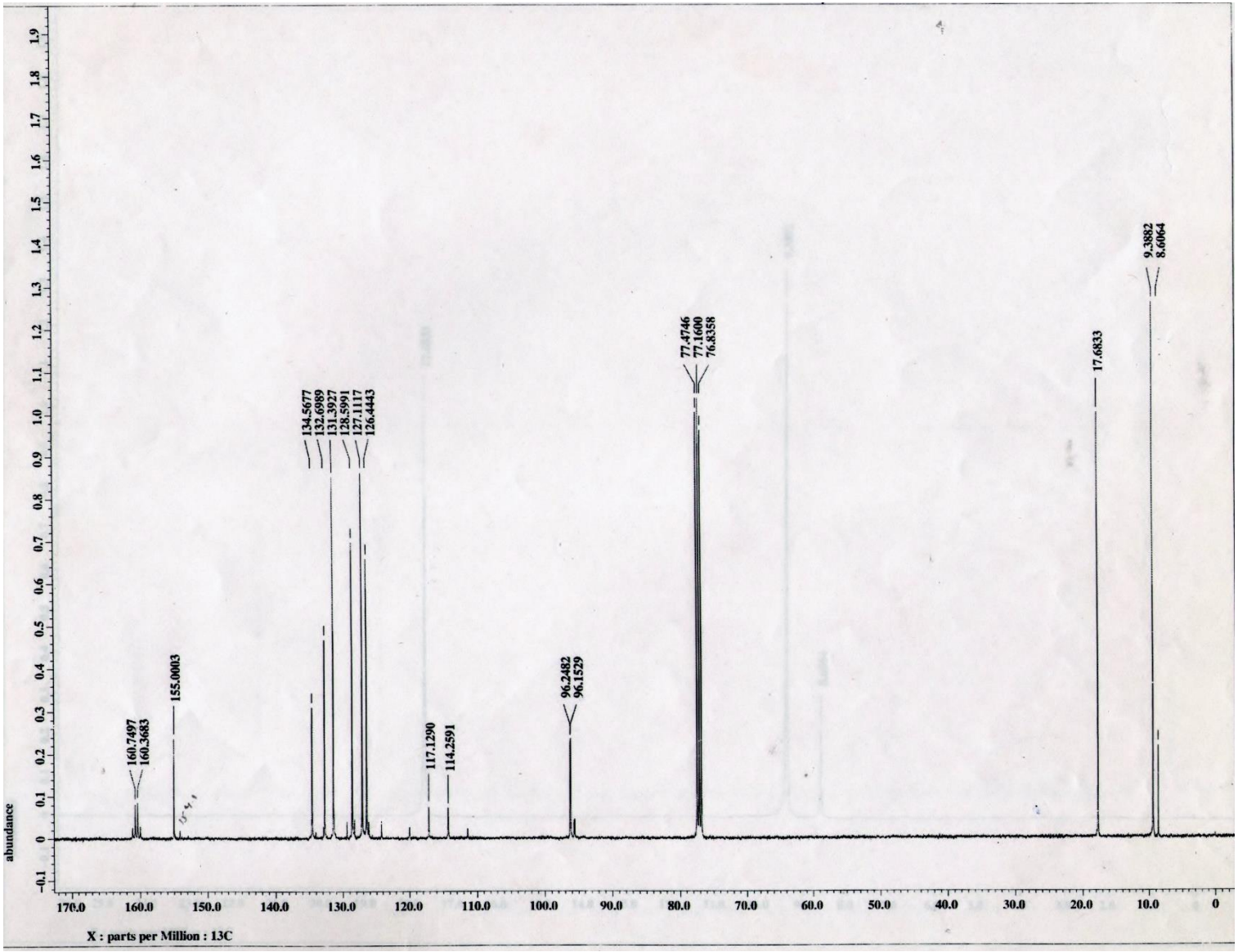

Fig. S13 ^{13}C NMR (100.5 MHz, $CDCl_3$) spectrum of **9**

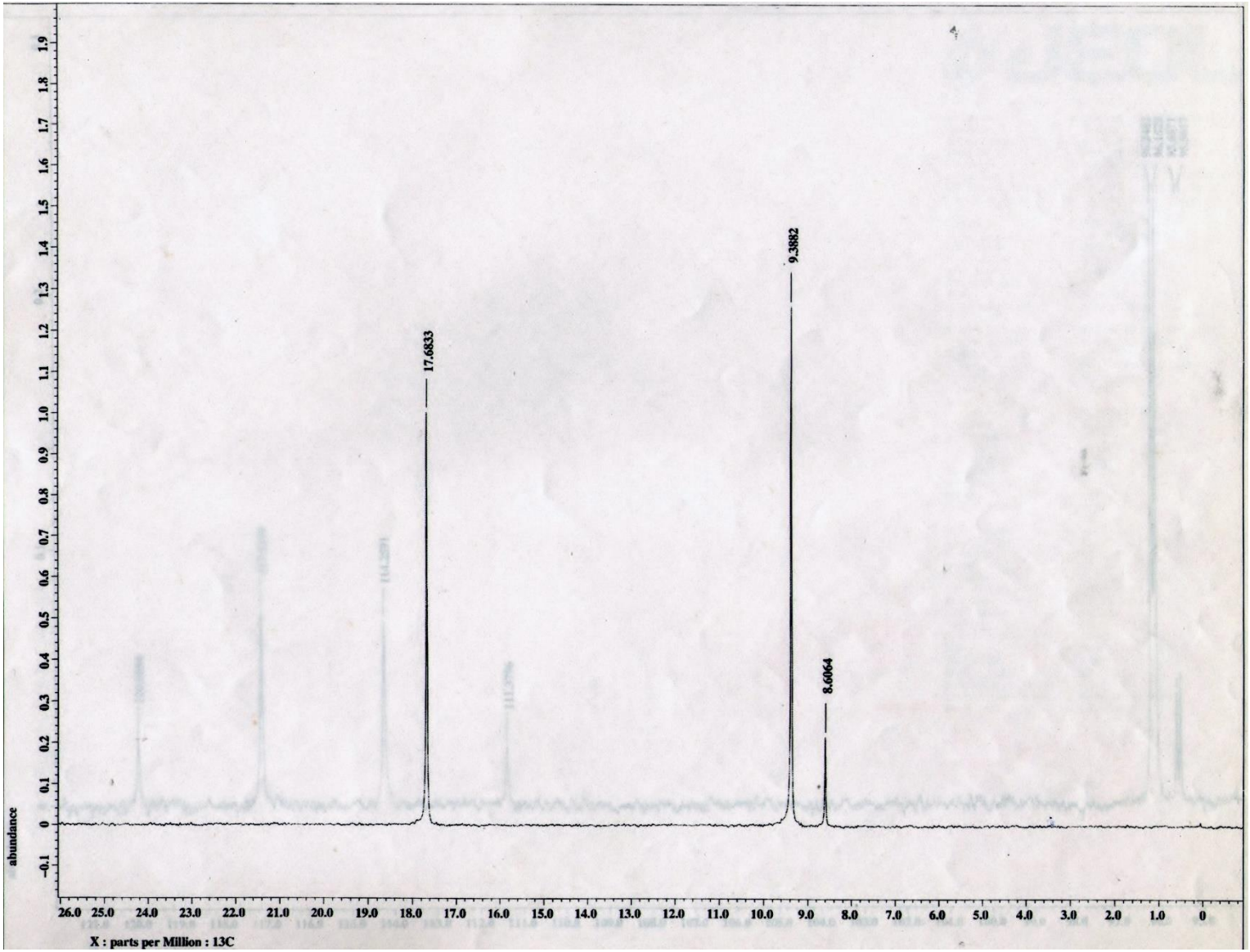

Fig. S14 ^{13}C NMR (100.5 MHz, $CDCl_3$) spectrum of **9** in the indicated region

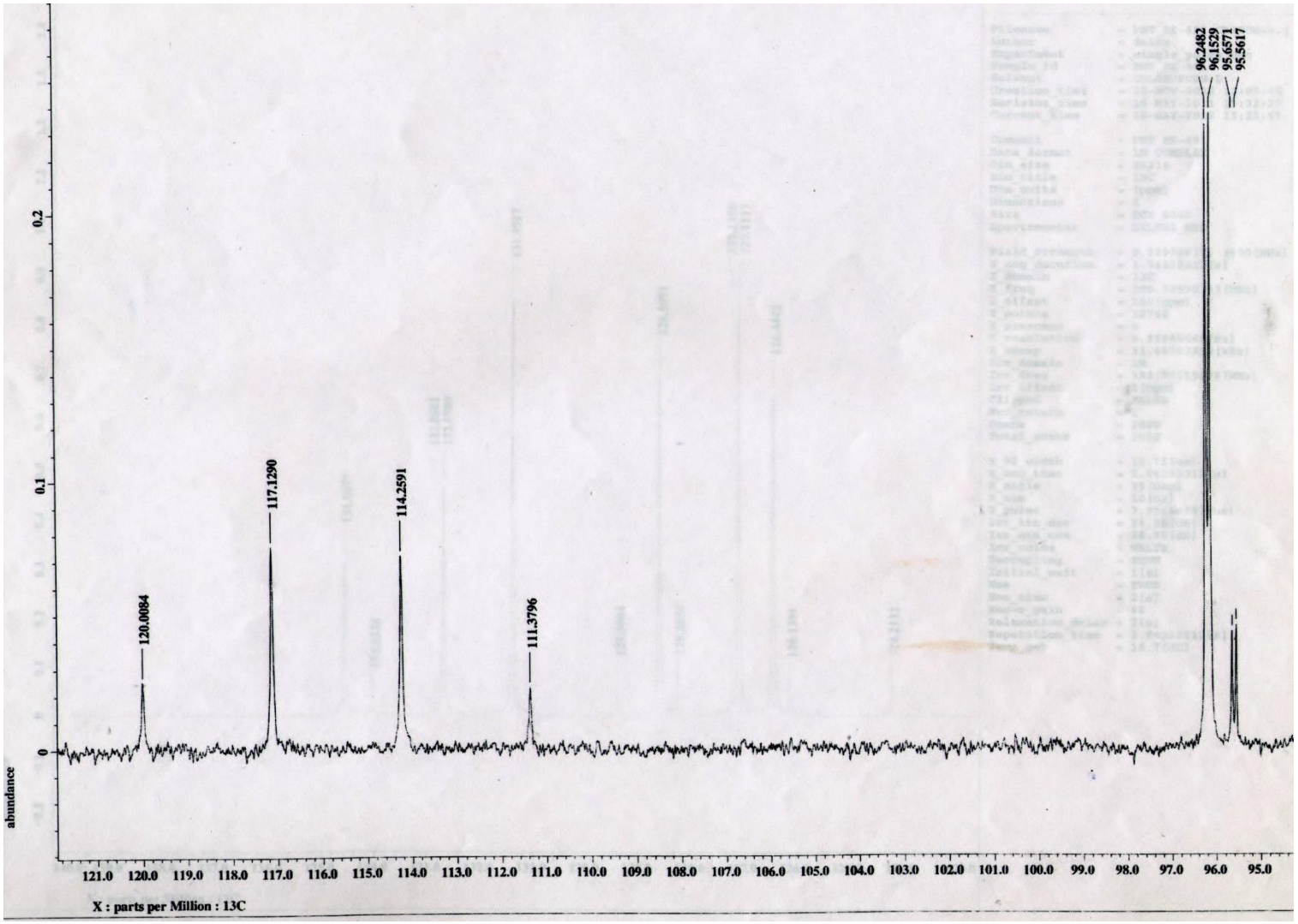

Fig. S15 ^{13}C NMR (100.5 MHz, $CDCl_3$) spectrum of **9** in the indicated region

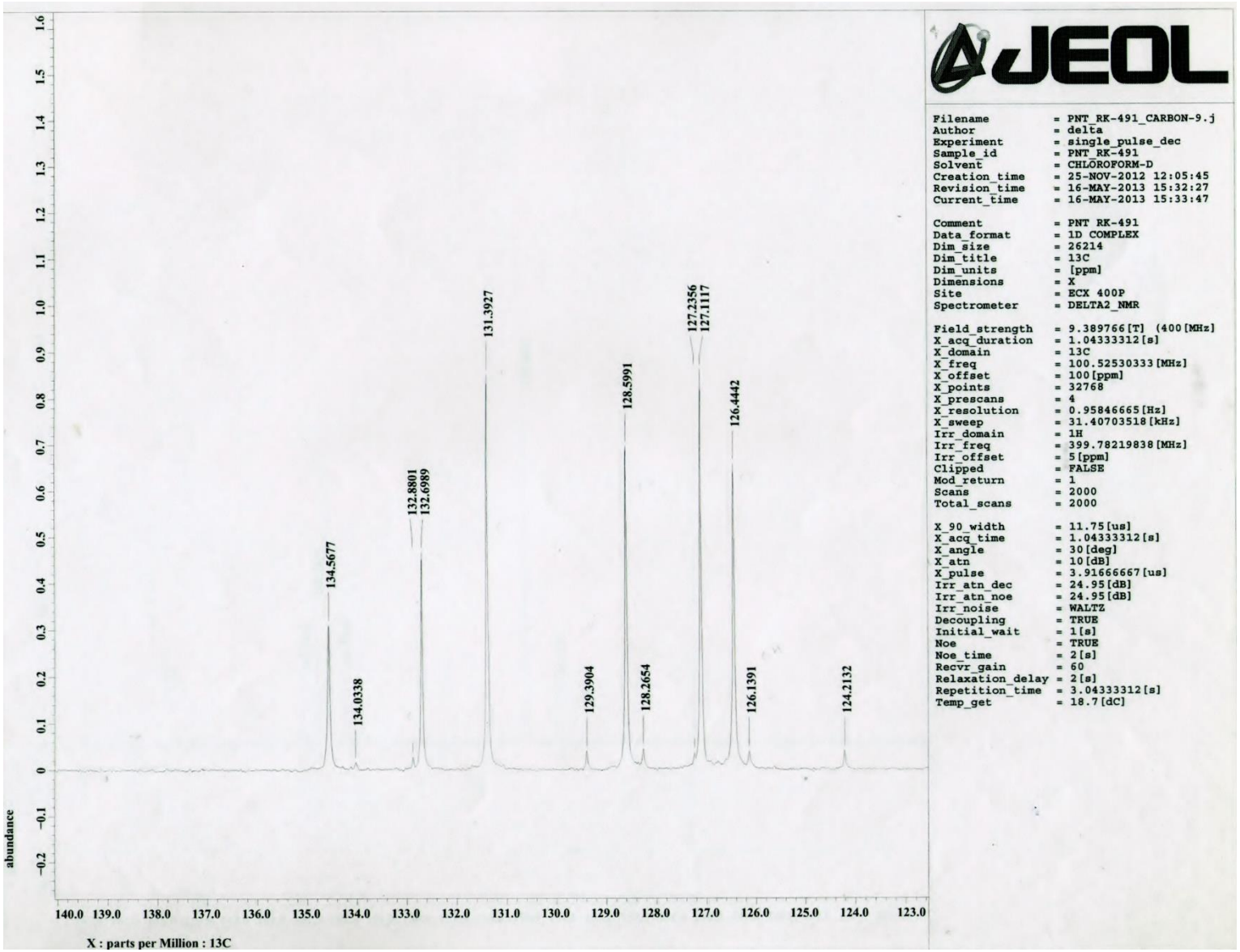

Fig. S16 ^{13}C NMR (100.5 MHz, $CDCl_3$) spectrum of **9** in the indicated region

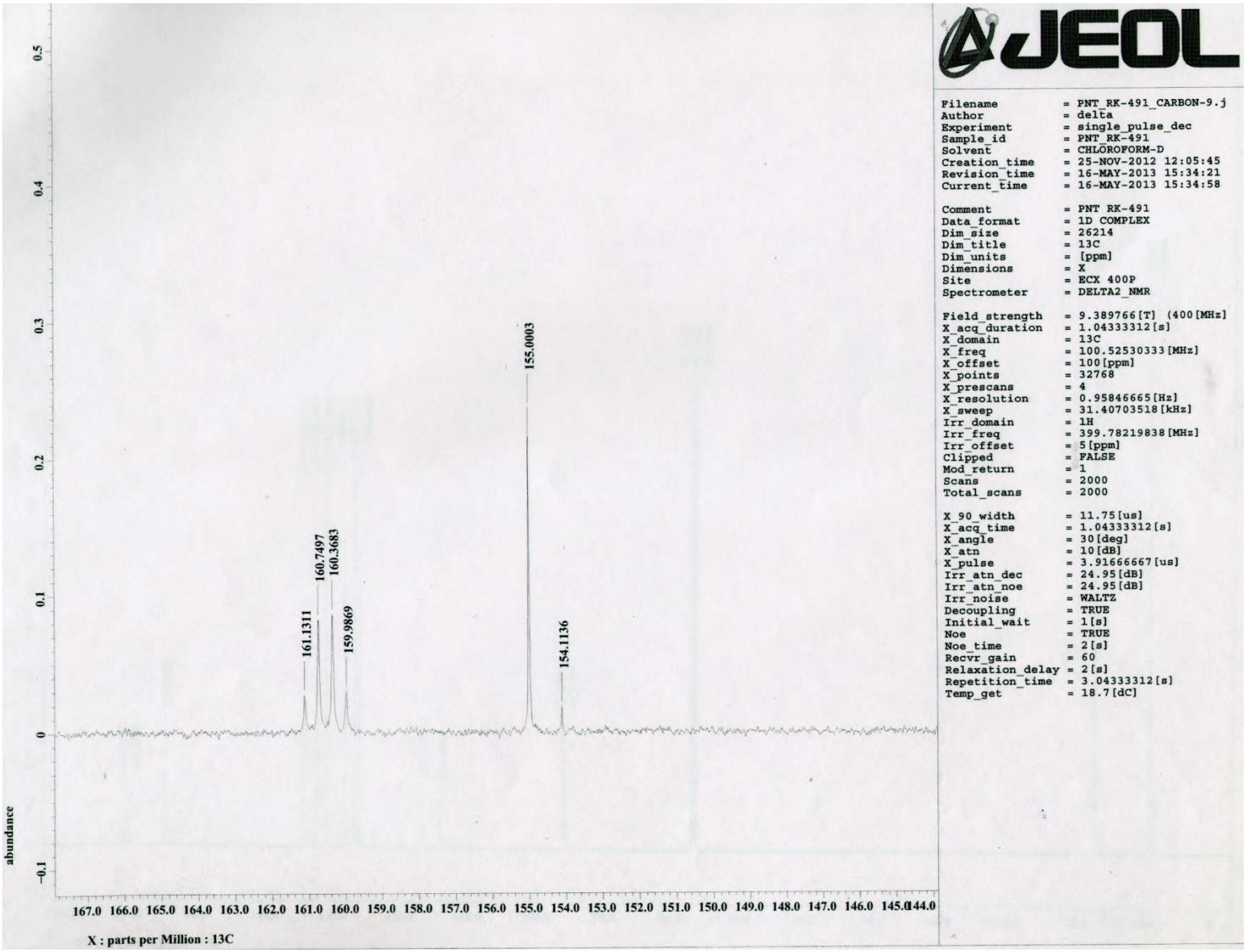

Fig. S17 ^{13}C NMR (100.5 MHz, $CDCl_3$) spectrum of **9** in the indicated region

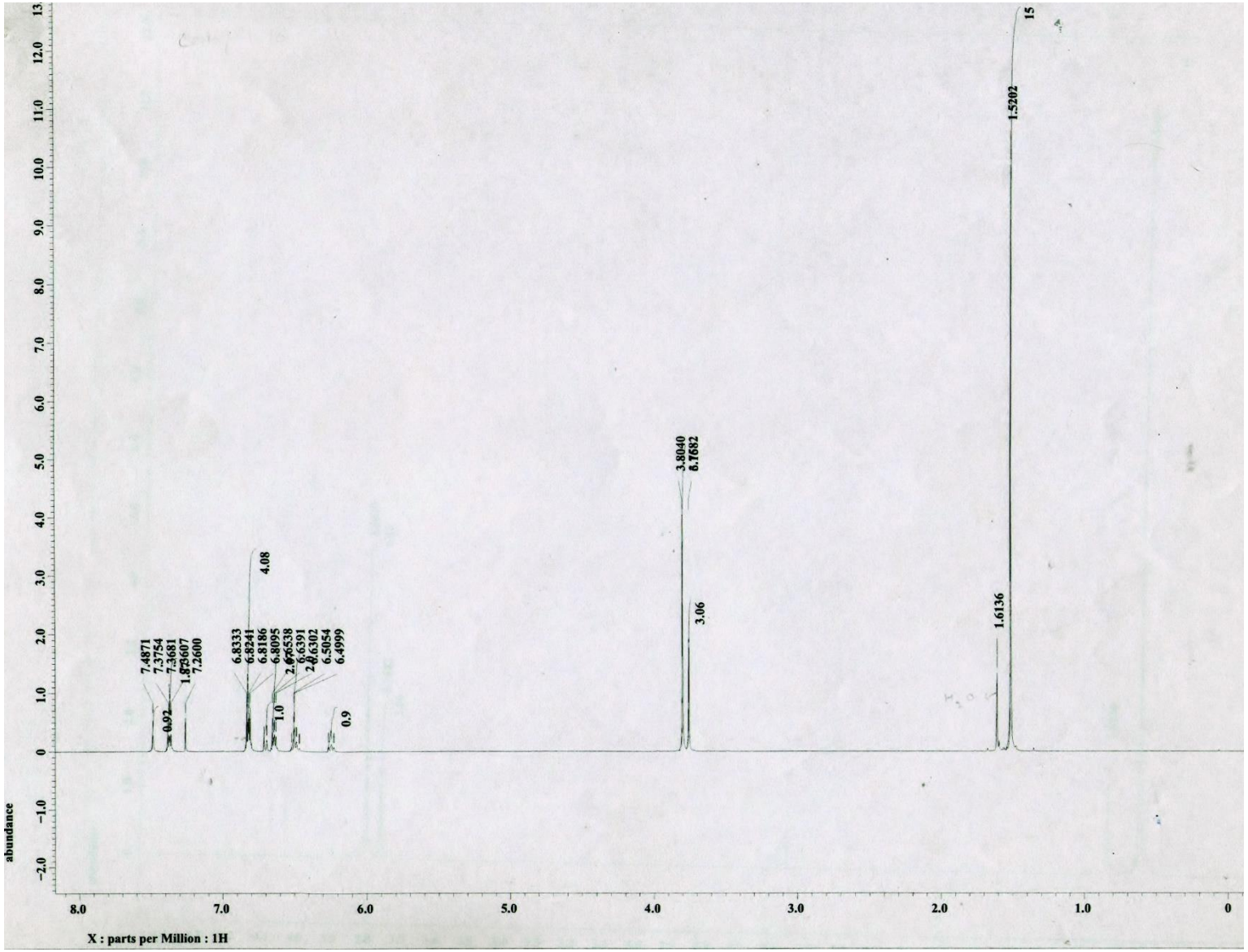

Fig. S18 ^{1}H NMR (400 MHz, $CDCl_3$) spectrum of **10**

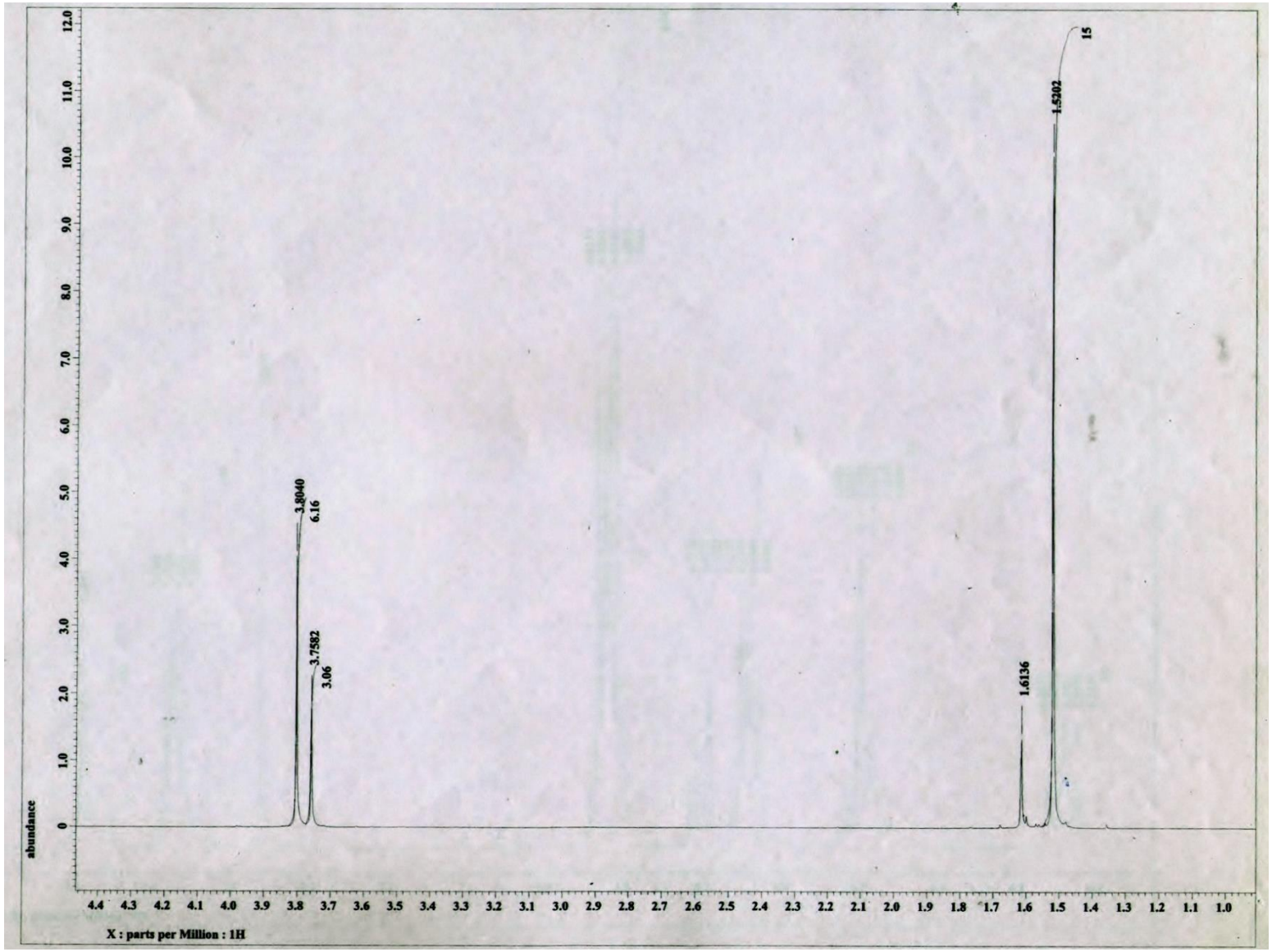

Fig. S19 ^{1}H NMR (400 MHz, $CDCl_3$) spectrum of **10** in the indicated region

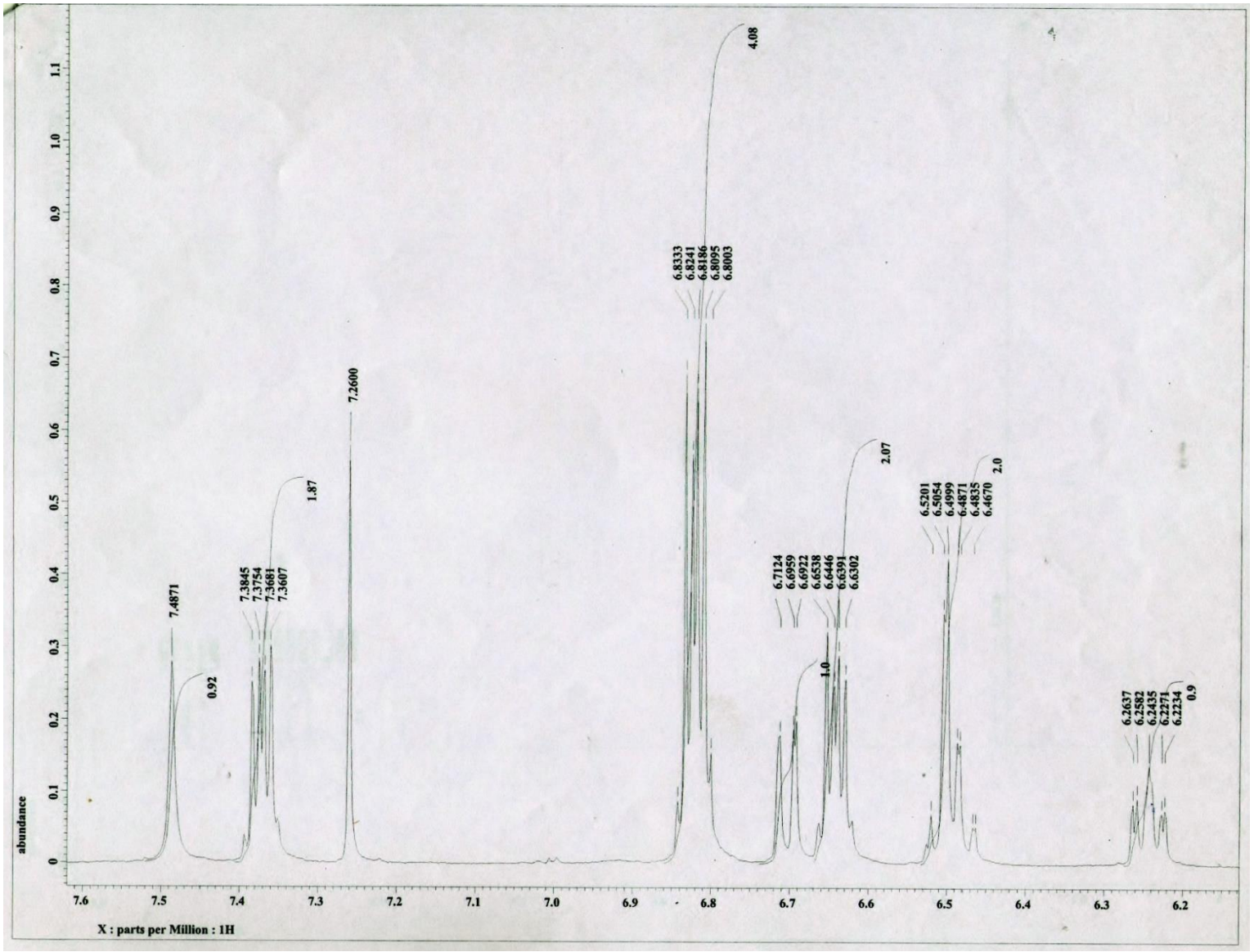

Fig. S20 ^{1}H NMR (400 MHz, $CDCl_3$) spectrum of **10** in the indicated region

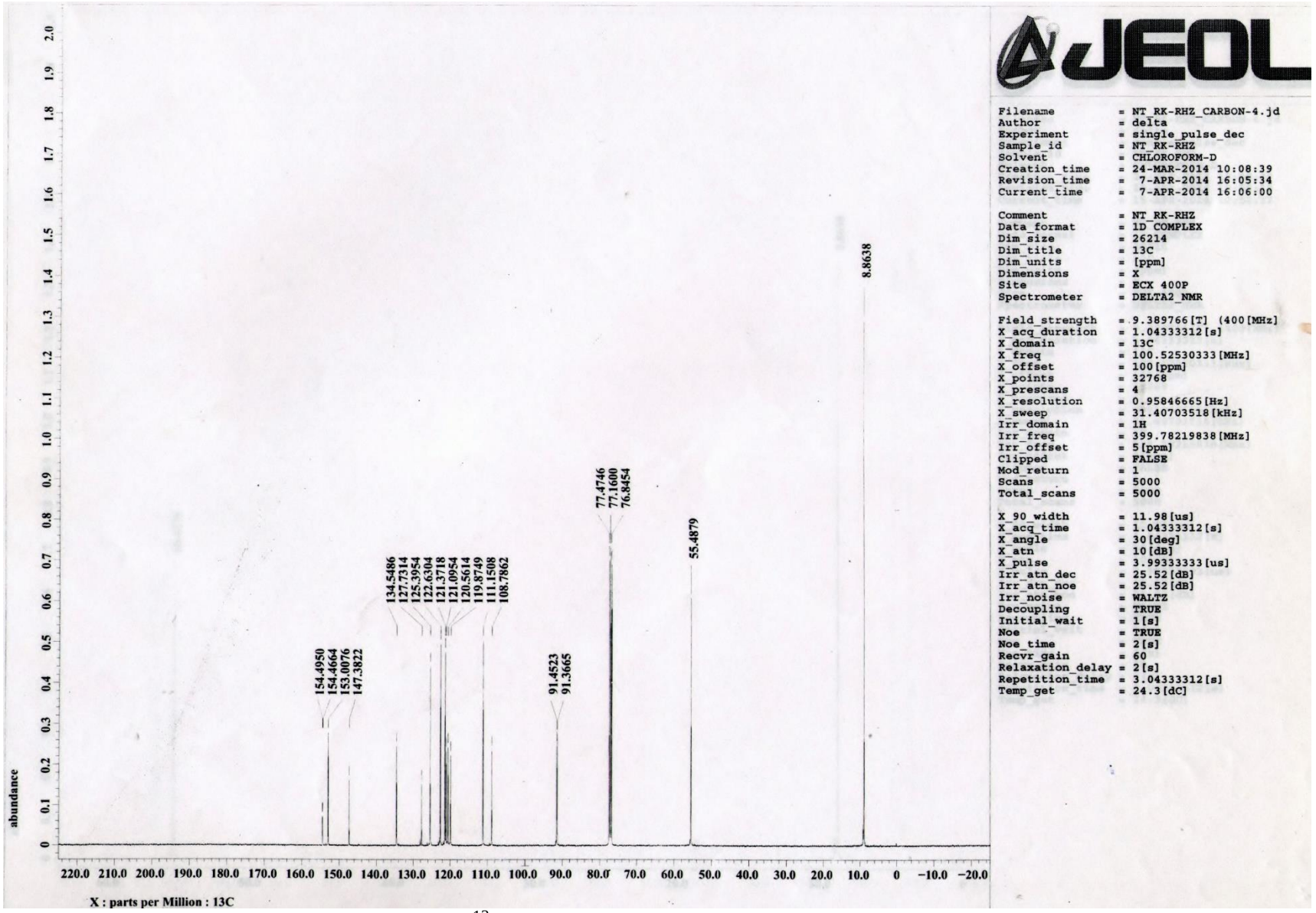

Fig. S21 ^{13}C NMR (100.5 MHz, $CDCl_3$) spectrum of **10**

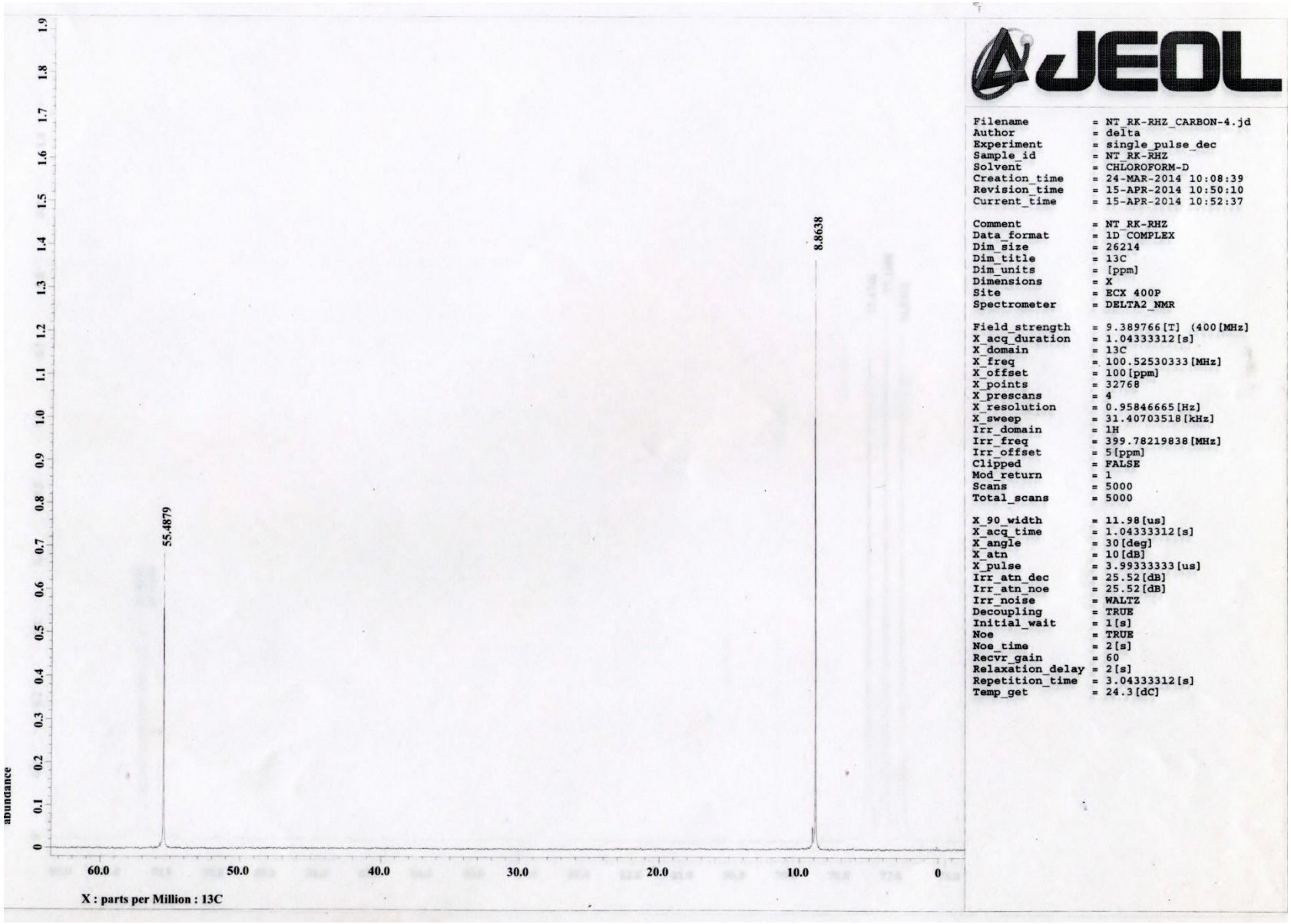

Fig. S22 ^{13}C NMR (100.5 MHz, $CDCl_3$) spectrum of **10** in the indicated region

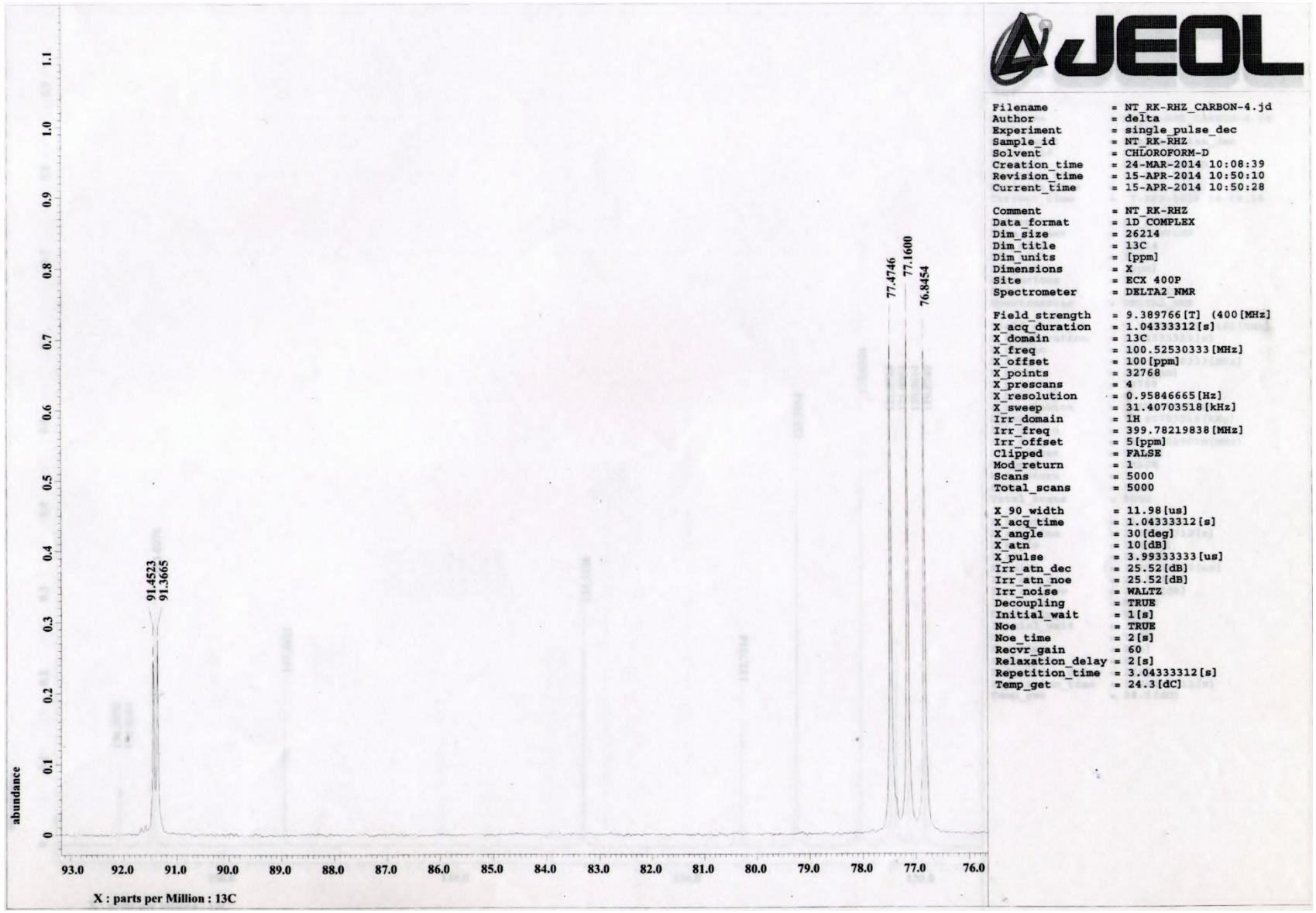

Fig. S23 ^{13}C NMR (100.5 MHz, $CDCl_3$) spectrum of **10** in the indicated region

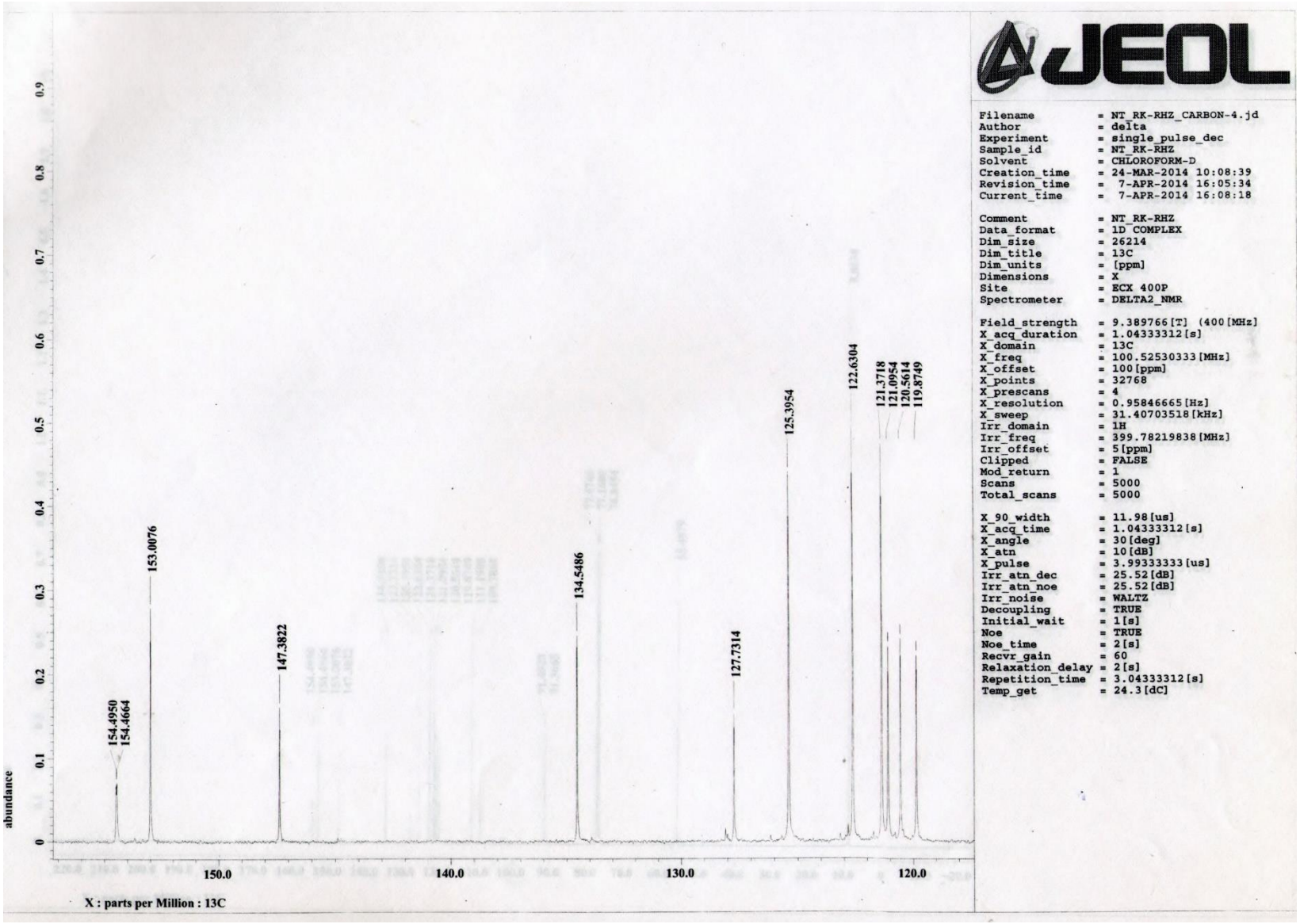

Fig. S24 ^{13}C NMR (100.5 MHz, $CDCl_3$) spectrum of **10** in the indicated region

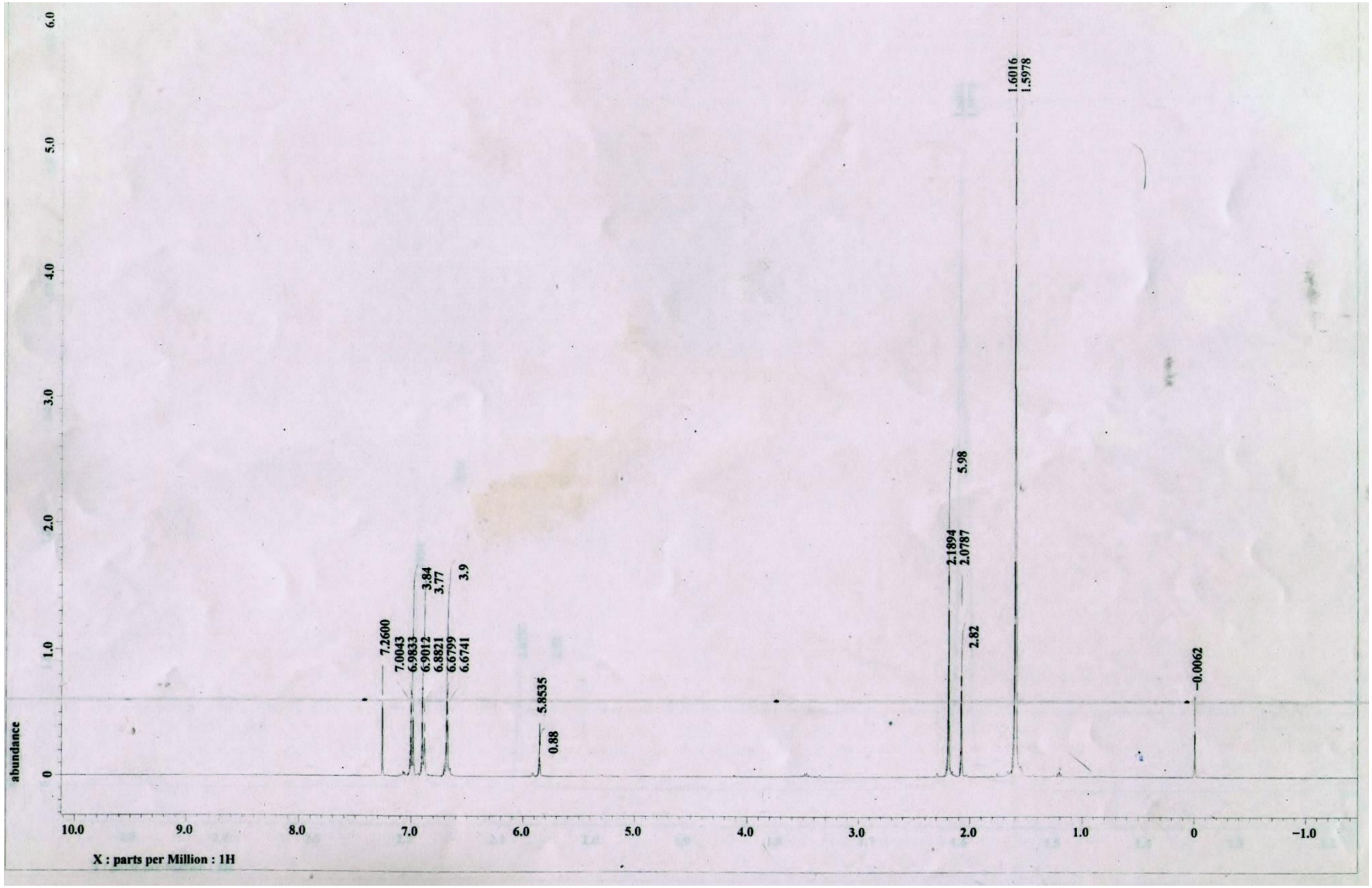

Fig. S25 ^{1}H NMR (400 MHz, $CDCl_3$) spectrum of **11**

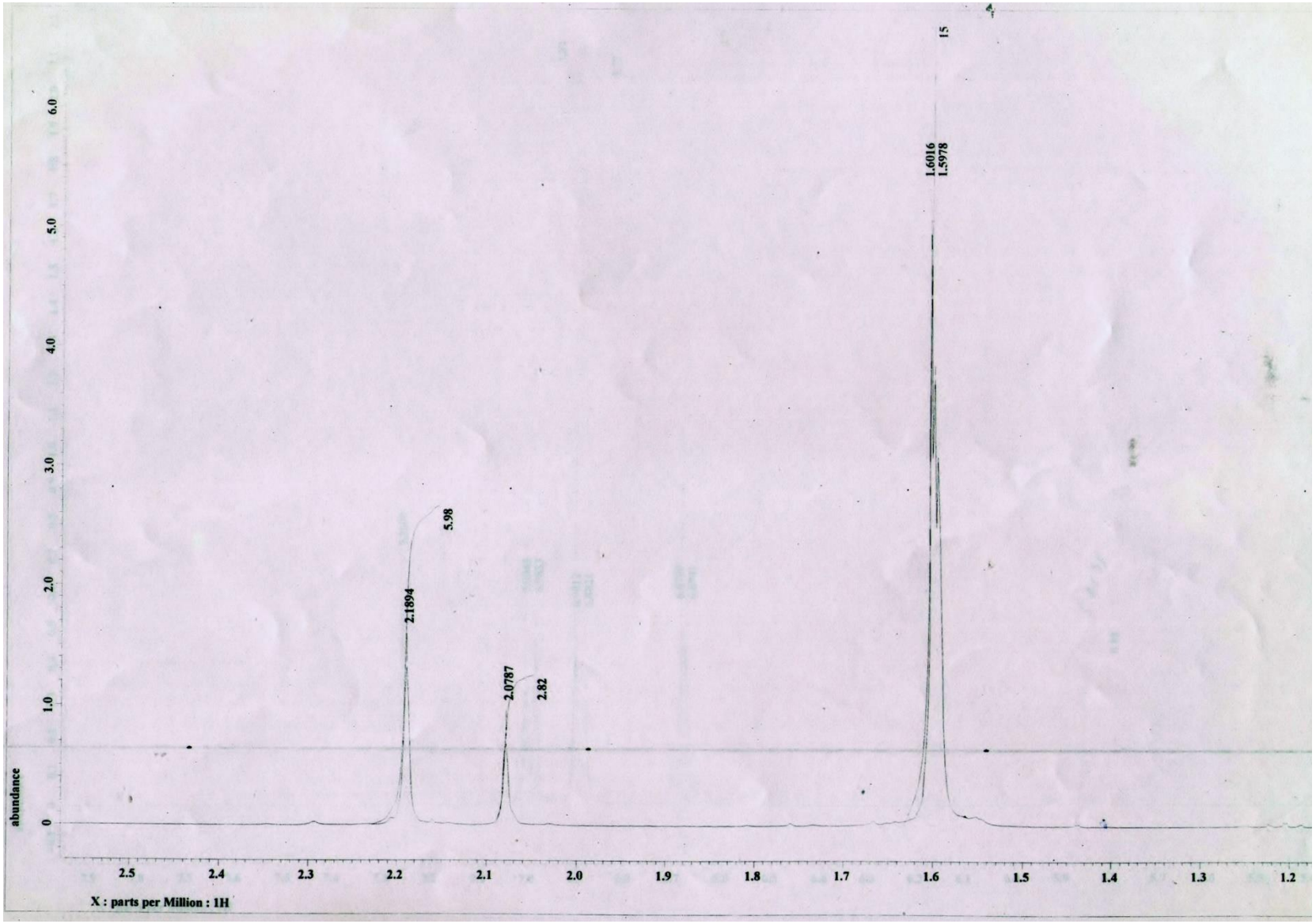

Fig. S26 ^{1}H NMR (400 MHz, $CDCl_3$) spectrum of **11** in the indicated region

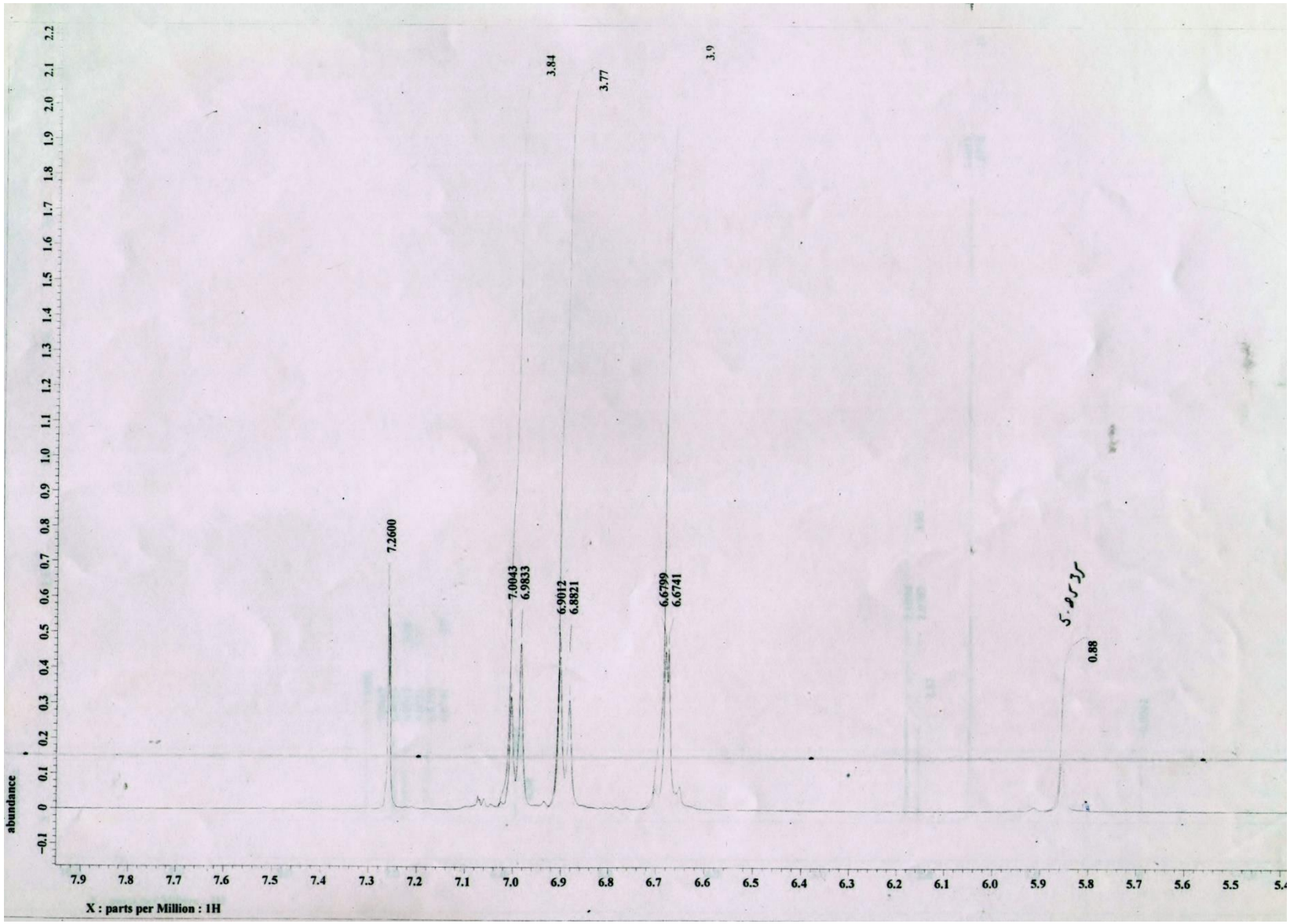

Fig. S27 ^{1}H NMR (400 MHz, $CDCl_3$) spectrum of **11** in the indicated region

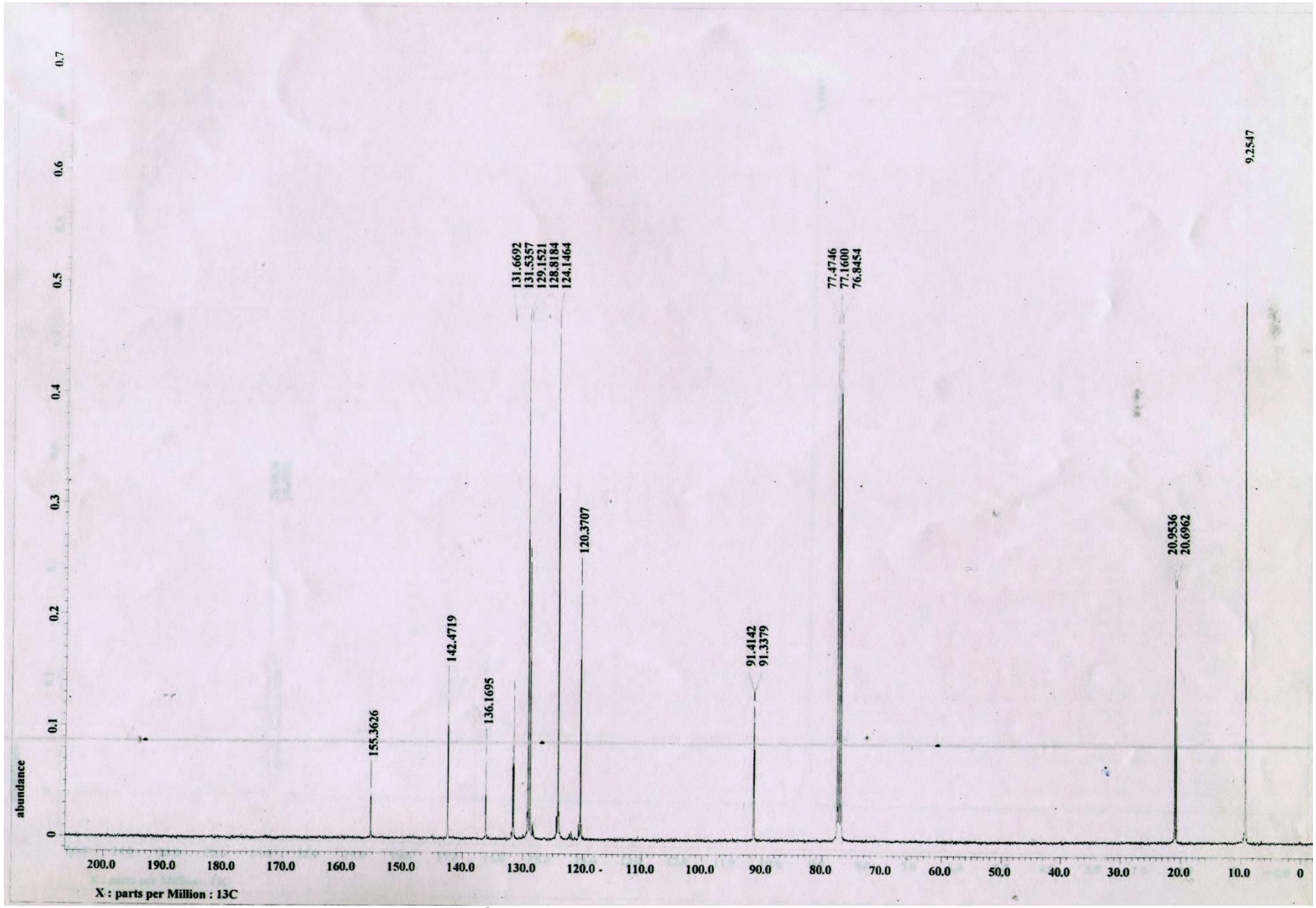

Fig. S28 ^{13}C NMR (100.5 MHz, $CDCl_3$) spectrum of **11**

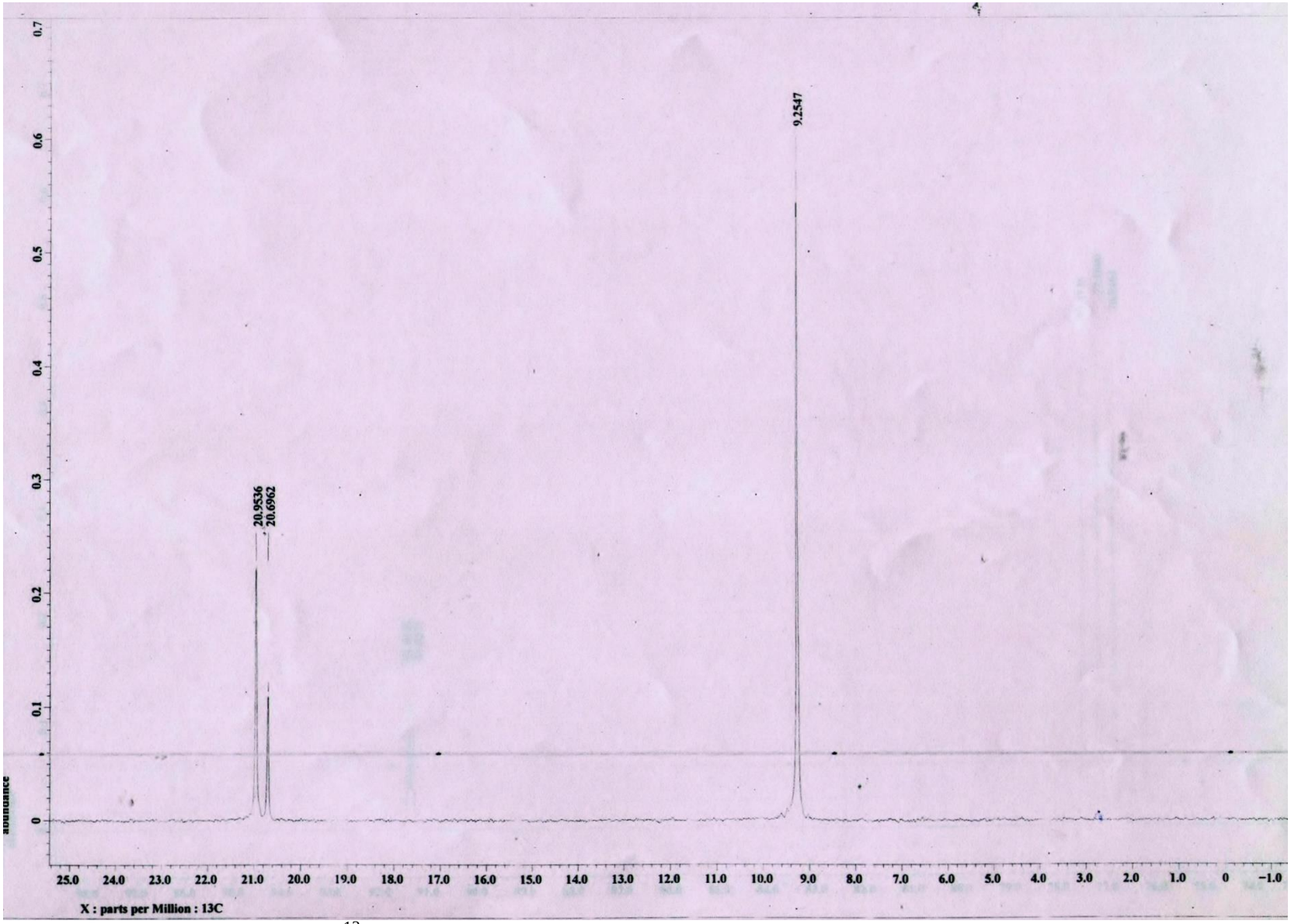

Fig. S29 ^{13}C NMR (100.5 MHz, $CDCl_3$) spectrum of **11** in the indicated region

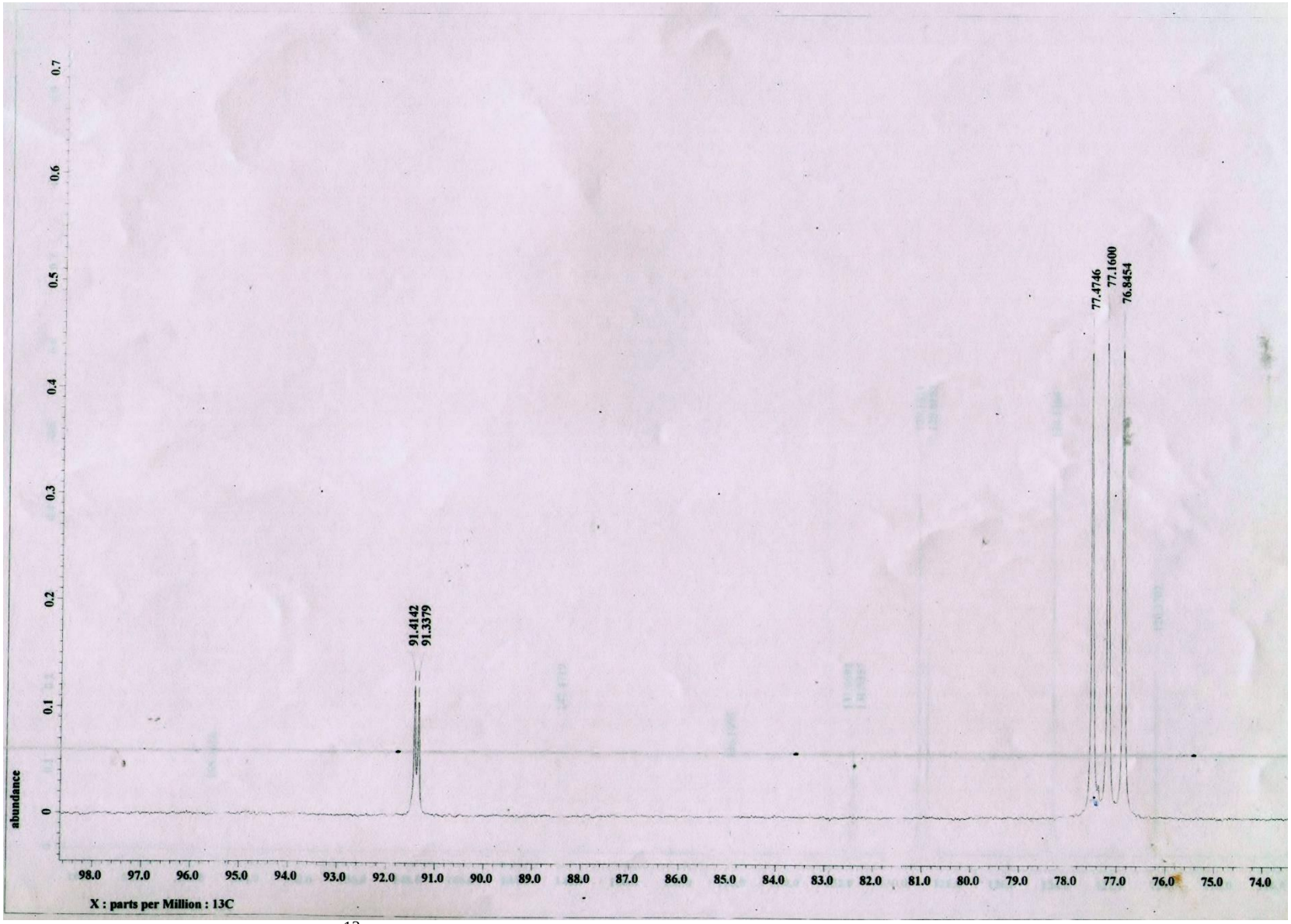

Fig. S30 ^{13}C NMR (100.5 MHz, $CDCl_3$) spectrum of **11** in the indicated region

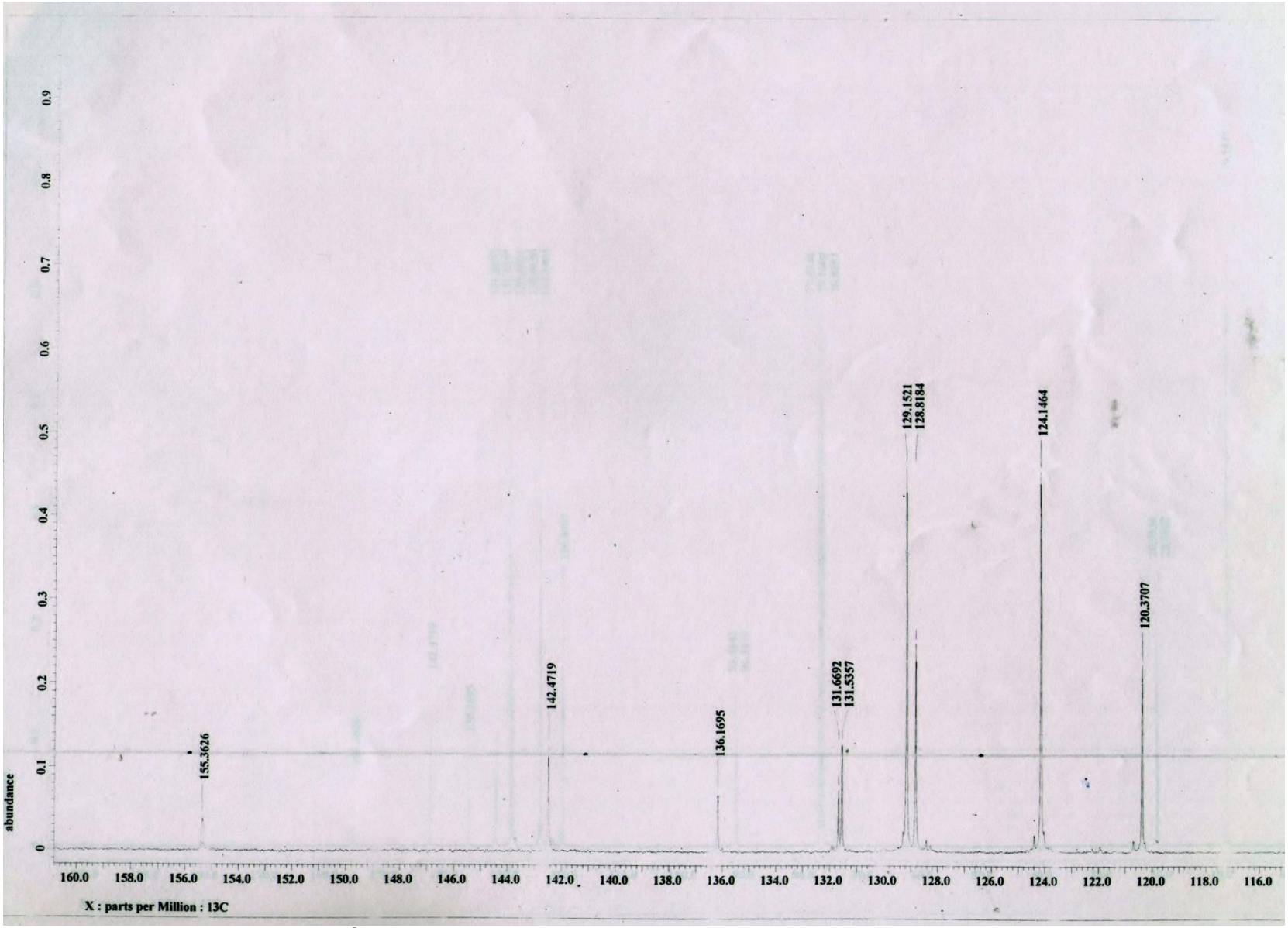

Fig. S31 ^{13}C NMR (100.5 MHz, $CDCl_3$) spectrum of **11** in the indicated region

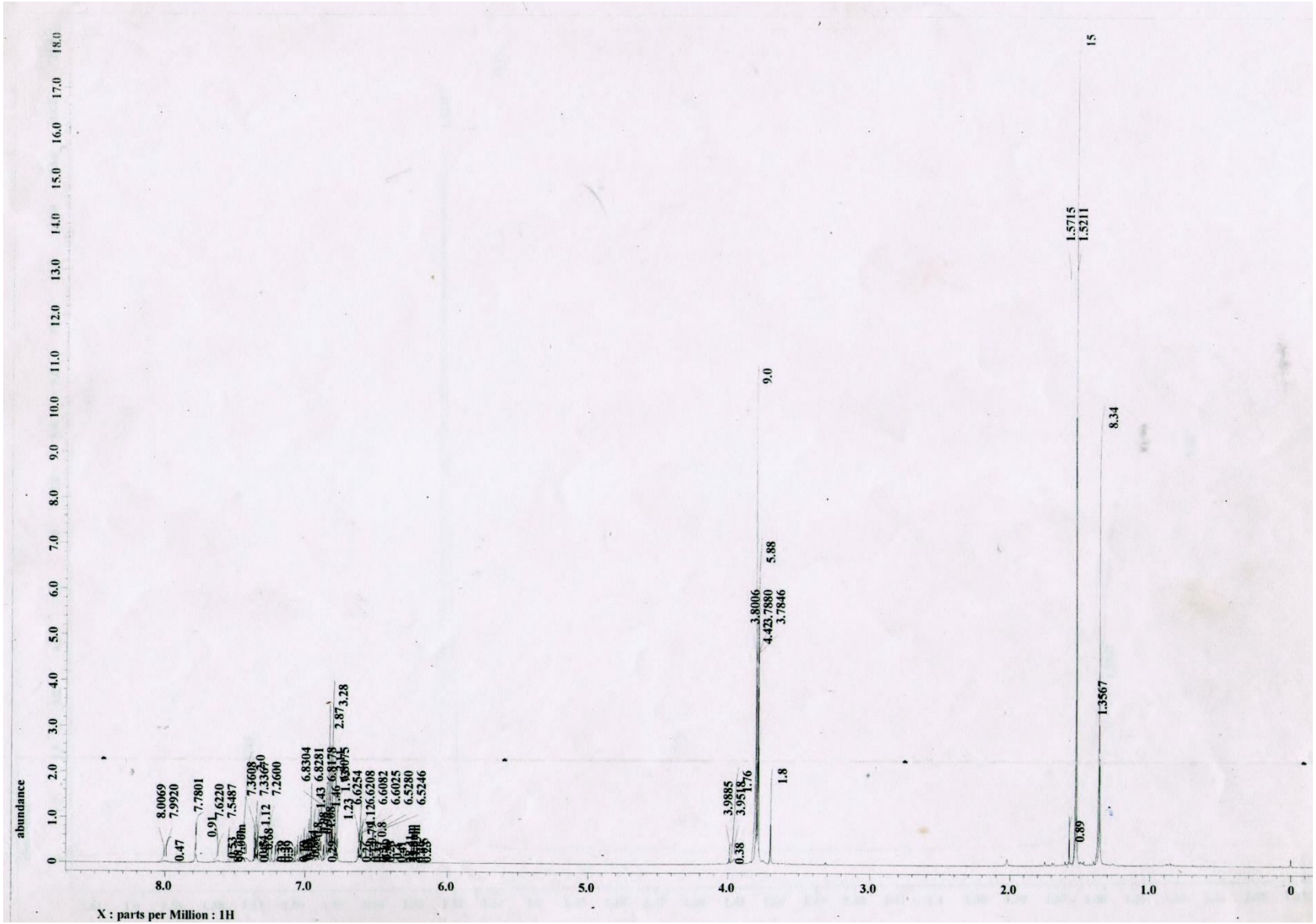

Fig. S32 ^{1}H NMR (400 MHz, $CDCl_3$) spectrum of **12**

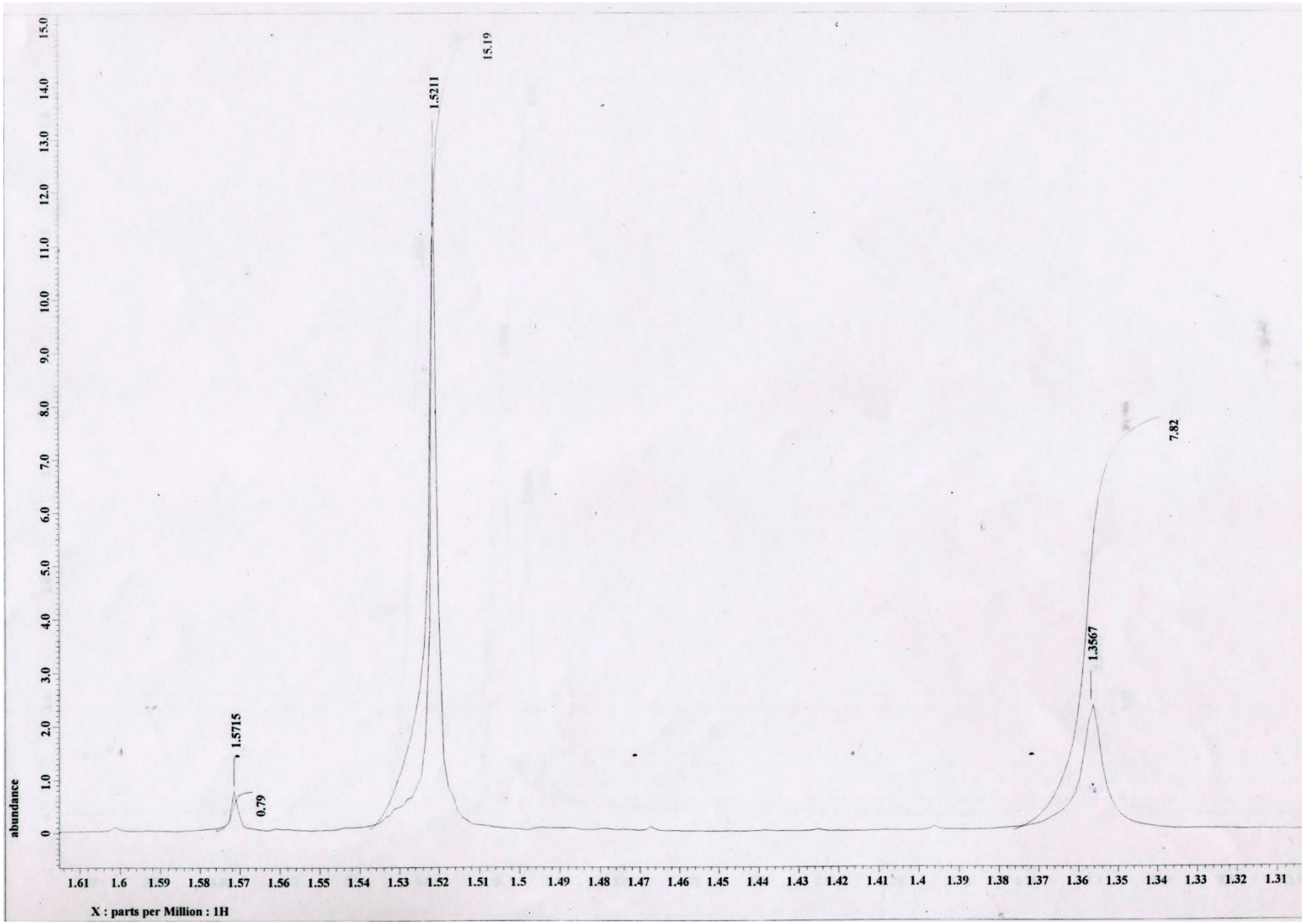

Fig. S33 ^{1}H NMR (400 MHz, $CDCl_3$) spectrum of **12** in the indicated region

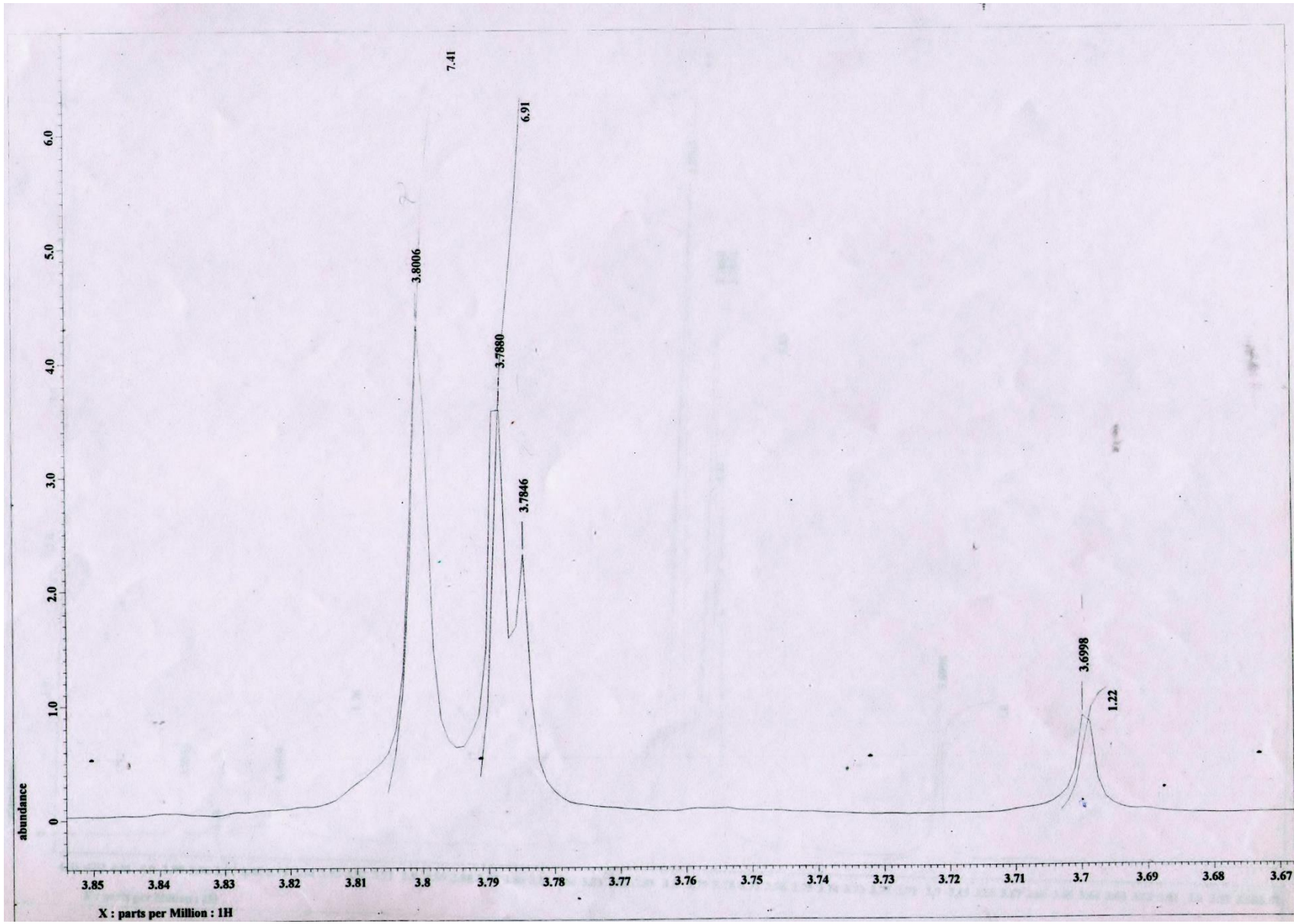

Fig. S34 ^{1}H NMR (400 MHz, $CDCl_3$) spectrum of **12** in the indicated region

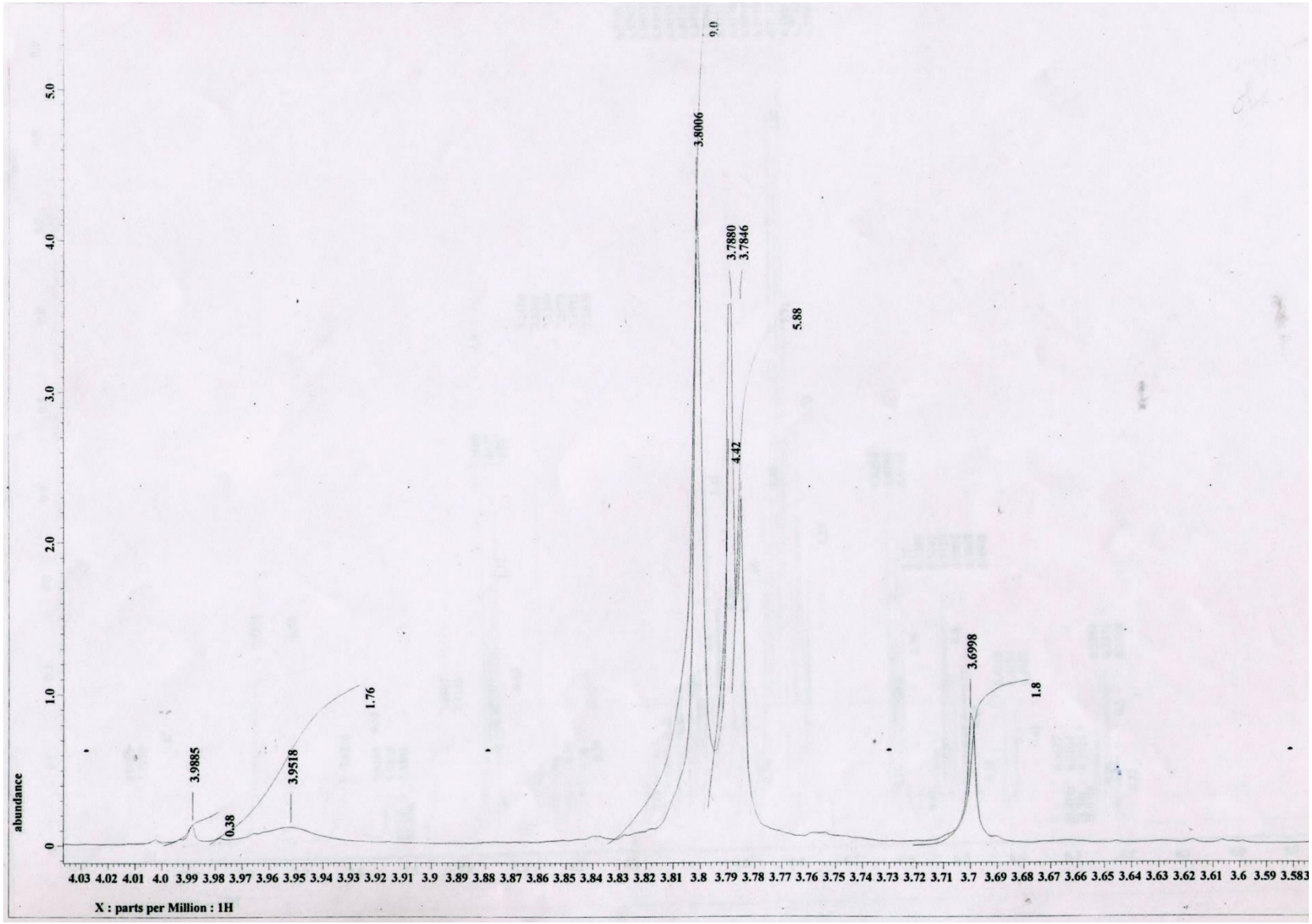

Fig. S35 ^{1}H NMR (400 MHz, $CDCl_3$) spectrum of **12** in the indicated region

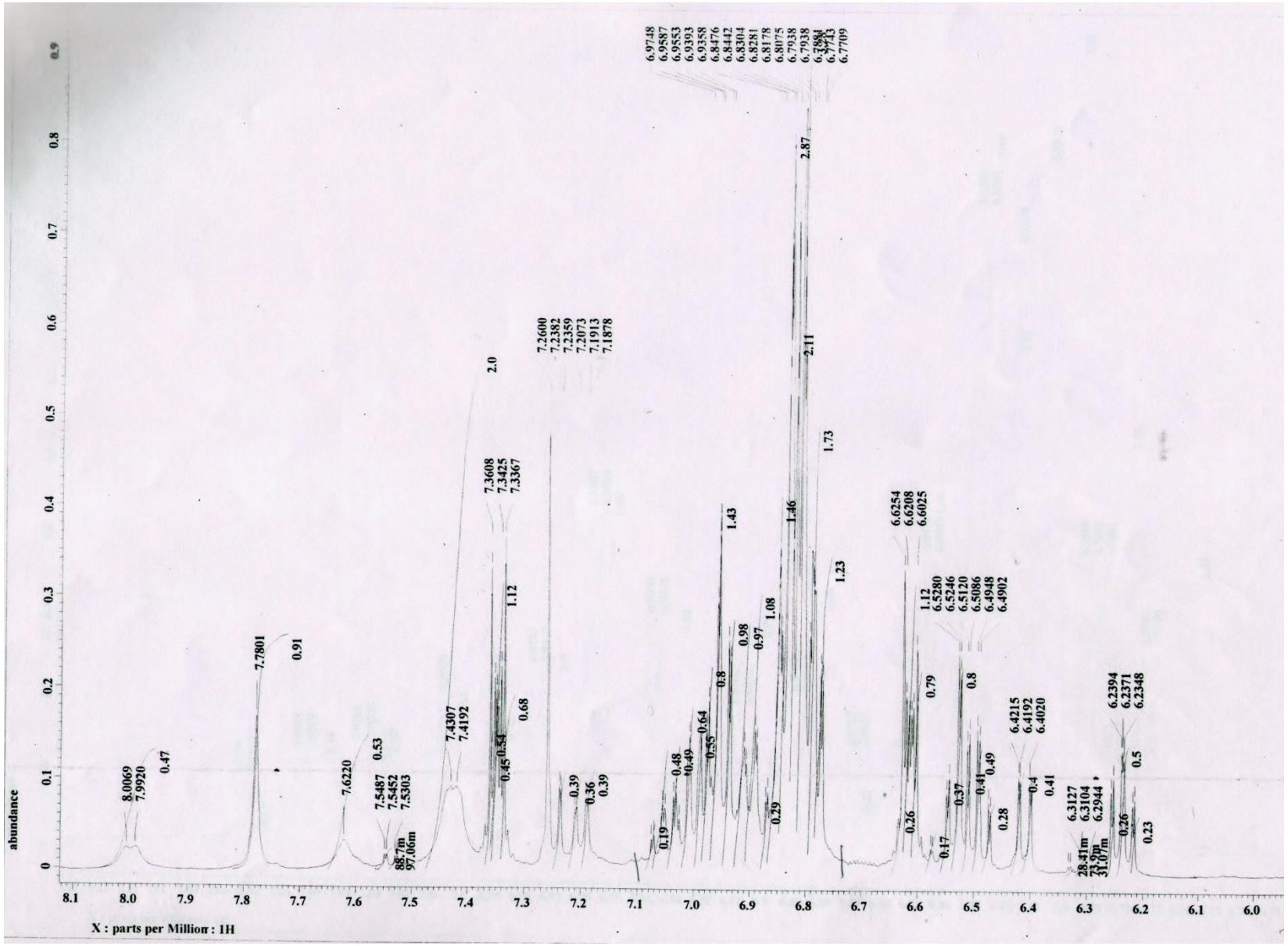

Fig. S36 ^{1}H NMR (400 MHz, $CDCl_3$) spectrum of **12** in the indicated region

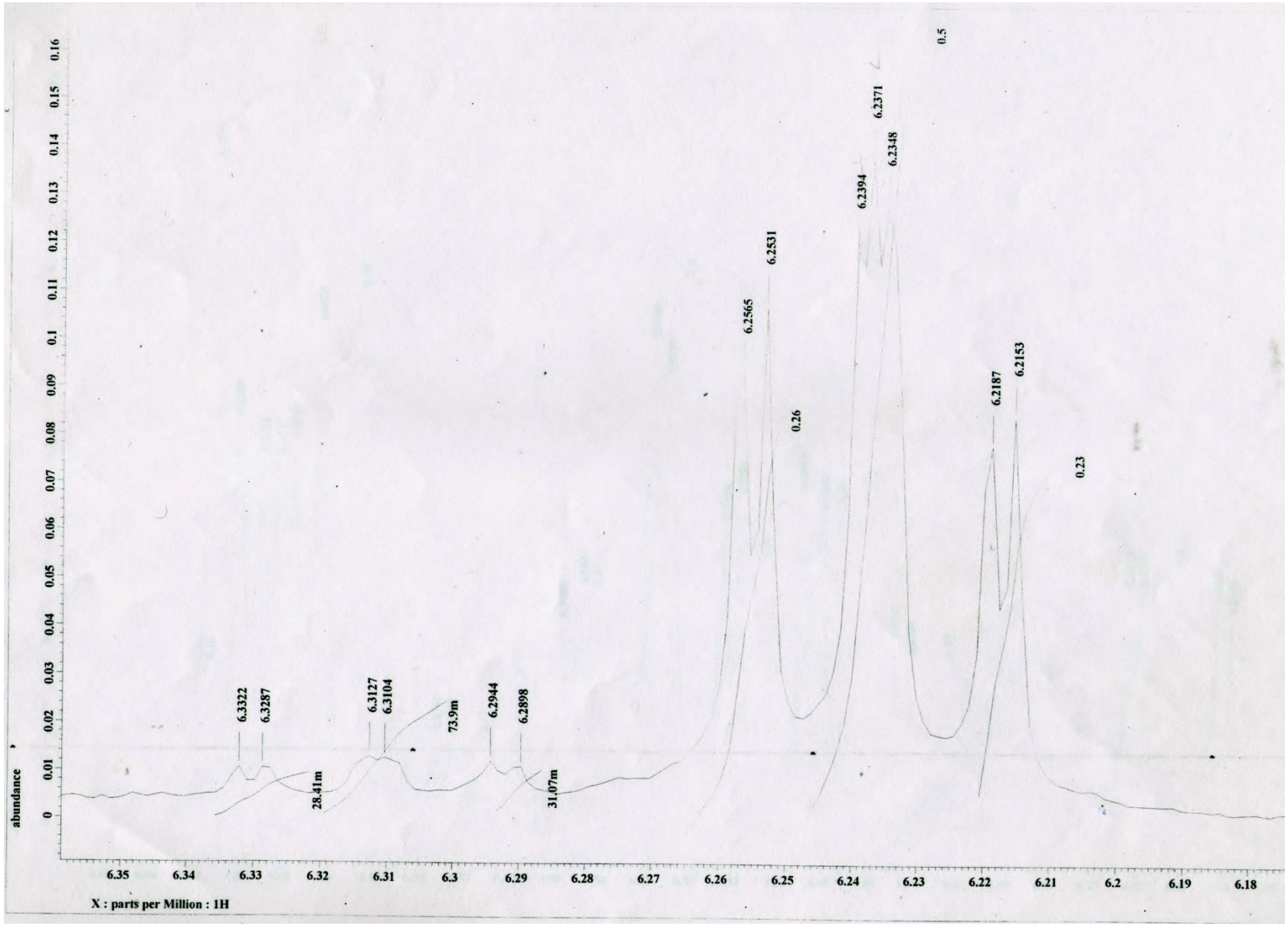

Fig. S37 ^{1}H NMR (400 MHz, $CDCl_3$) spectrum of **12** in the indicated region

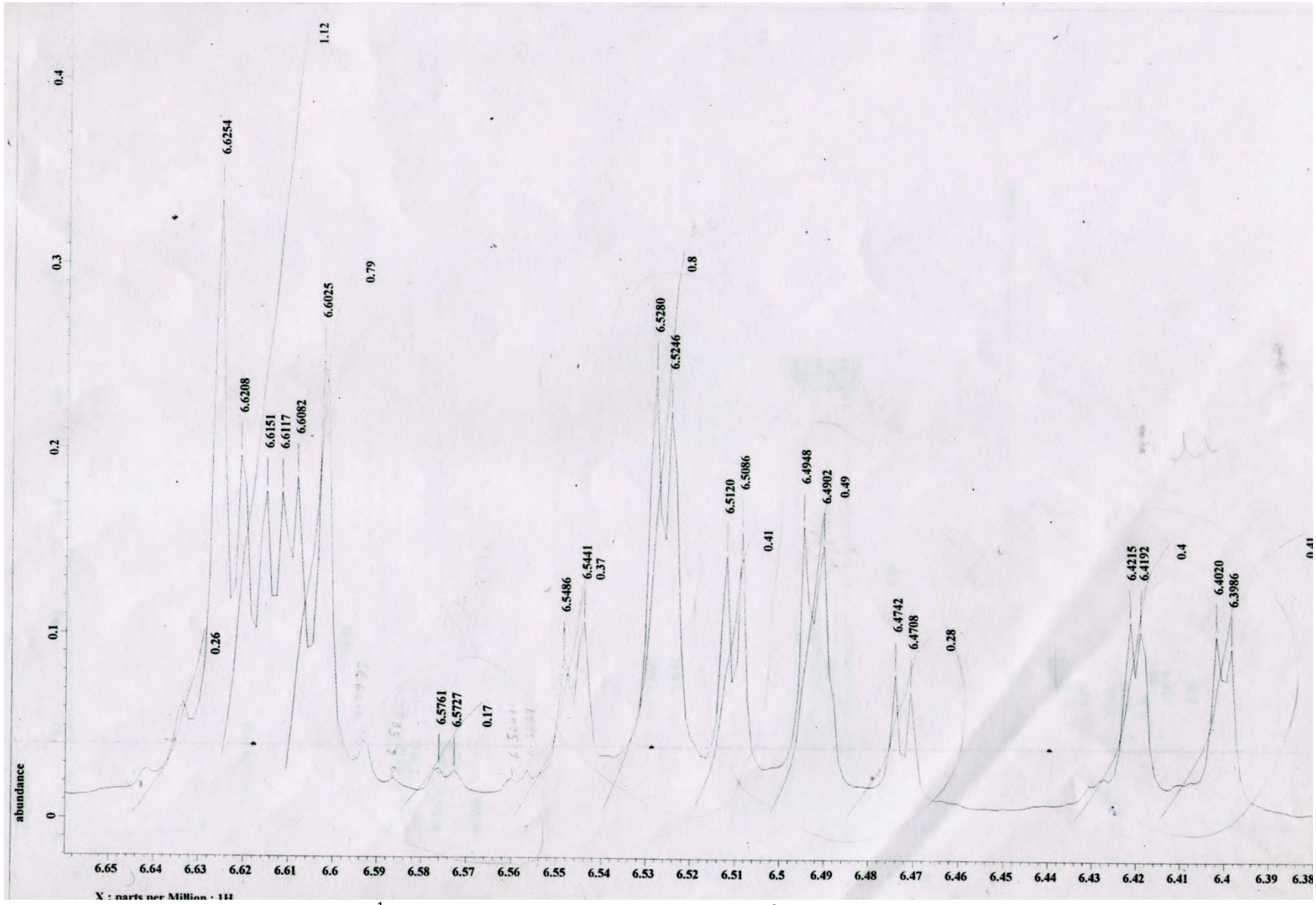

Fig. S38 ^{1}H NMR (400 MHz, $CDCl_3$) spectrum of **12** in the indicated region

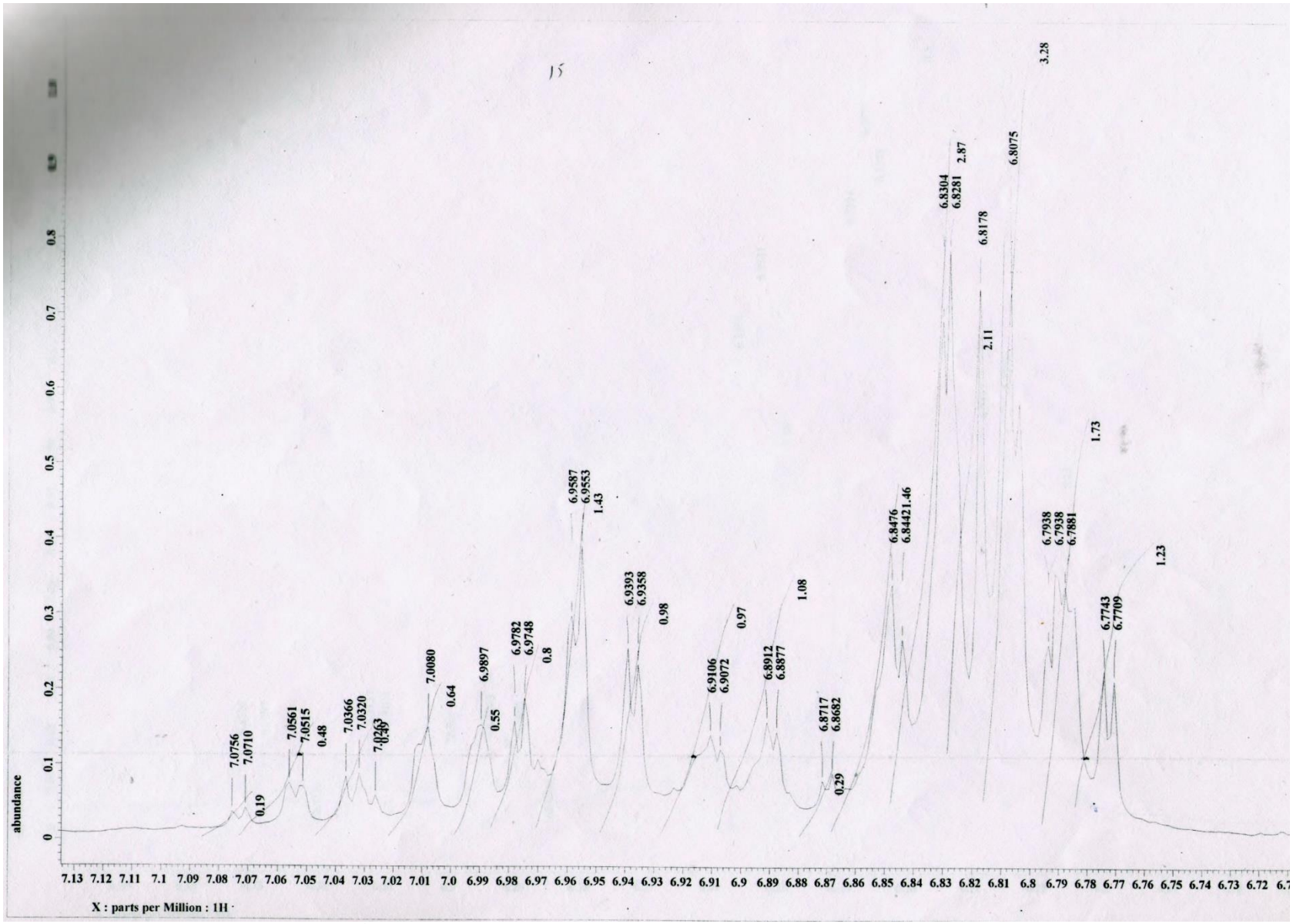

Fig. S39 ^{1}H NMR (400 MHz, $CDCl_3$) spectrum of **12** in the indicated region

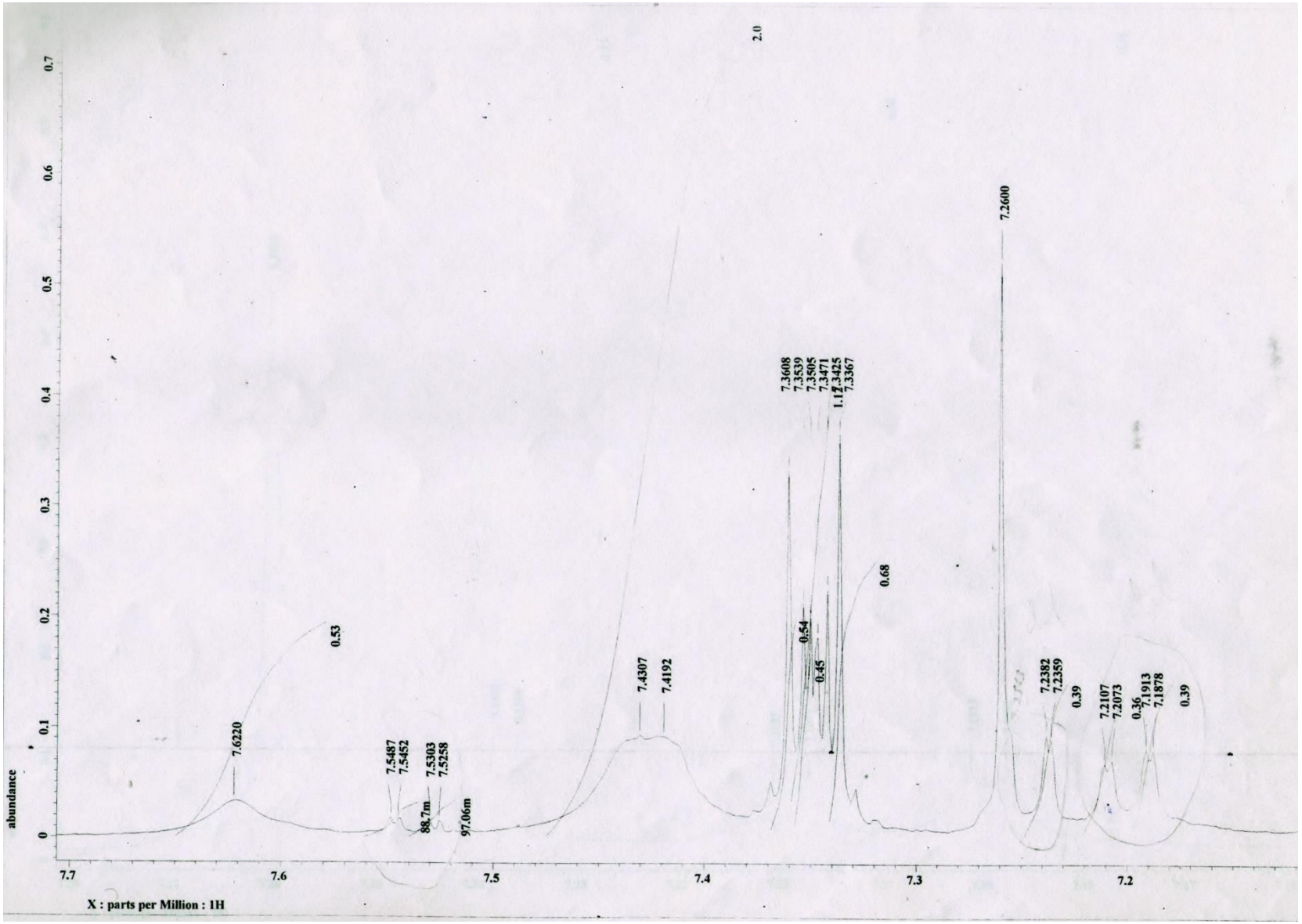

Fig. S40 ^{1}H NMR (400 MHz, $CDCl_3$) spectrum of **12** in the indicated region

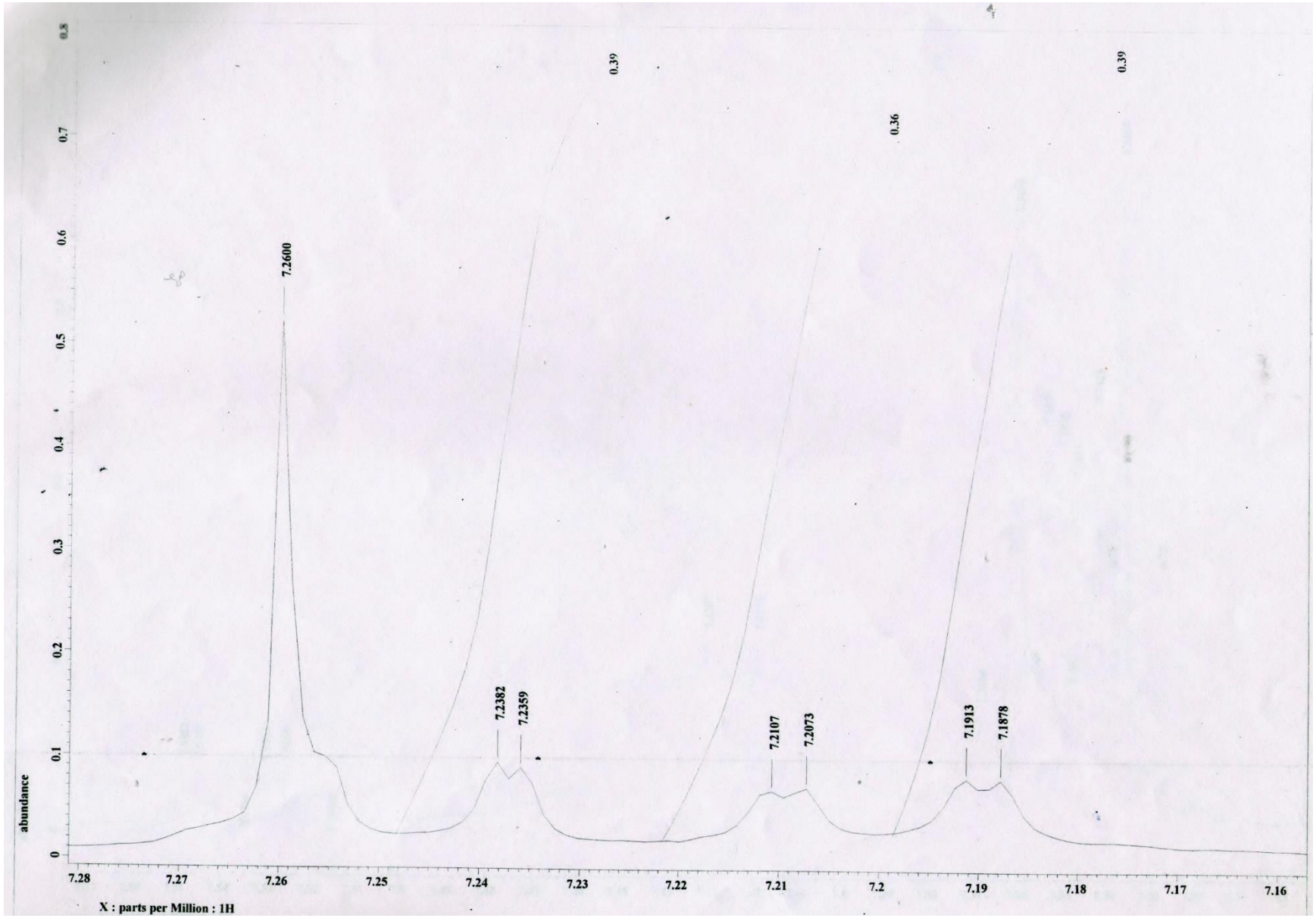

Fig. S41 ^{1}H NMR (400 MHz, $CDCl_3$) spectrum of **12** in the indicated region

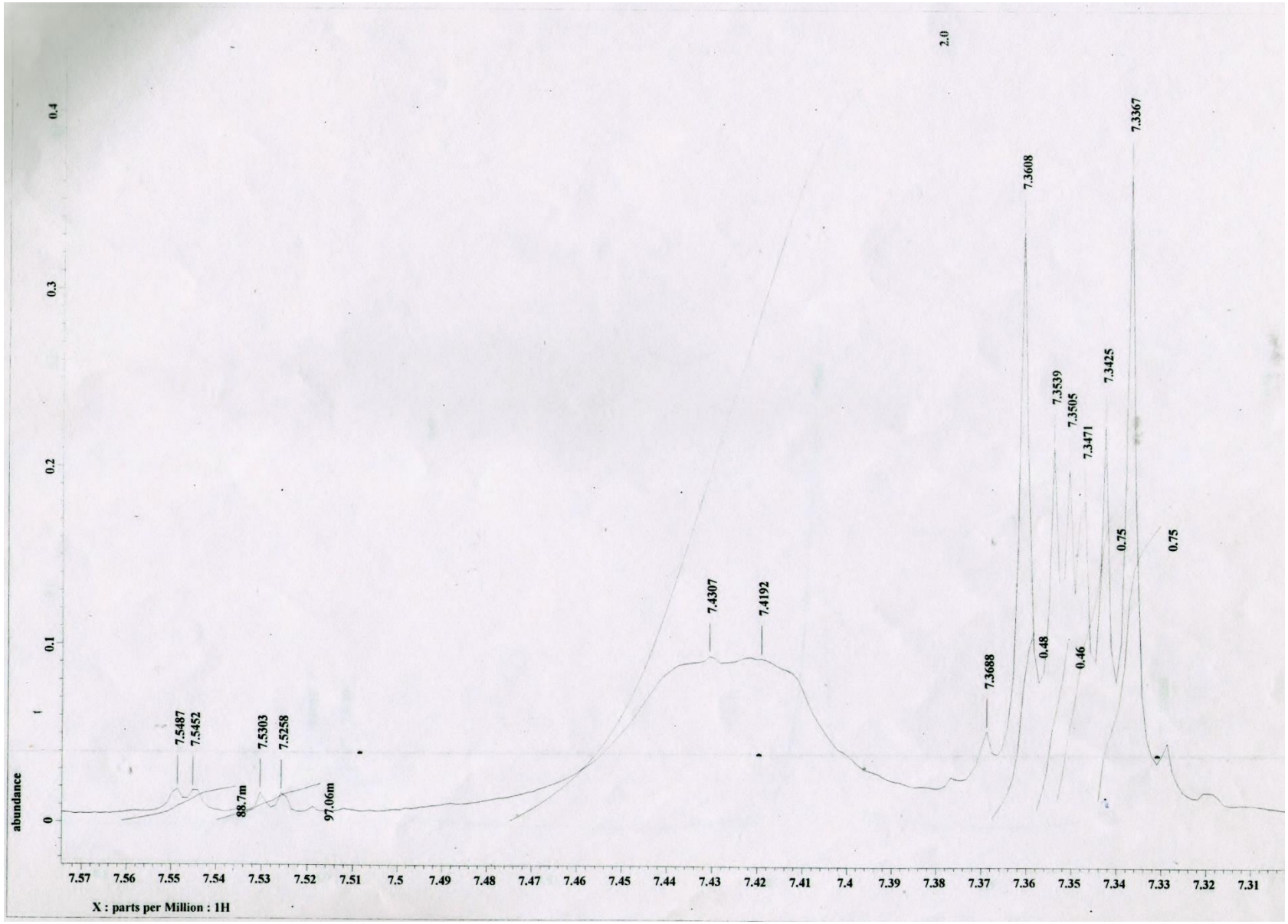

Fig. S42 ^{1}H NMR (400 MHz, $CDCl_3$) spectrum of **12** in the indicated region

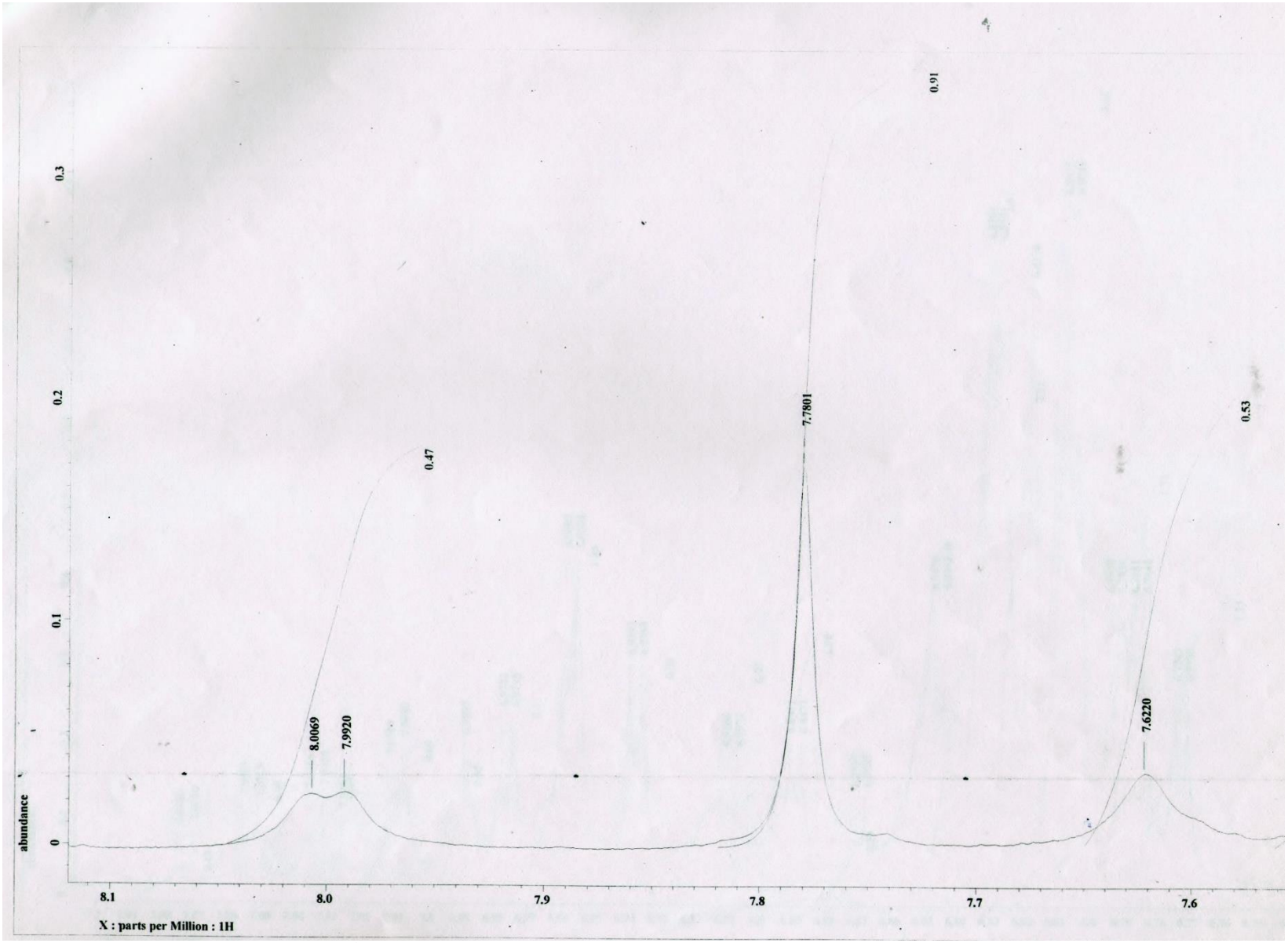

Fig. S43 ^{1}H NMR (400 MHz, $CDCl_3$) spectrum of **12** in the indicated region

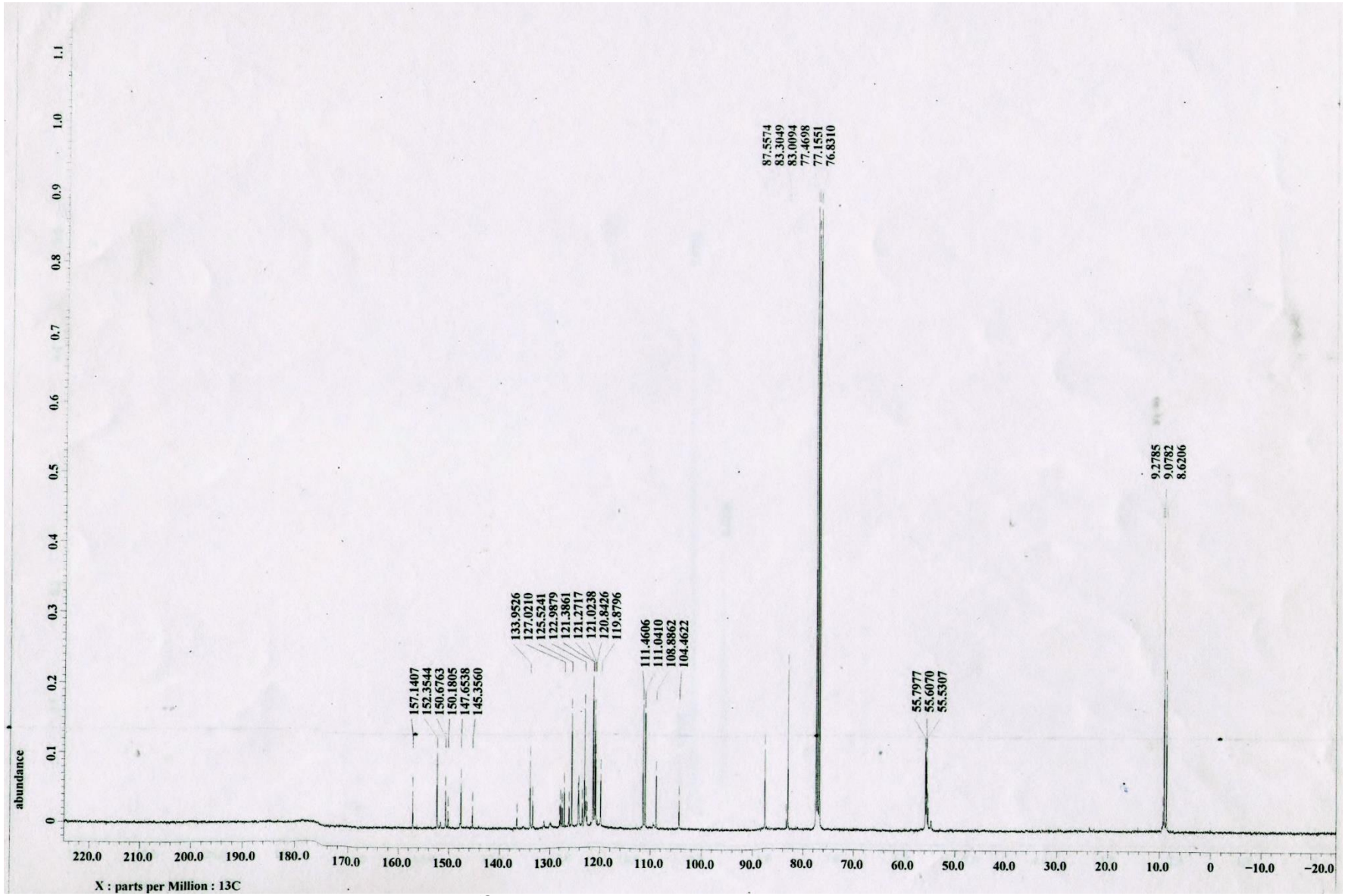

Fig. S44 ^{13}C NMR (100.5 MHz, $CDCl_3$) spectrum of **12**

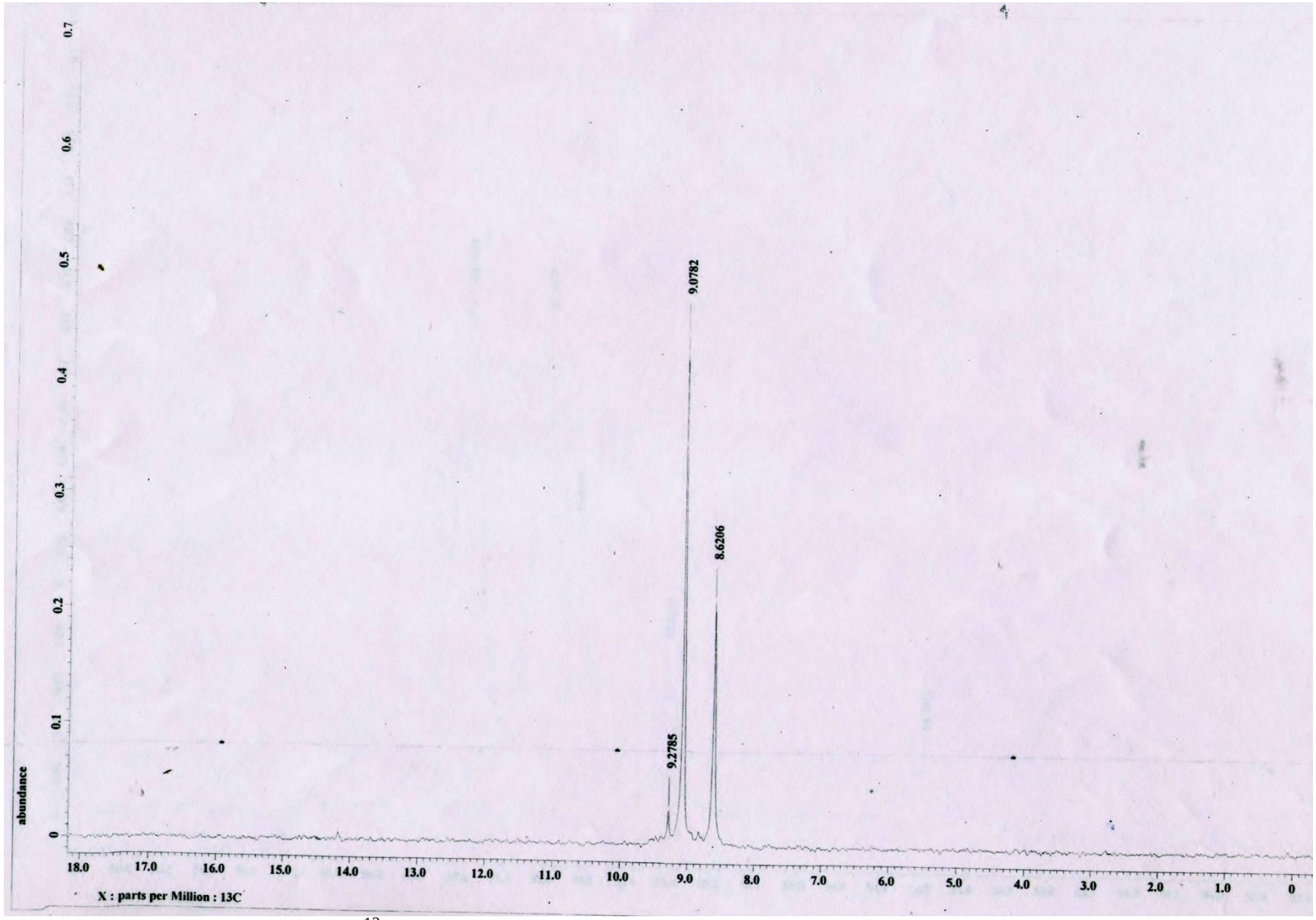

Fig. S45 ^{13}C NMR (100.5 MHz, $CDCl_3$) spectrum of **12** in the indicated region

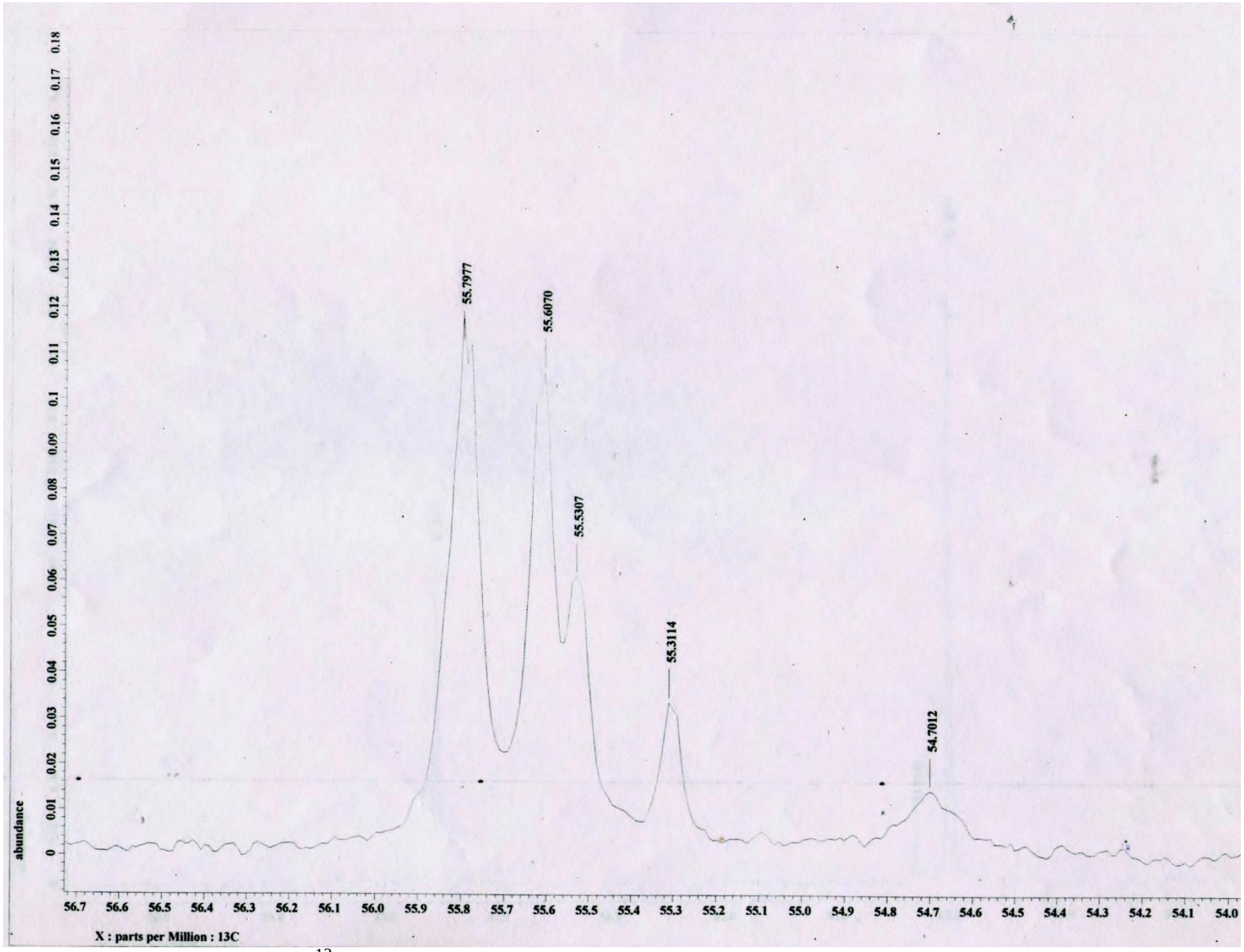

Fig. S46 ^{13}C NMR (100.5 MHz, $CDCl_3$) spectrum of **12** in the indicated region

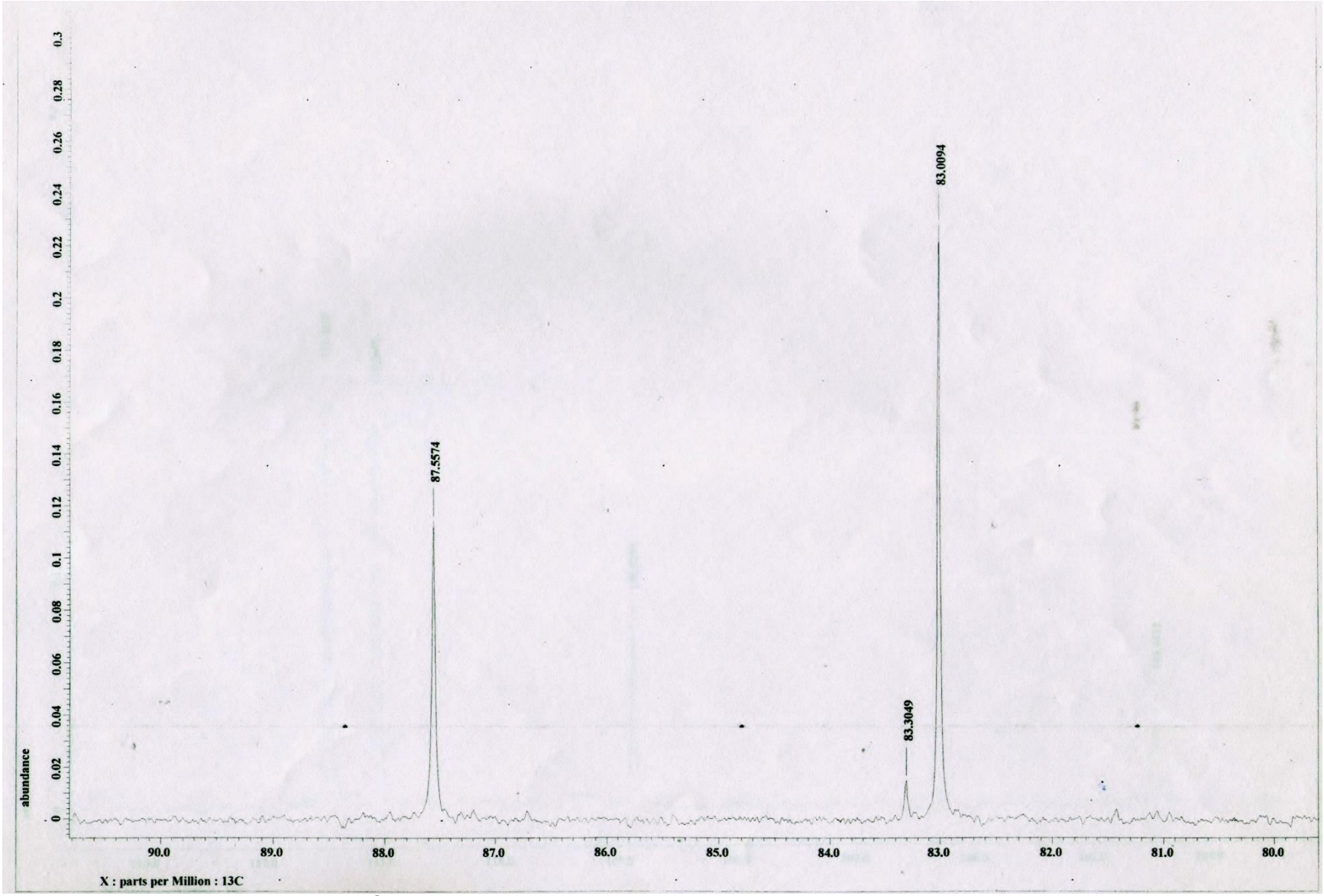

Fig. S47 ^{13}C NMR (100.5 MHz, $CDCl_3$) spectrum of **12** in the indicated region

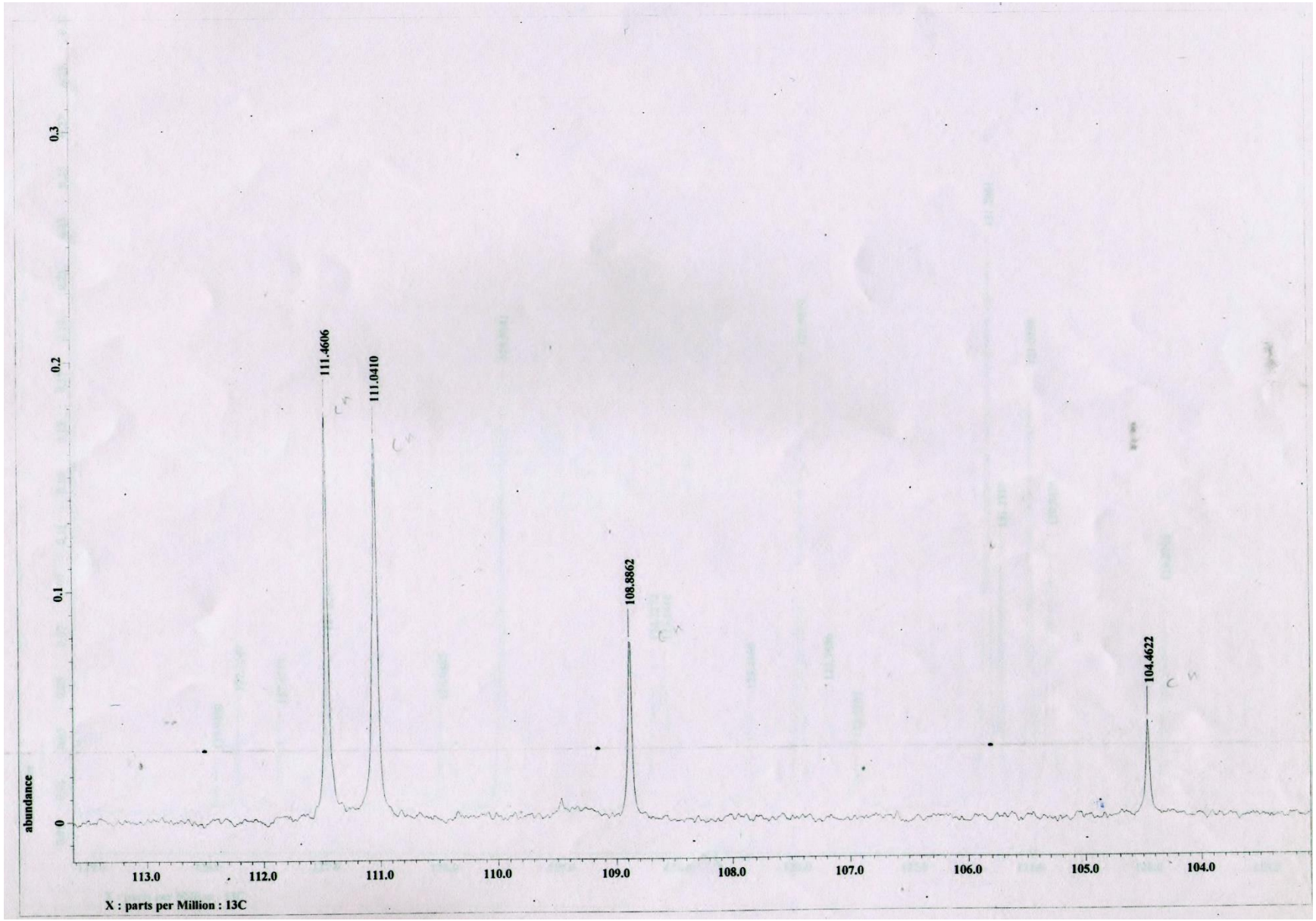

Fig. S48 ^{13}C NMR (100.5 MHz, $CDCl_3$) spectrum of **12** in the indicated region

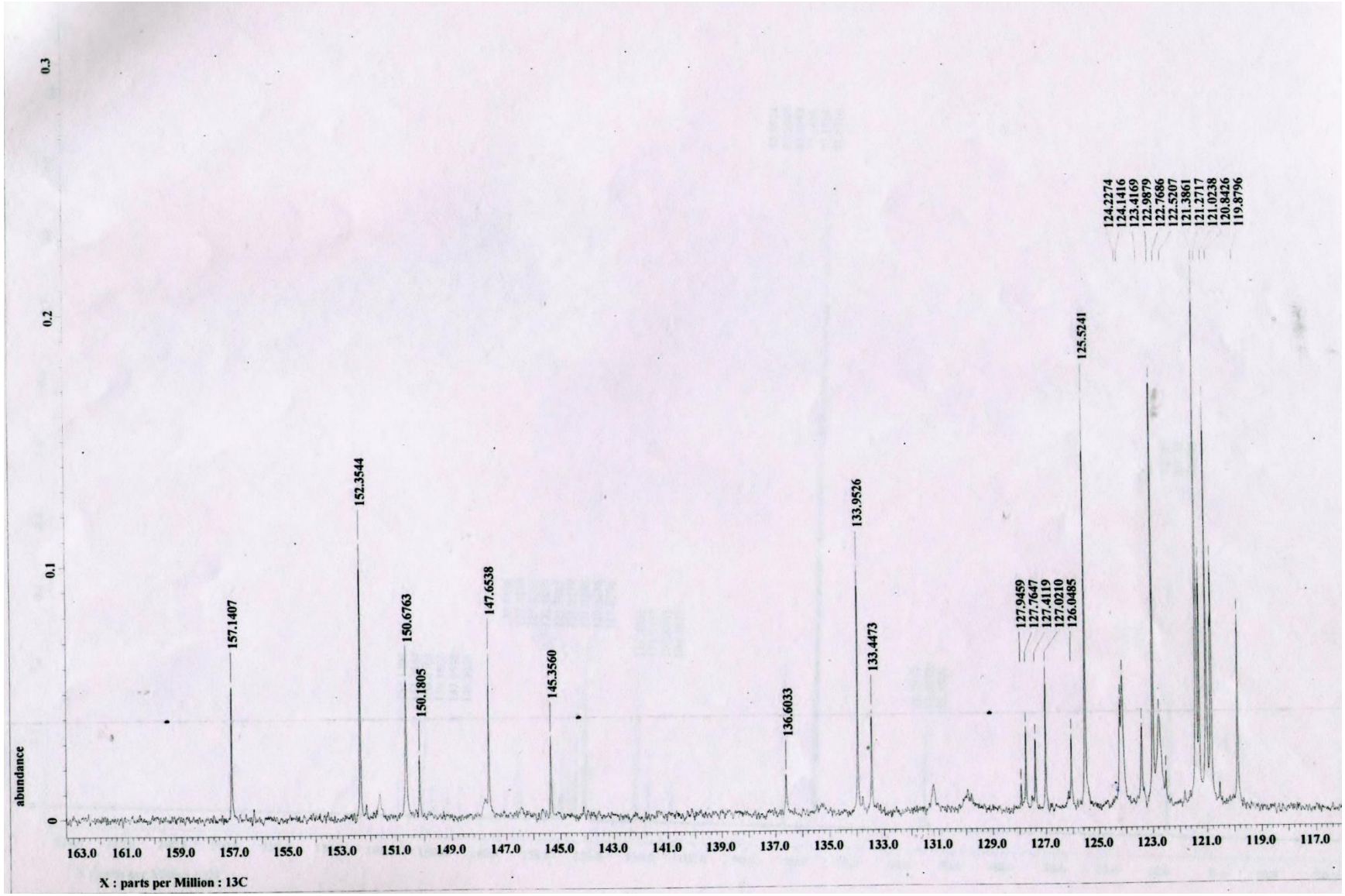

Fig. S49 ^{13}C NMR (100.5 MHz, $CDCl_3$) spectrum of **12** in the indicated region

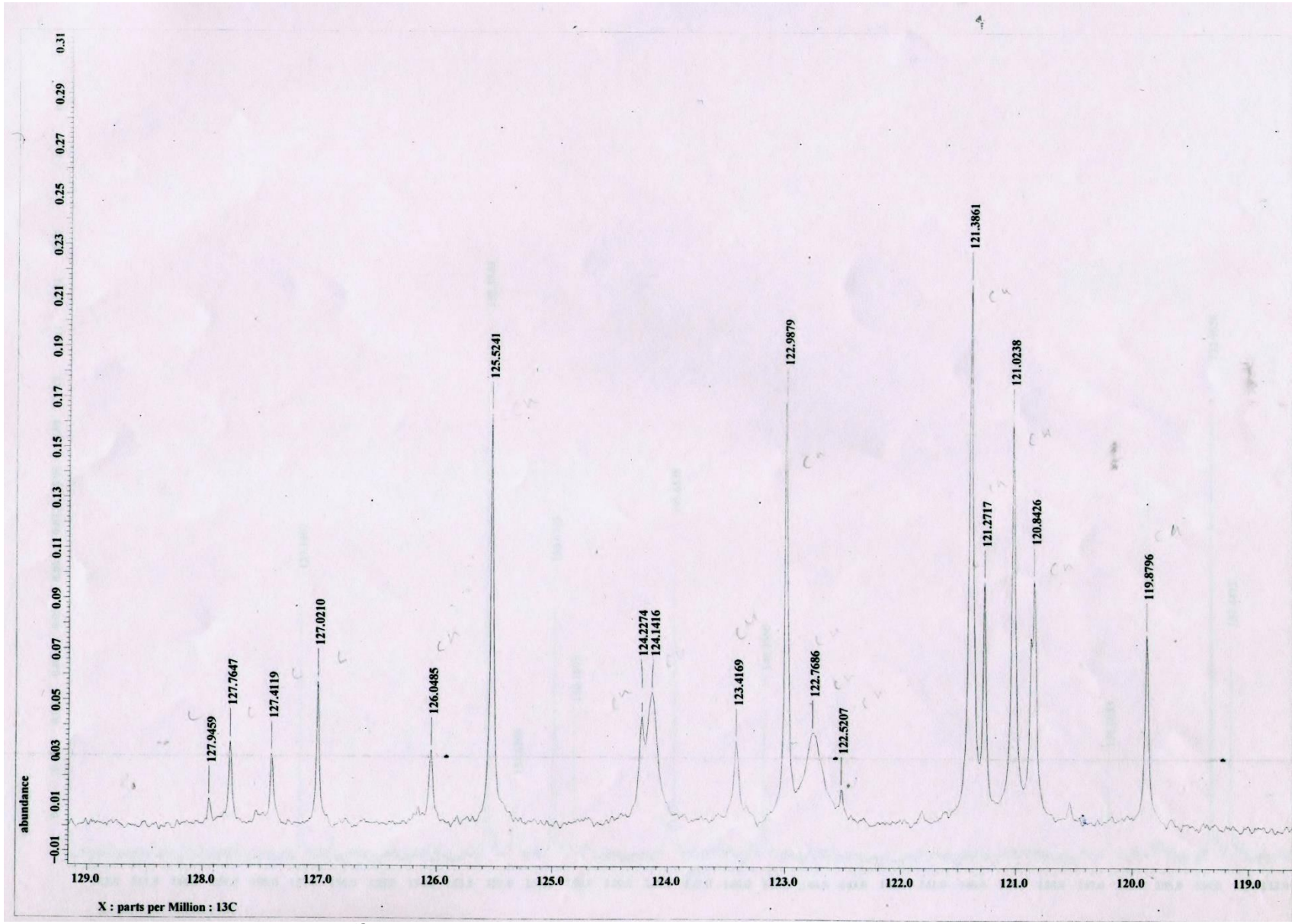

Fig. S50 ^{13}C NMR (100.5 MHz, $CDCl_3$) spectrum of **12** in the indicated region

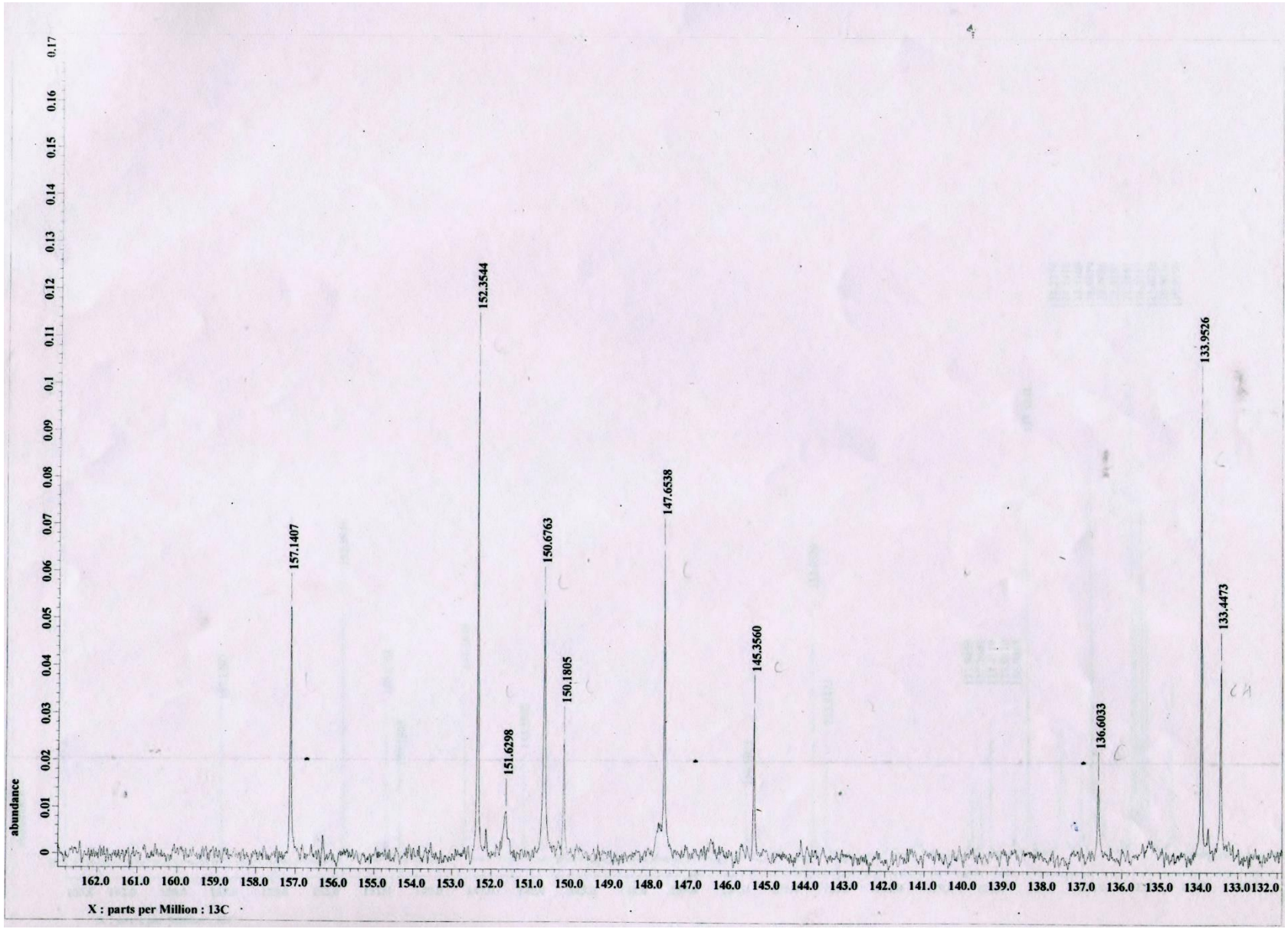

Fig. S51 ^{13}C NMR (100.5 MHz, $CDCl_3$) spectrum of **12** in the indicated region

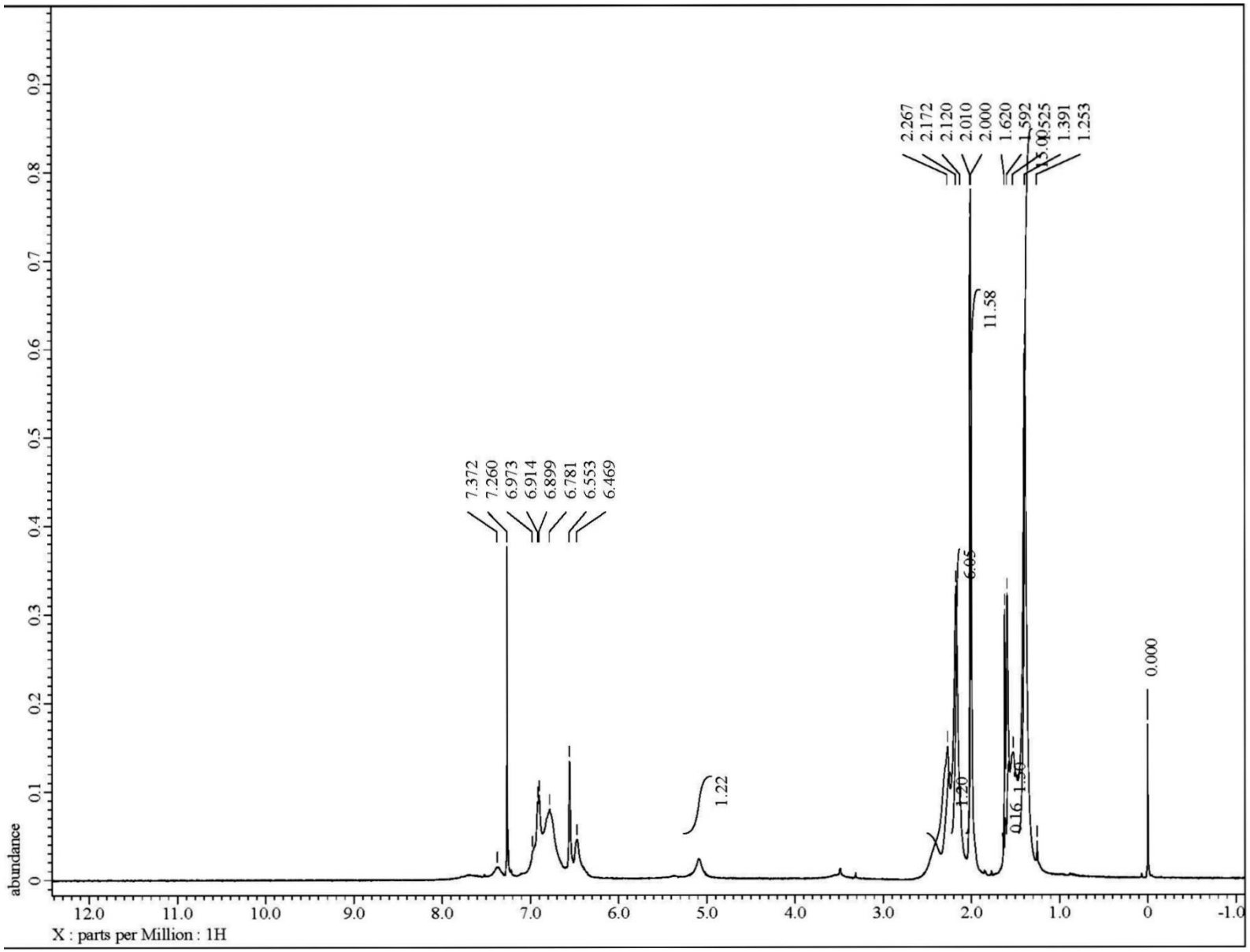

Fig. S52 ^{1}H NMR (400 MHz, $CDCl_3$) spectrum of **13** in the indicated region

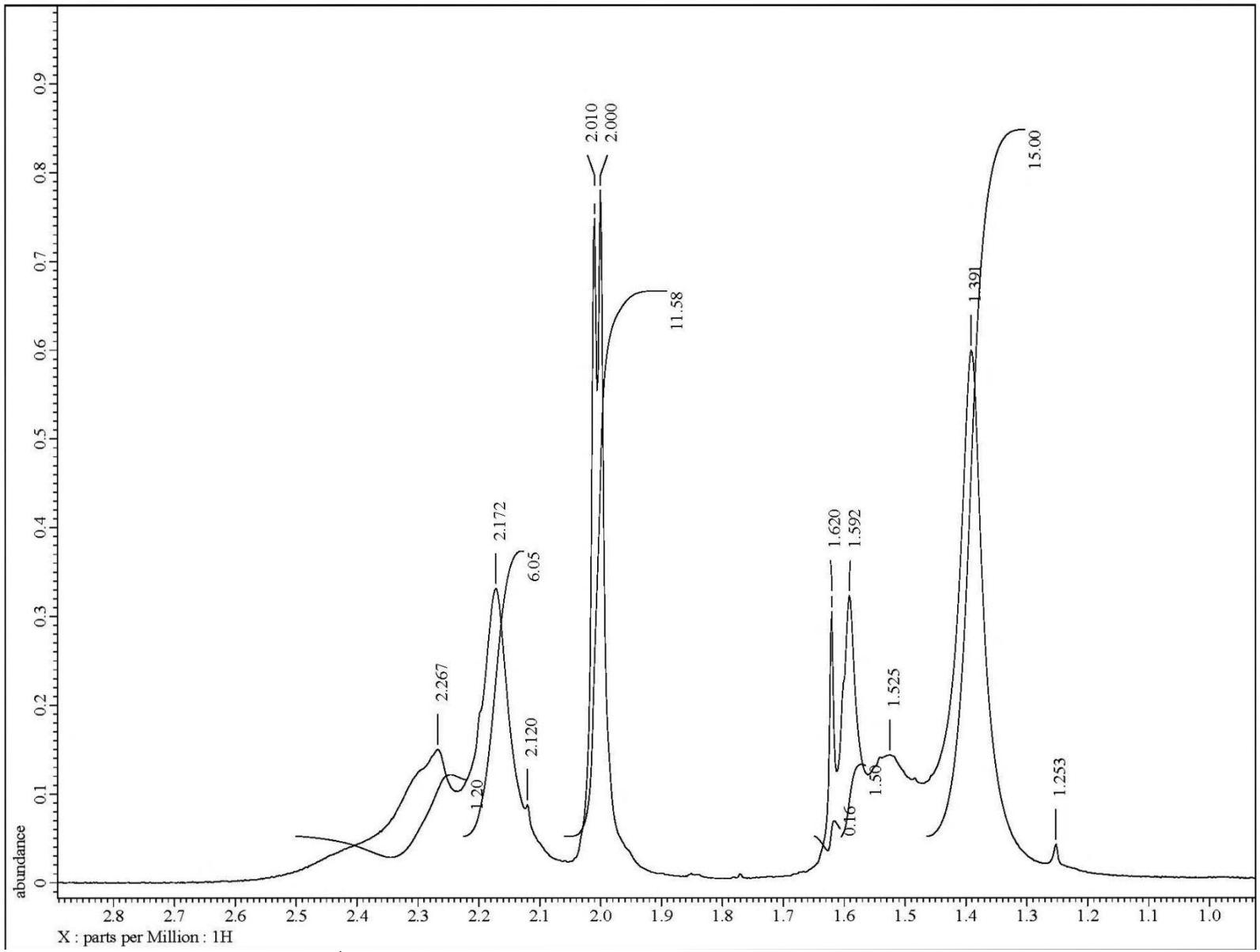

Fig. S53 ^{1}H NMR (400 MHz, $CDCl_3$) spectrum of **13** in the indicated region

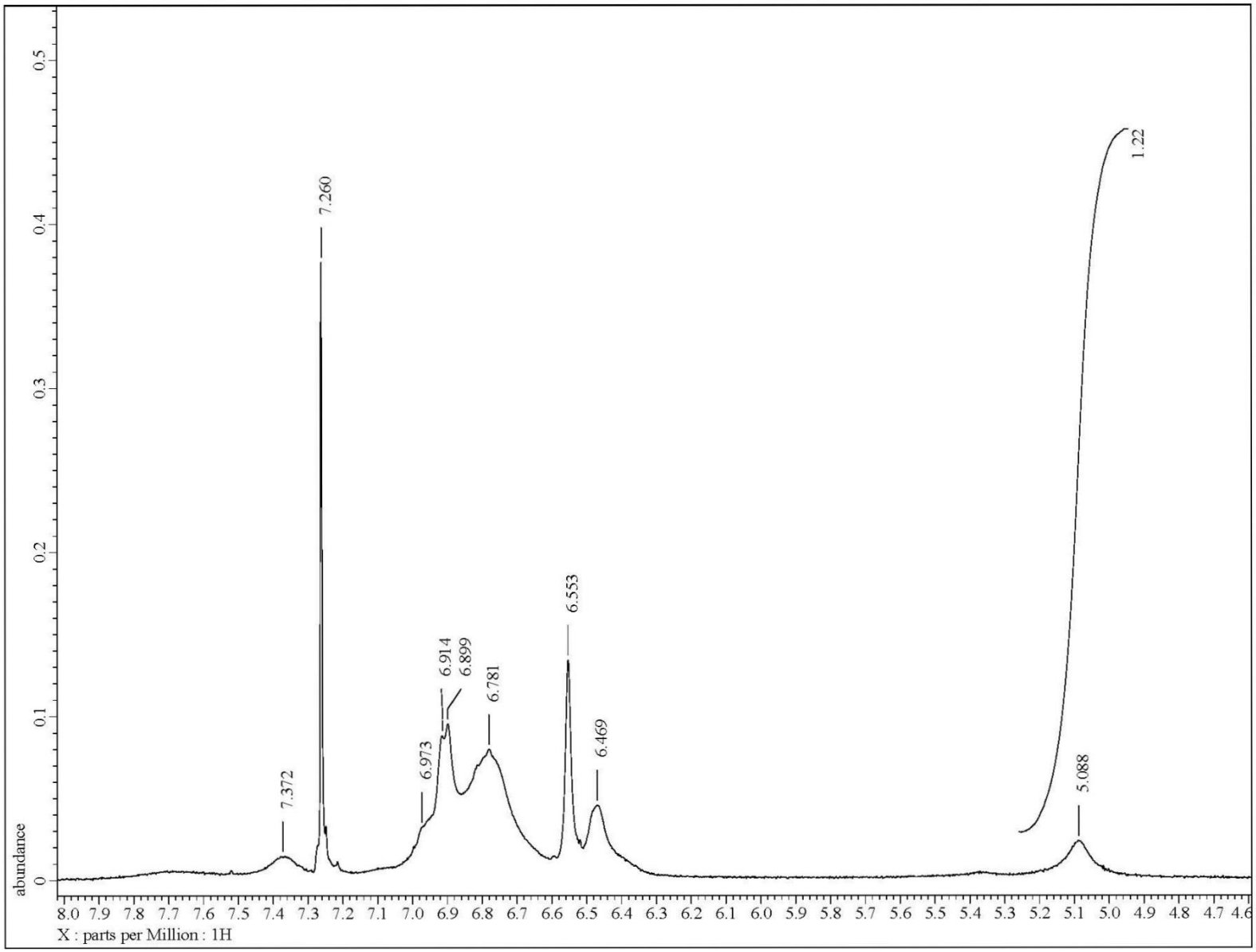

Fig. S54 ^{1}H NMR (400 MHz, $CDCl_3$) spectrum of **13** in the indicated region

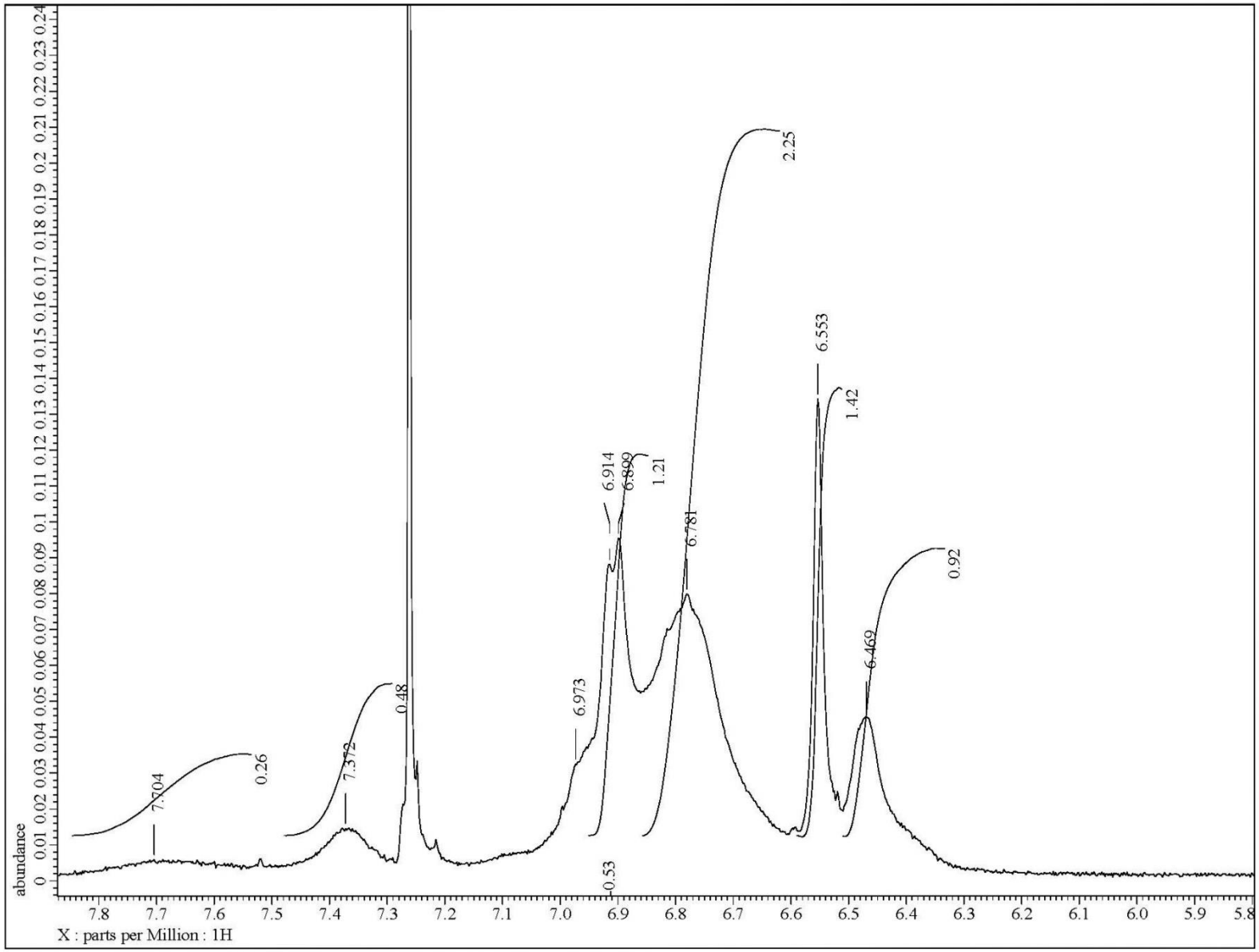

Fig. S55 ^{1}H NMR (400 MHz, $CDCl_3$) spectrum of **13** in the indicated region

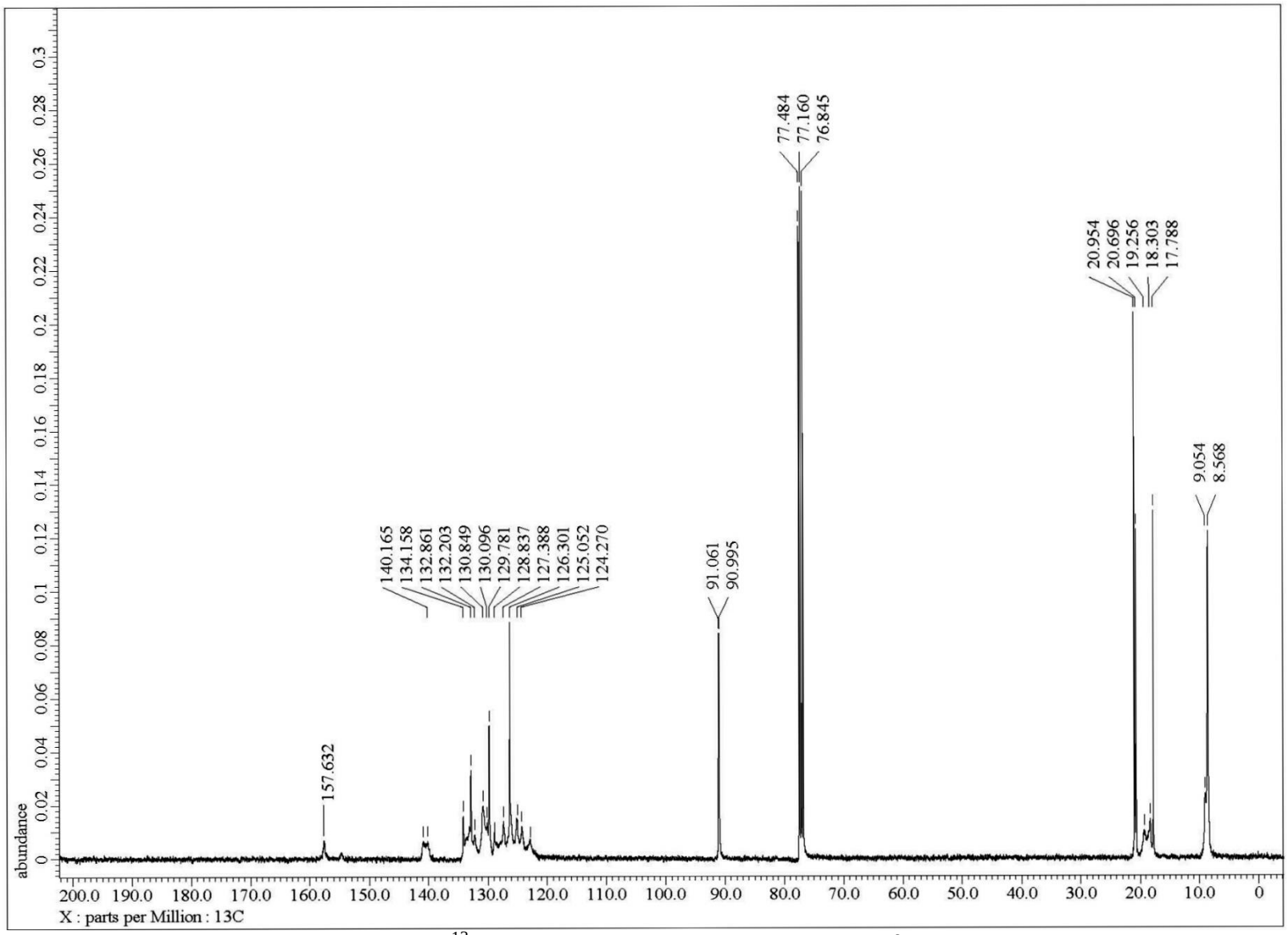

Fig. S56 ^{13}C NMR (100.5 MHz, $CDCl_3$) spectrum of **13**

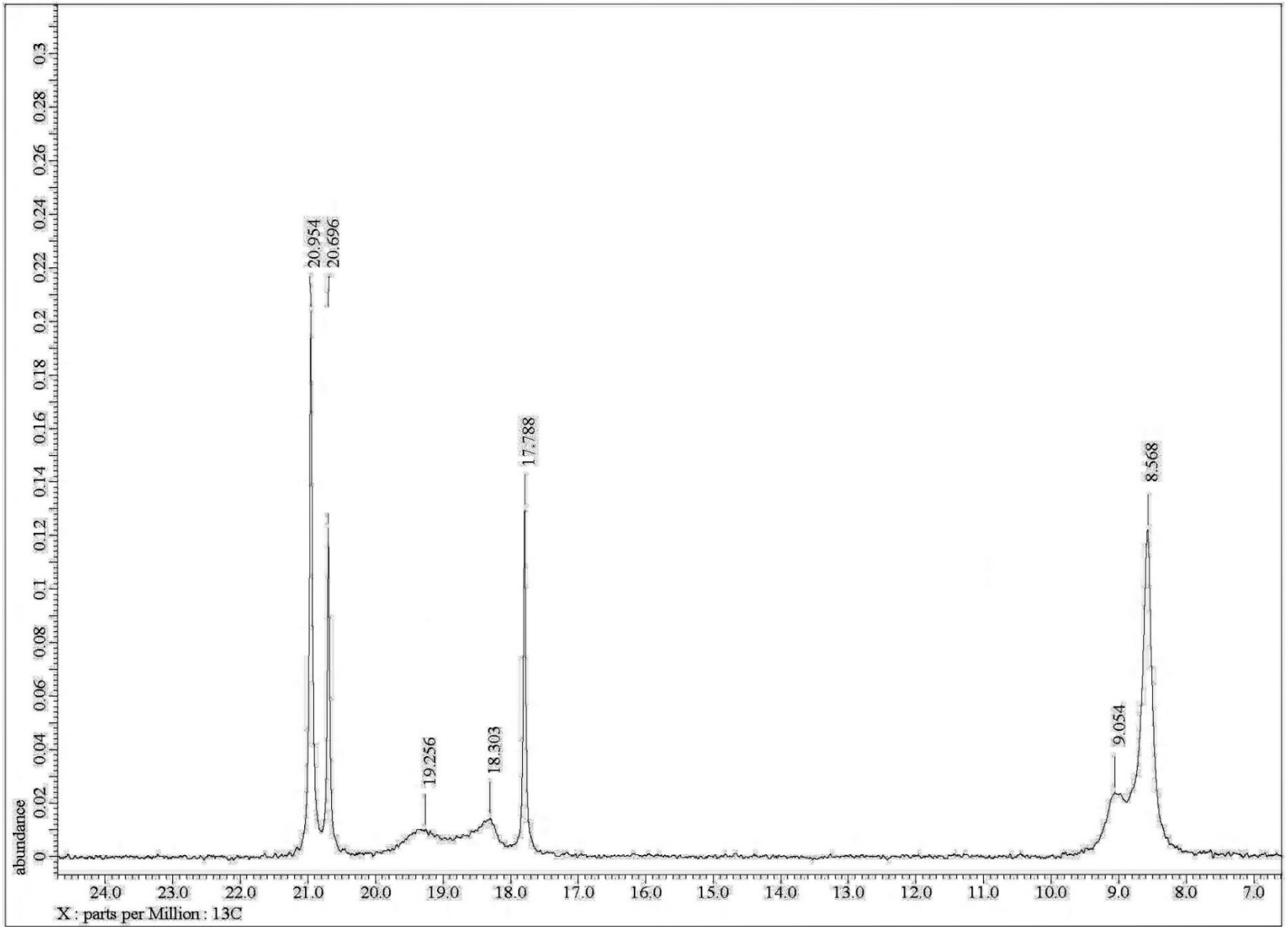

Fig. S57 ^{13}C NMR (100.5 MHz, $CDCl_3$) spectrum of **13** in the indicated region

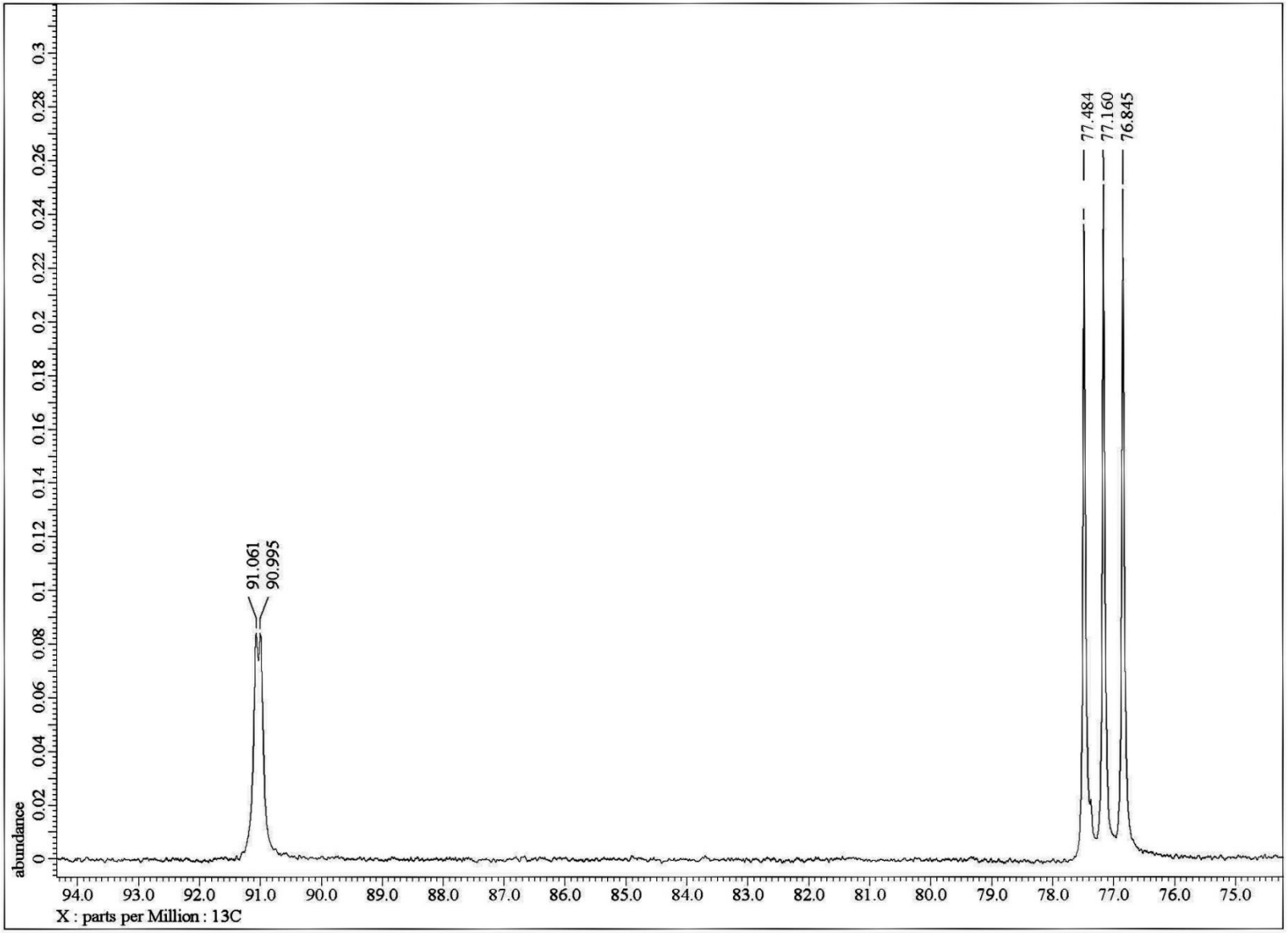

Fig. S58 ^{13}C NMR (100.5 MHz, $CDCl_3$) spectrum of **13** in the indicated region

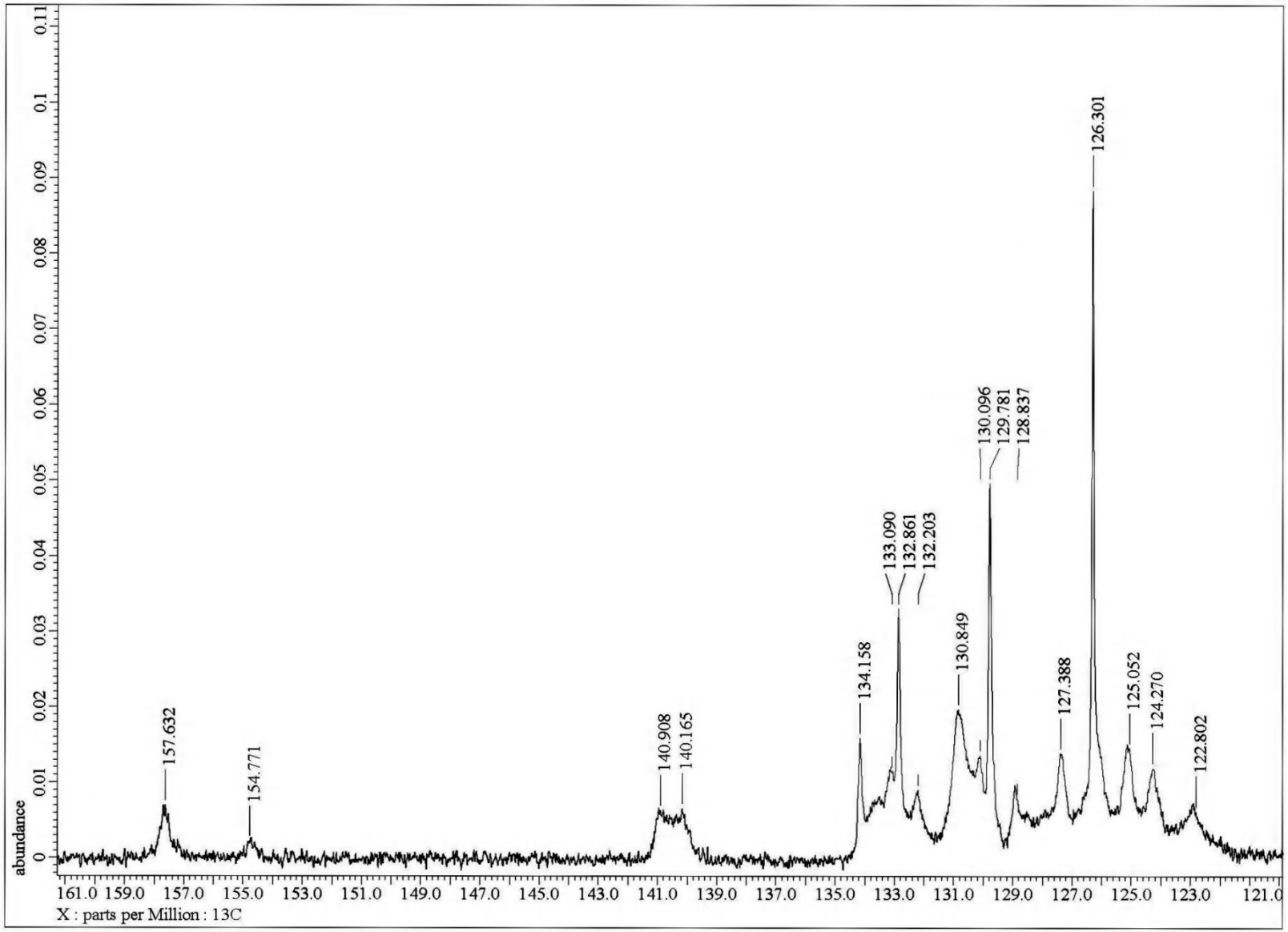

Fig. S59 ^{13}C NMR (100.5 MHz, $CDCl_3$) spectrum of **13** in the indicated region

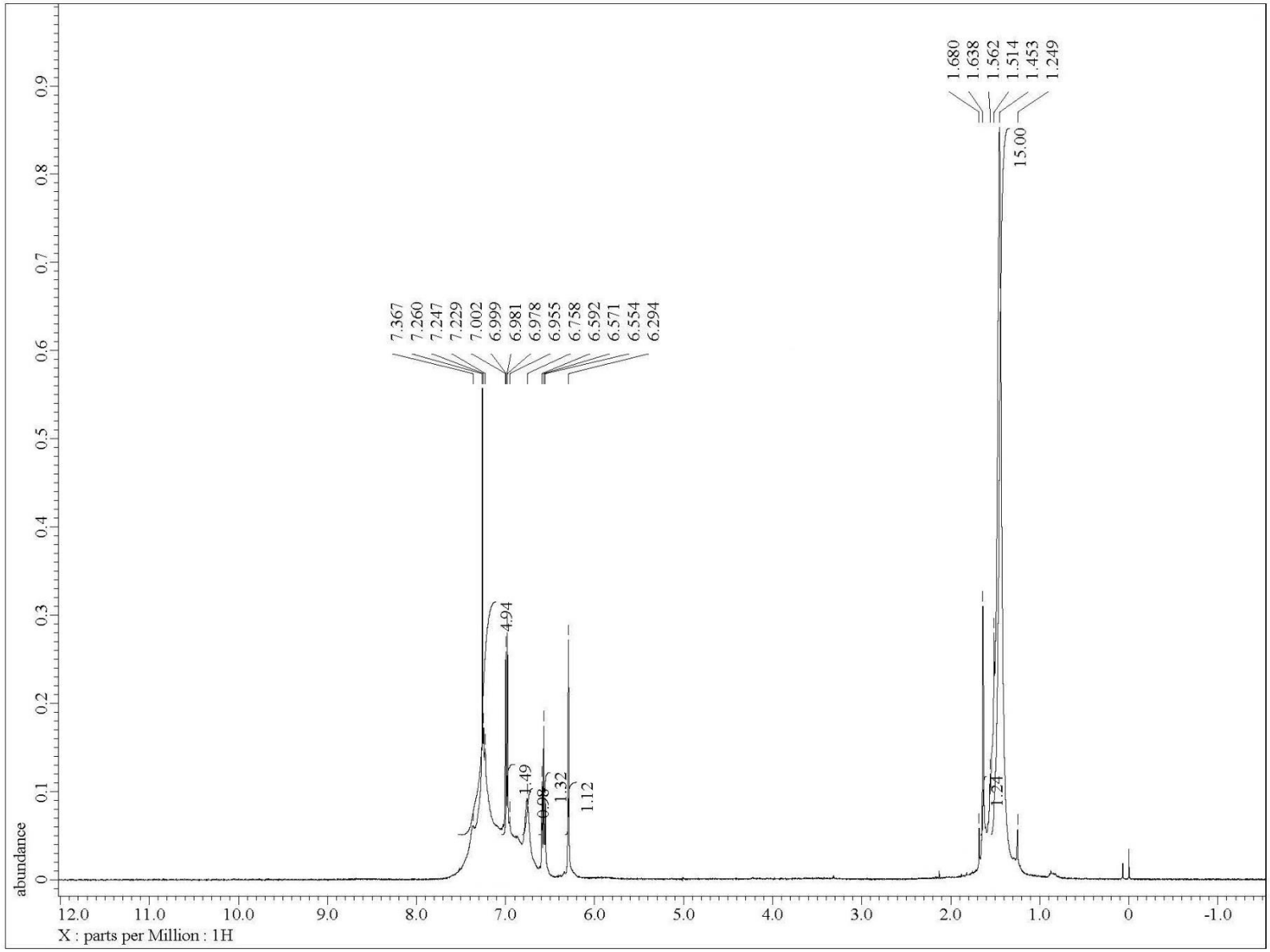

Fig. S60 ^{1}H NMR (400 MHz, $CDCl_3$) spectrum of **14** at 1.49×10^{-2} M concentration

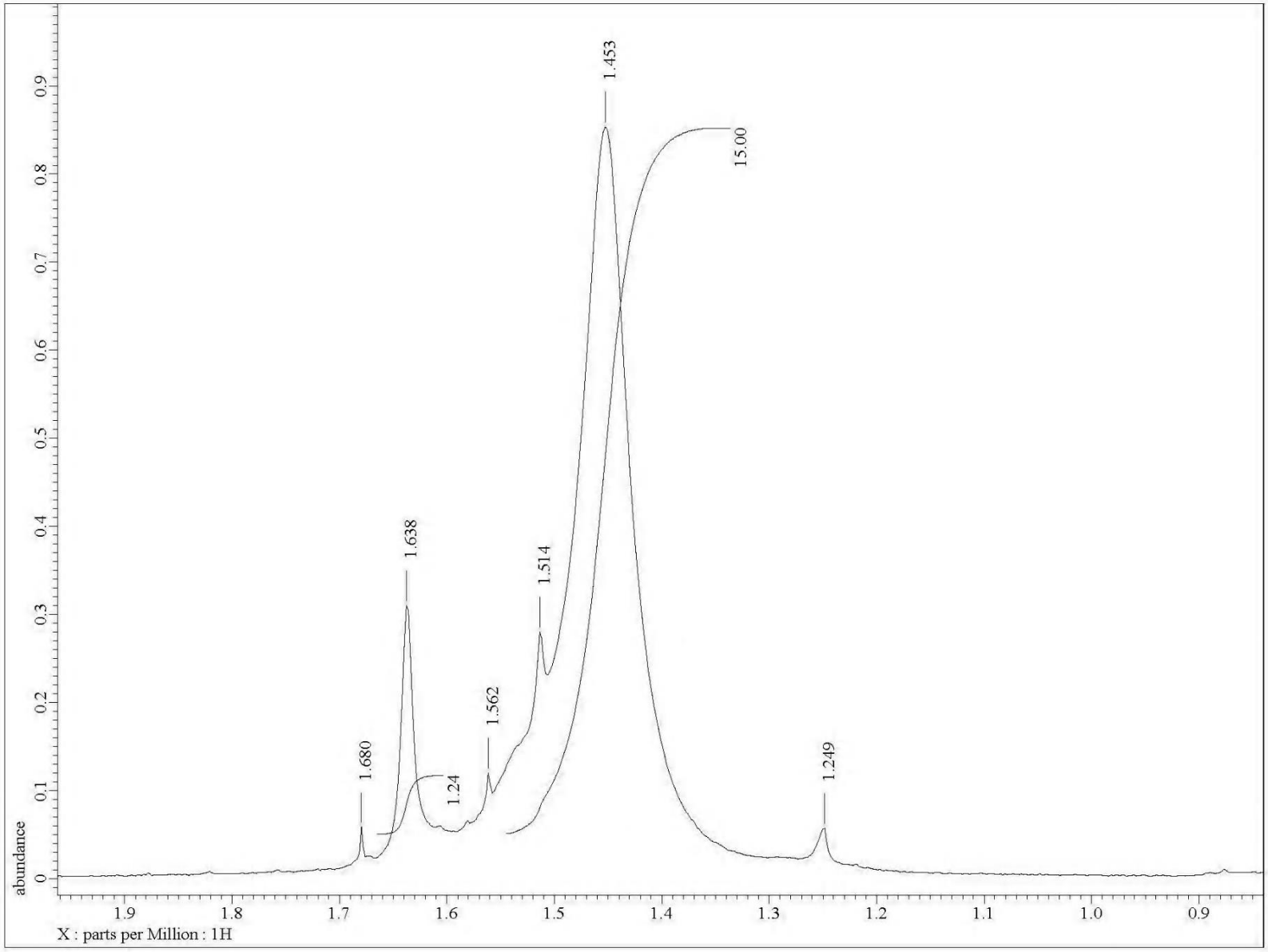

Fig. S61 ^{1}H NMR (400 MHz, $CDCl_3$) spectrum of **14** at 1.49×10^{-2} M concentration in the indicated region

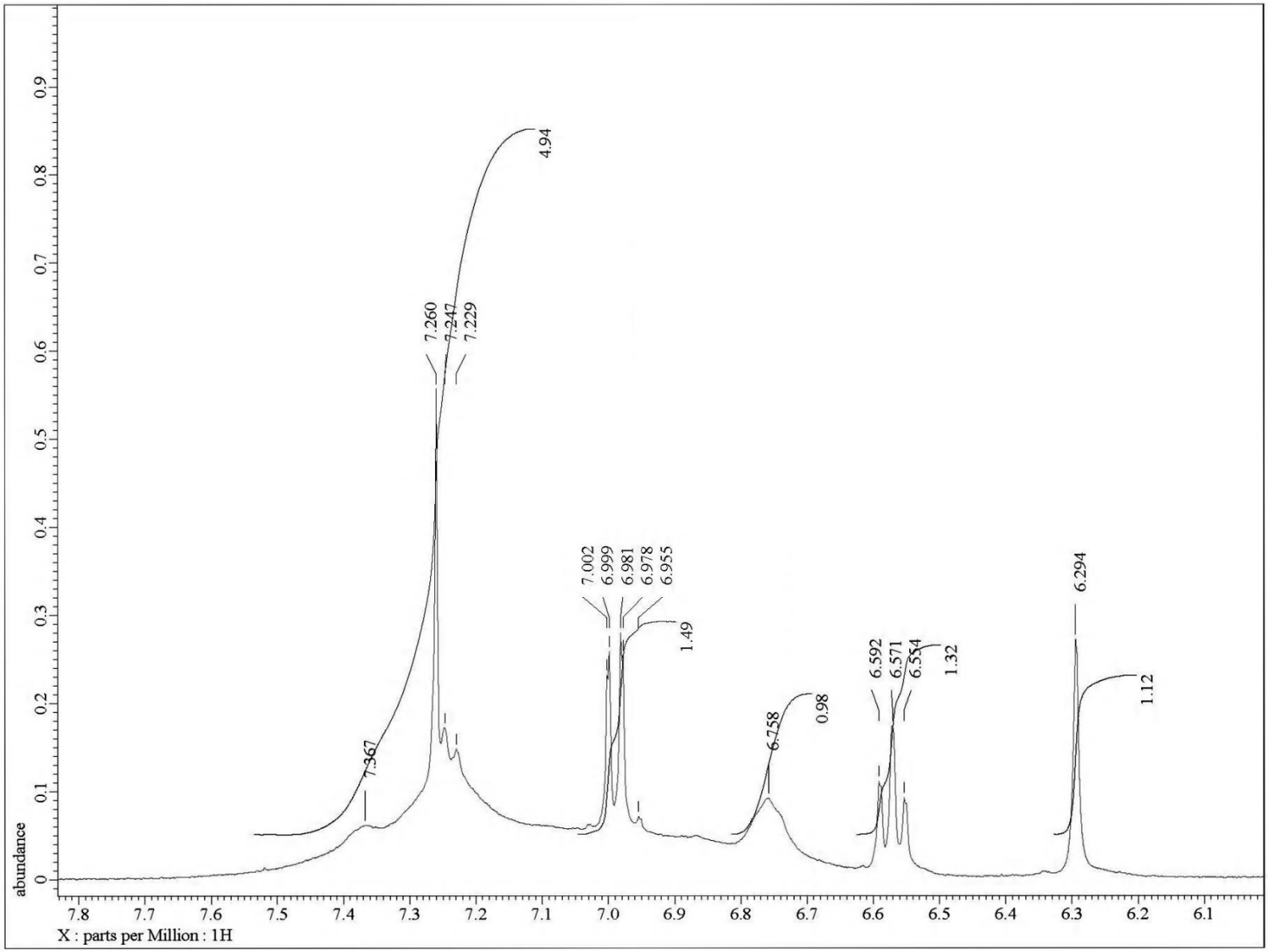

Fig. S62 ^{1}H NMR (400 MHz, $CDCl_3$) spectrum of **14** at 1.49×10^{-2} M concentration in the indicated region

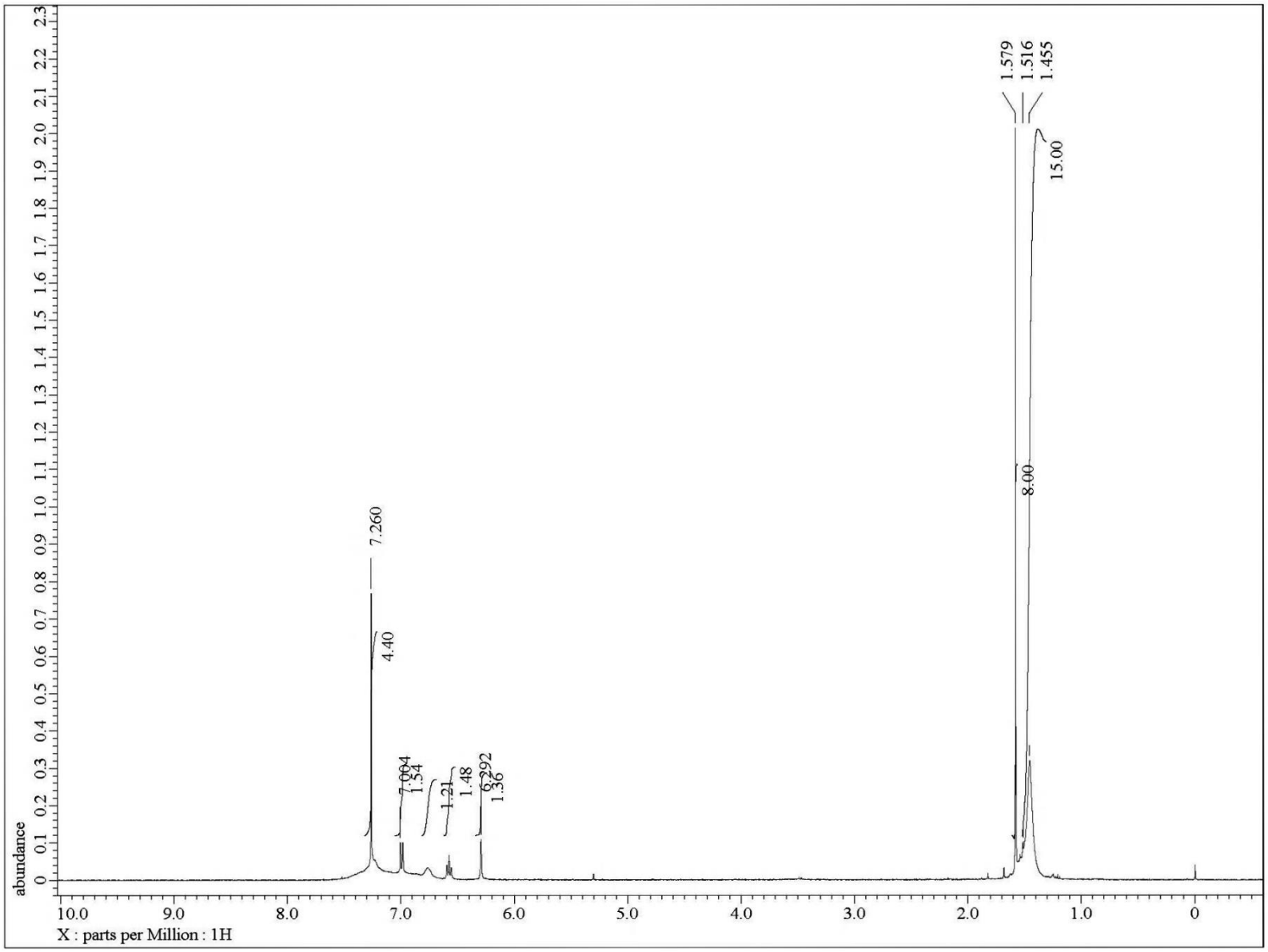

Fig. S63 ^{1}H NMR (400 MHz, $CDCl_3$) spectrum of **14** at 1.49×10^{-1} M concentration

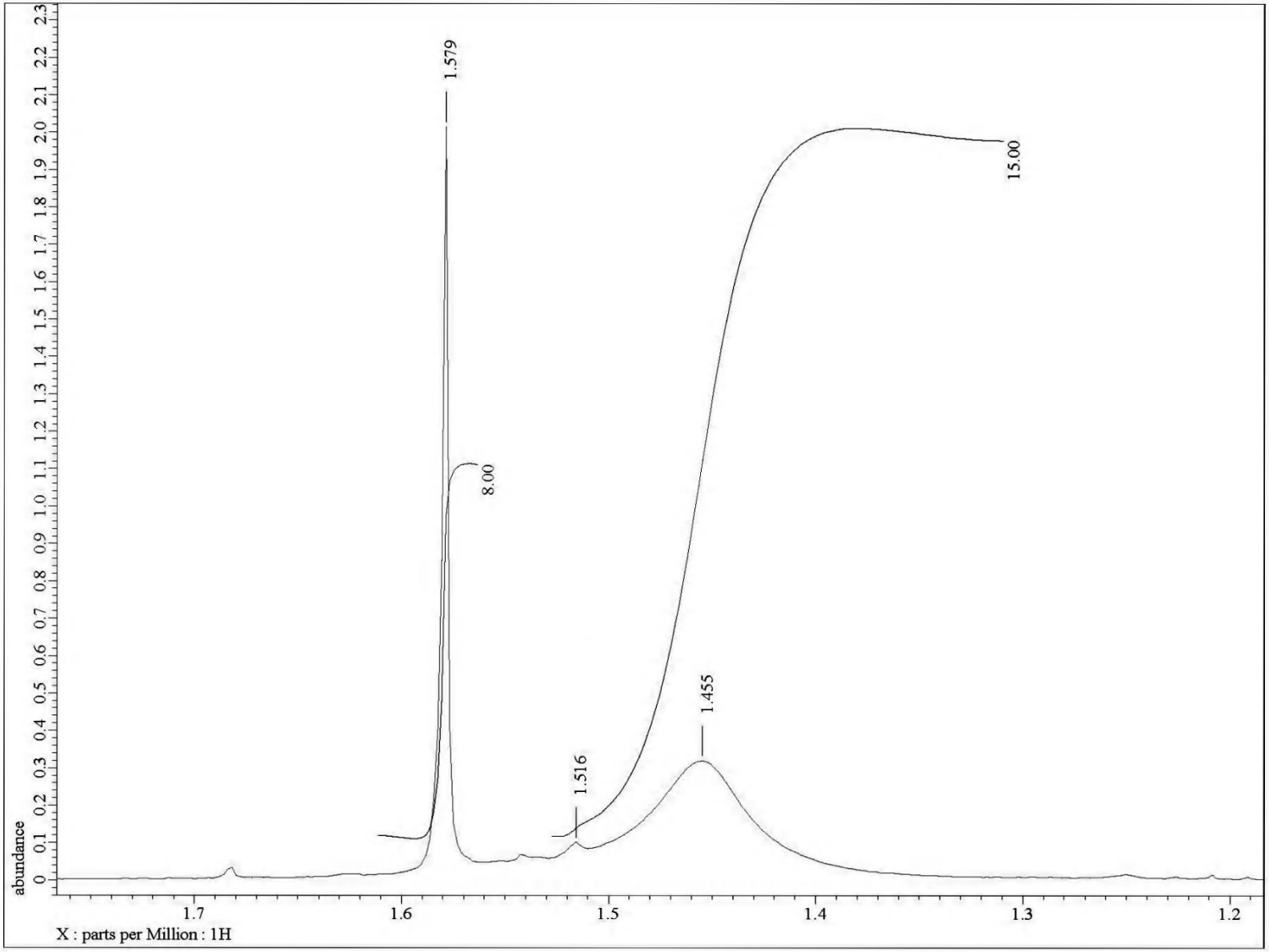

Fig. S64 ^{1}H NMR (400 MHz, $CDCl_3$) spectrum of **14** at 1.49×10^{-1} M concentration in the indicated region

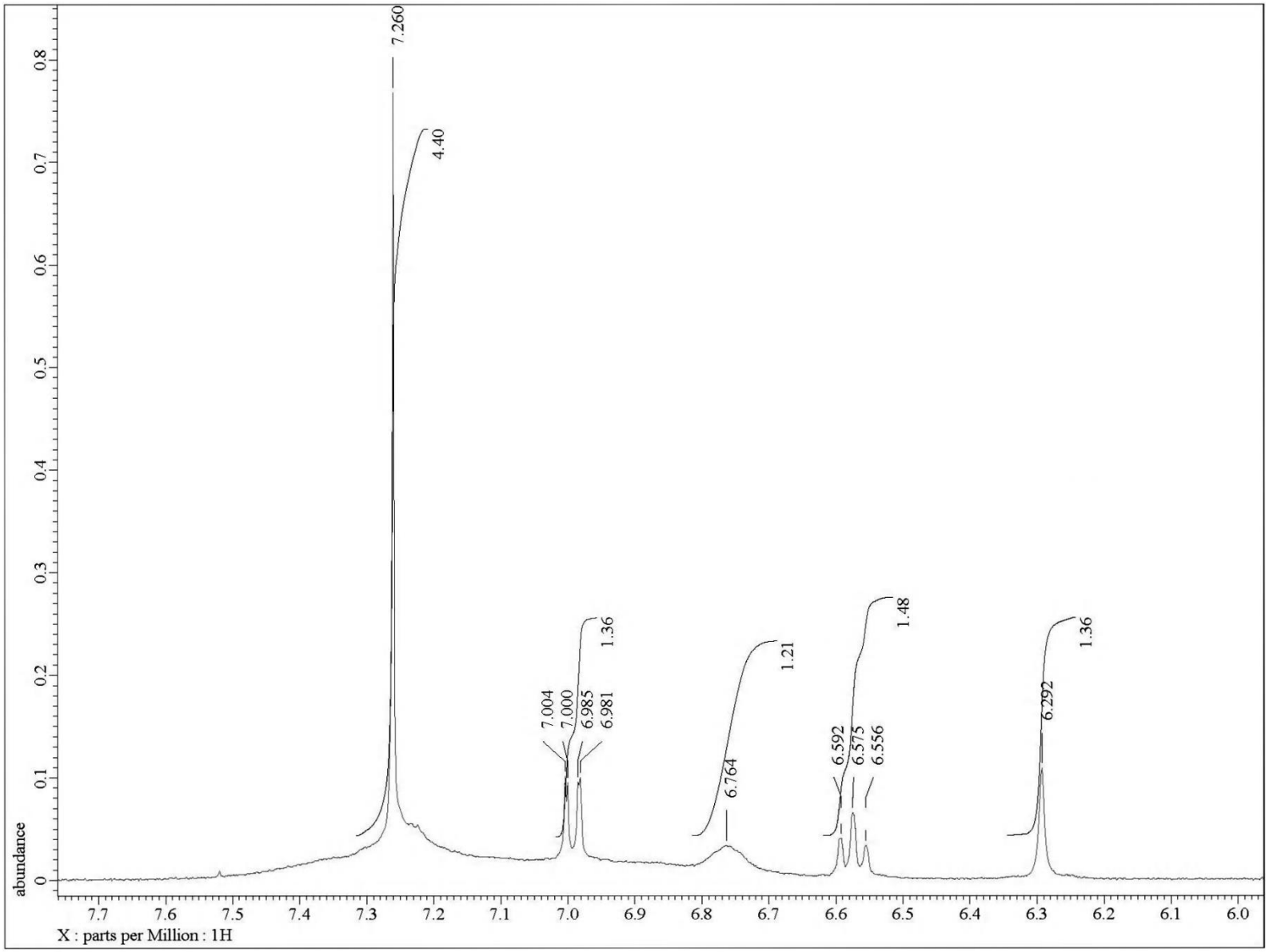

Fig. S65 ^{1}H NMR (400 MHz, $CDCl_3$) spectrum of **14** at 1.49×10^{-1} M concentration in the indicated region

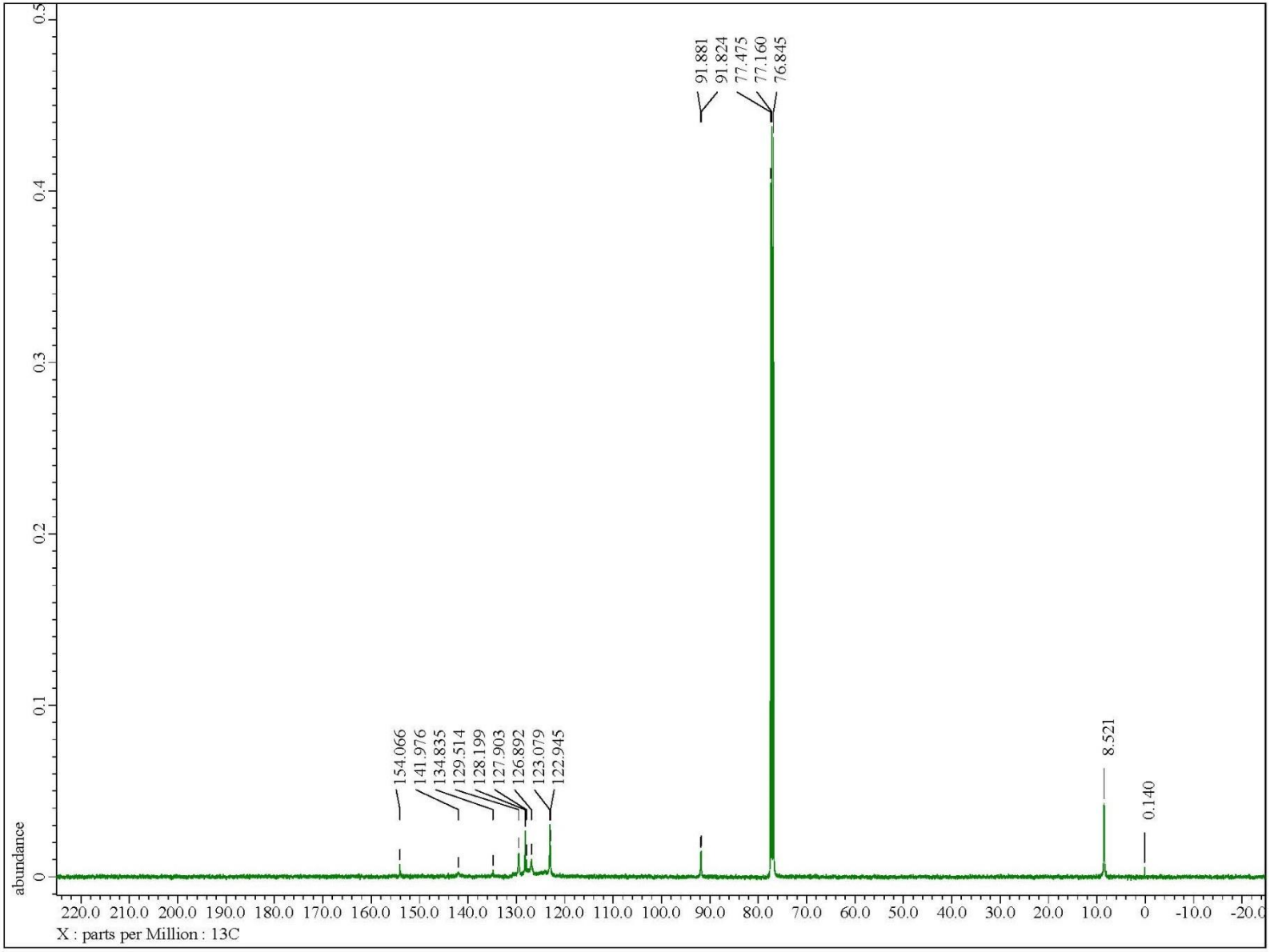

Fig. S66 ^{13}C NMR (100.5 MHz, $CDCl_3$) spectrum of **14**

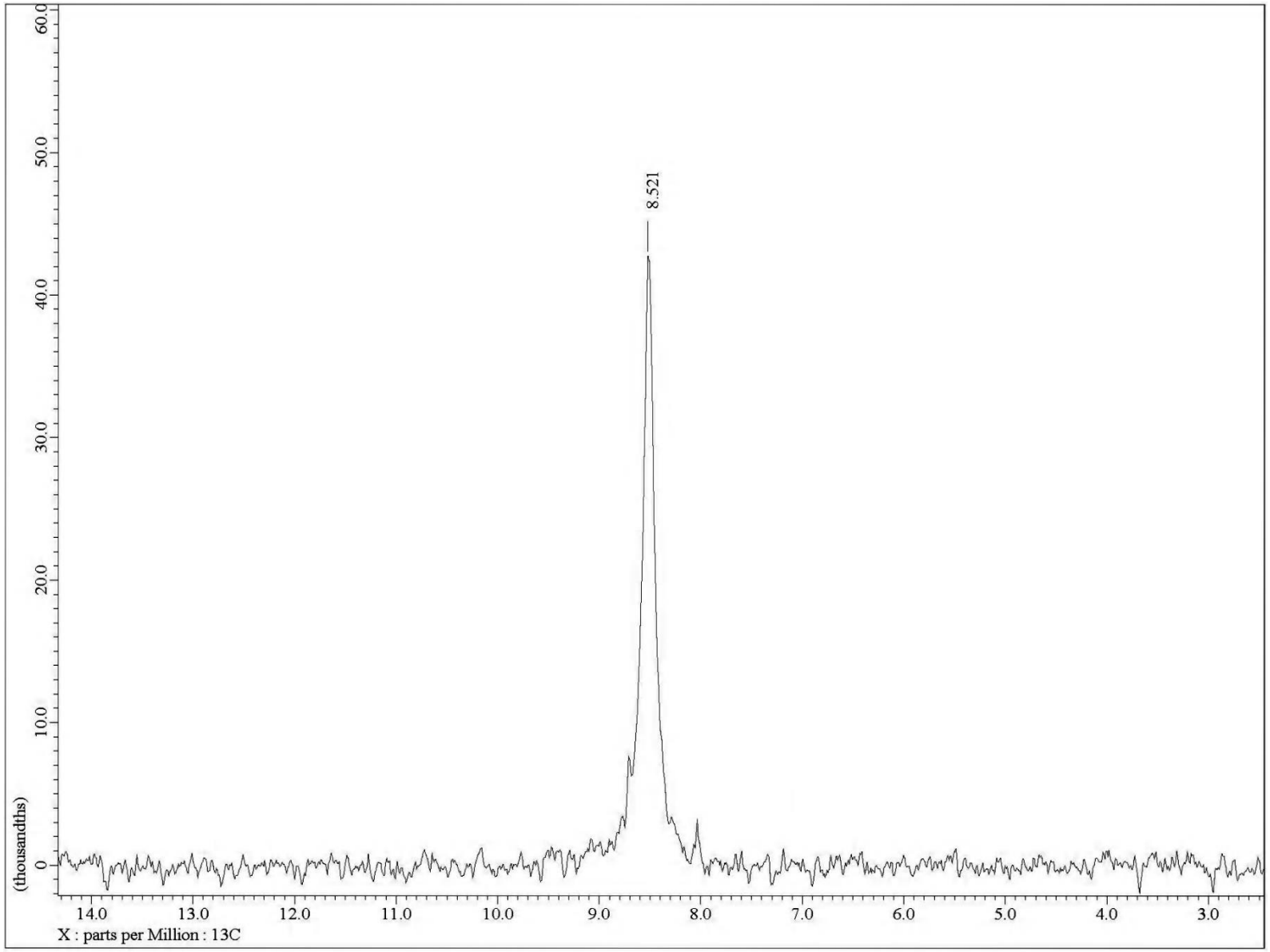

Fig. S67 ^{13}C NMR (100.5 MHz, $CDCl_3$) spectrum of **14** in the indicated region

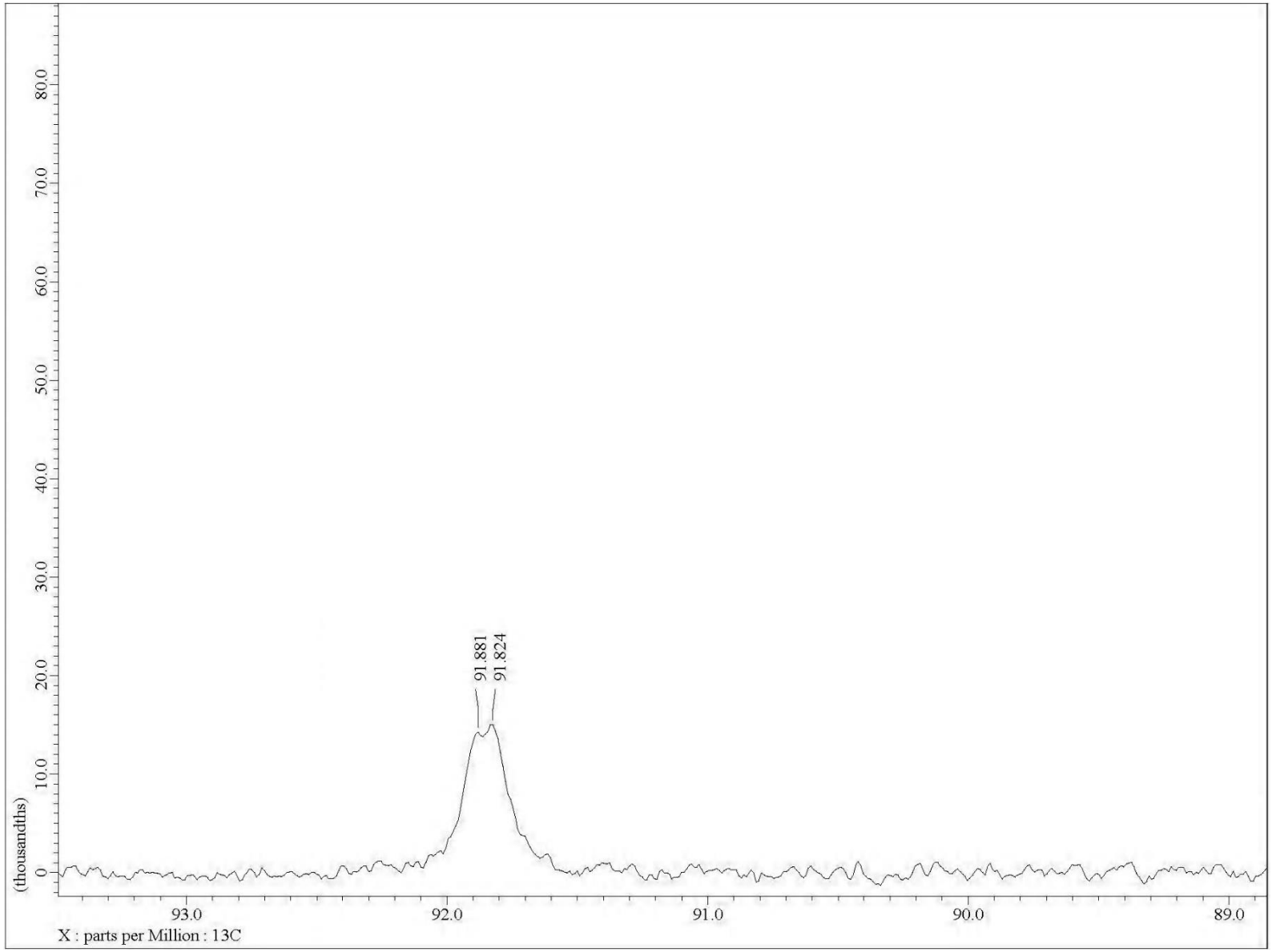

Fig. S68 ^{13}C NMR (100.5 MHz, $CDCl_3$) spectrum of **14** in the indicated region

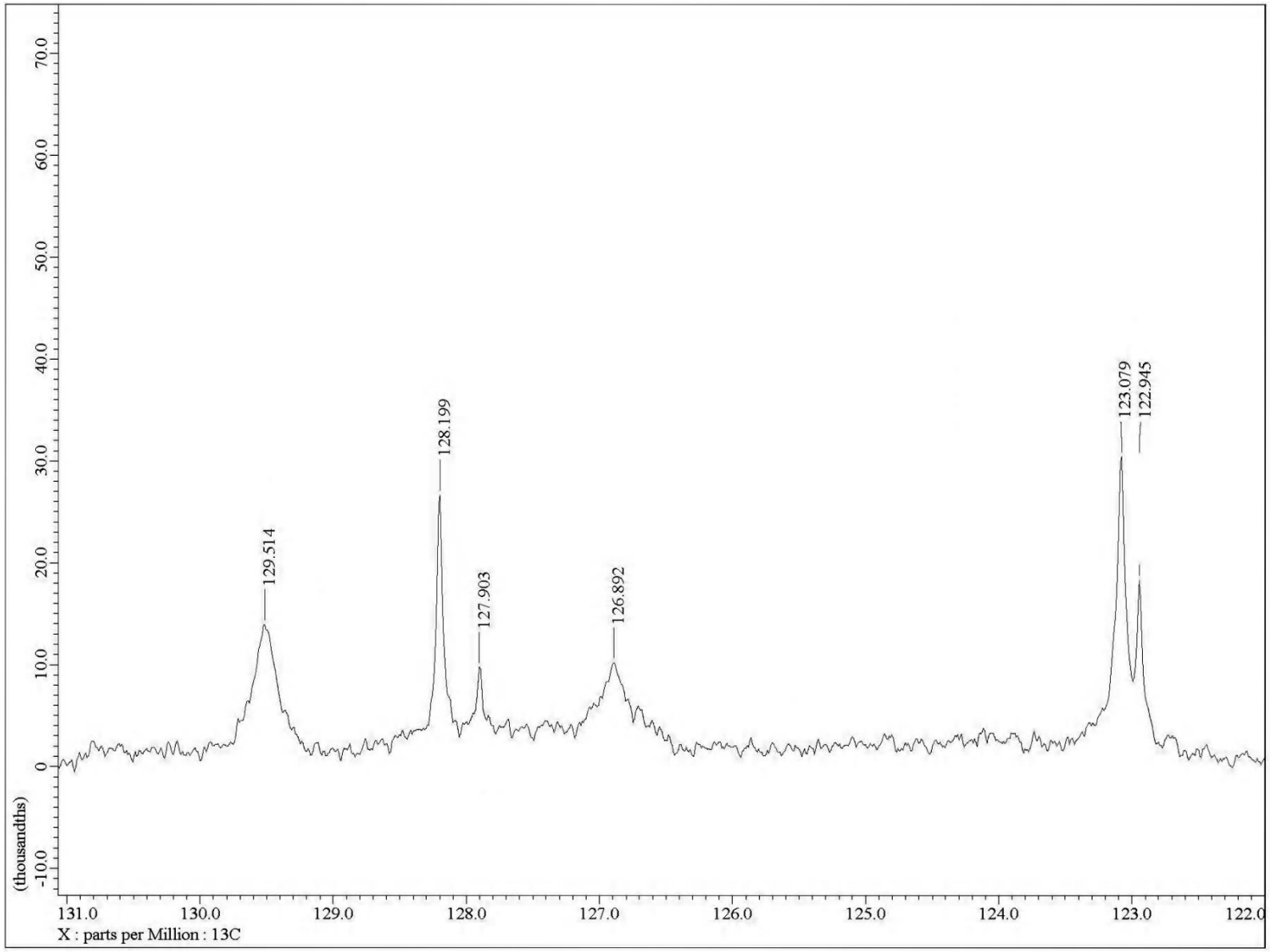

Fig. S69 ^{13}C NMR (100.5 MHz, $CDCl_3$) spectrum of **14** in the indicated region

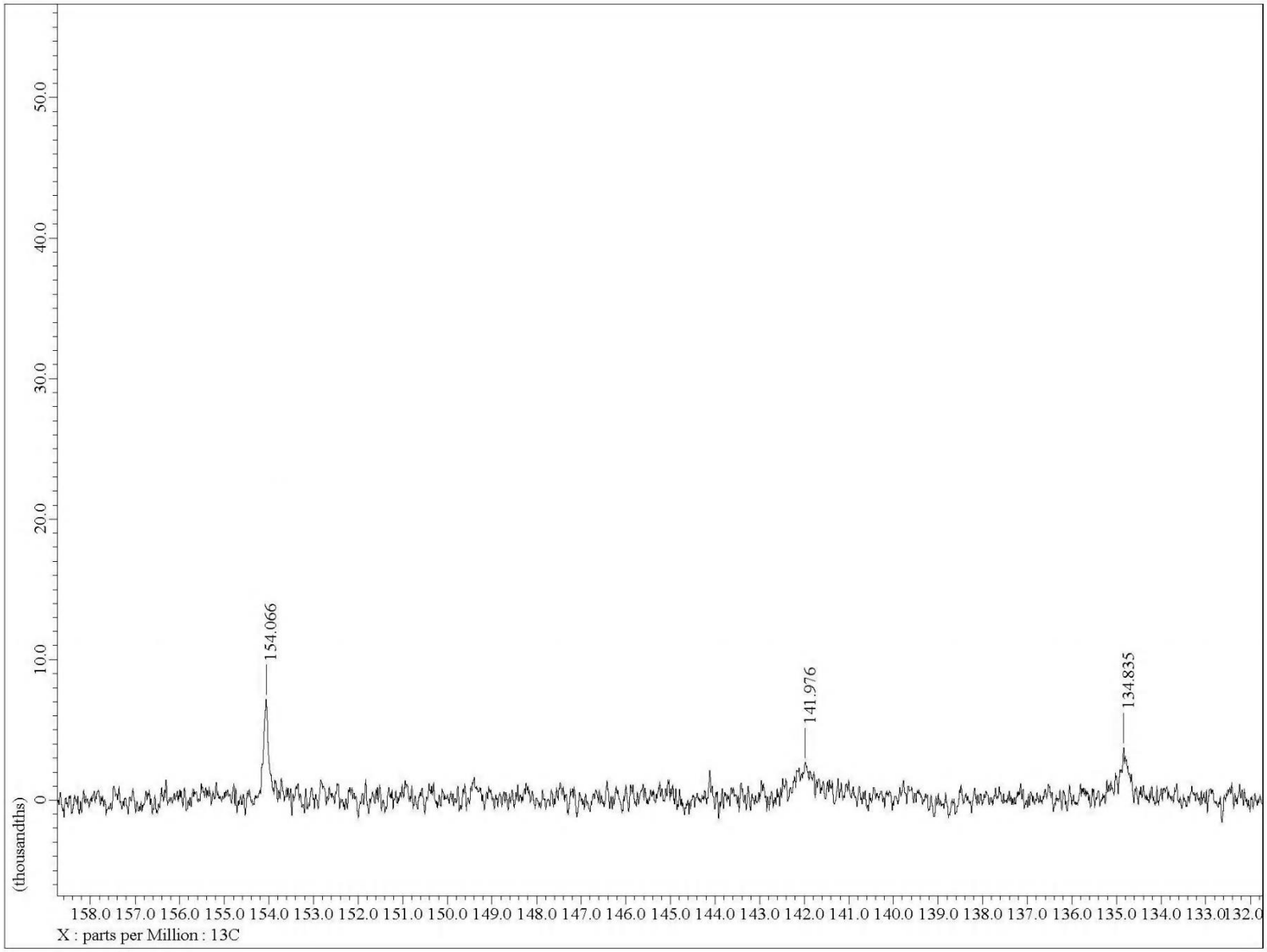

Fig. S70 ^{13}C NMR (100.5 MHz, $CDCl_3$) spectrum of **14** in the indicated region

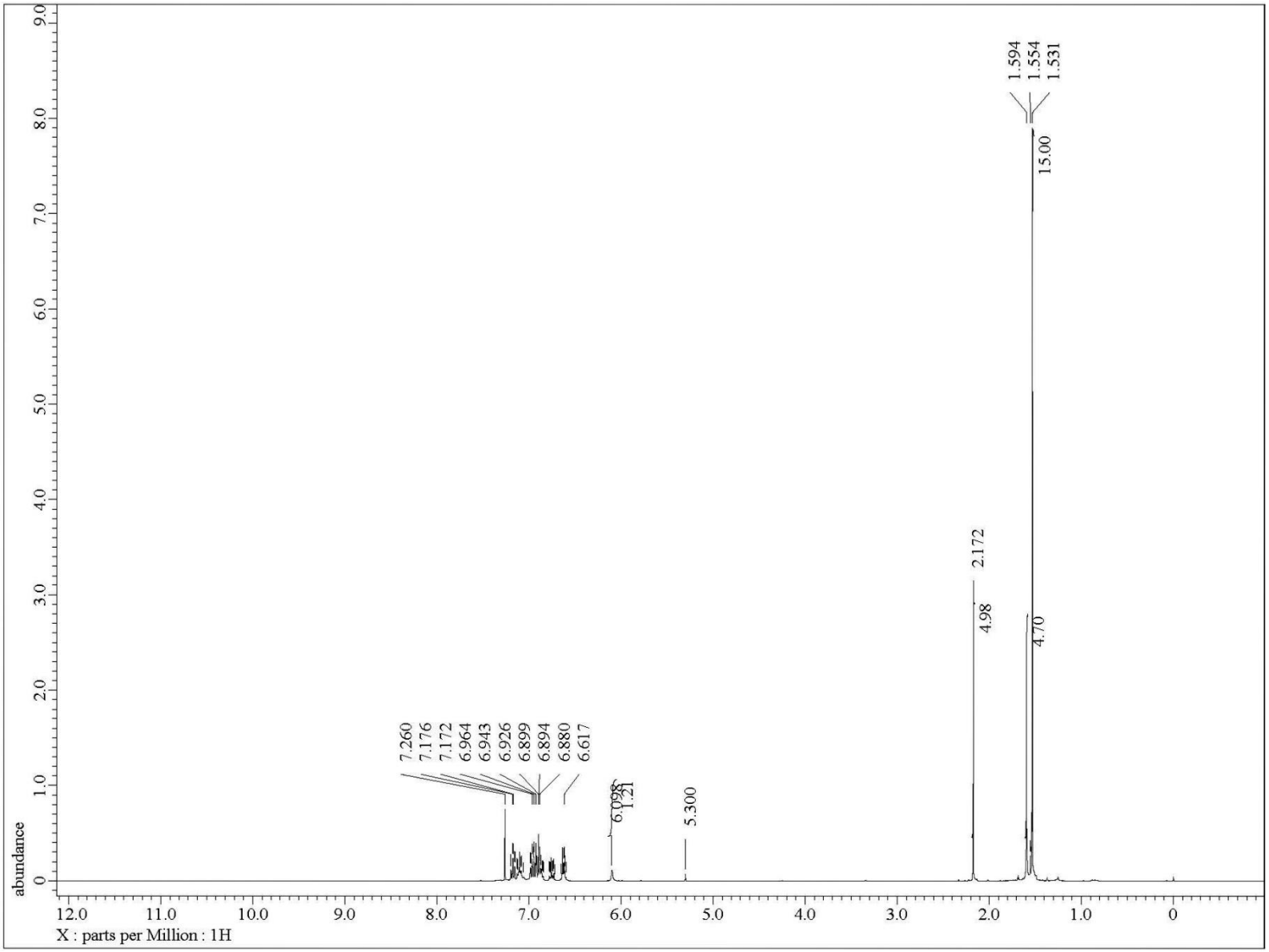

Fig. S71 ^{1}H NMR (400 MHz, $CDCl_3$) spectrum of **15** at 1.45×10^{-1} M concentration

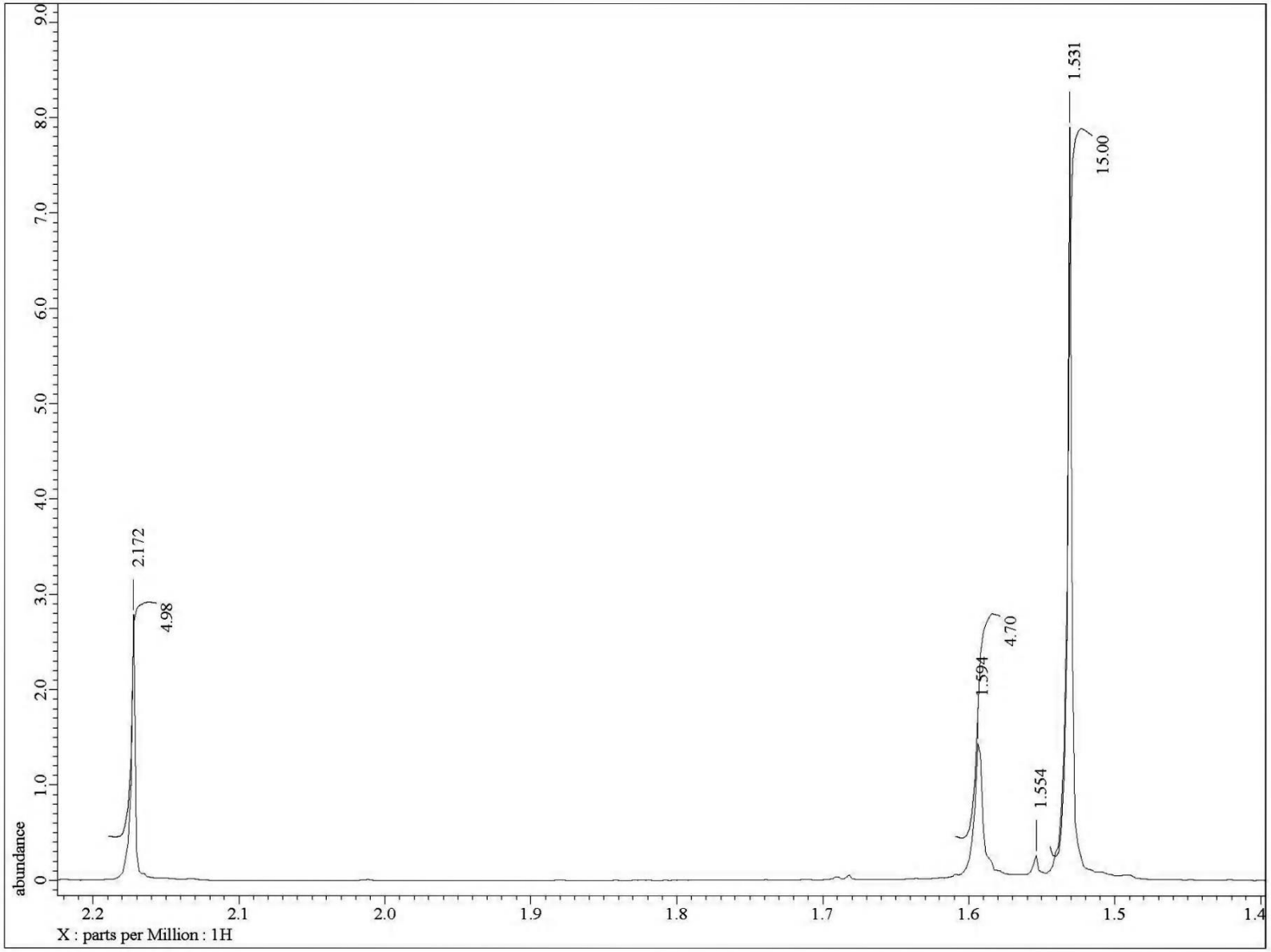

Fig. S72 ^{1}H NMR (400 MHz, $CDCl_3$) spectrum of **15** at 1.45×10^{-1} M concentration in the indicated region

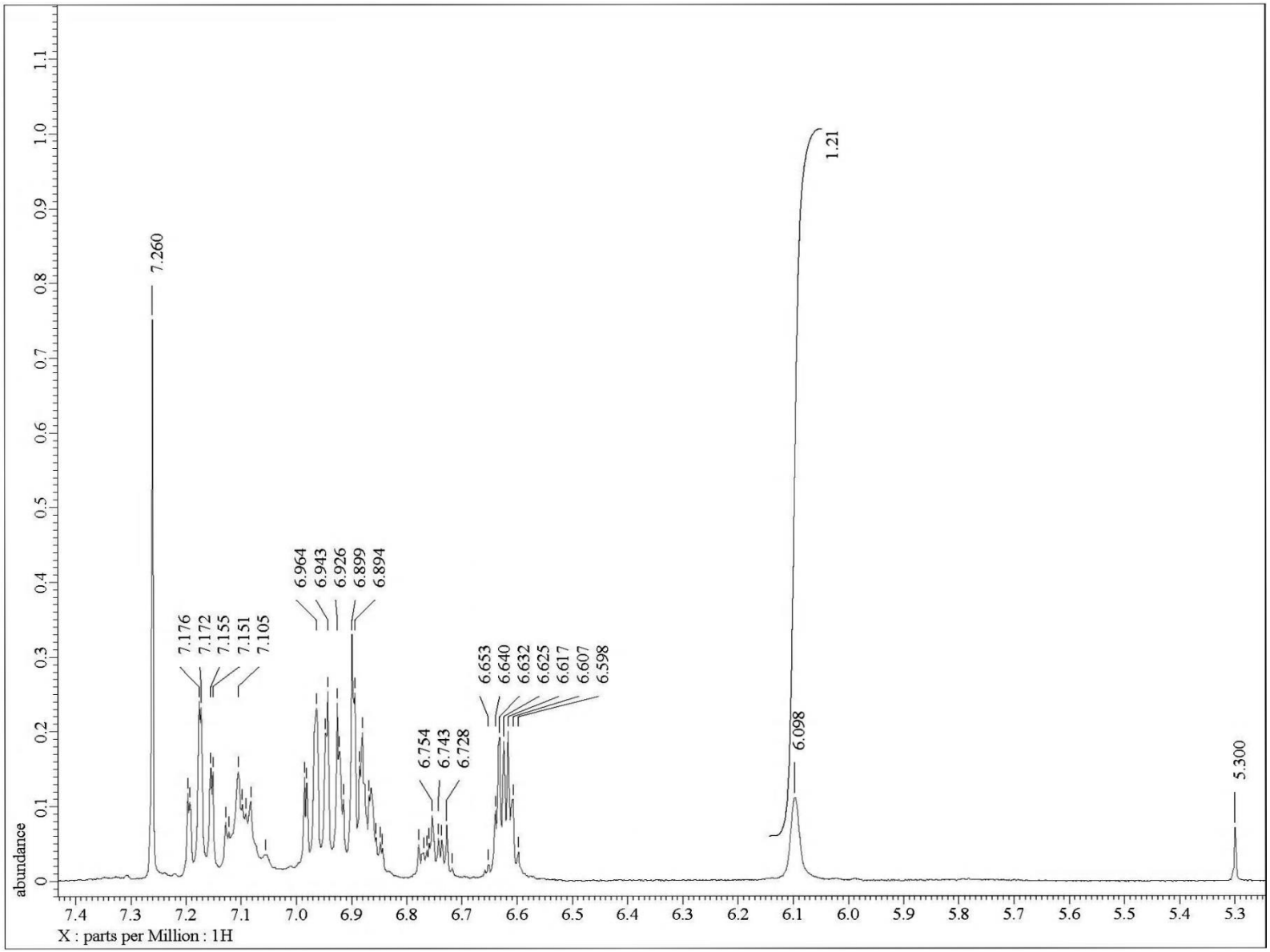

Fig. S73 ^{1}H NMR (400 MHz, $CDCl_3$) spectrum of **15** at 1.45×10^{-1} M concentration in the indicated region

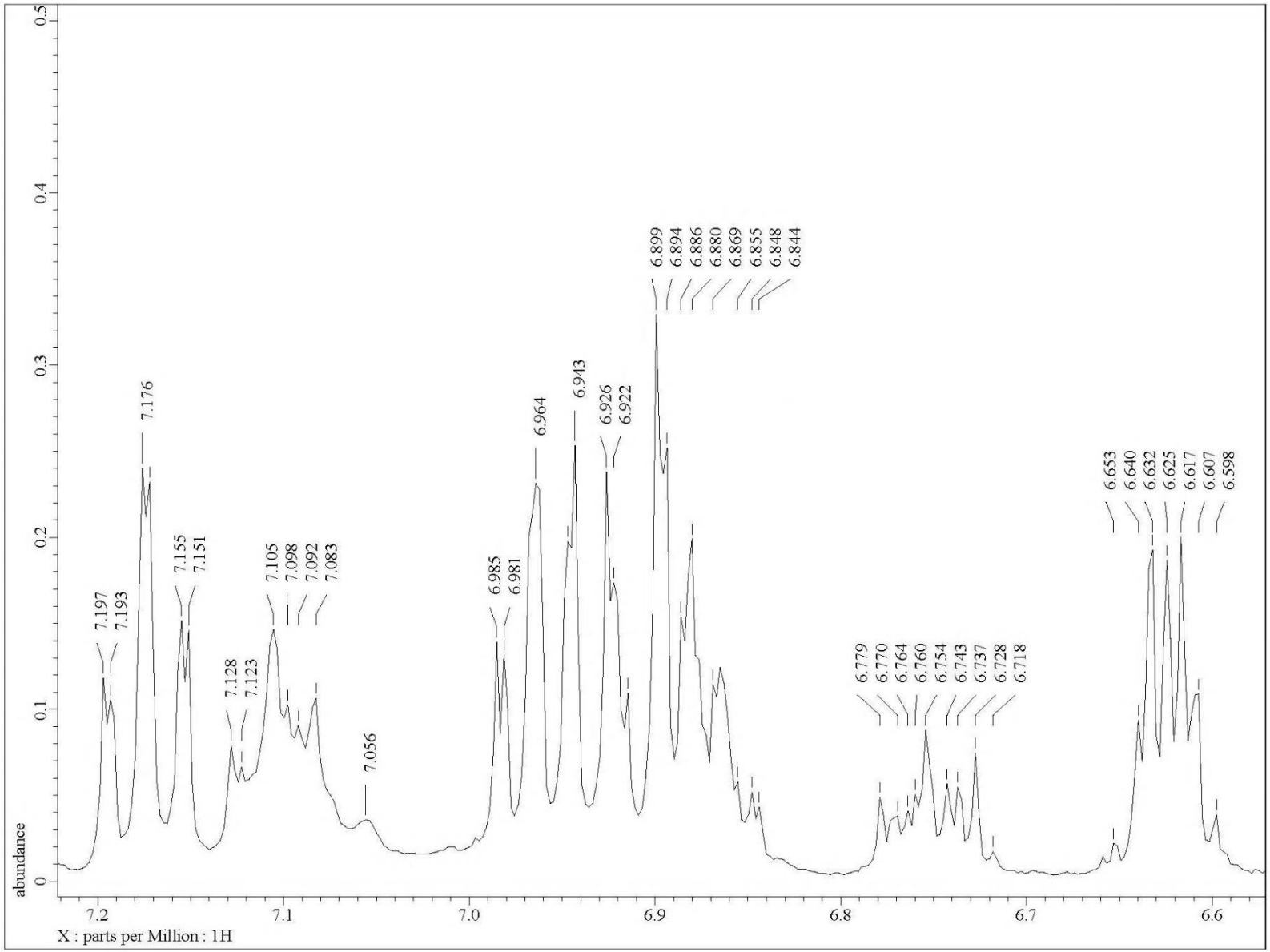

Fig. S74 ^{1}H NMR (400 MHz, $CDCl_3$) spectrum of **15** at 1.45×10^{-1} M concentration in the indicated region

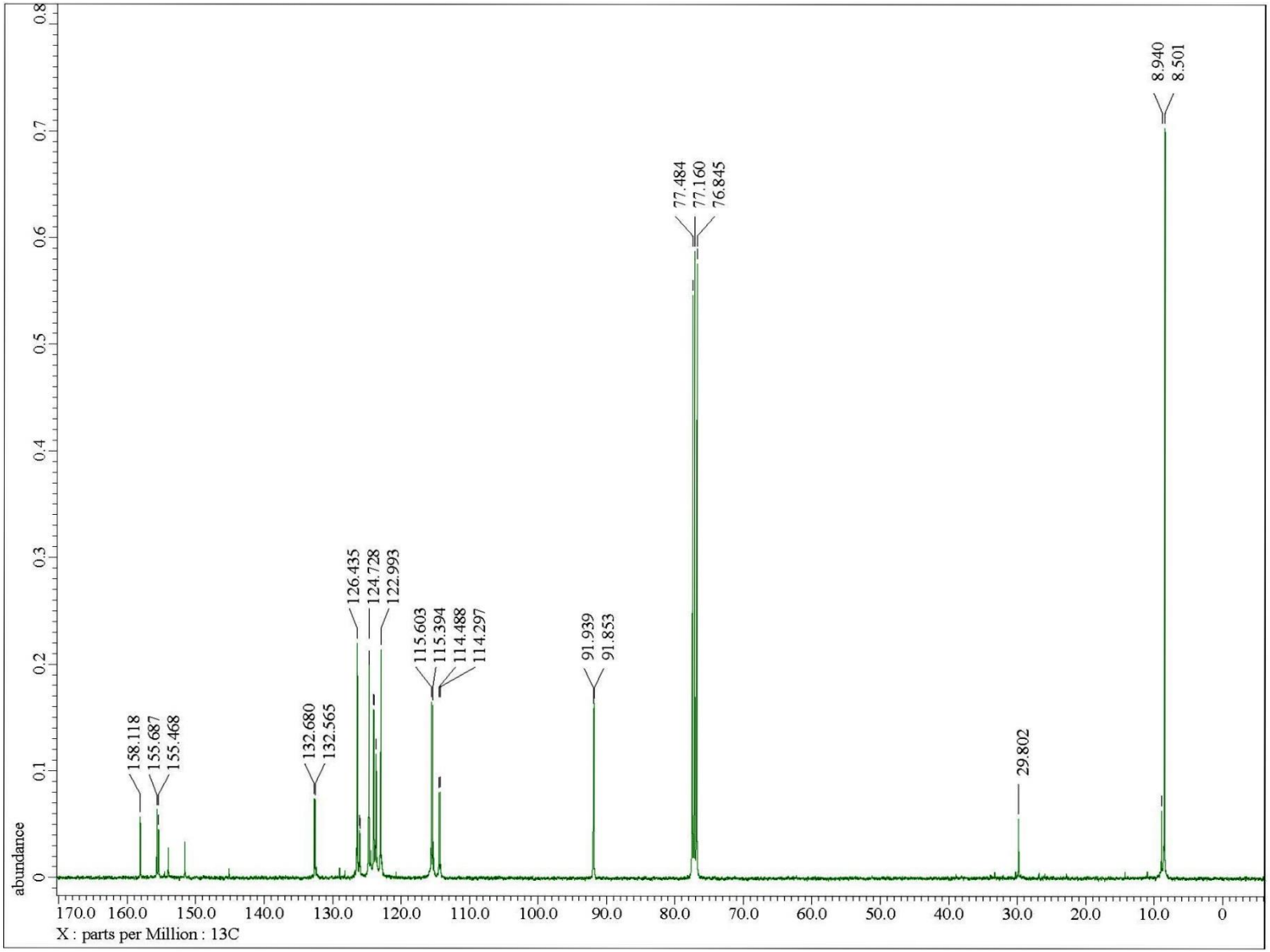

Fig. S75 ^{13}C NMR (100.5 MHz, $CDCl_3$) spectrum of **15** at 1.45×10^{-1} M concentration

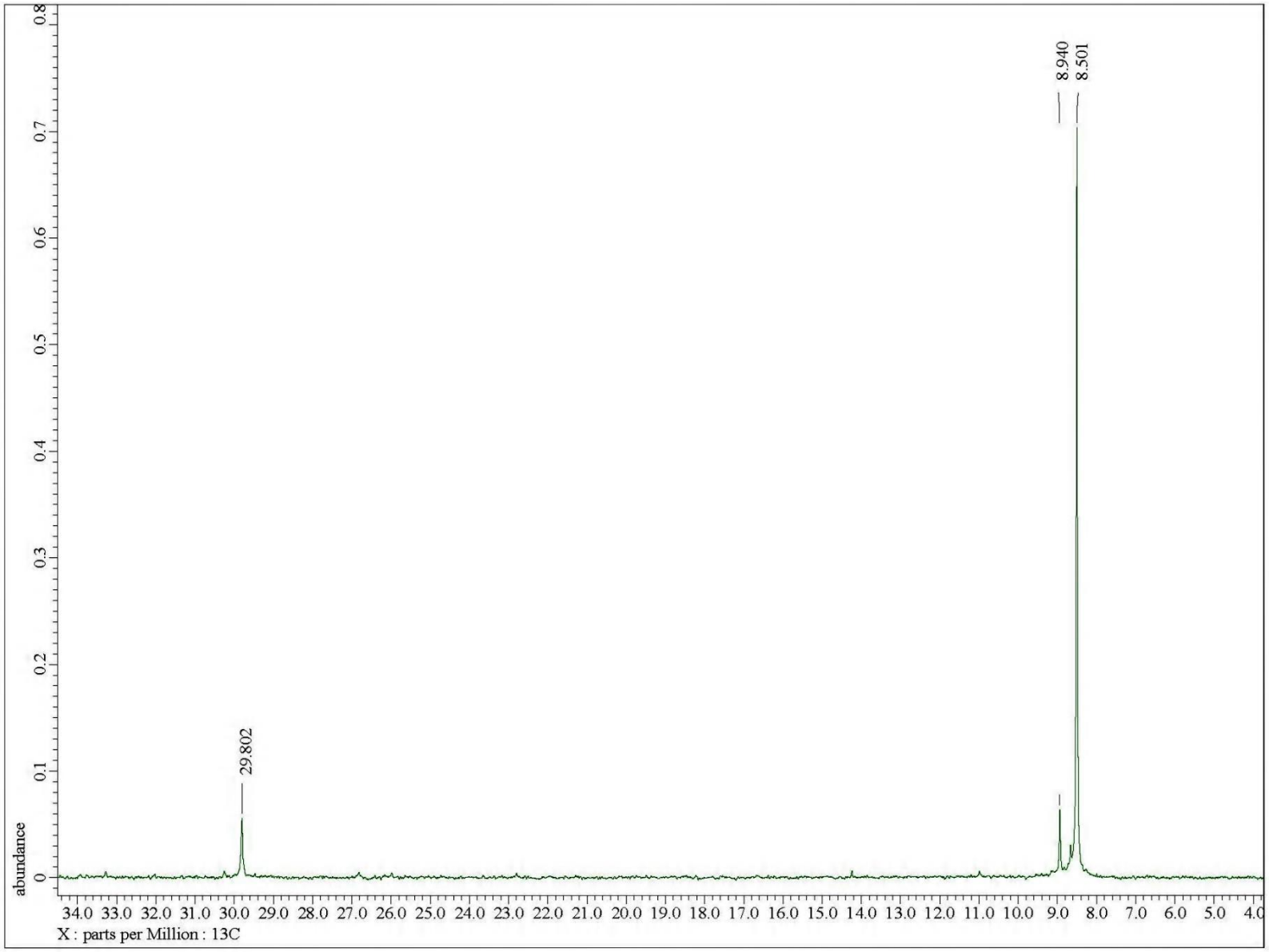

Fig. S76 ^{13}C NMR (100.5 MHz, $CDCl_3$) spectrum of **15** at 1.45×10^{-1} M concentration in the indicated region

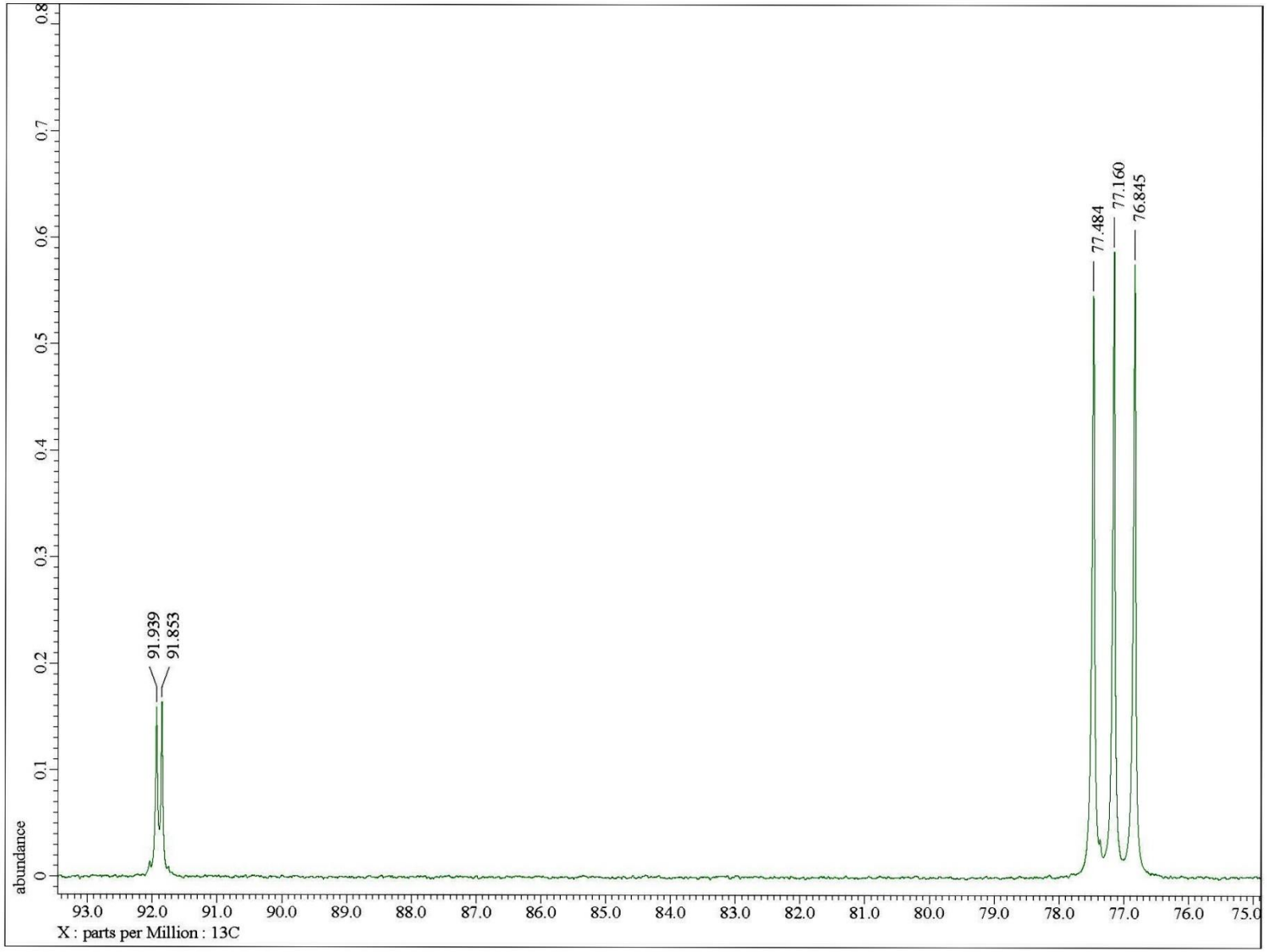

Fig. S77 ^{13}C NMR (100.5 MHz, $CDCl_3$) spectrum of **15** at 1.45×10^{-1} M concentration in the indicated region

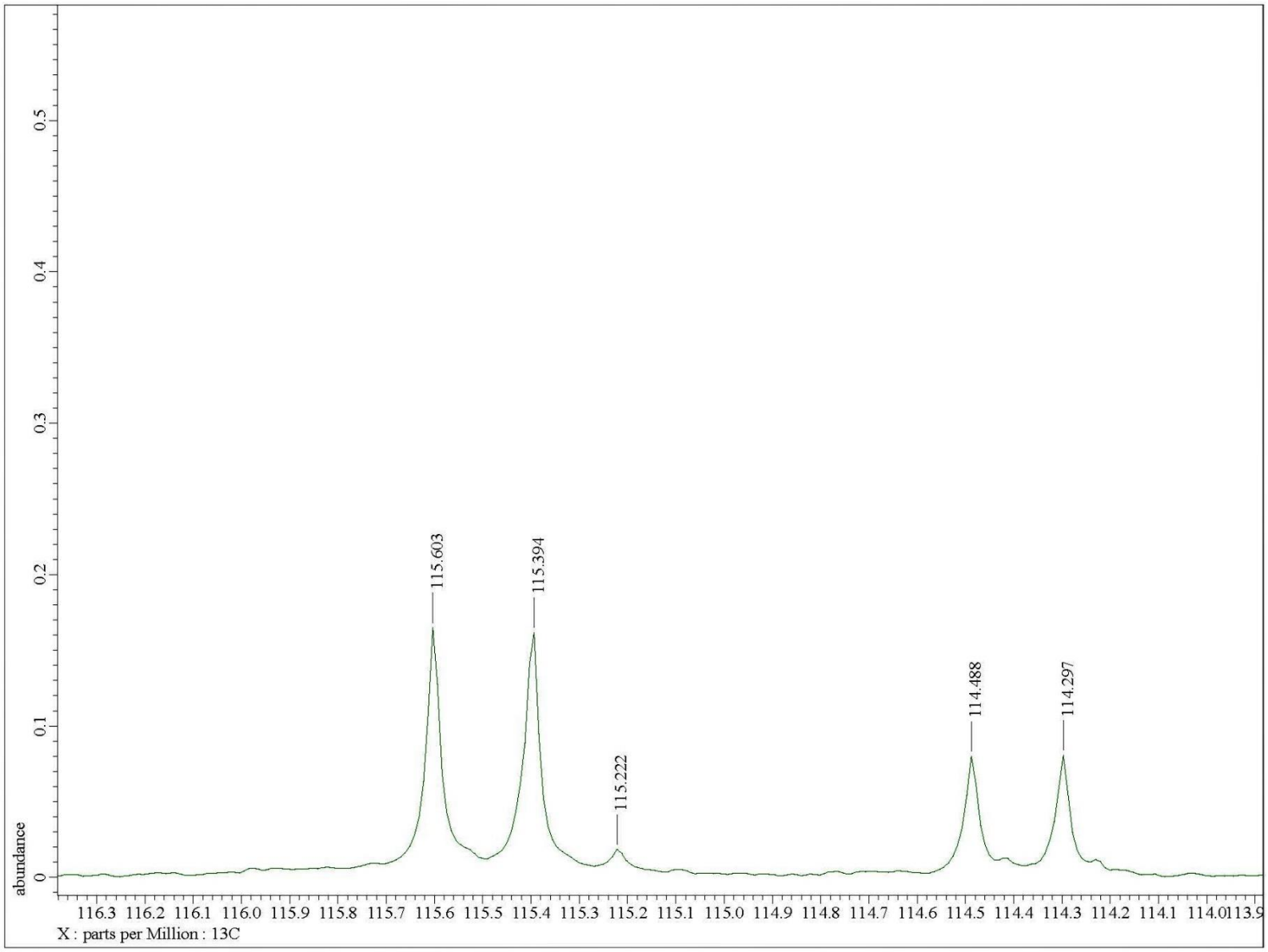

Fig. S78 ^{13}C NMR (100.5 MHz, $CDCl_3$) spectrum of **15** at 1.45×10^{-1} M concentration in the indicated region

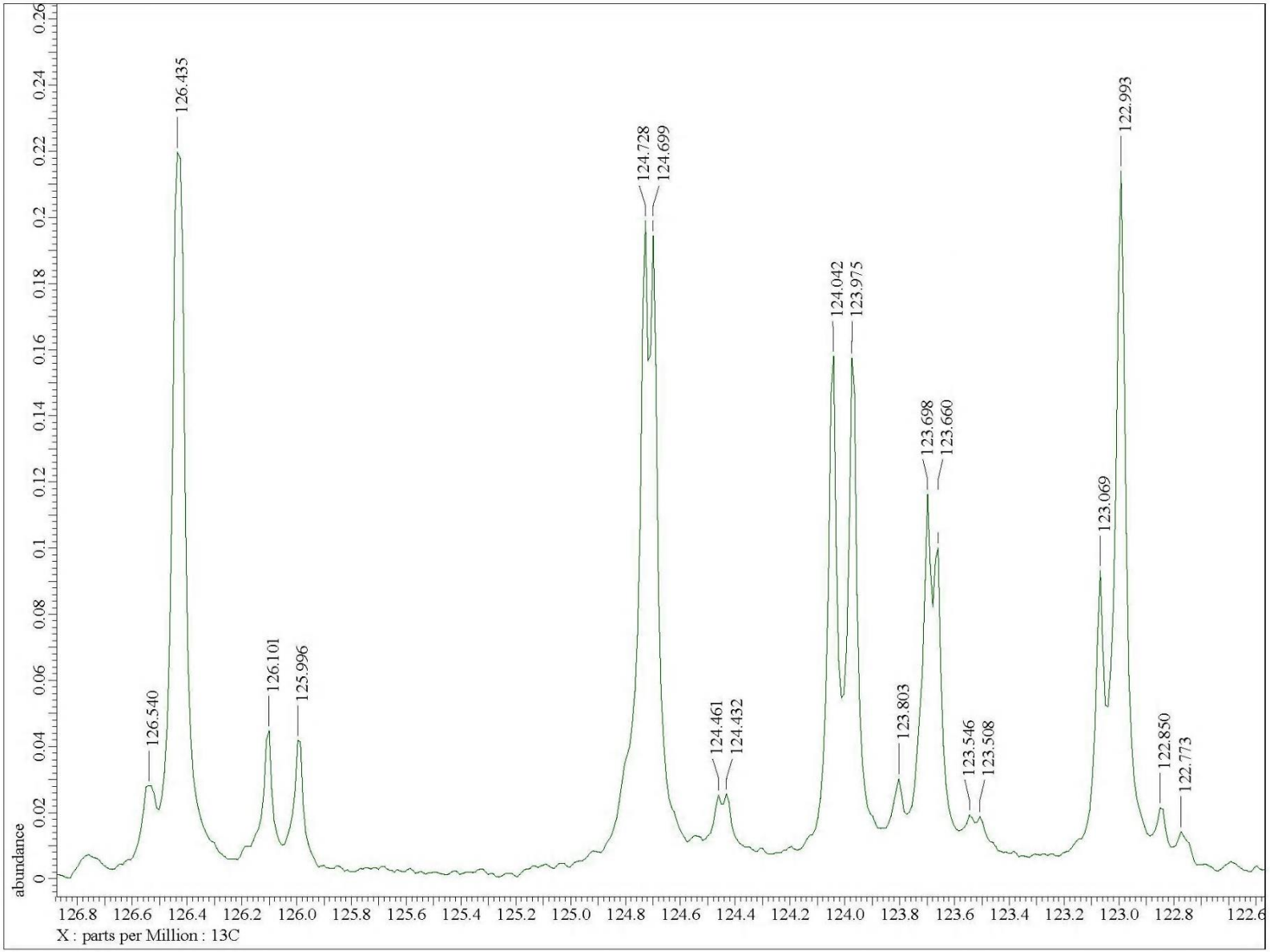

Fig. S79 ^{13}C NMR (100.5 MHz, $CDCl_3$) spectrum of **15** at 1.45×10^{-1} M concentration in the indicated region

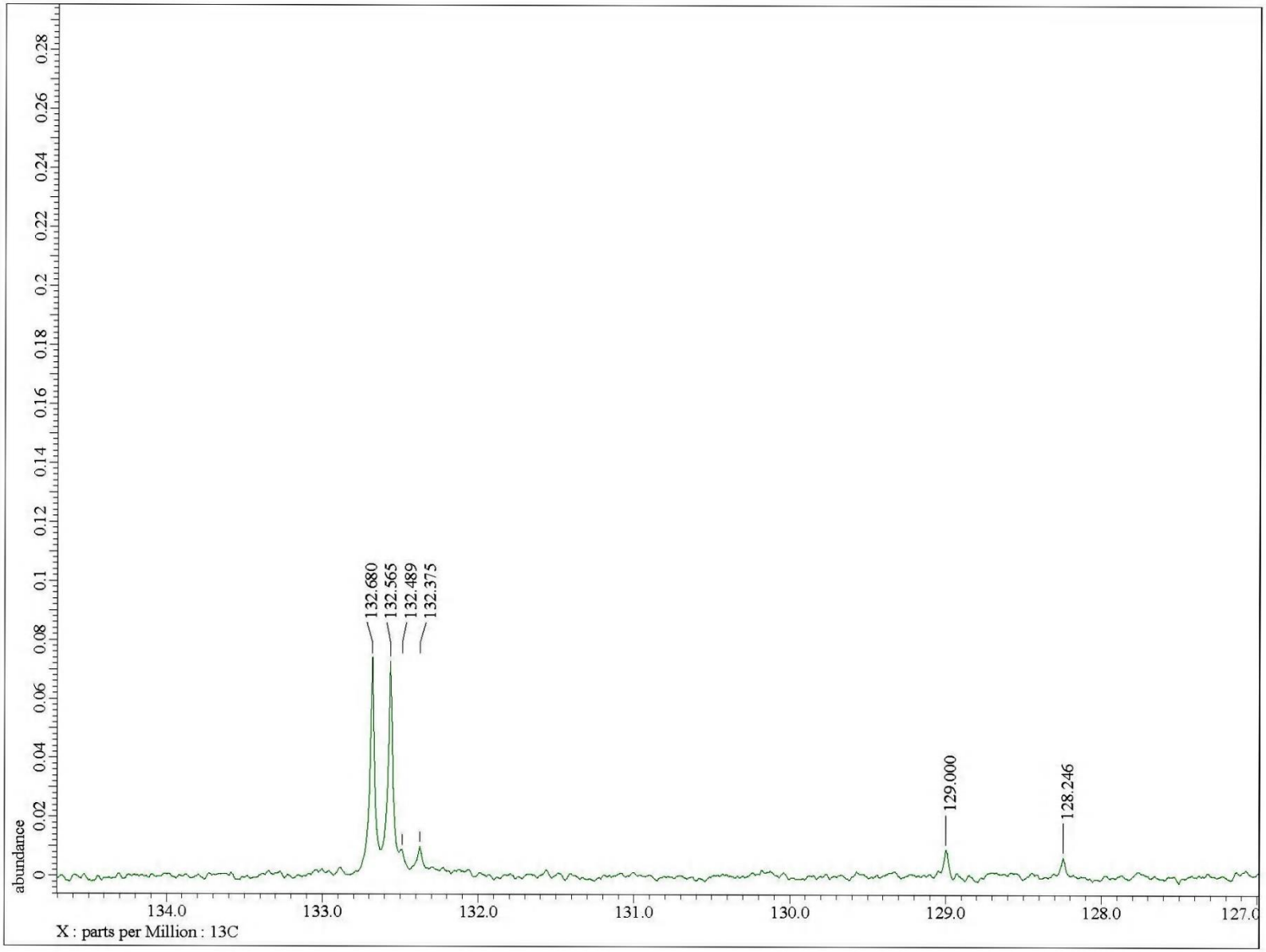

Fig. S80 ^{13}C NMR (100.5 MHz, $CDCl_3$) spectrum of **15** at 1.45×10^{-1} M concentration in the indicated region

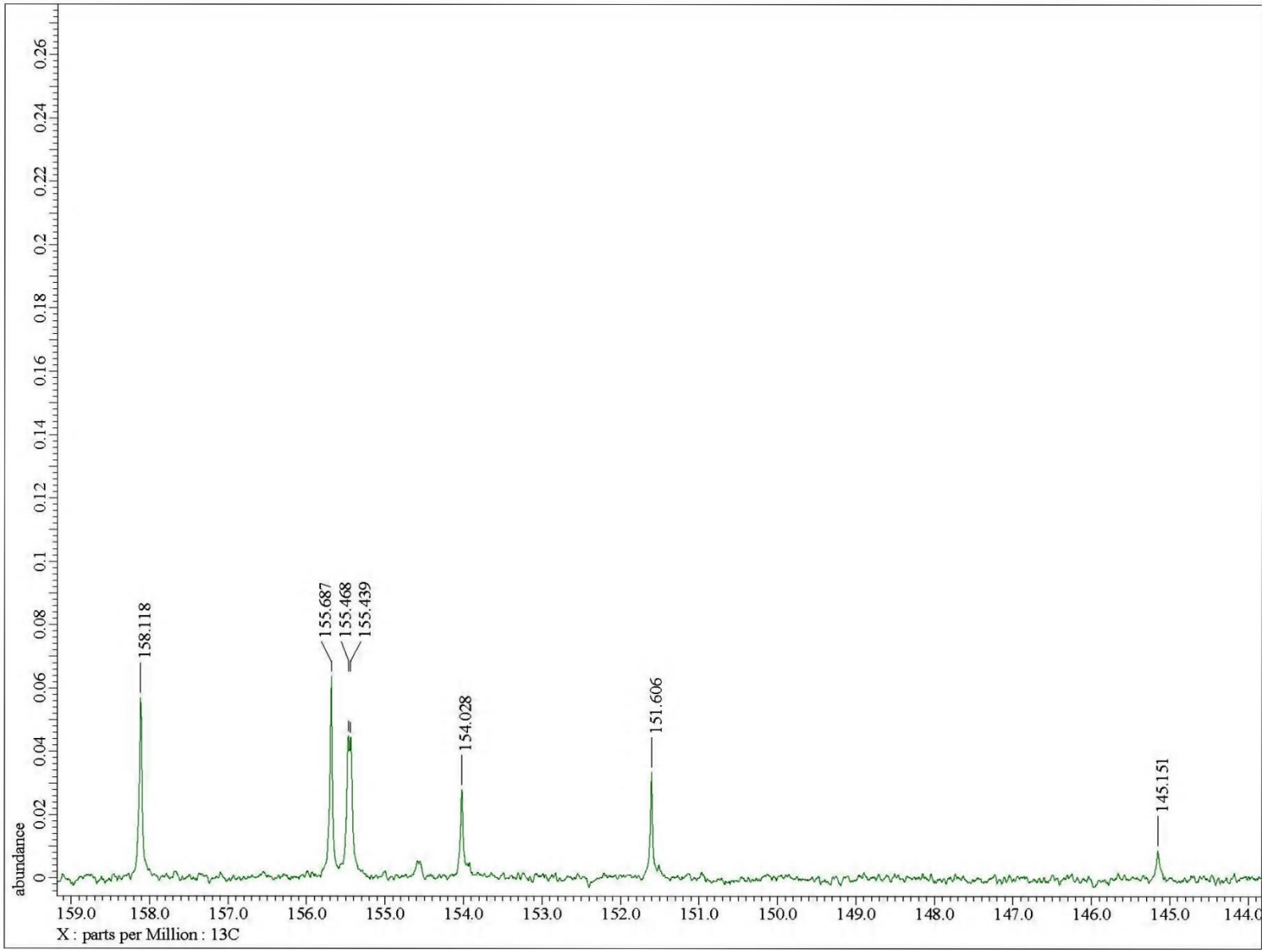

Fig. S81 ^{13}C NMR (100.5 MHz, $CDCl_3$) spectrum of **15** at 1.45×10^{-1} M concentration in the indicated region

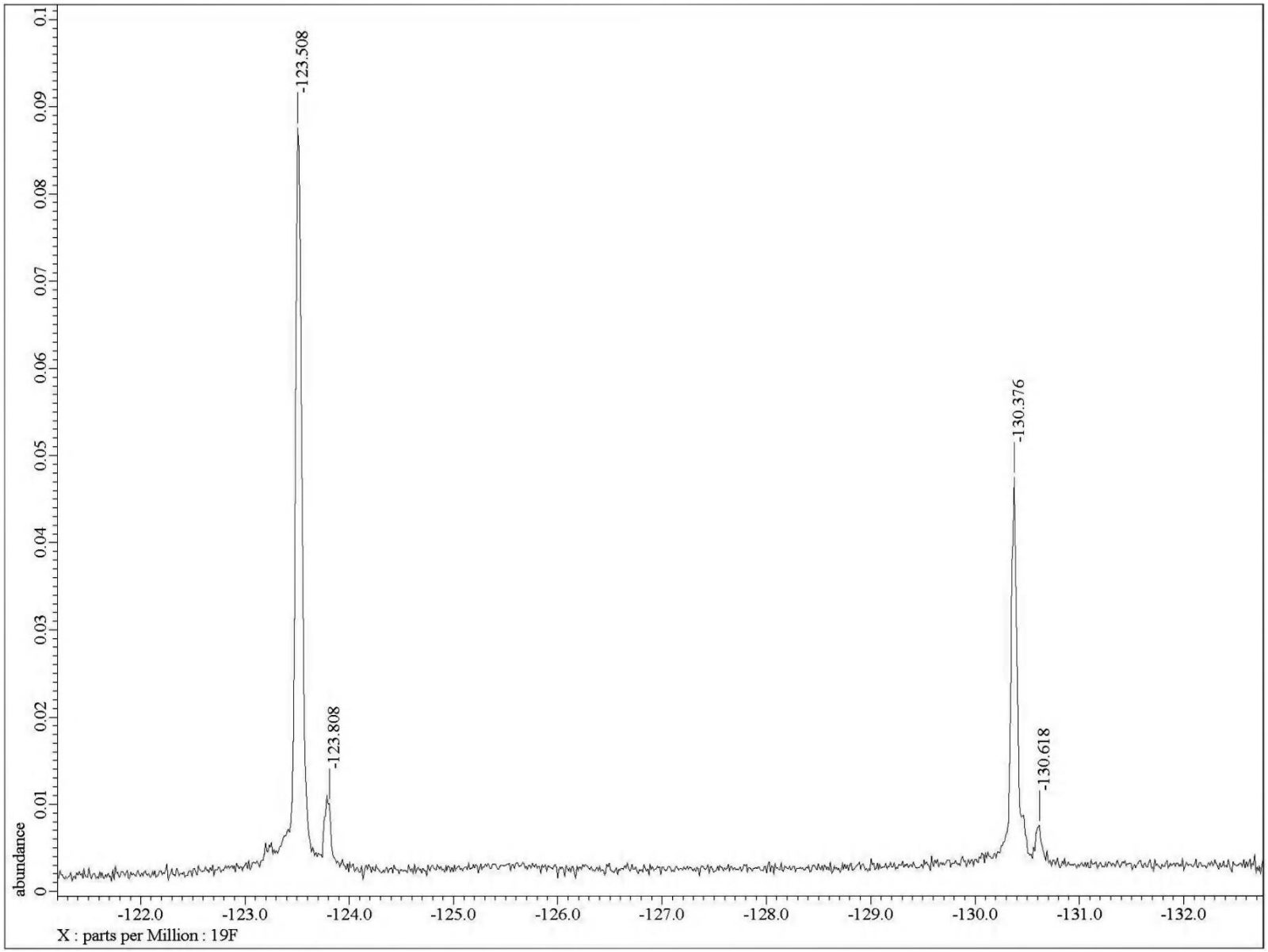

Fig. S82 ^{19}F NMR (376.5 MHz, $CDCl_3$) spectrum of **15** at 1.45×10^{-1} M concentration

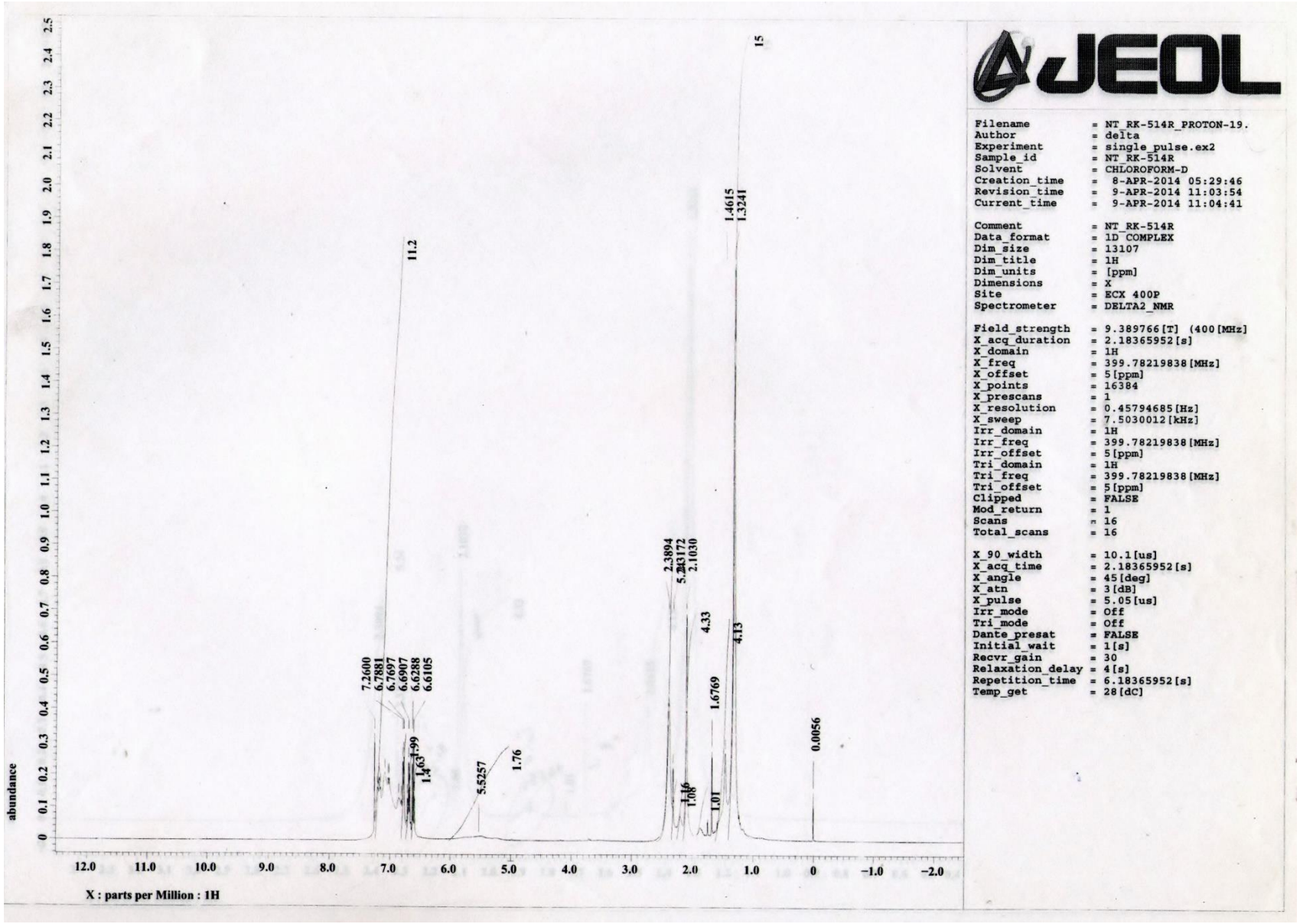

Fig. S83 ^{1}H NMR (400 MHz, $CDCl_3$) spectrum of **16**

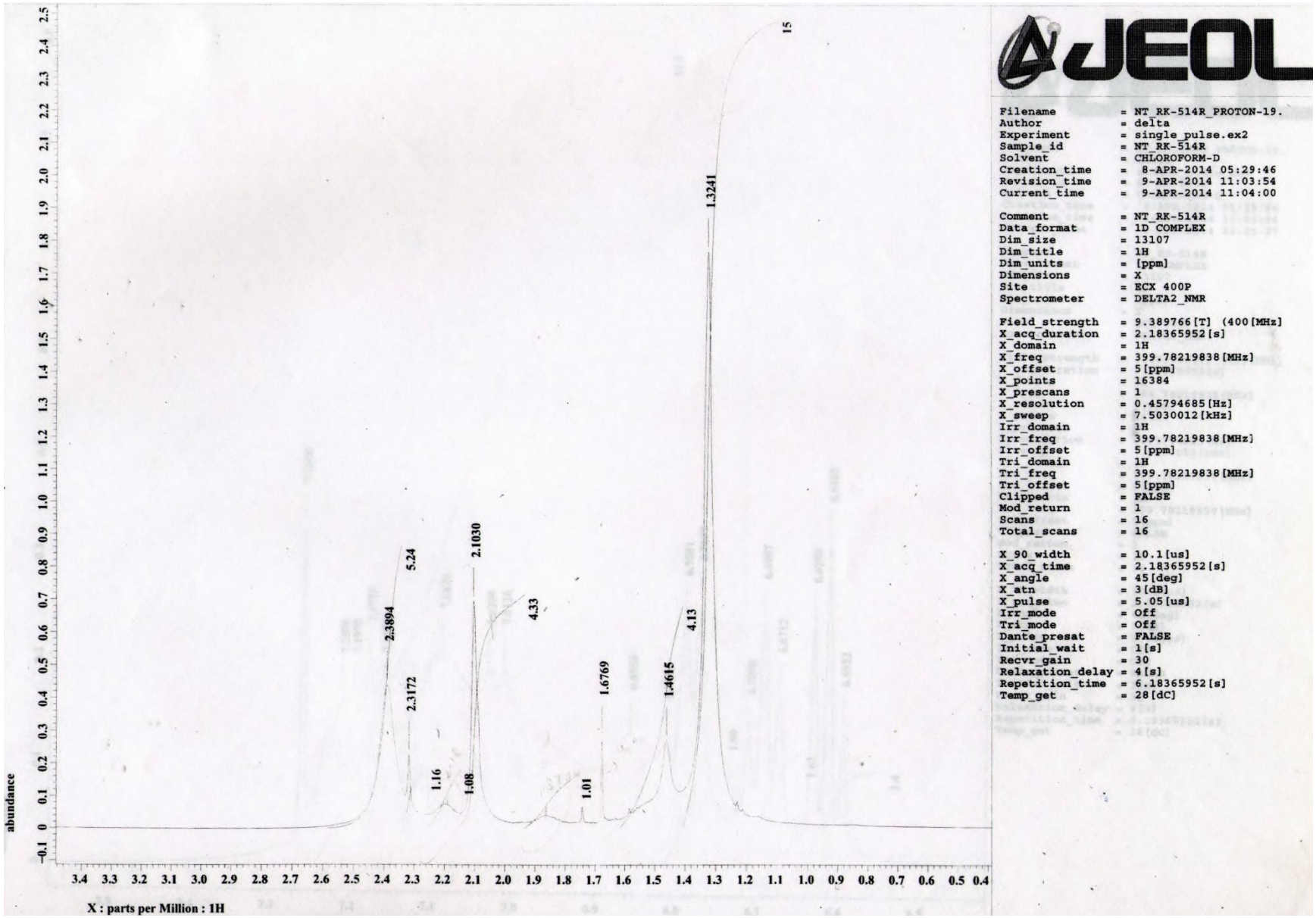

Fig. S84 ^{1}H NMR (400 MHz, $CDCl_3$) spectrum of **16** in the indicated region

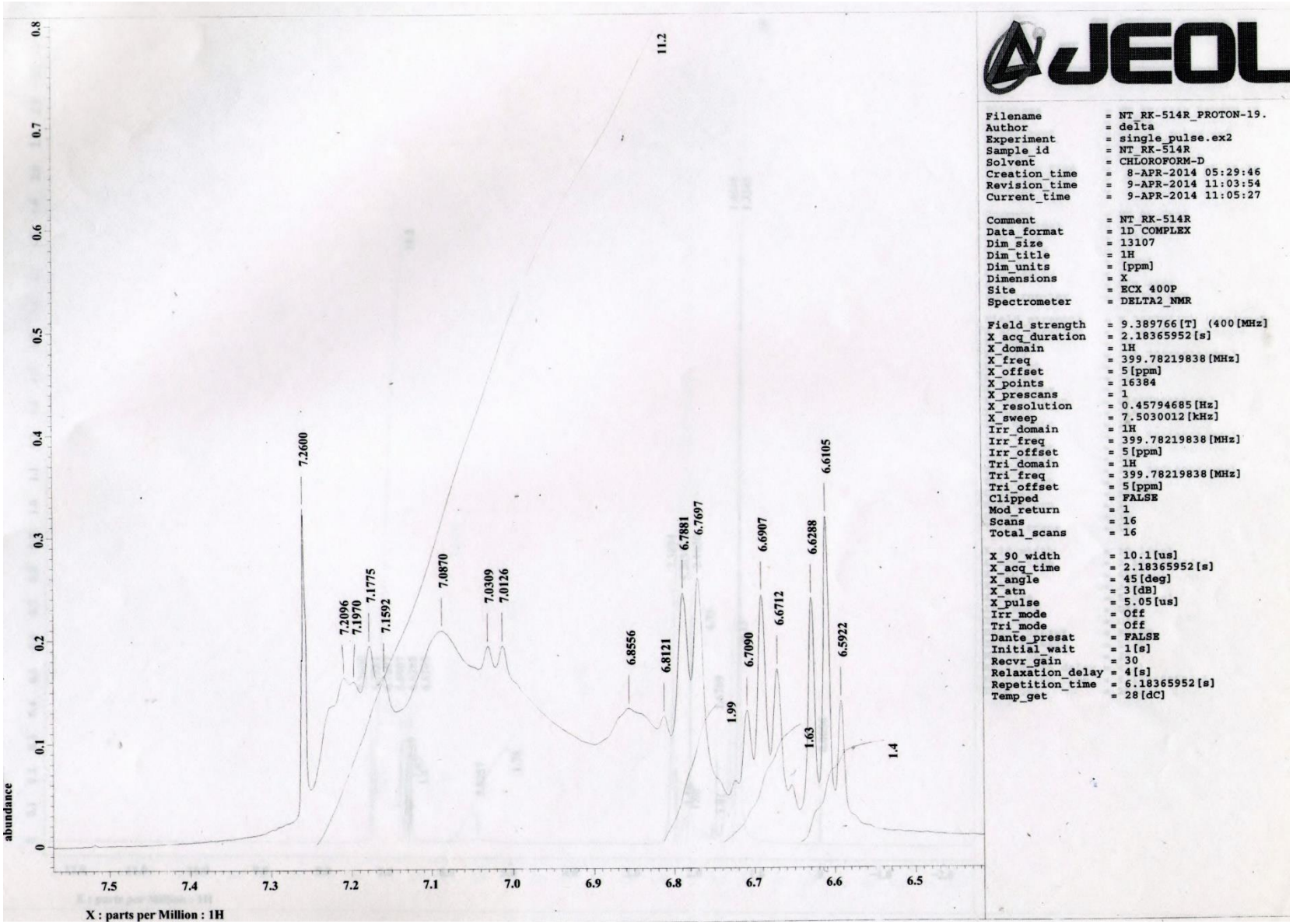

Fig. S85 ^{1}H NMR (400 MHz, $CDCl_3$) spectrum of **16** in the indicated region

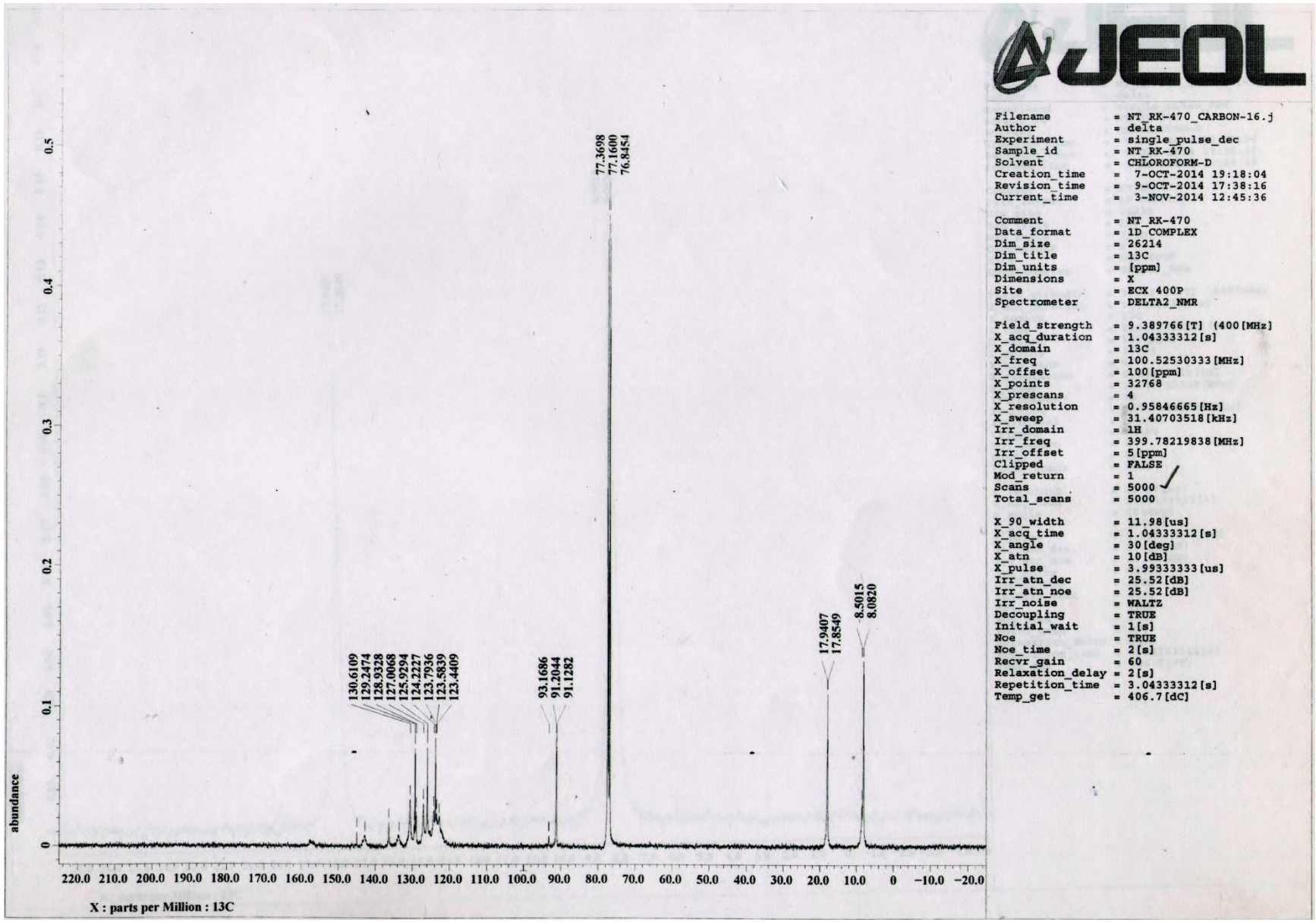

Fig. S86 ^{13}C NMR (100.5 MHz, $CDCl_3$) spectrum of **16**

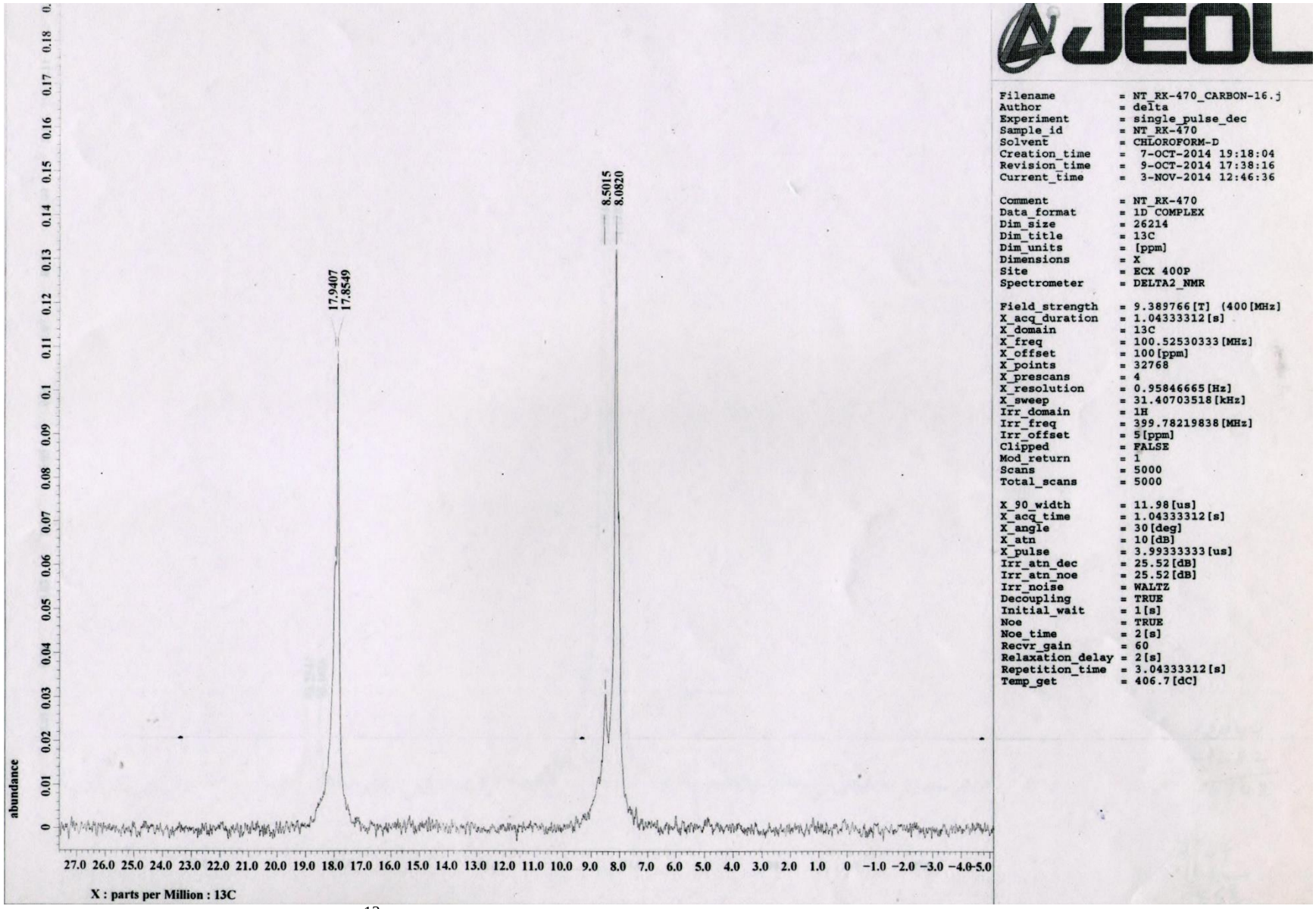

Fig. S87 ^{13}C NMR (100.5 MHz, $CDCl_3$) spectrum of **16** in the indicated region

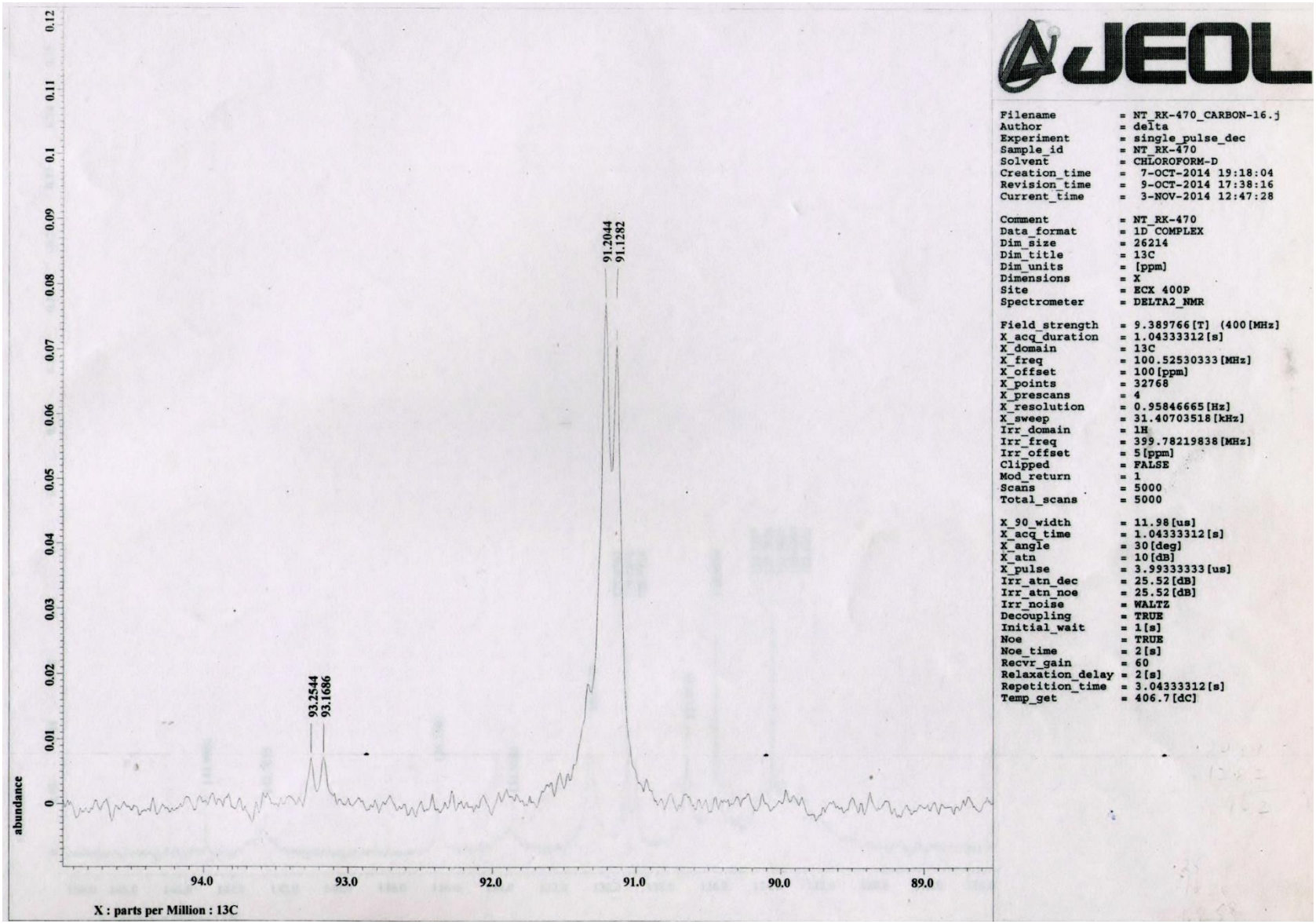

Fig. S88 ^{13}C NMR (100.5 MHz, $CDCl_3$) spectrum of **16** in the indicated region

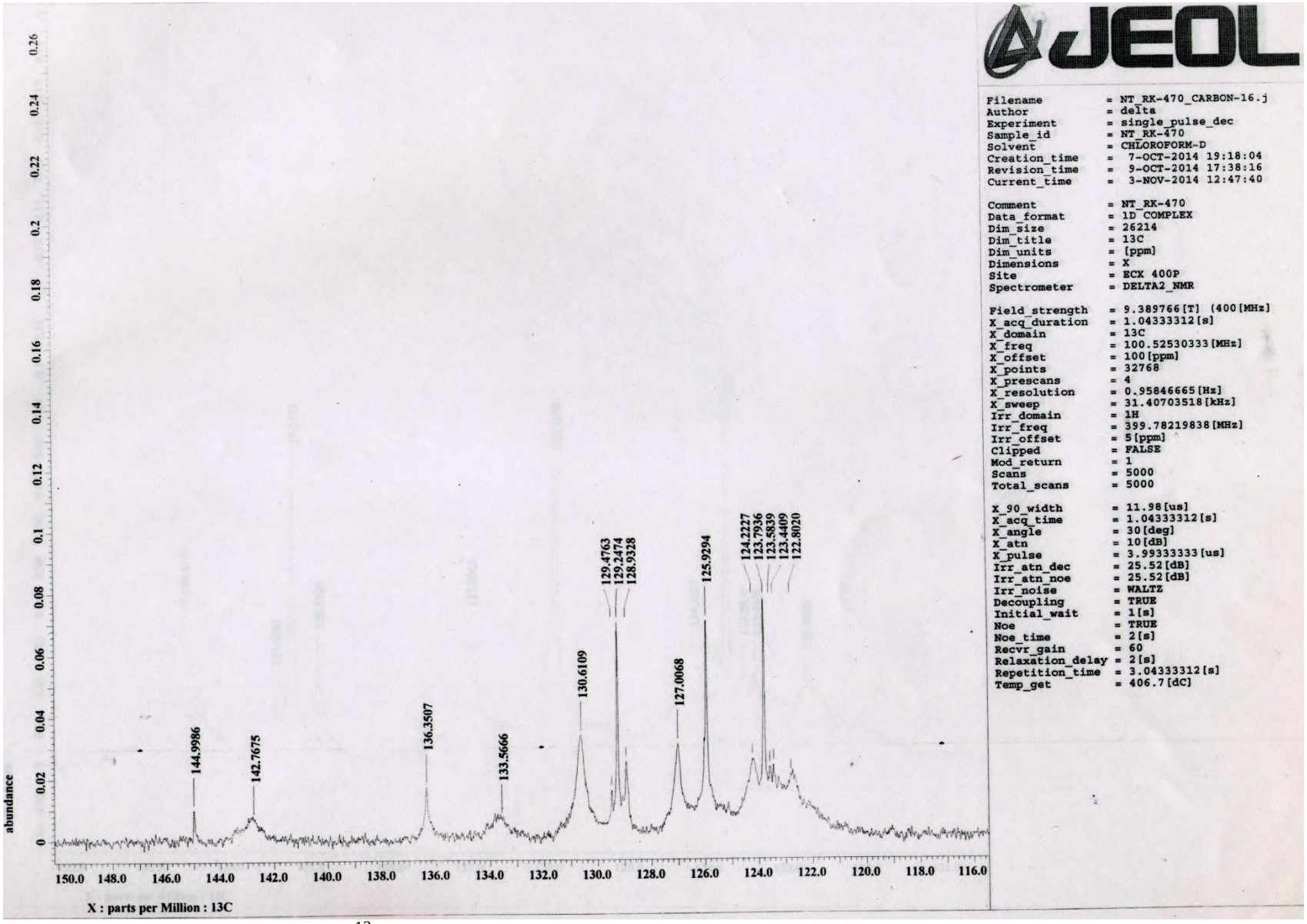

Fig. S89 ^{13}C NMR (100.5 MHz, $CDCl_3$) spectrum of **16** in the indicated region

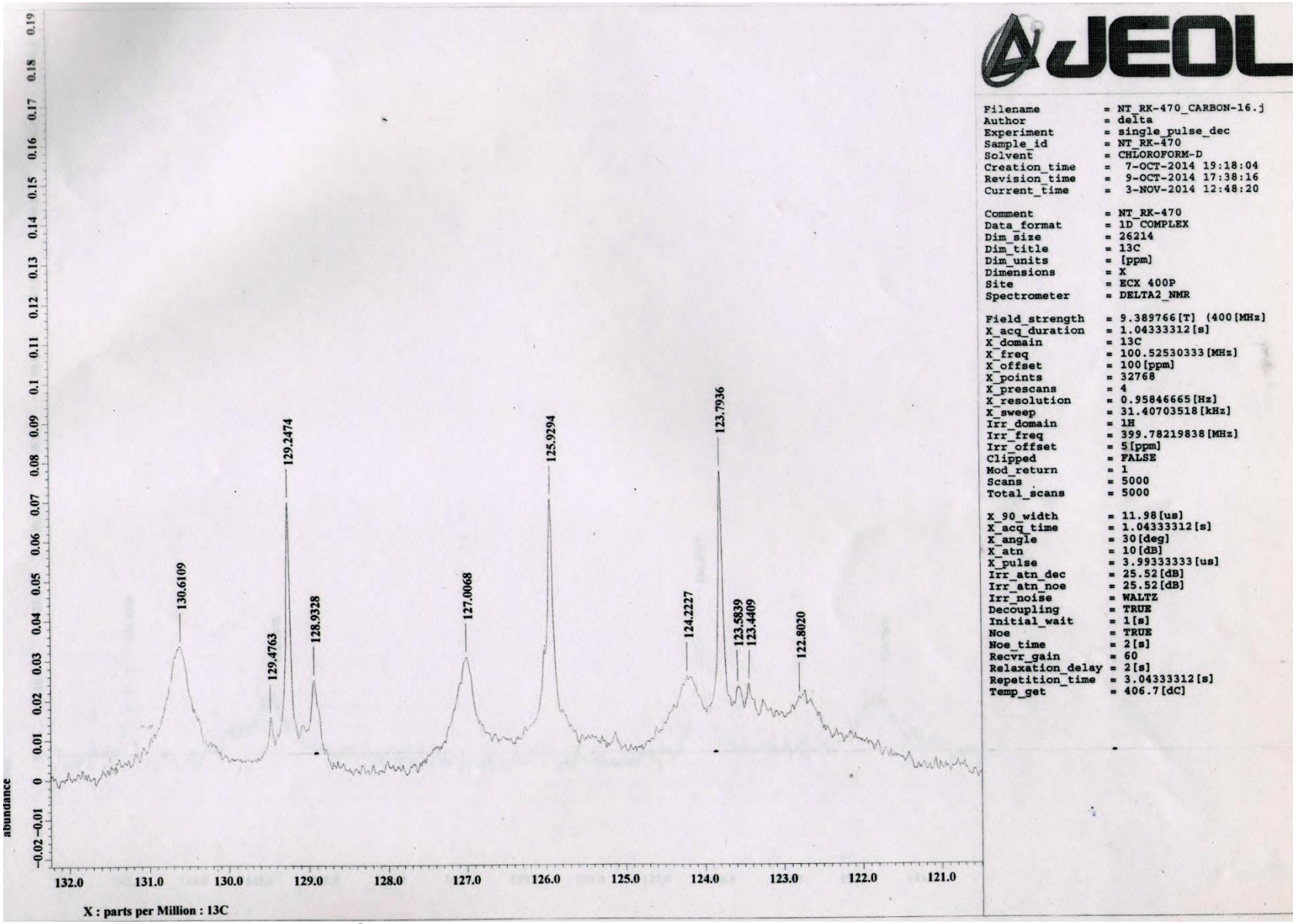

Fig. S90 ^{13}C NMR (100.5 MHz, $CDCl_3$) spectrum of **16** in the indicated region

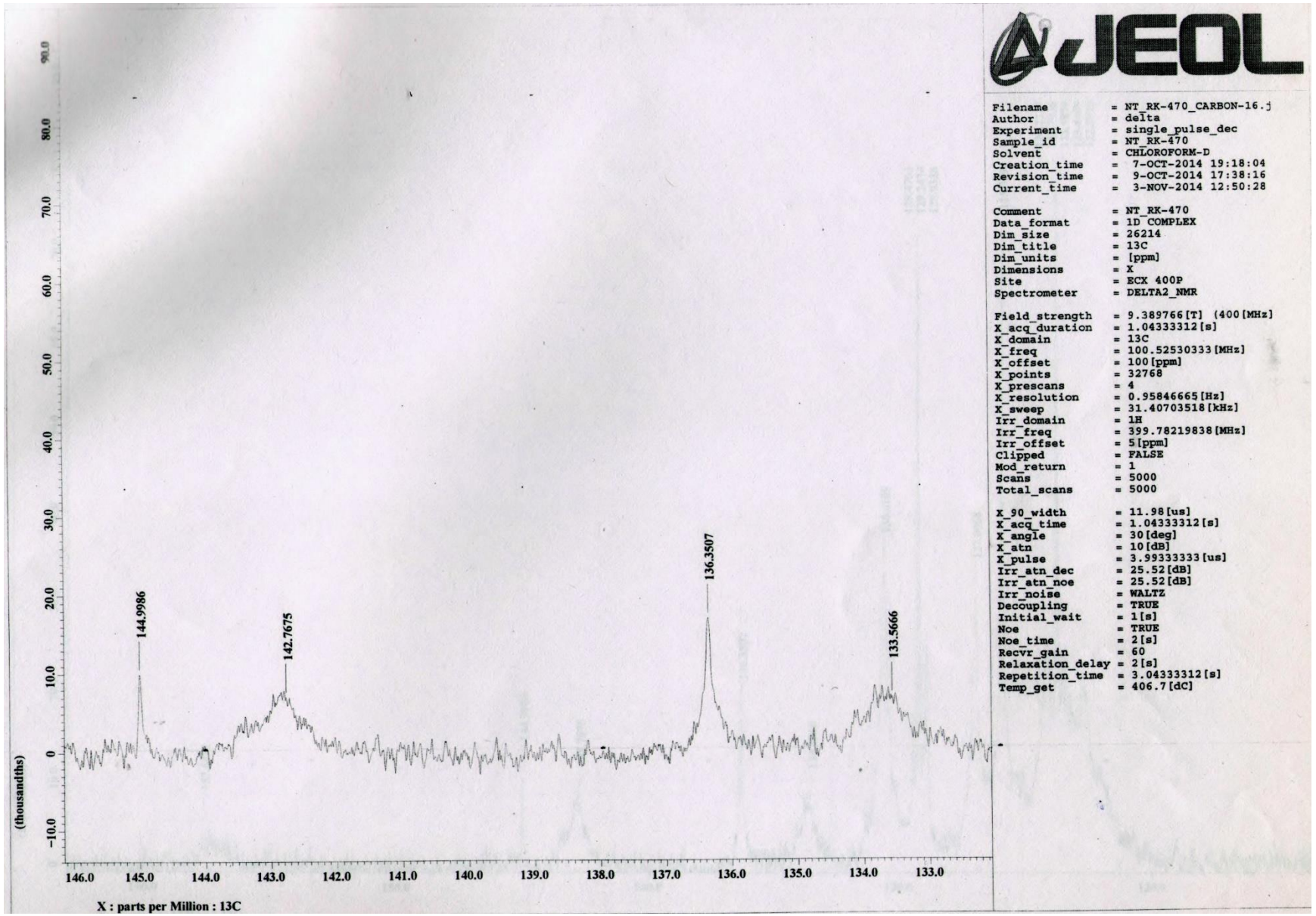

Fig. S91 ^{13}C NMR (100.5 MHz, $CDCl_3$) spectrum of **16** in the indicated region

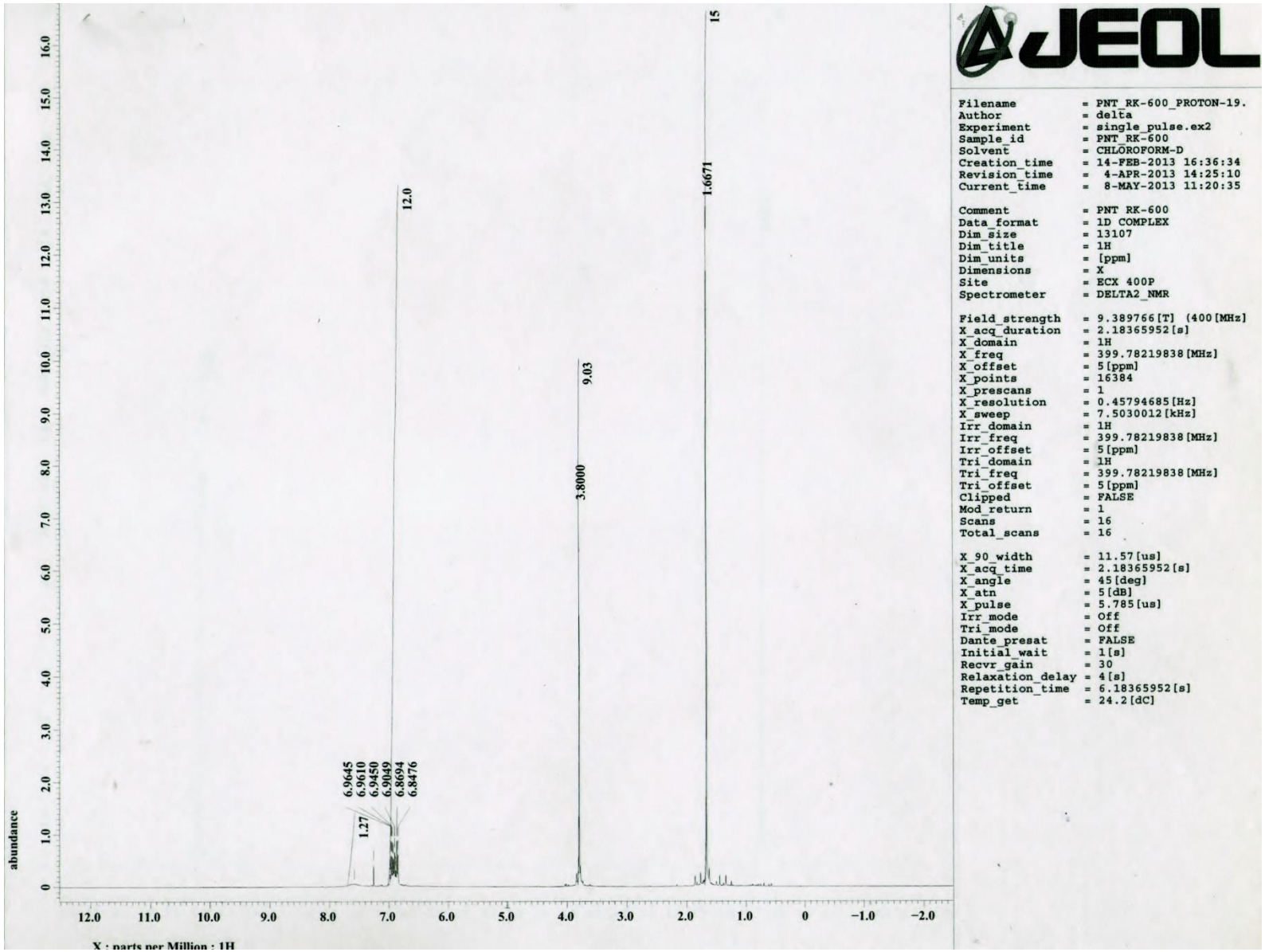

Fig. S92 ^{1}H NMR (400 MHz, $CDCl_3$) spectrum of **17**

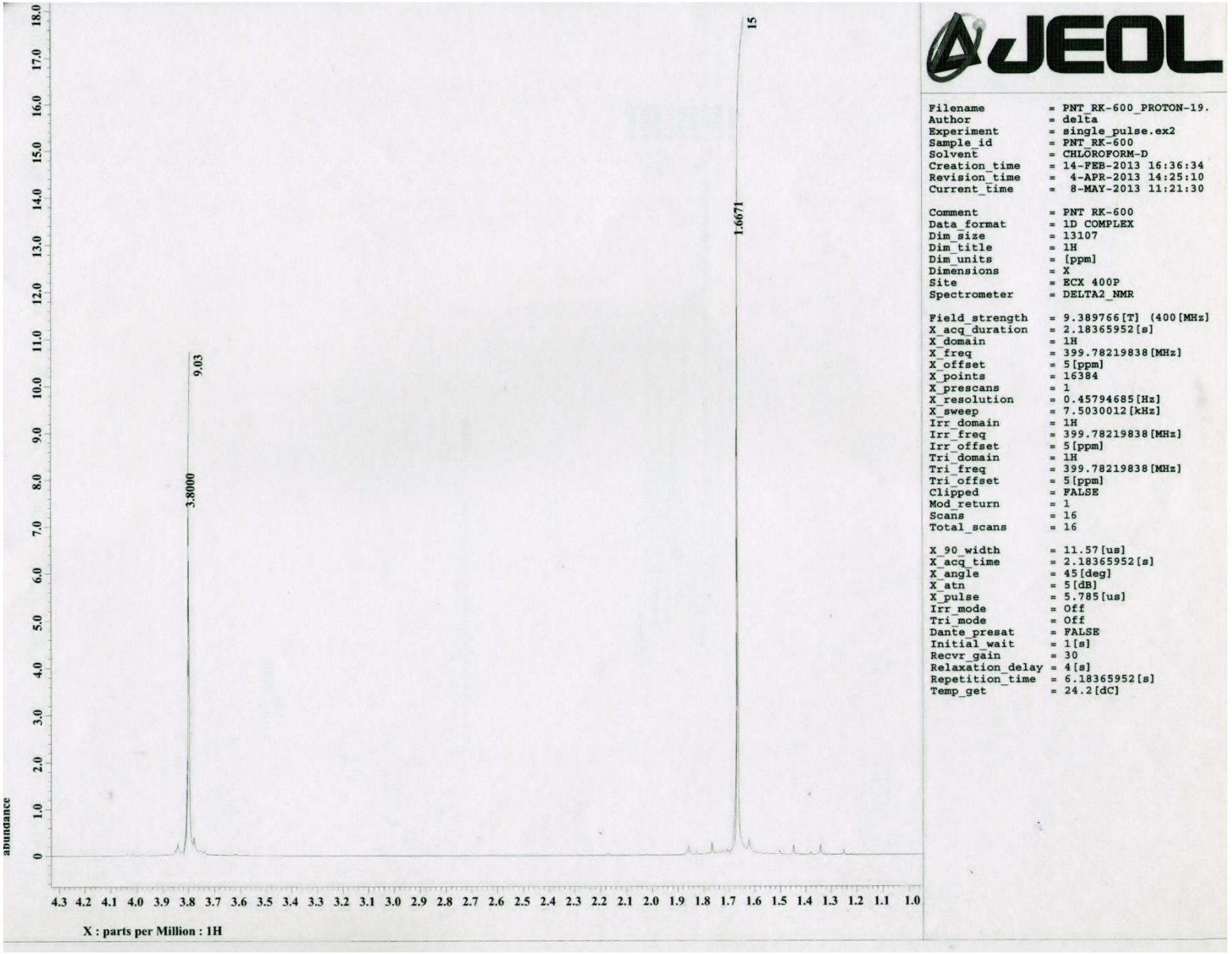

Fig. S93 ^{1}H NMR (400 MHz, $CDCl_3$) spectrum of **17** in the indicated region

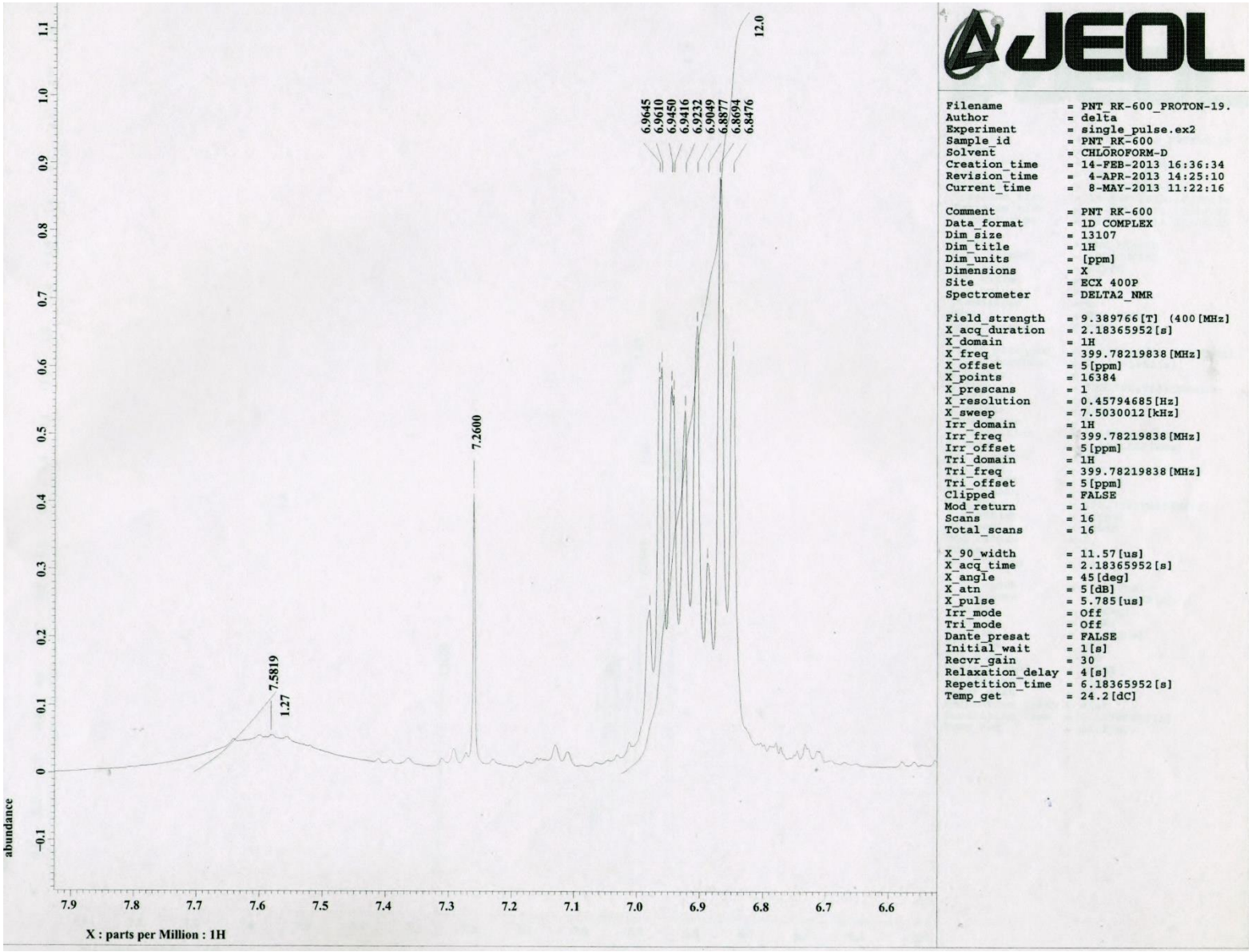

Fig. S94 ^{1}H NMR (400 MHz, $CDCl_3$) spectrum of **17** in the indicated region

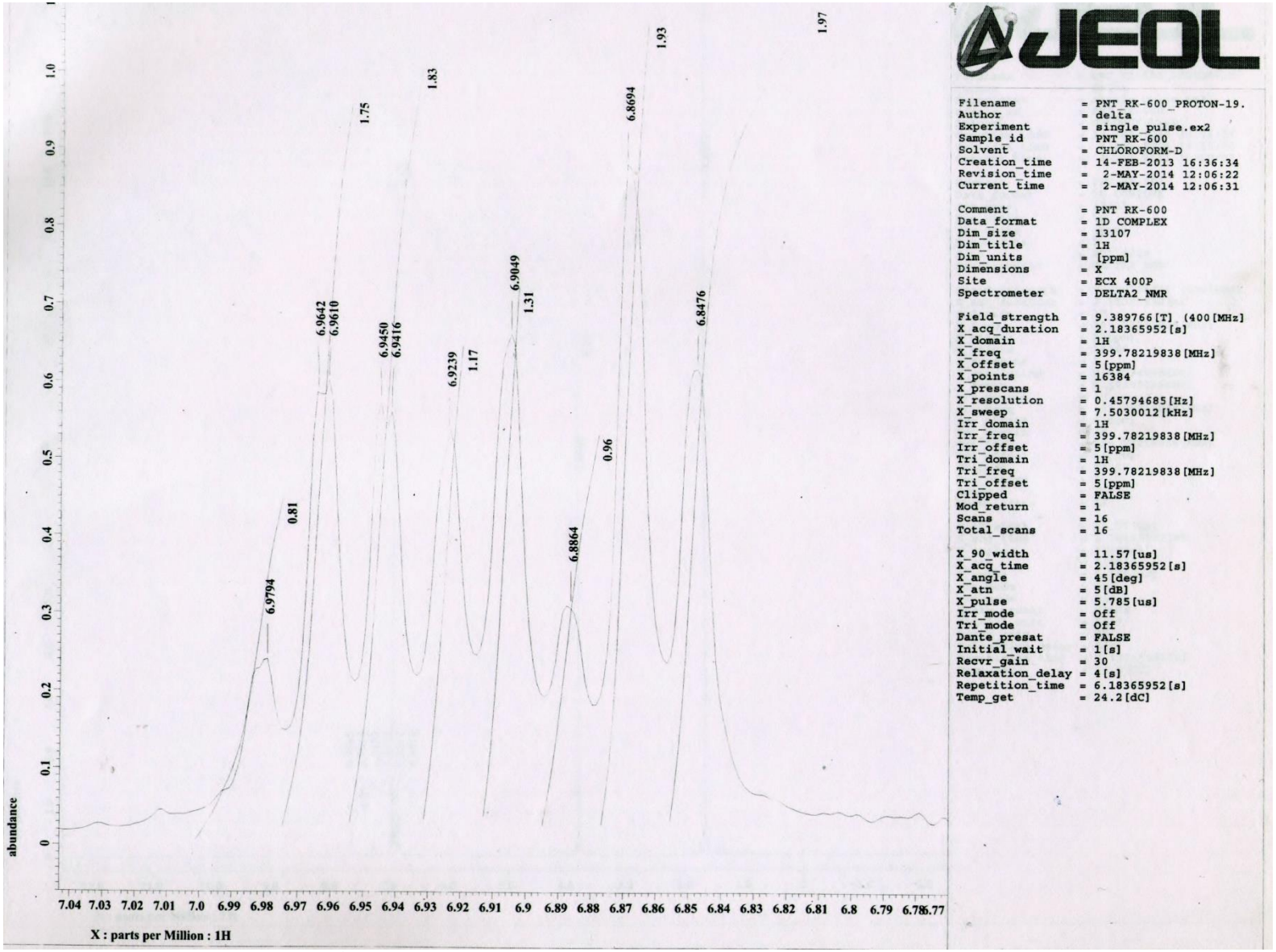

Fig. S95 ^{1}H NMR (400 MHz, $CDCl_3$) spectrum of **17** in the indicated region

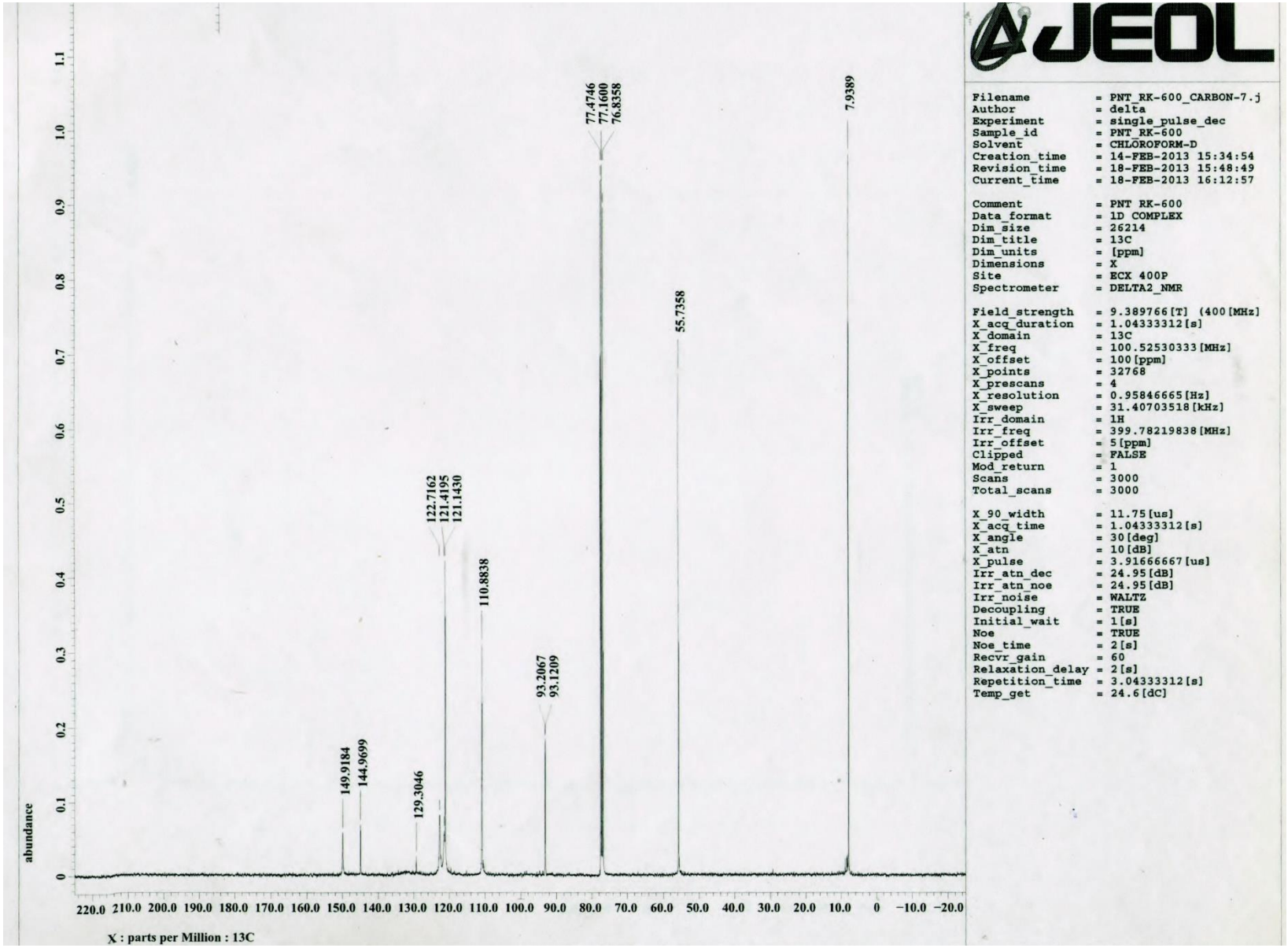

Fig. S96 ^{13}C NMR (100.5 MHz, $CDCl_3$) spectrum of **17**

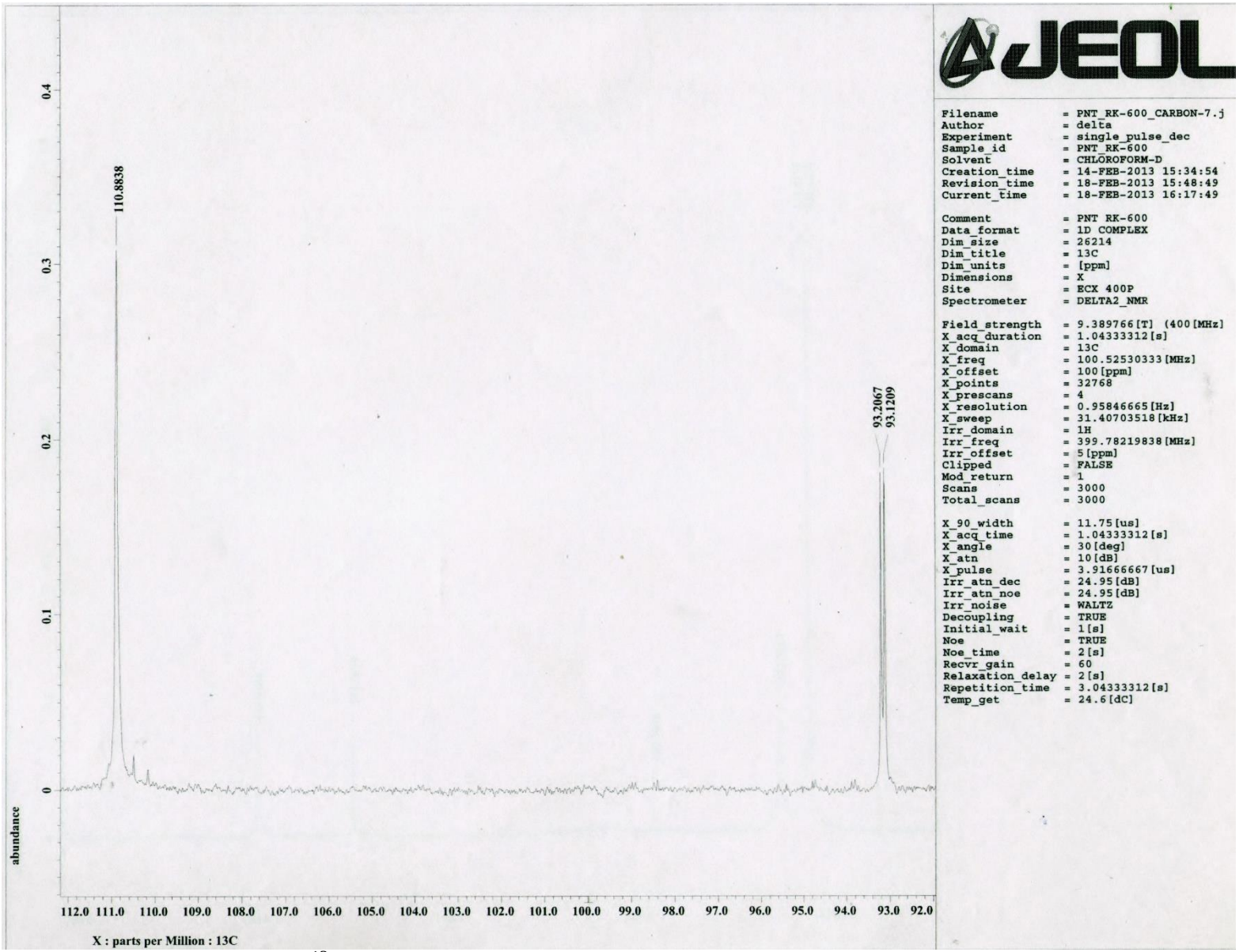

Fig. S97 ^{13}C NMR (100.5 MHz, $CDCl_3$) spectrum of **17** in the indicated region

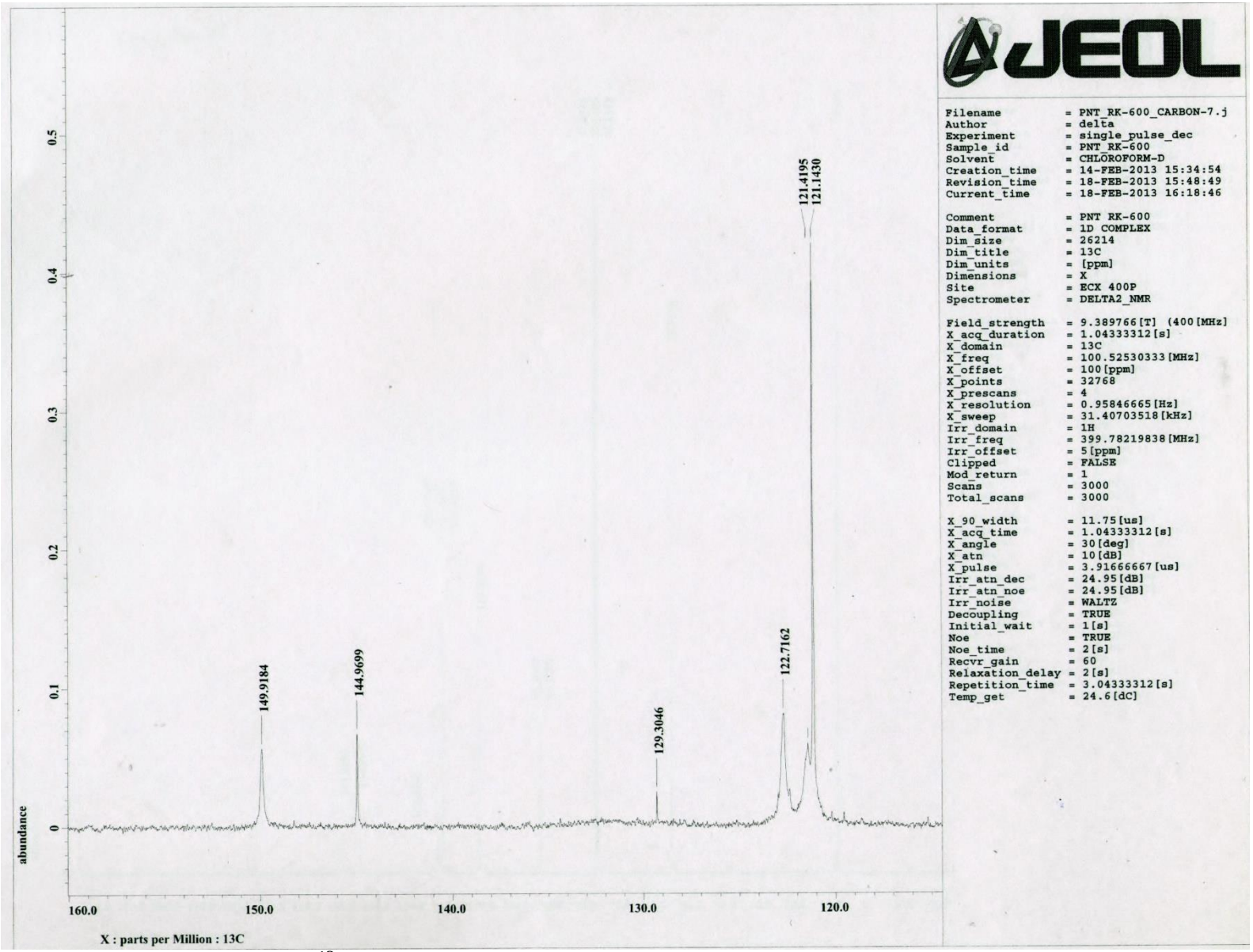

Fig. S98 ^{13}C NMR (100.5 MHz, $CDCl_3$) spectrum of **17** in the indicated region

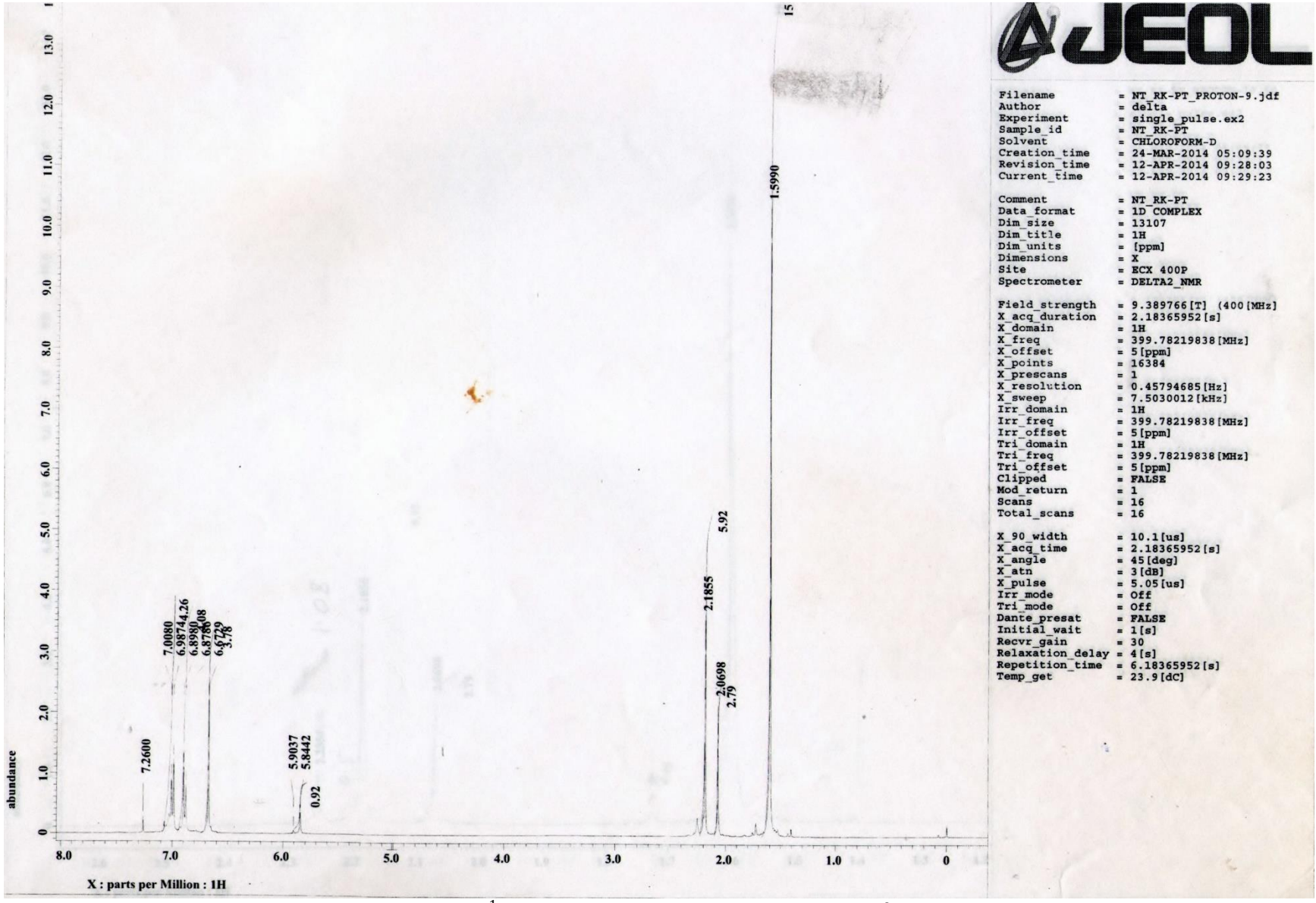

Fig. S99 ^{1}H NMR (400 MHz, $CDCl_3$) spectrum of **18**

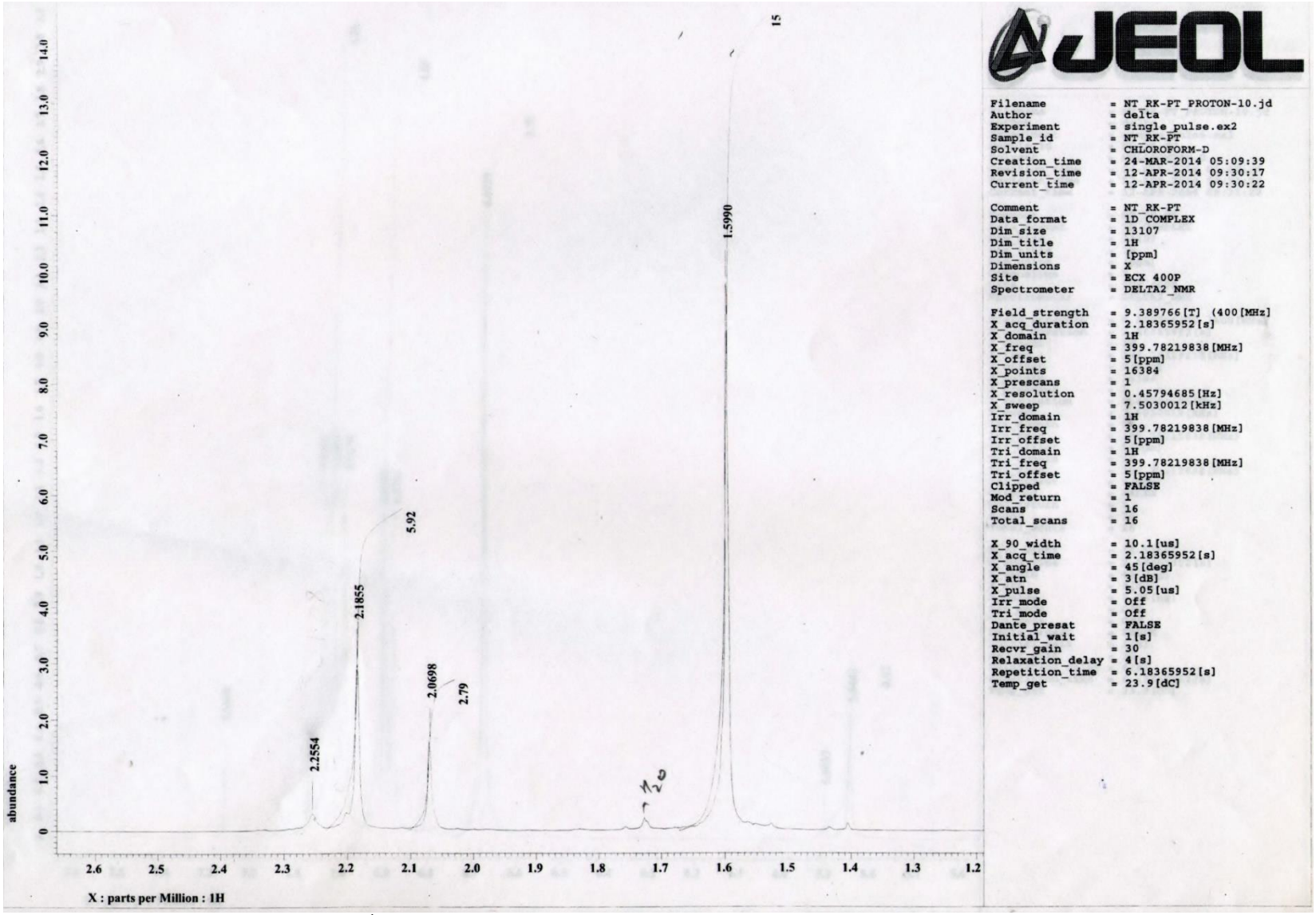

Fig. S100 ^{1}H NMR (400 MHz, $CDCl_3$) spectrum of **18** in the indicated region

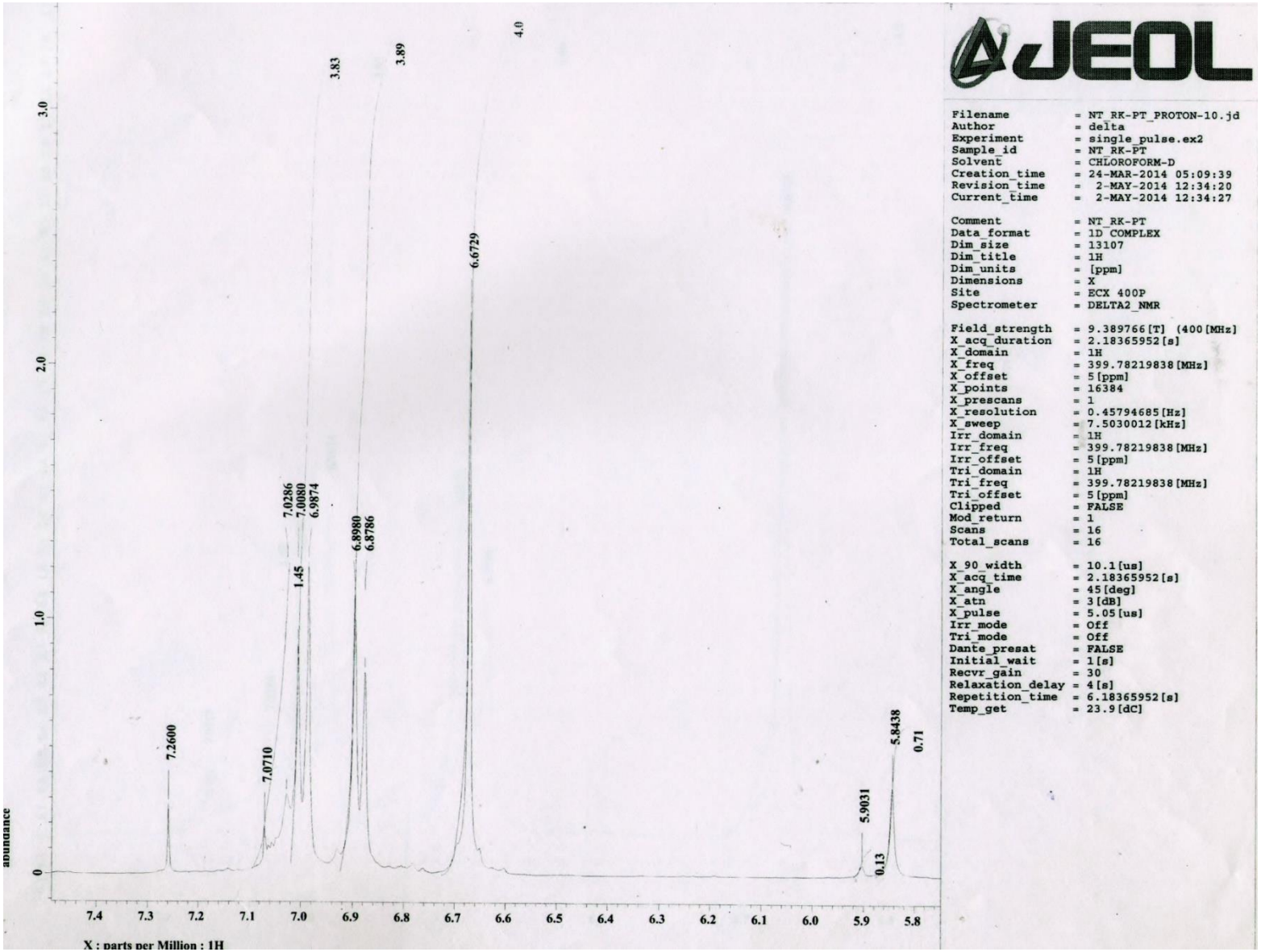

Fig. S101 ^{1}H NMR (400 MHz, $CDCl_3$) spectrum of **18** in the indicated region

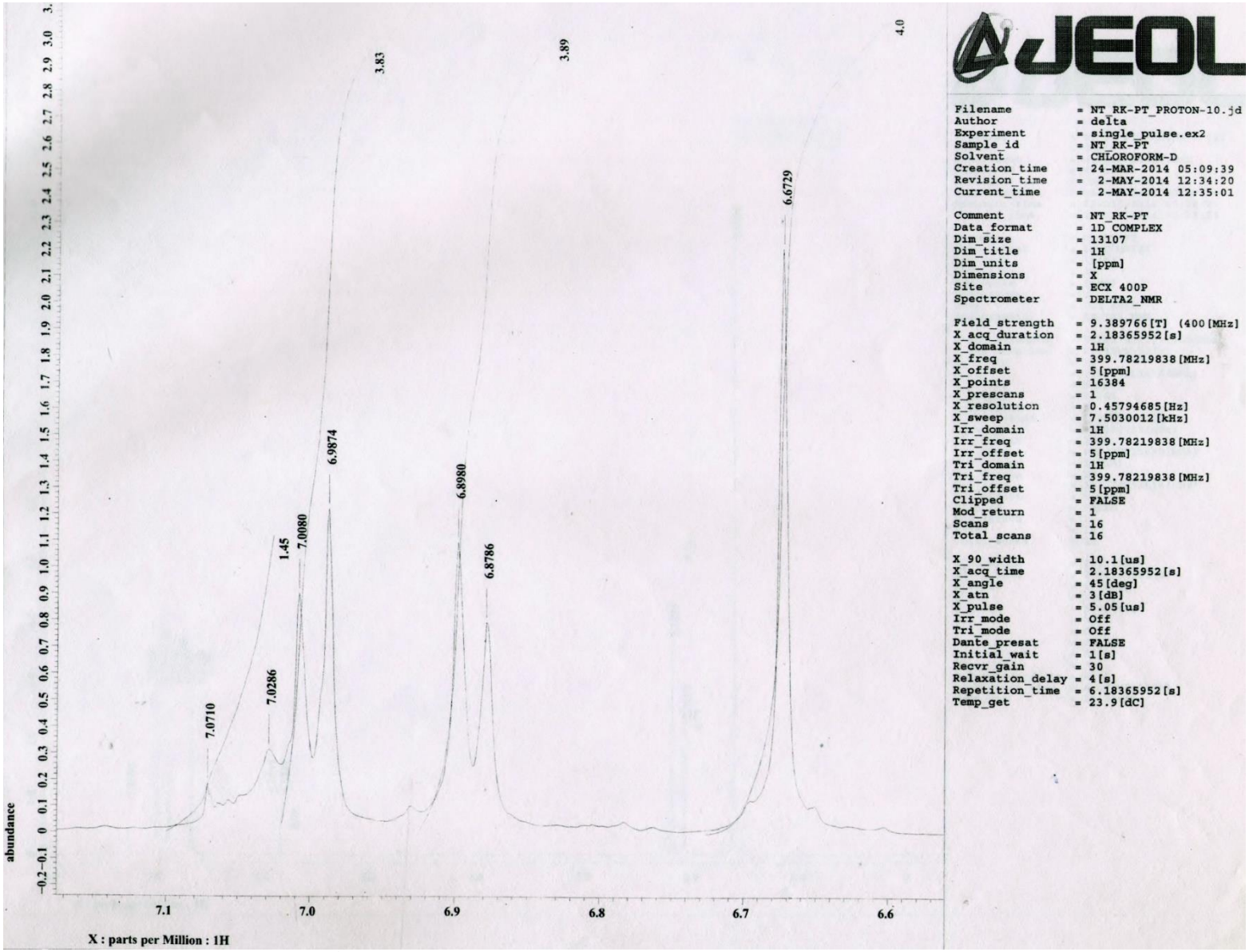

Fig. S102 ^{1}H NMR (400 MHz, $CDCl_3$) spectrum of **18** in the indicated region

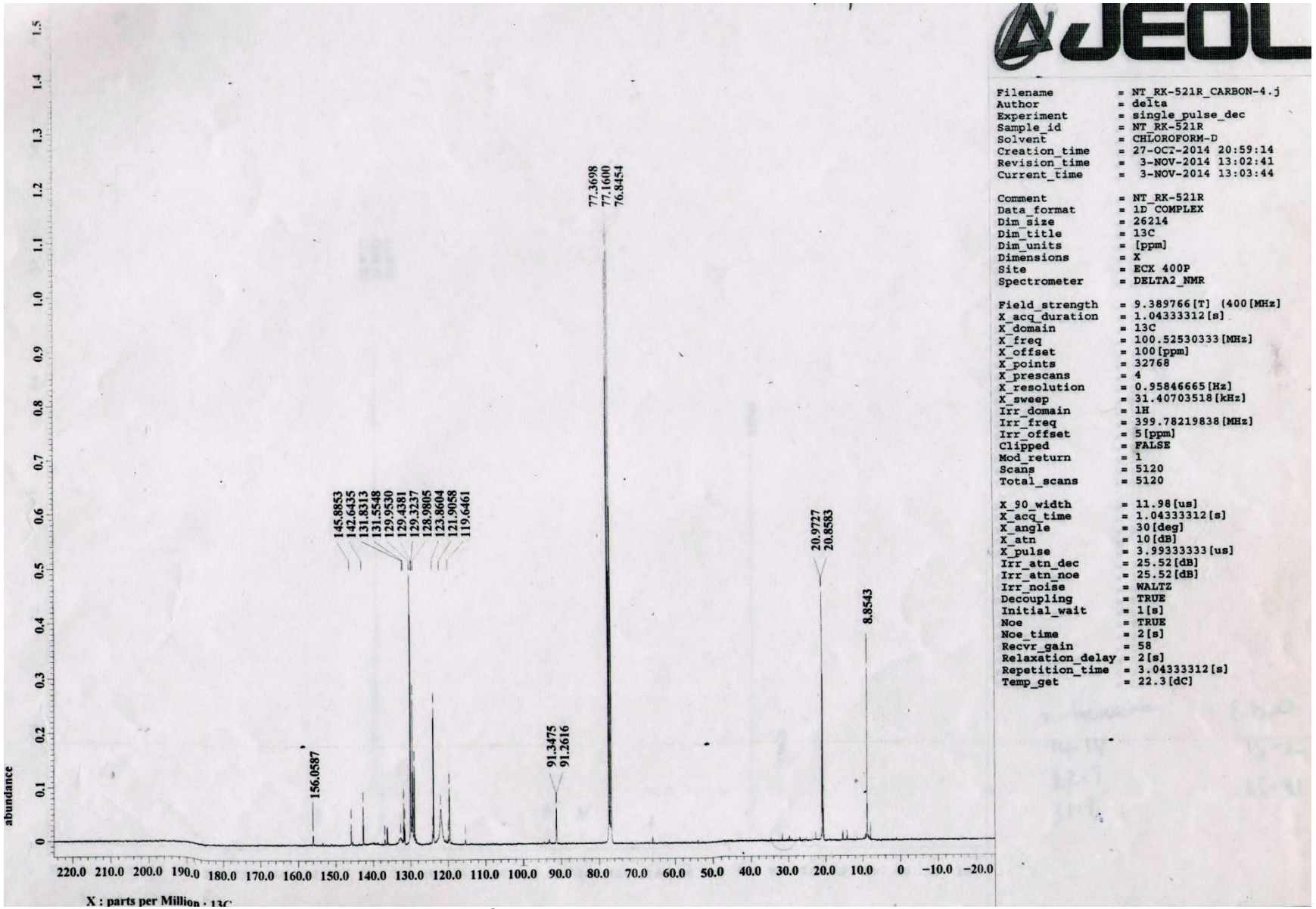

Fig. S103 ^{13}C NMR (100.5 MHz, $CDCl_3$) spectrum of **18**

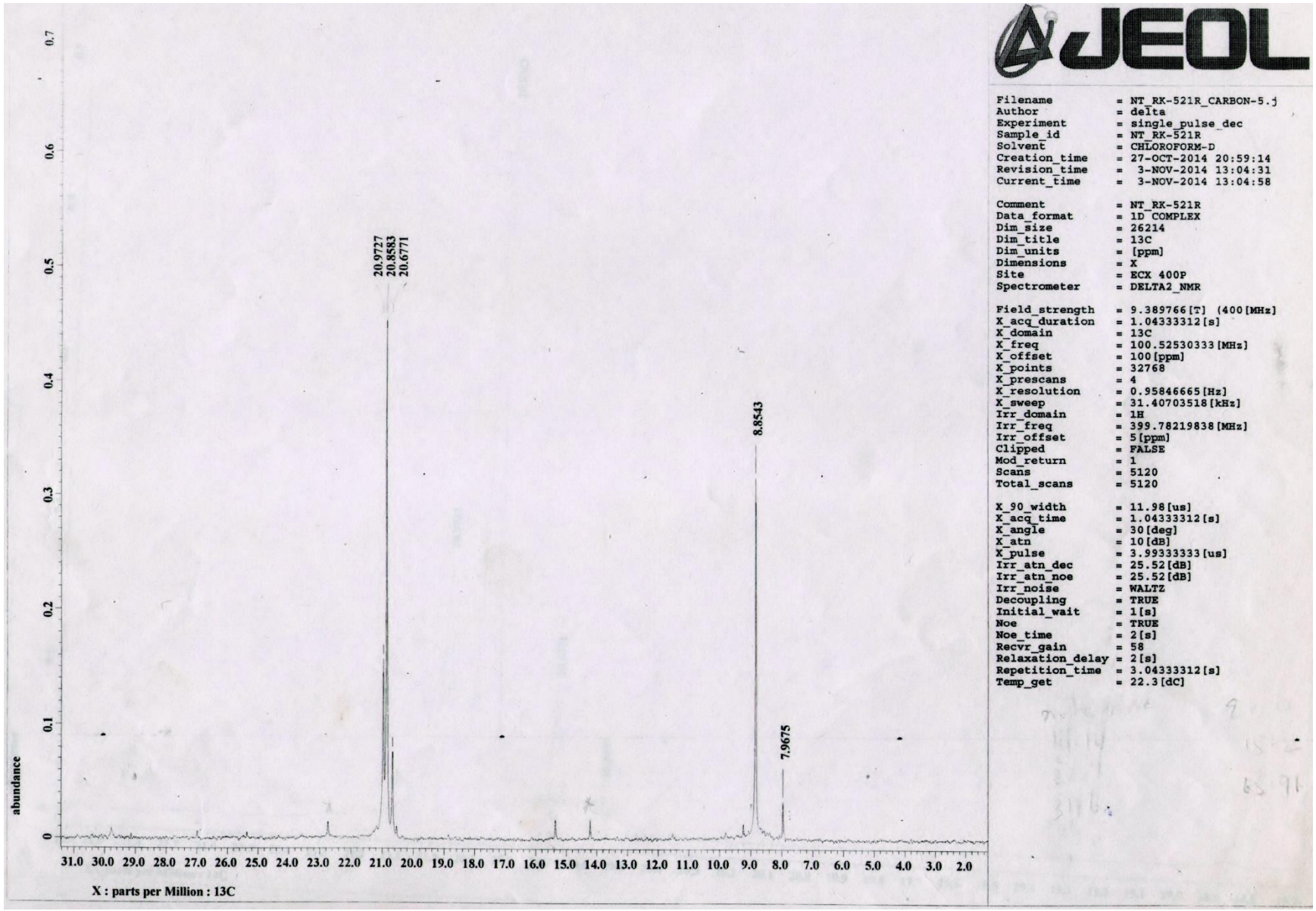

Fig. S104 ^{13}C NMR (100.5 MHz, $CDCl_3$) spectrum of **18** in the indicated region

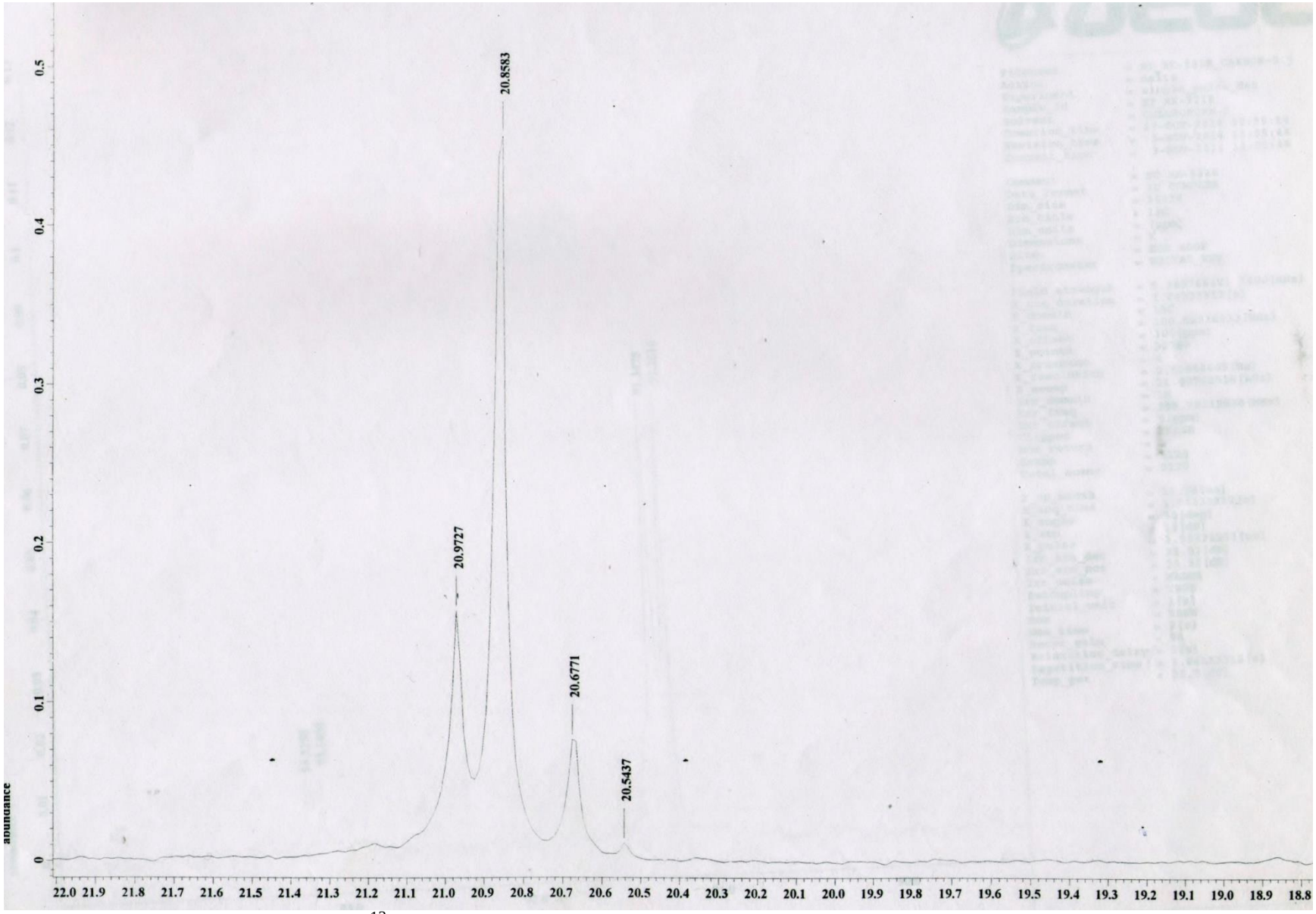

Fig. S105 ^{13}C NMR (100.5 MHz, $CDCl_3$) spectrum of **18** in the indicated region

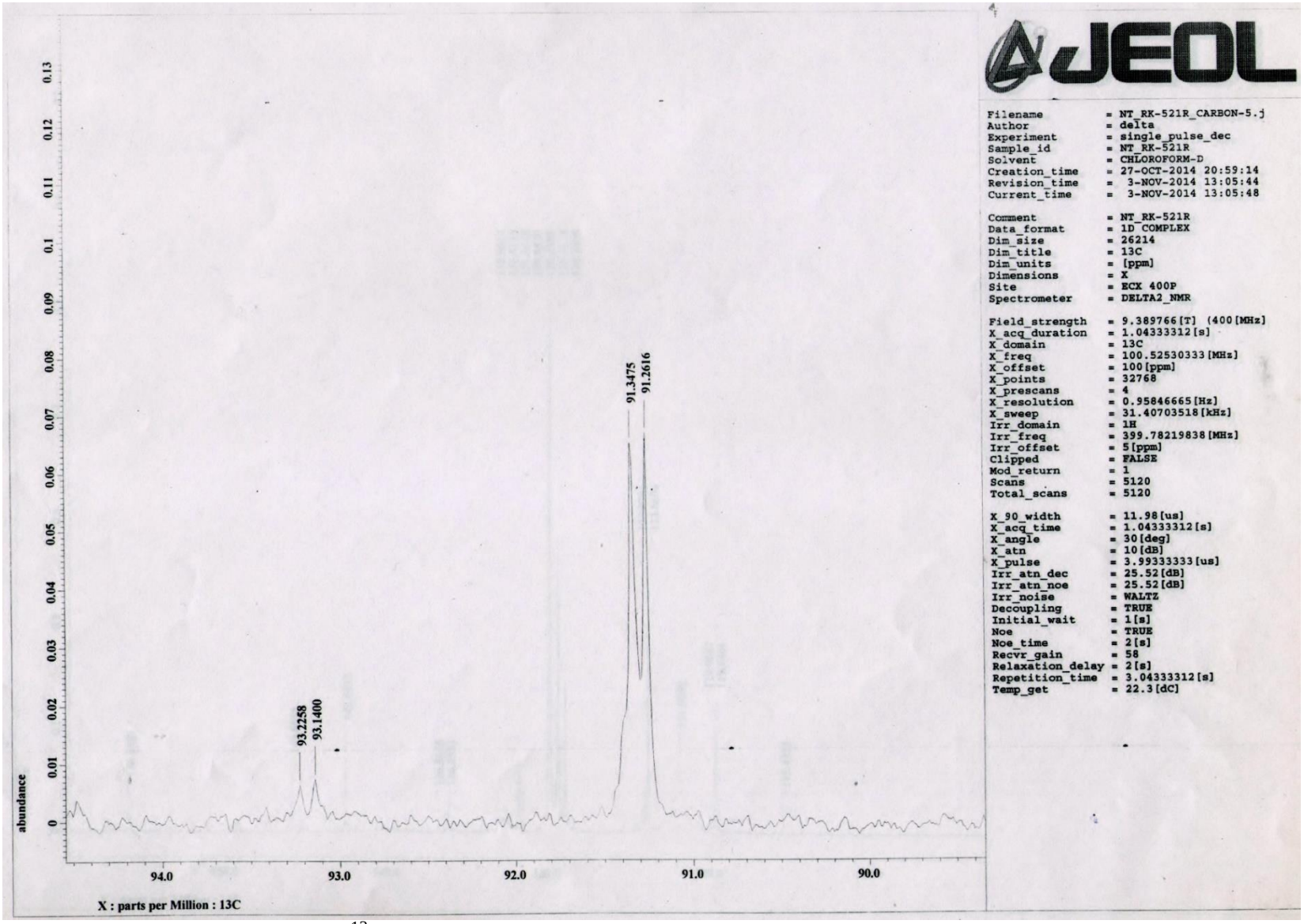

Fig. S106 ^{13}C NMR (100.5 MHz, $CDCl_3$) spectrum of **18** in the indicated region

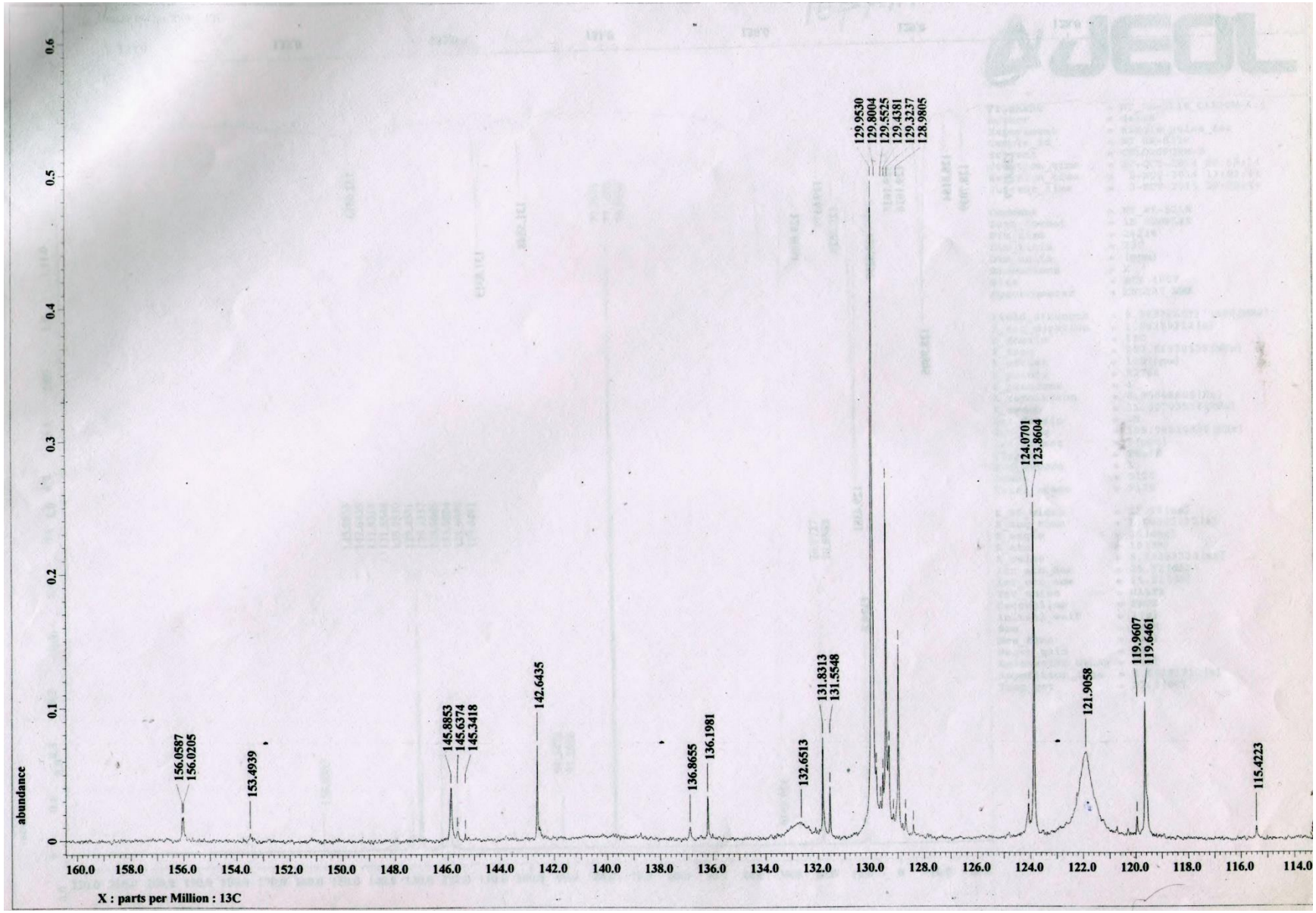

Fig. S107 ^{13}C NMR (100.5 MHz, $CDCl_3$) spectrum of **18** in the indicated region

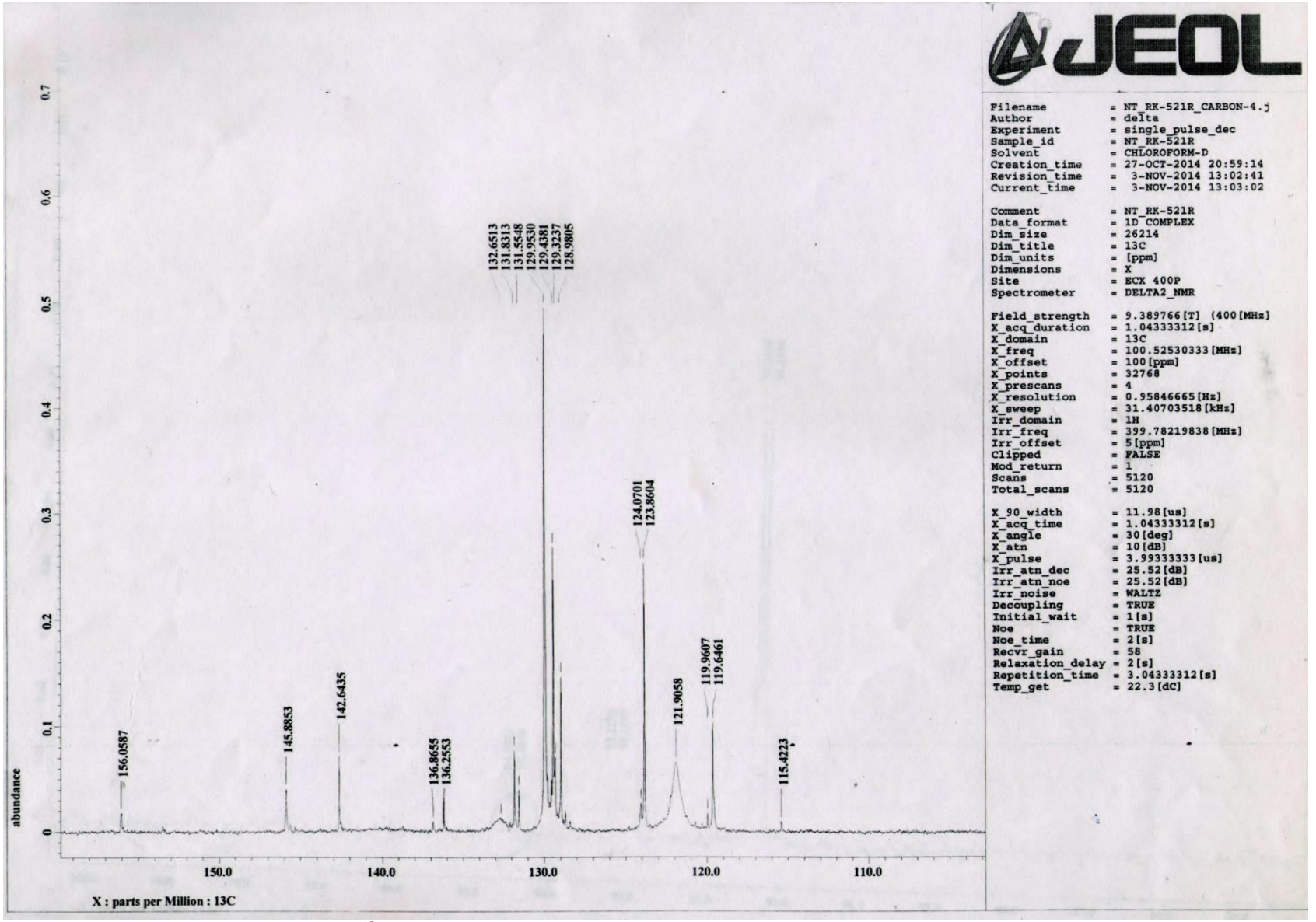

Fig. S108 ^{13}C NMR (100.5 MHz, $CDCl_3$) spectrum of **18** in the indicated region

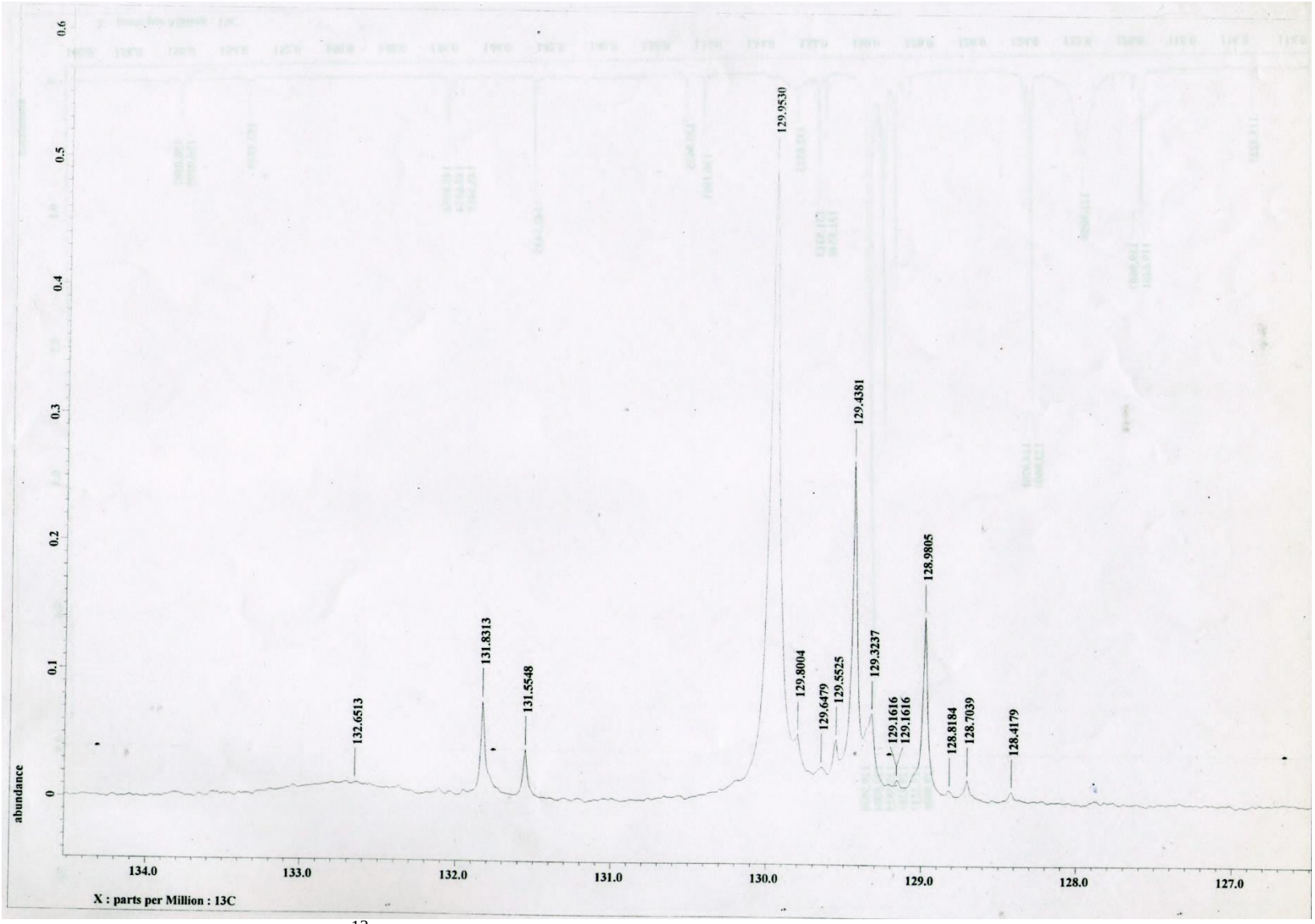

Fig. S109 ^{13}C NMR (100.5 MHz, $CDCl_3$) spectrum of **18** in the indicated region

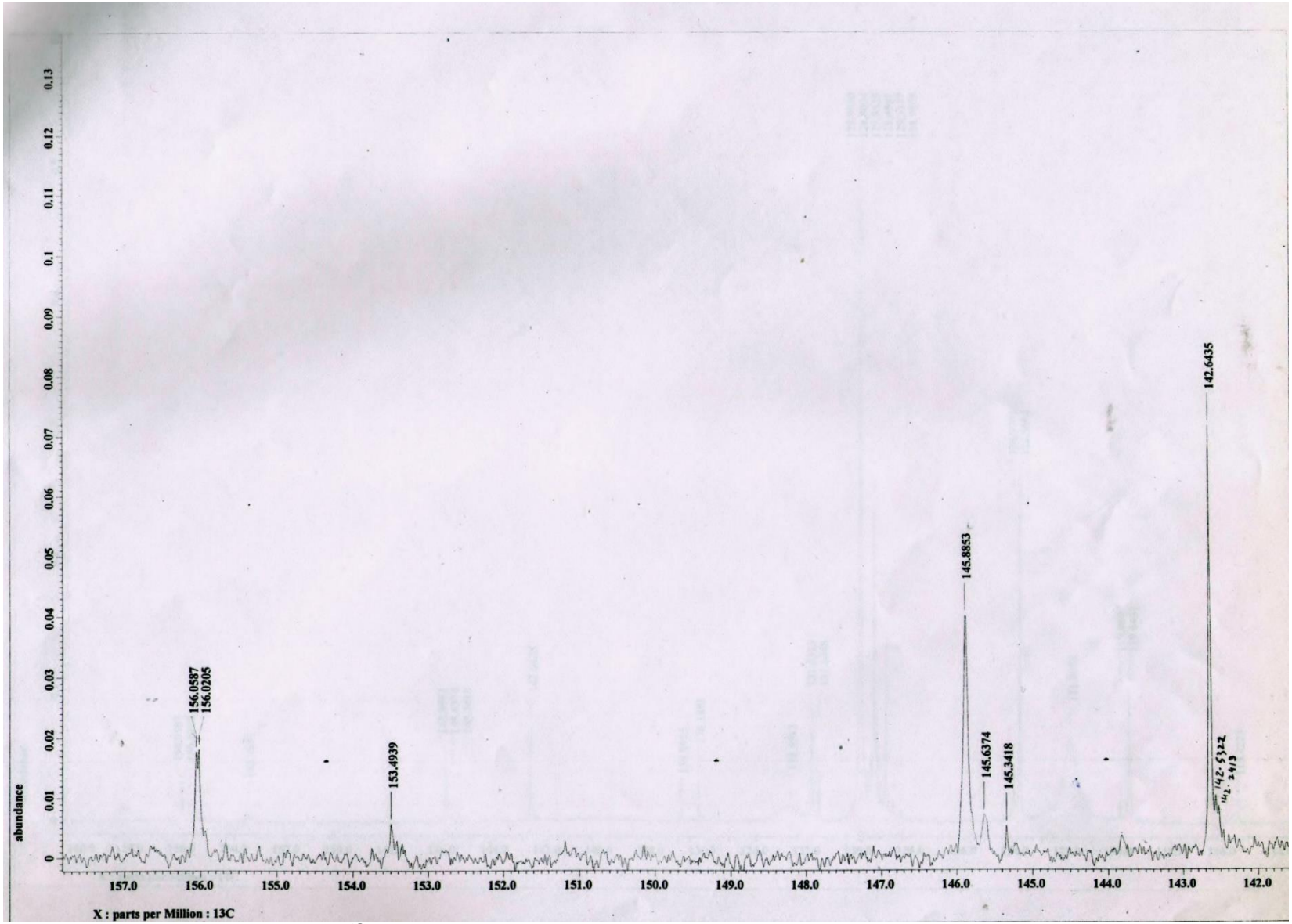

Fig. S110 ^{13}C NMR (100.5 MHz, $CDCl_3$) spectrum of **18** in the indicated region

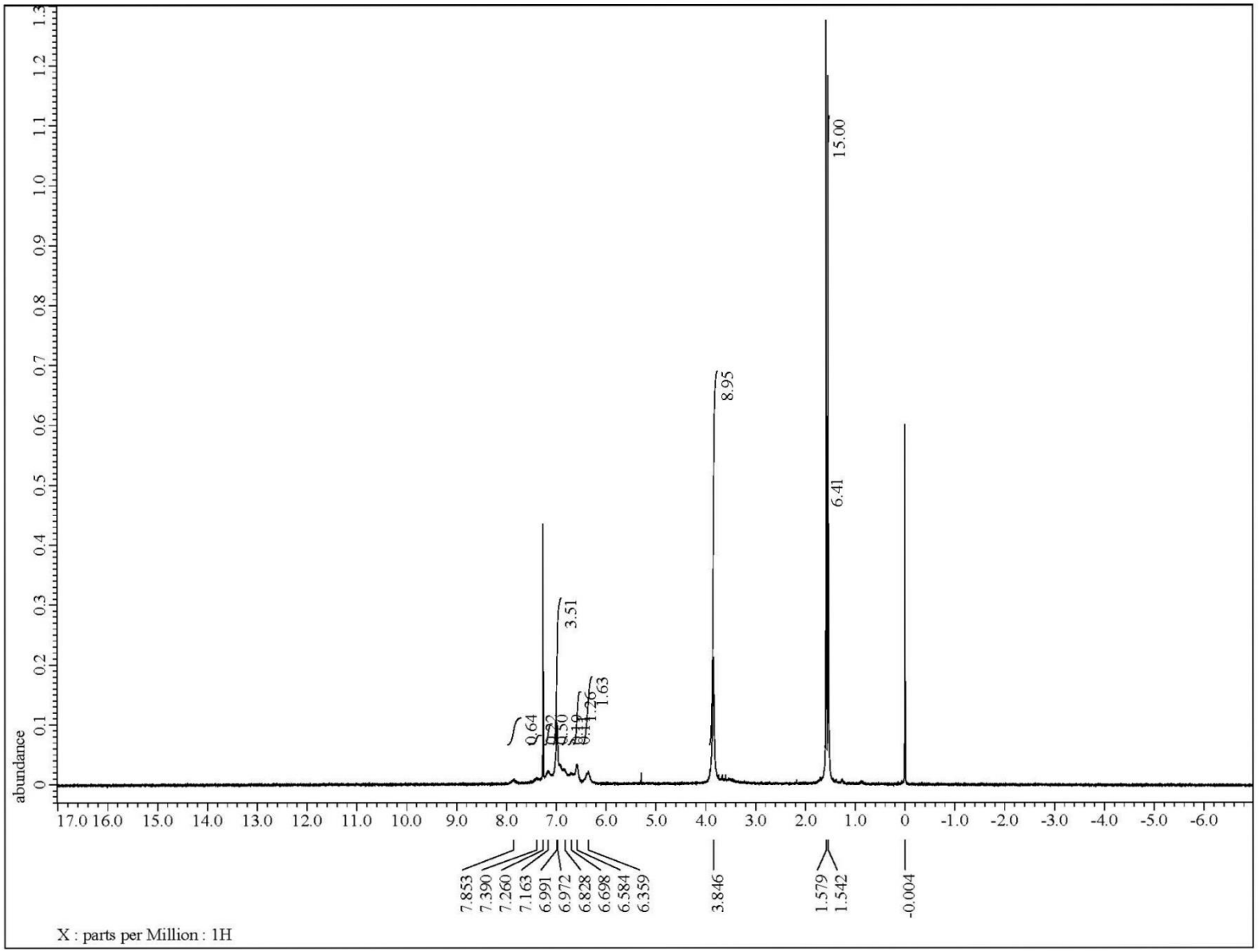

Fig. S111 ^{1}H NMR (400 MHz, $CDCl_3$) spectrum of **19** at 1.23×10^{-1} M concentration

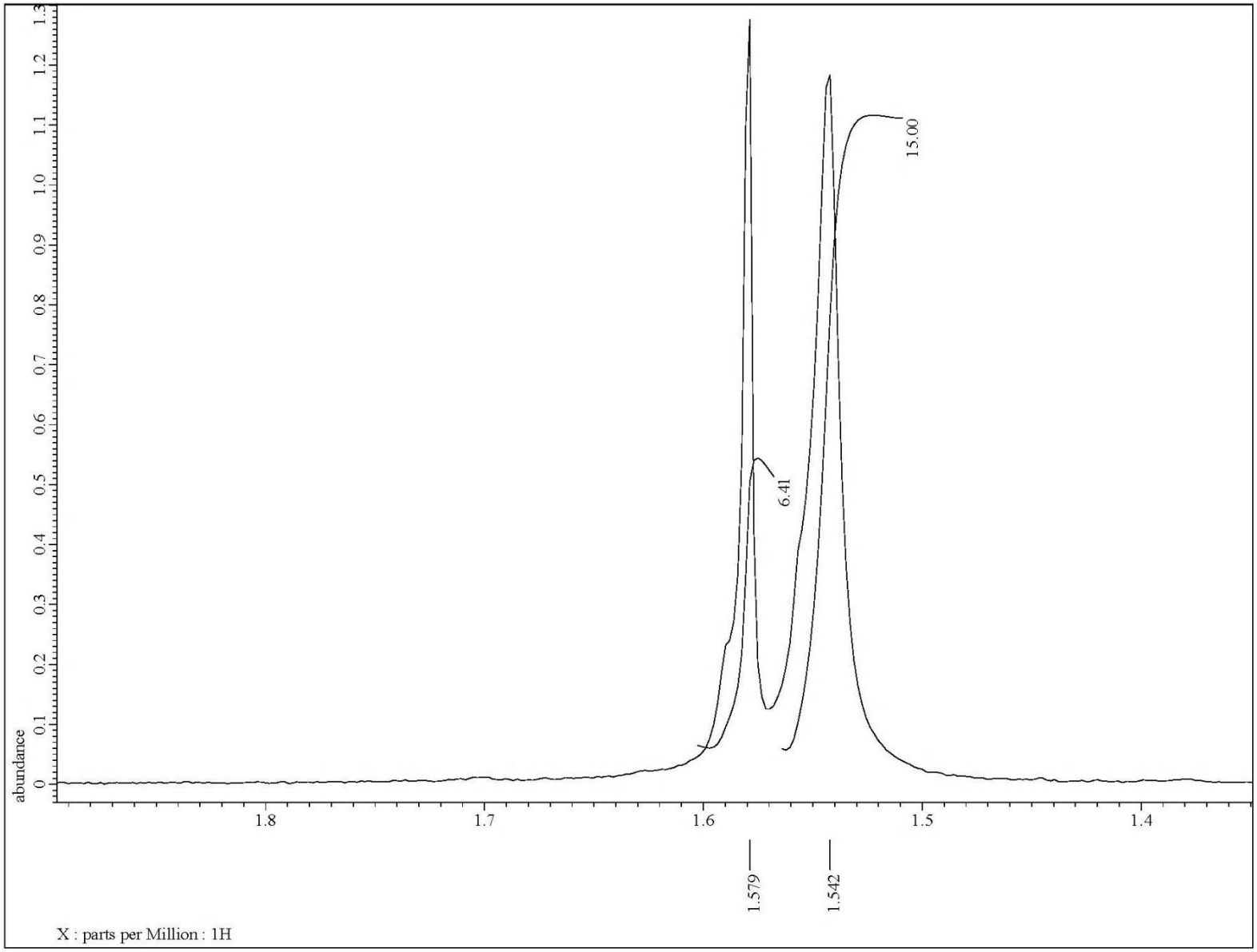

Fig. S112 ^{1}H NMR (400 MHz, $CDCl_3$) spectrum of **19** at 1.23×10^{-1} M concentration in the indicated region

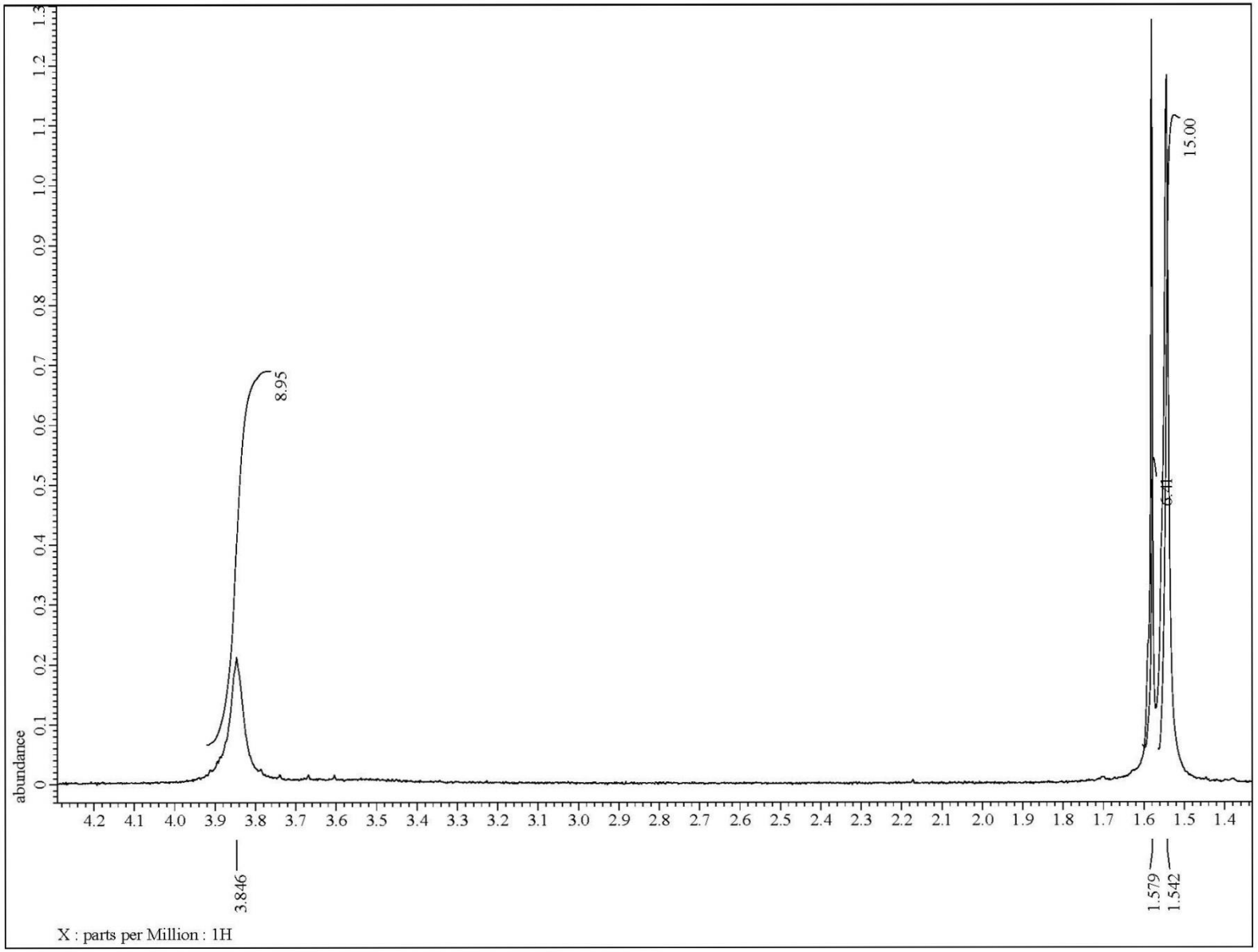

Fig. S113 ^{1}H NMR (400 MHz, $CDCl_3$) spectrum of **19** at 1.23×10^{-1} M concentration in the indicated region

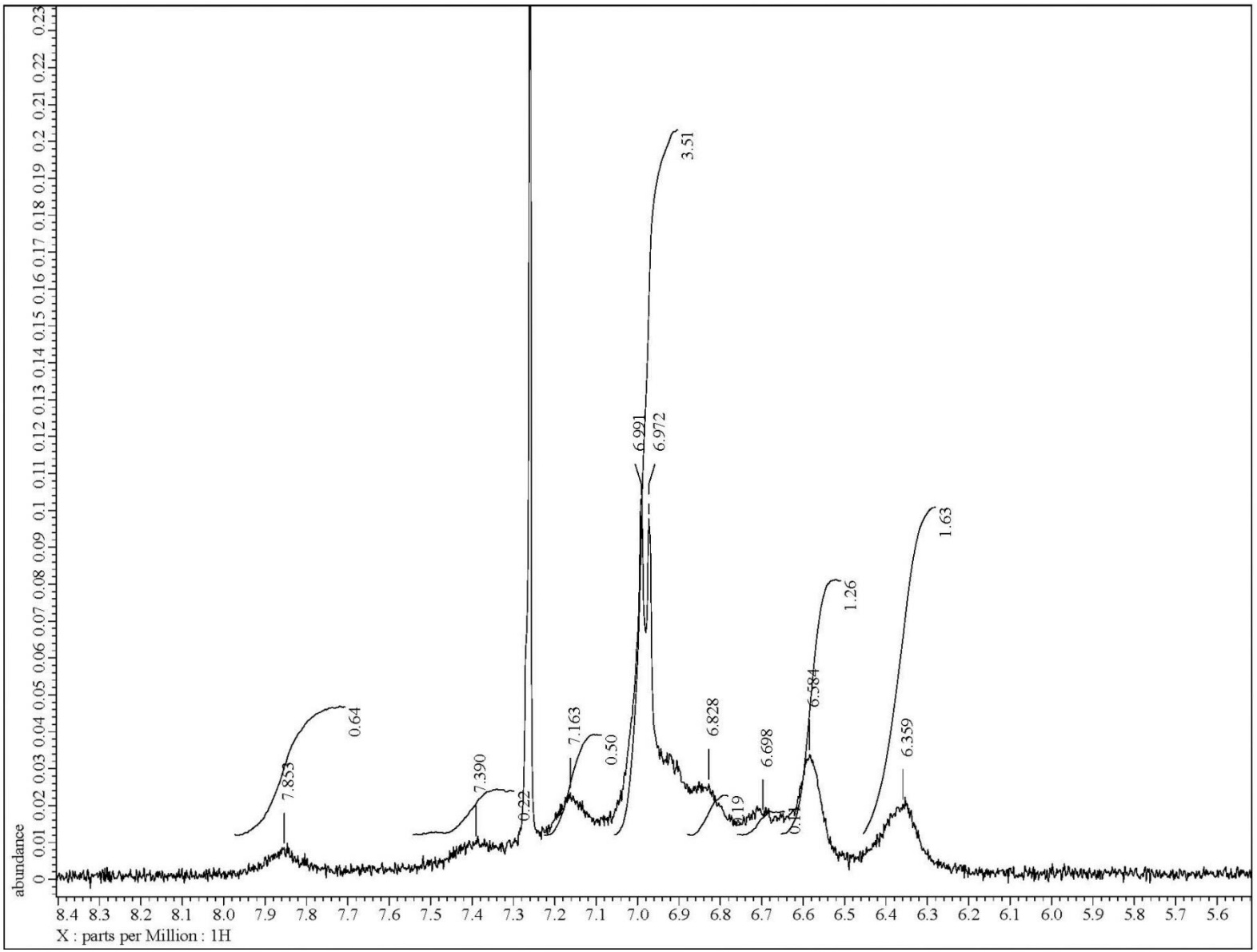

Fig. S114 ^{1}H NMR (400 MHz, $CDCl_3$) spectrum of **19** at 1.23×10^{-1} M concentration in the indicated region

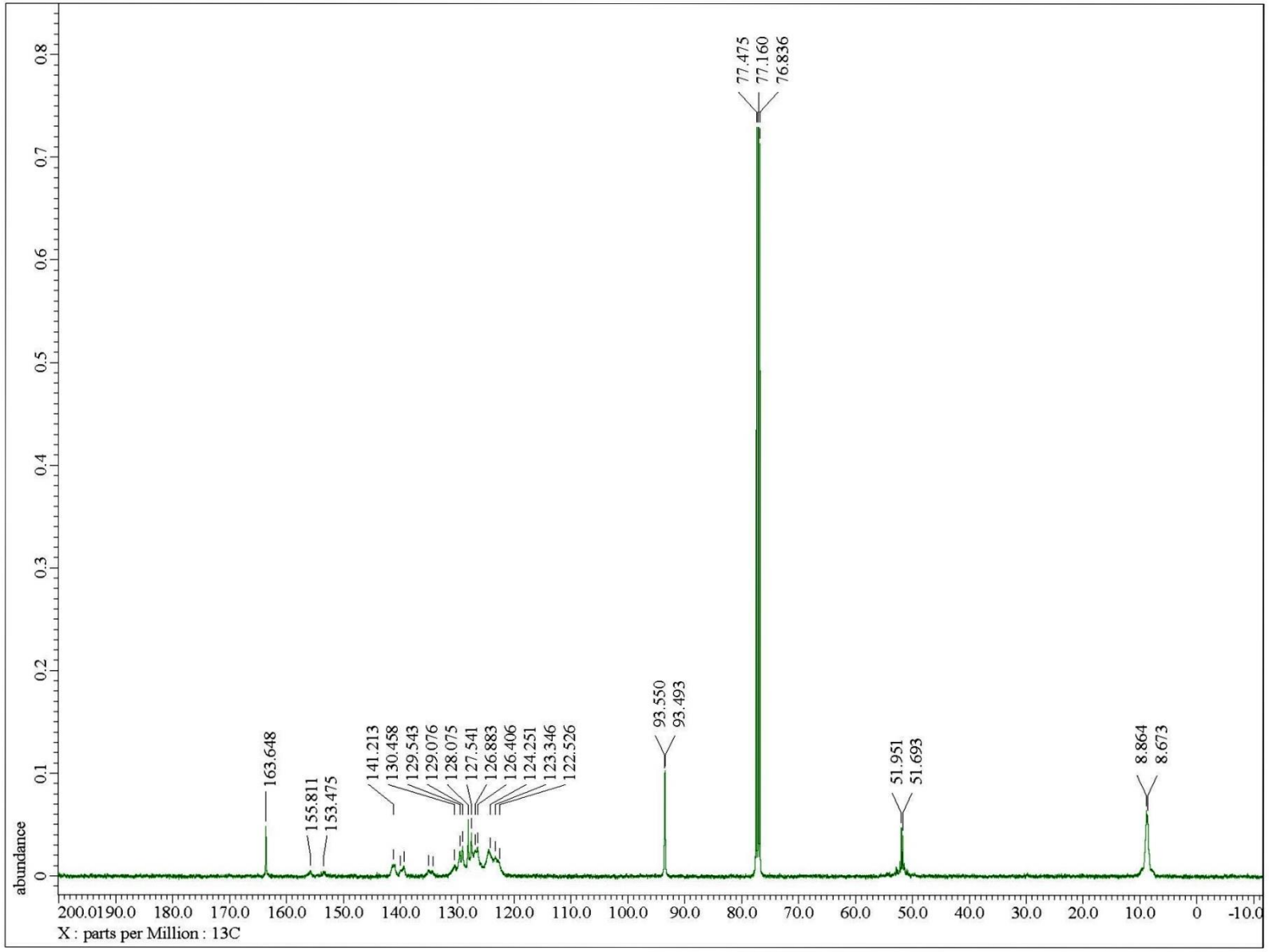

Fig. S115 ^{13}C NMR (100.5 MHz, $CDCl_3$) spectrum of **19** at 1.23×10^{-1} M concentration

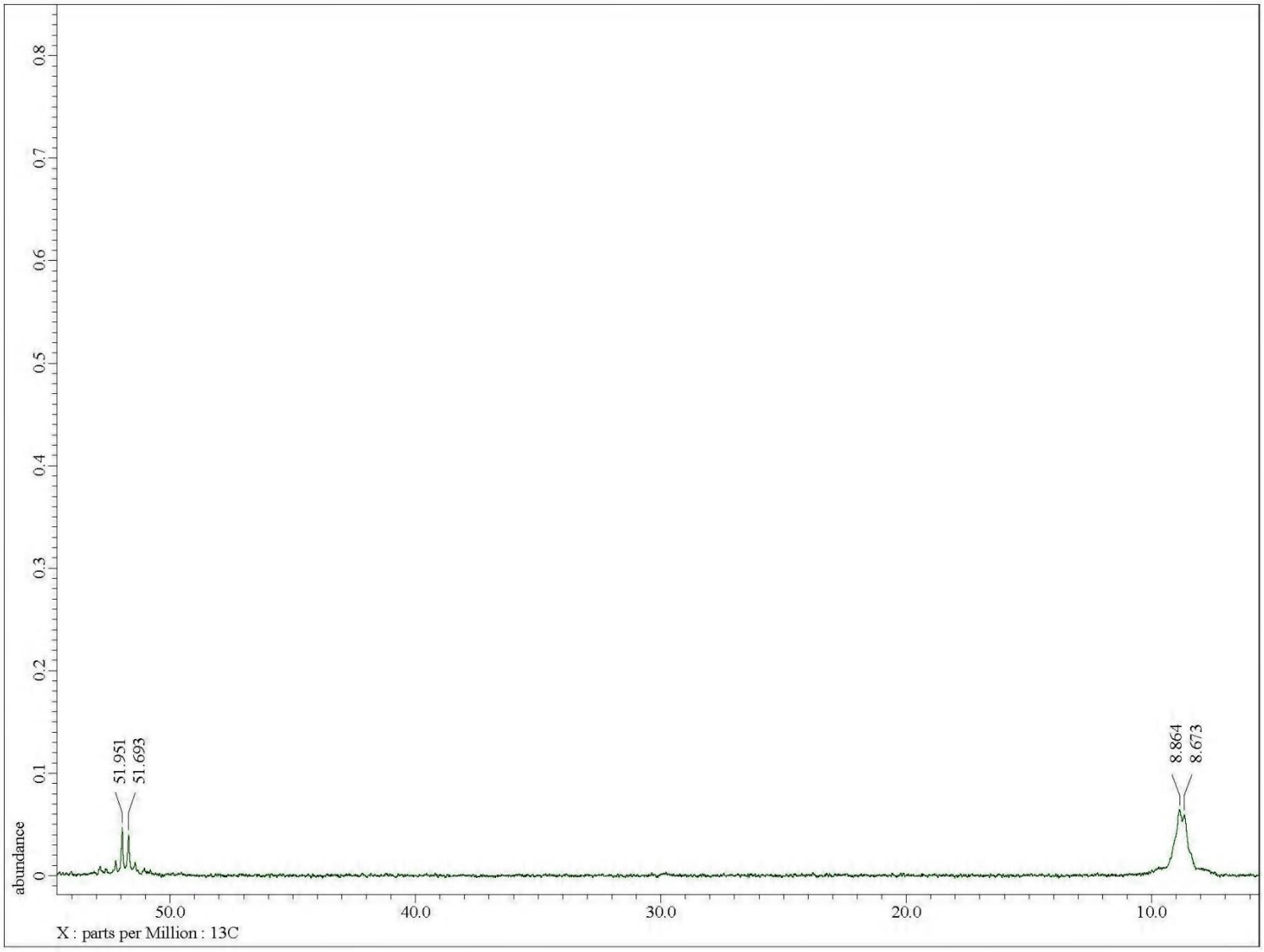

Fig. S116 ^{13}C NMR (100.5 MHz, $CDCl_3$) spectrum of **19** at 1.23×10^{-1} M concentration in the indicated region

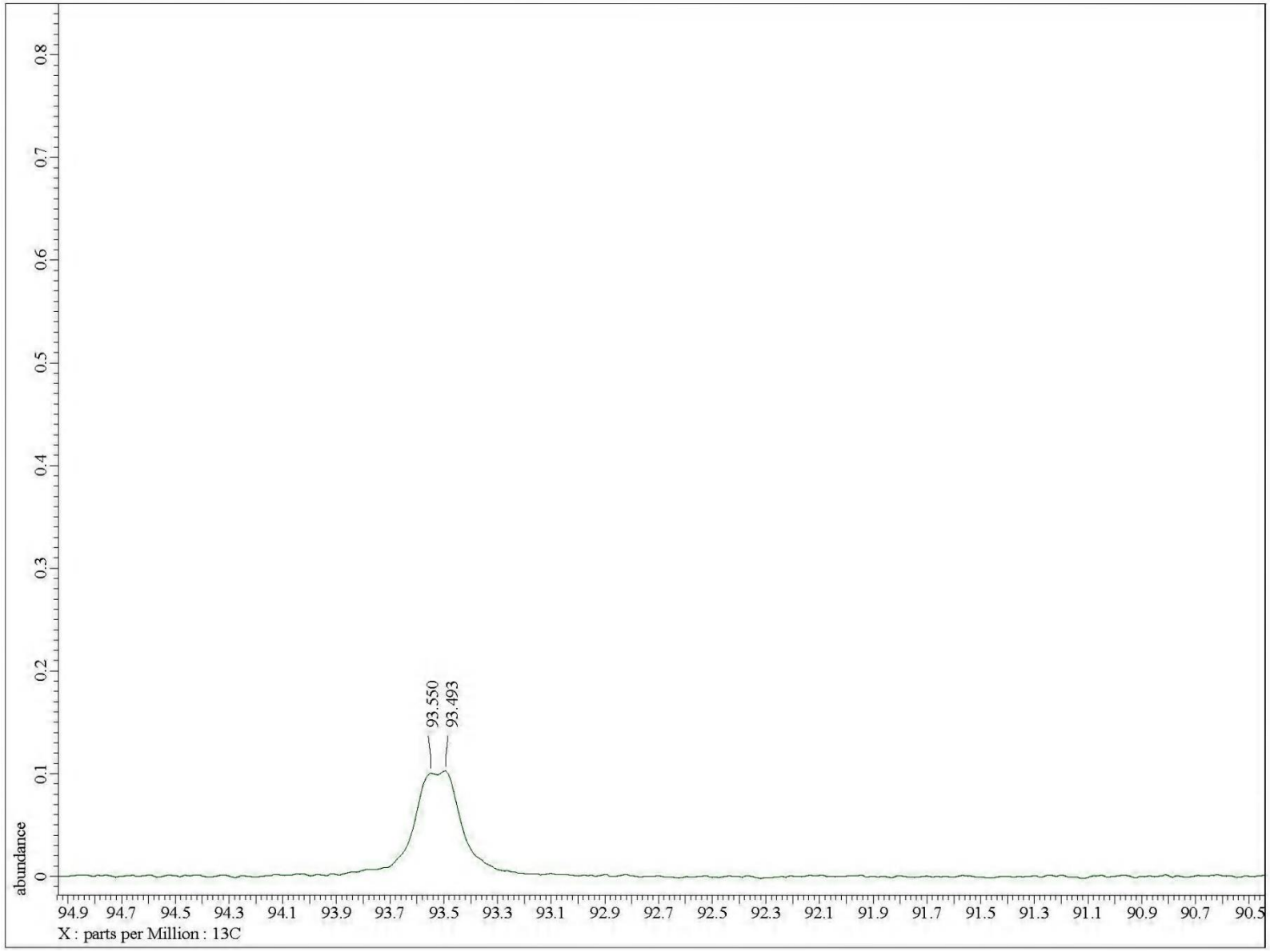

Fig. S117 ^{13}C NMR (100.5 MHz, $CDCl_3$) spectrum of **19** at 1.23×10^{-1} M concentration in the indicated region

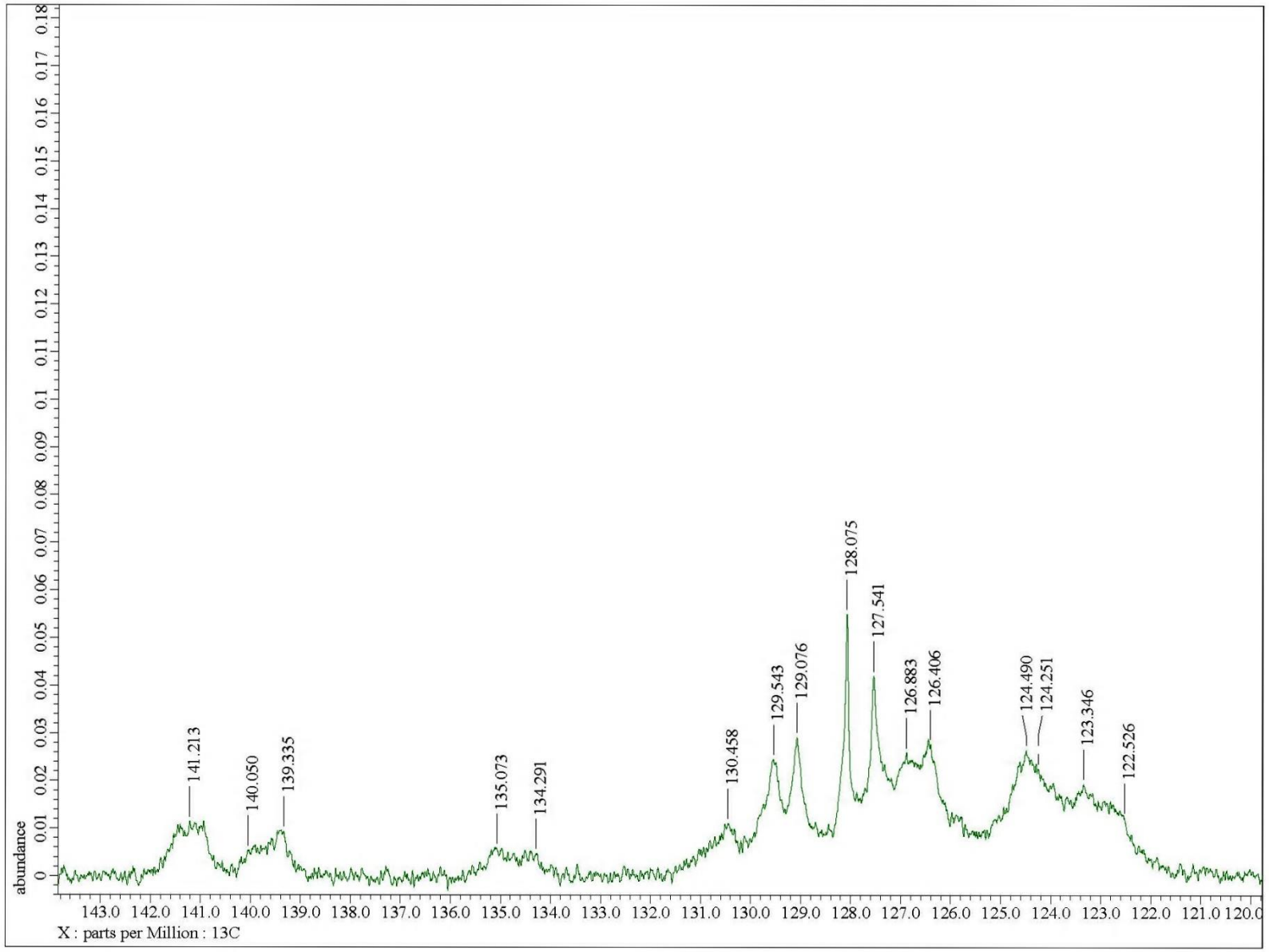

Fig. S118 ^{13}C NMR (100.5 MHz, $CDCl_3$) spectrum of **19** at 1.23×10^{-1} M concentration in the indicated region

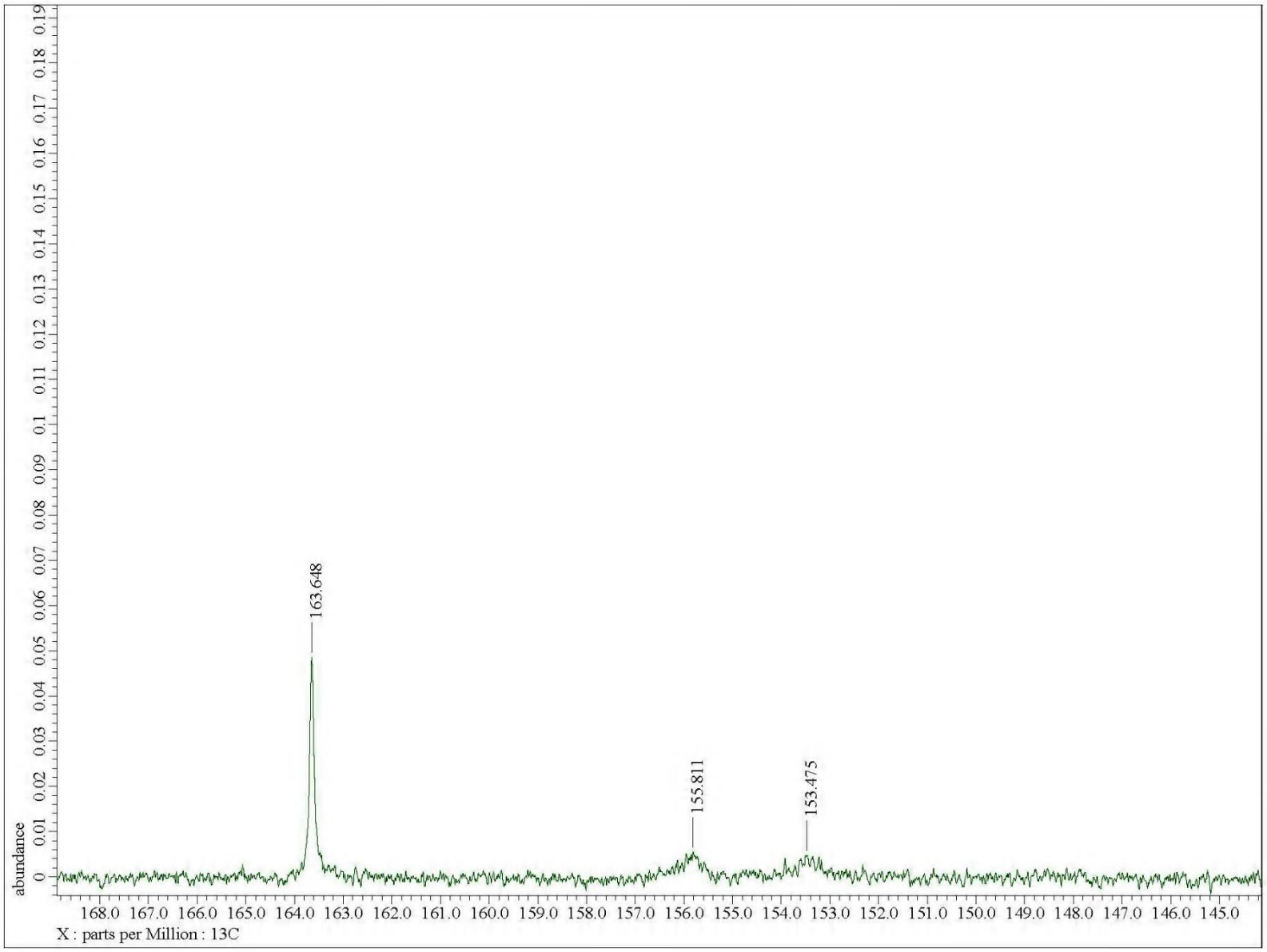

Fig. S119 ^{13}C NMR (100.5 MHz, $CDCl_3$) spectrum of **19** at 1.23×10^{-1} M concentration in the indicated region

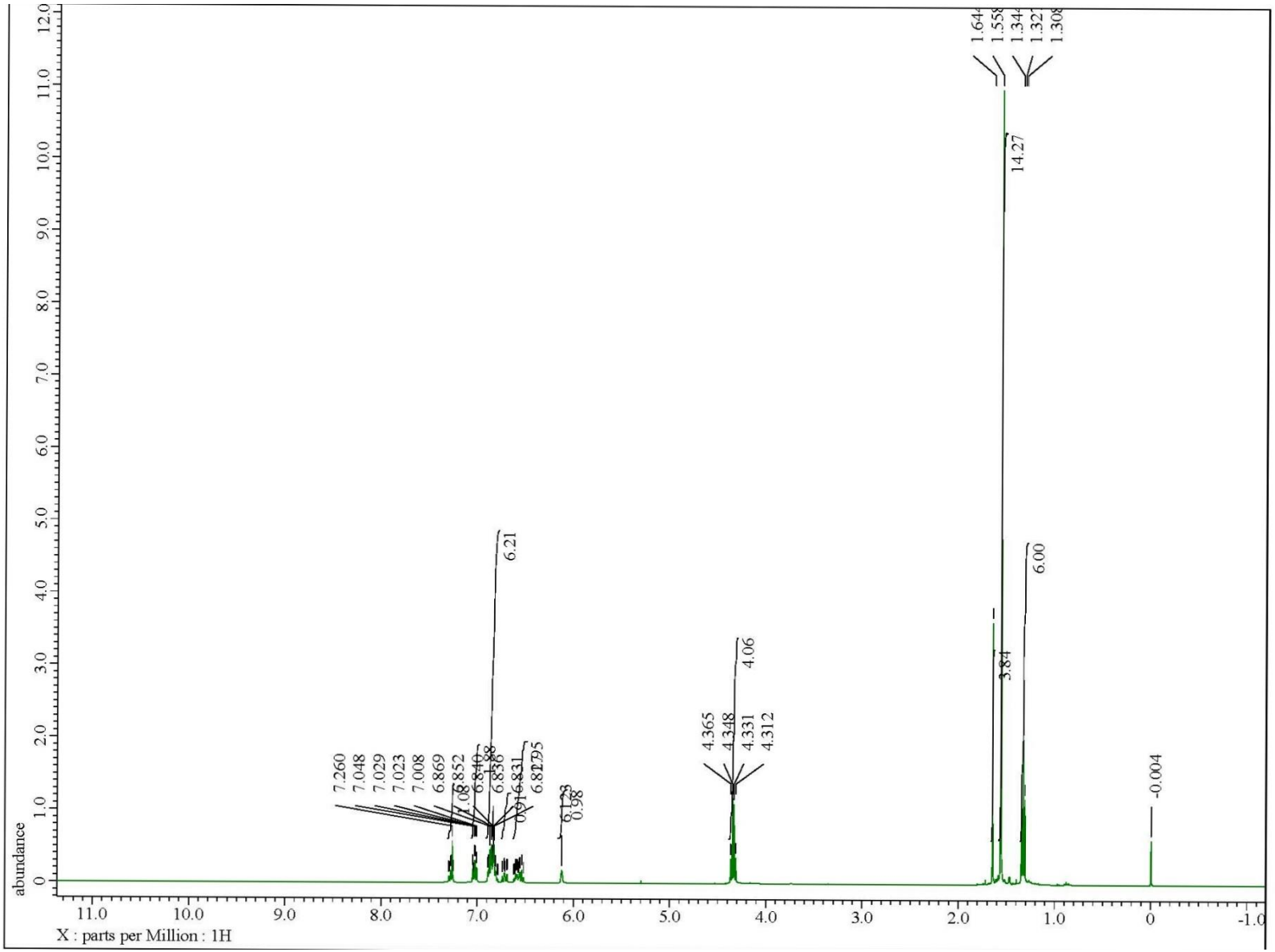

Fig. S120 ^{1}H NMR (400 MHz, $CDCl_3$) spectrum of **20** at 1.27×10^{-1} M concentration

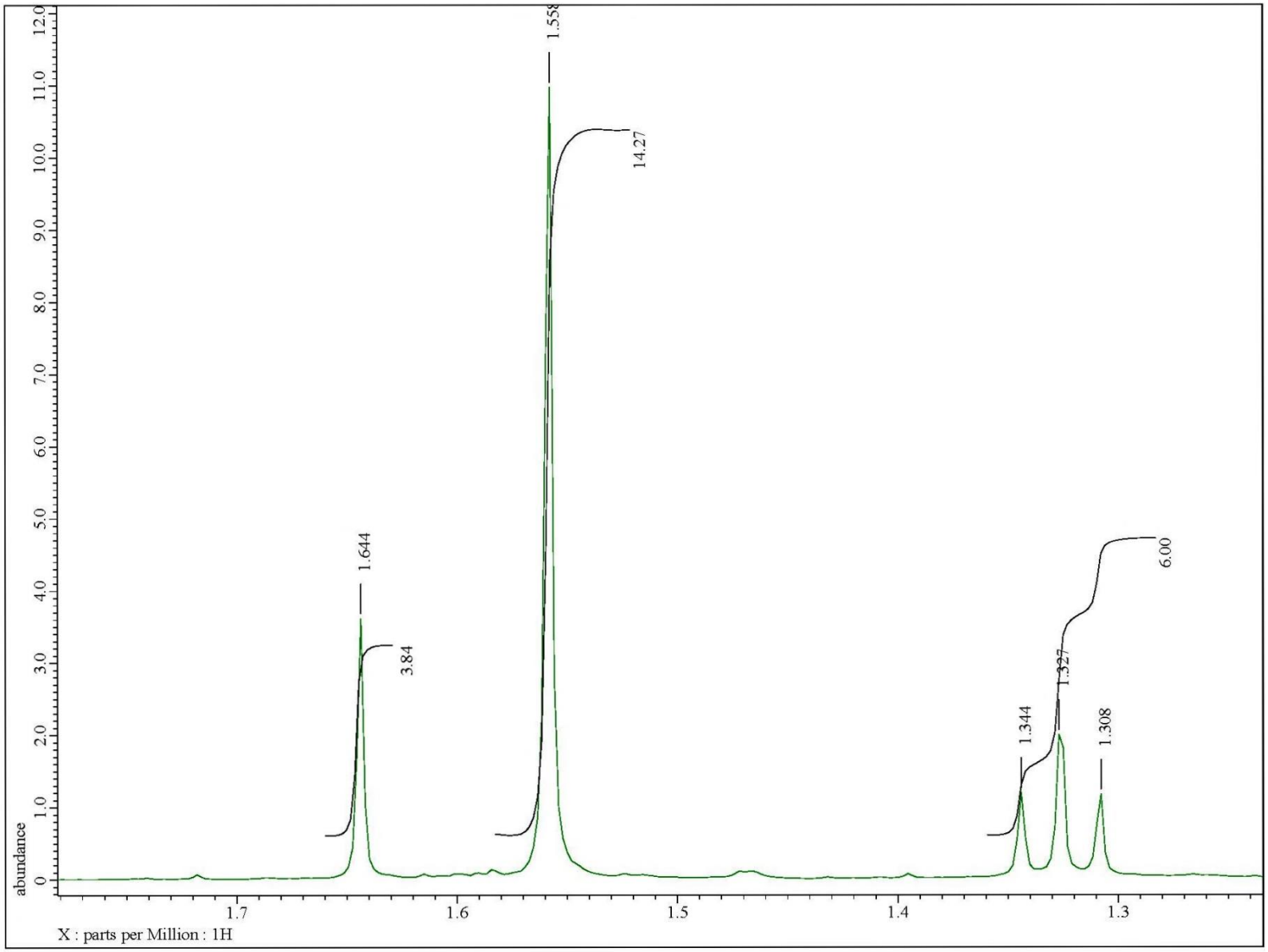

Fig. S121 ^{1}H NMR (400 MHz, $CDCl_3$) spectrum of **20** at 1.27×10^{-1} M concentration in the indicated region

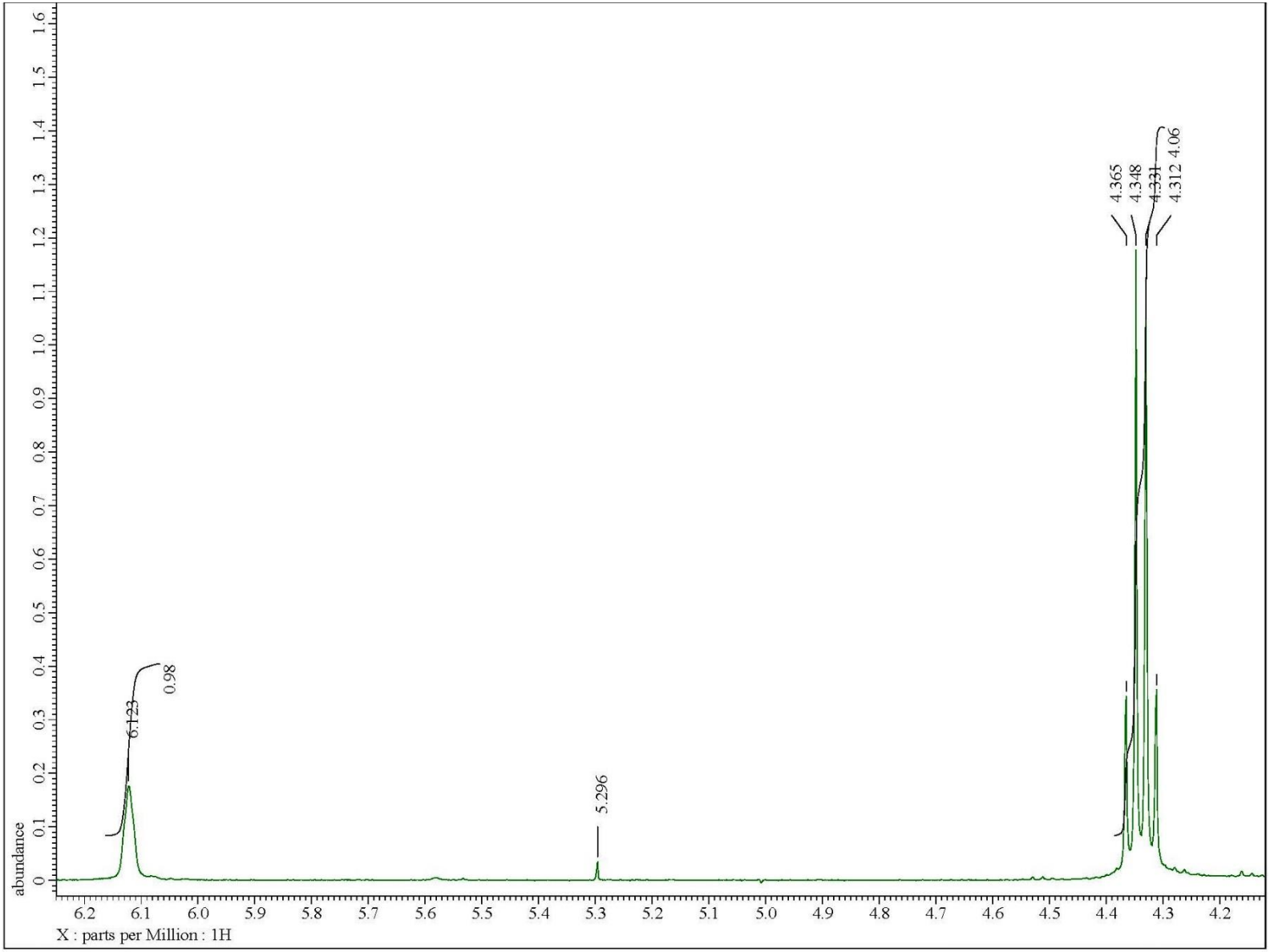

Fig. S122 ^{1}H NMR (400 MHz, $CDCl_3$) spectrum of **20** at 1.27×10^{-1} M concentration in the indicated region

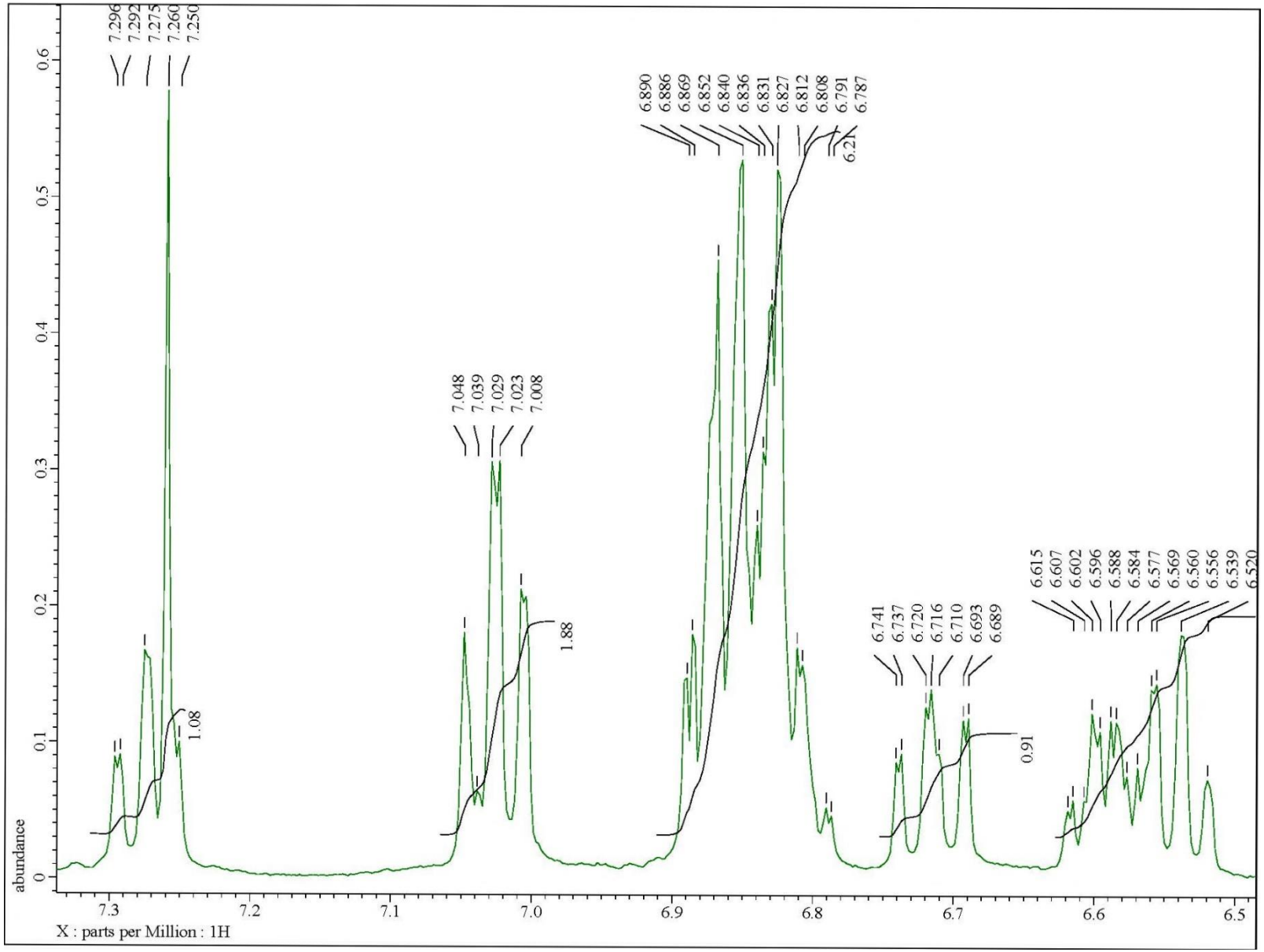

Fig. S123 ^{1}H NMR (400 MHz, $CDCl_3$) spectrum of **20** at 1.27×10^{-1} M concentration in the indicated region

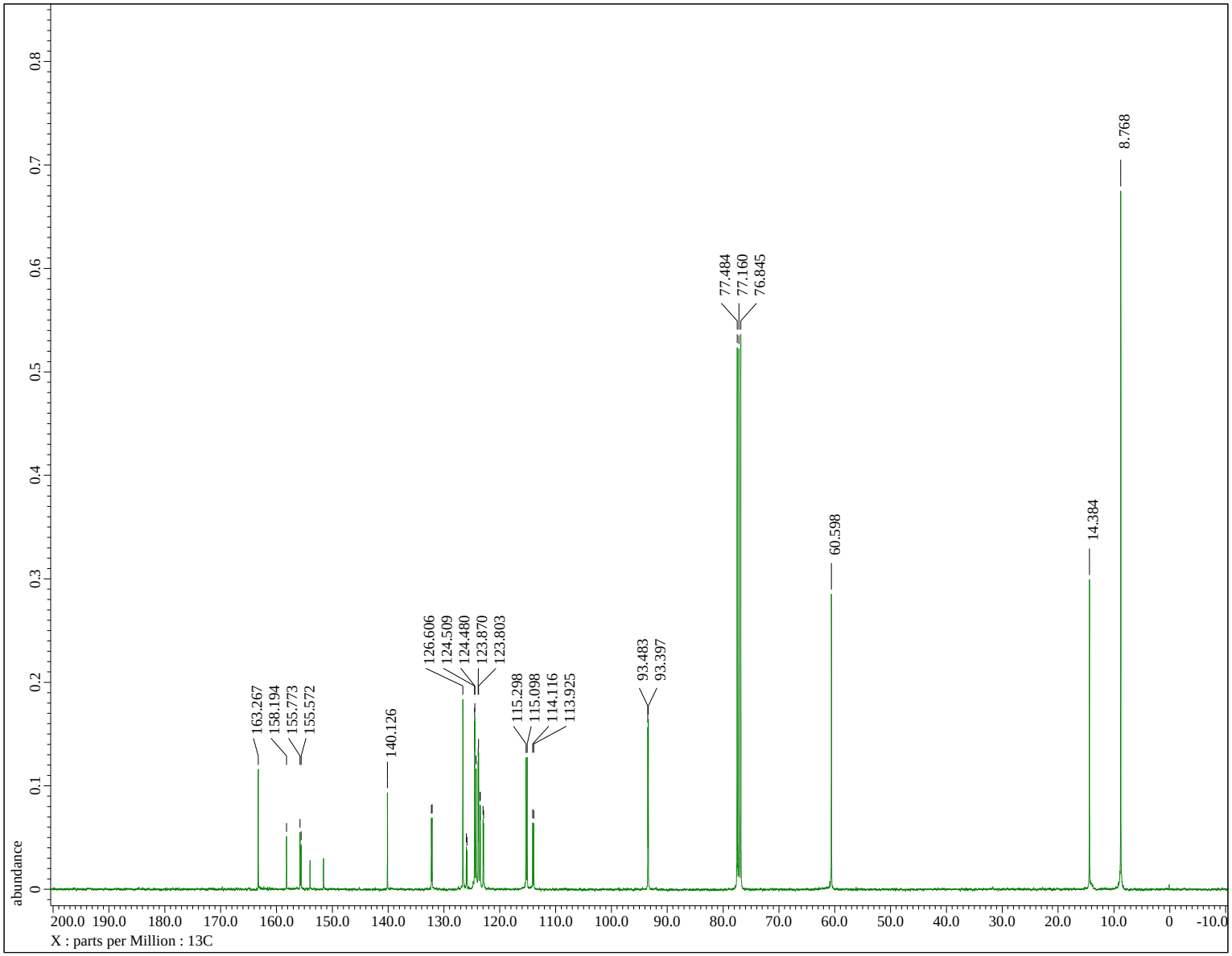

Fig. S124 ^{13}C NMR (100.5 MHz, $CDCl_3$) spectrum of **20** at 1.27×10^{-1} M concentration

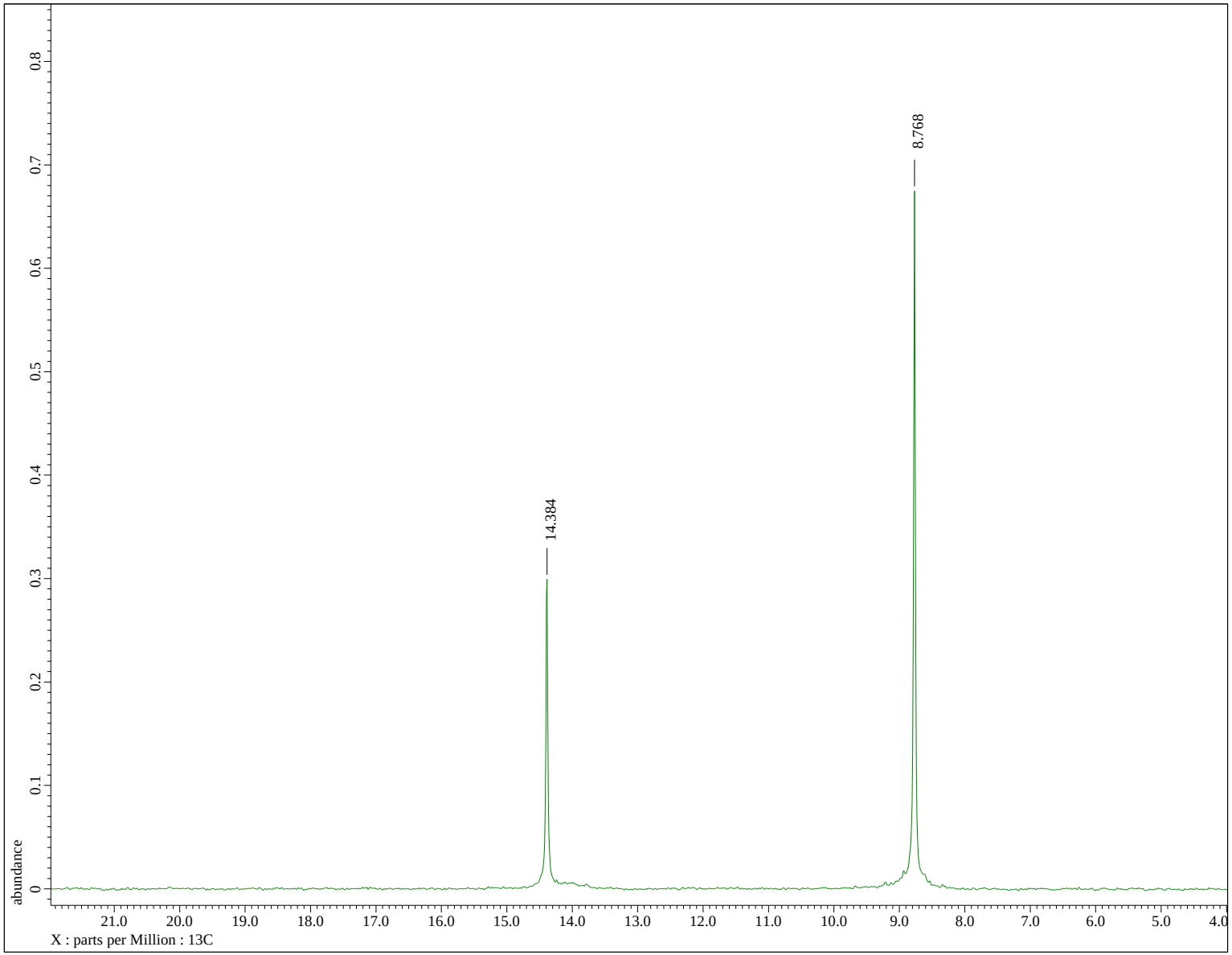

Fig. S125 ^{13}C NMR (100.5 MHz, $CDCl_3$) spectrum of **20** at 1.27×10^{-1} M concentration in the indicated region

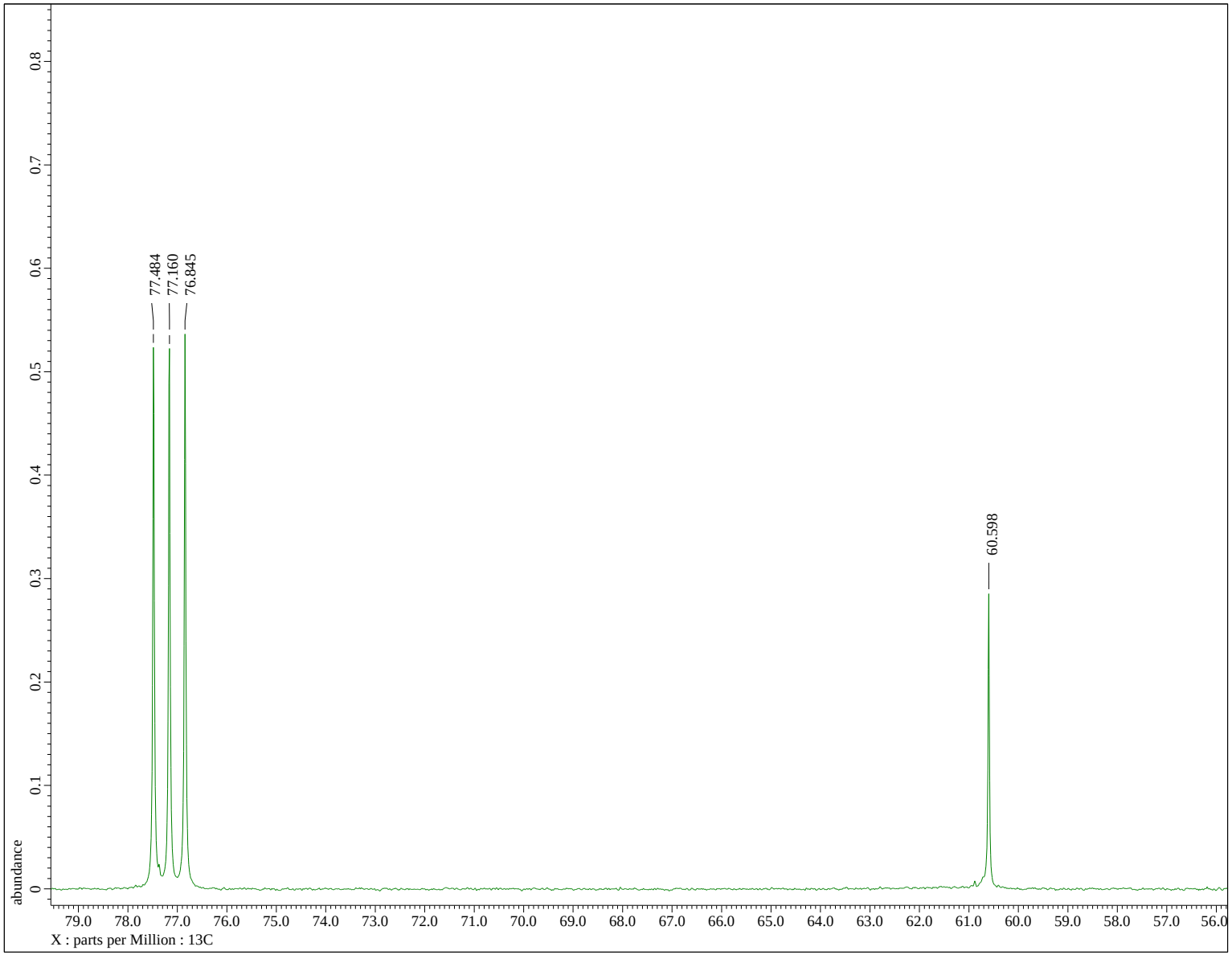

Fig. S126 ^{13}C NMR (100.5 MHz, $CDCl_3$) spectrum of **20** at 1.27×10^{-1} M concentration in the indicated region

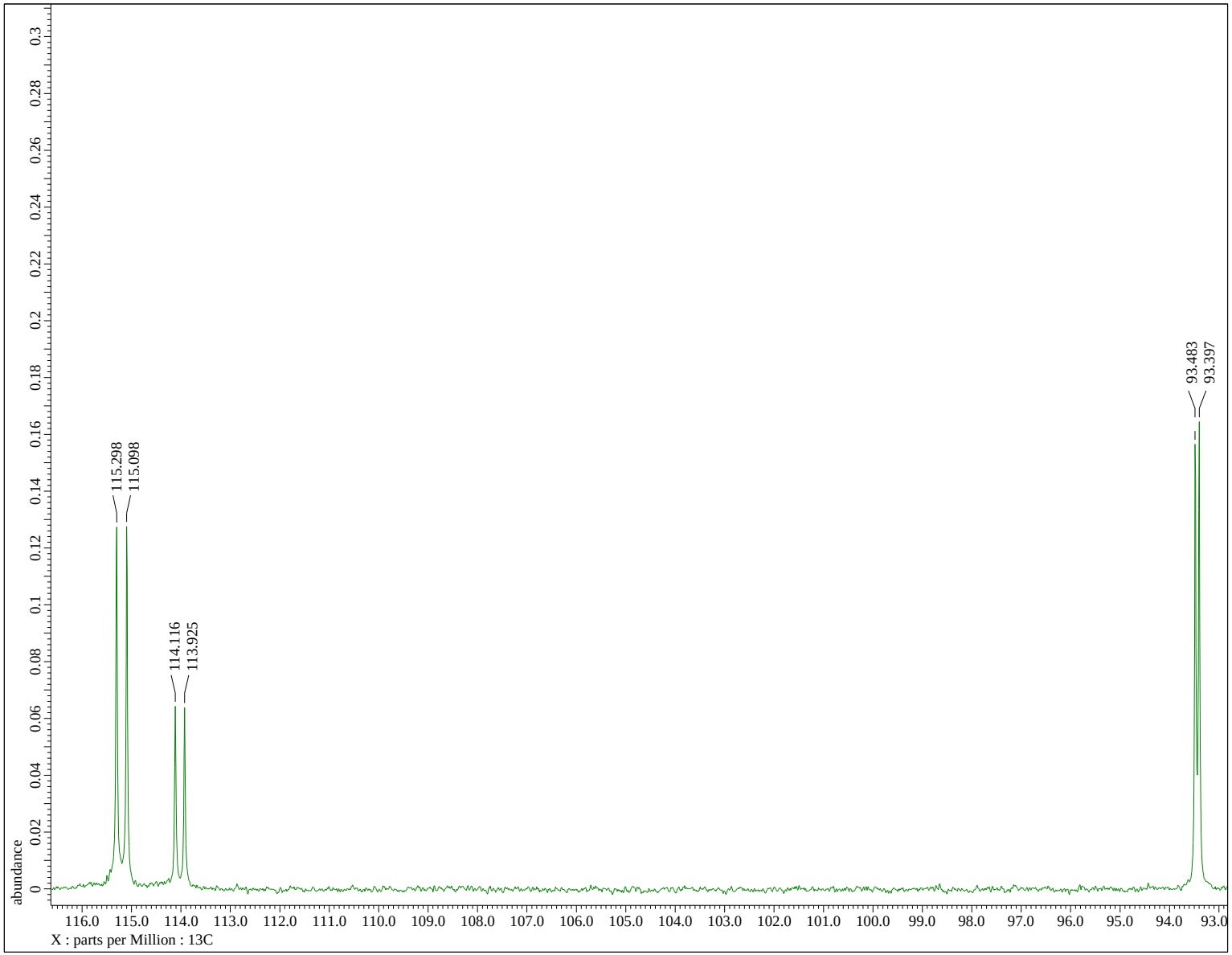

Fig. S127 ^{13}C NMR (100.5 MHz, $CDCl_3$) spectrum of **20** at 1.27×10^{-1} M concentration in the indicated region

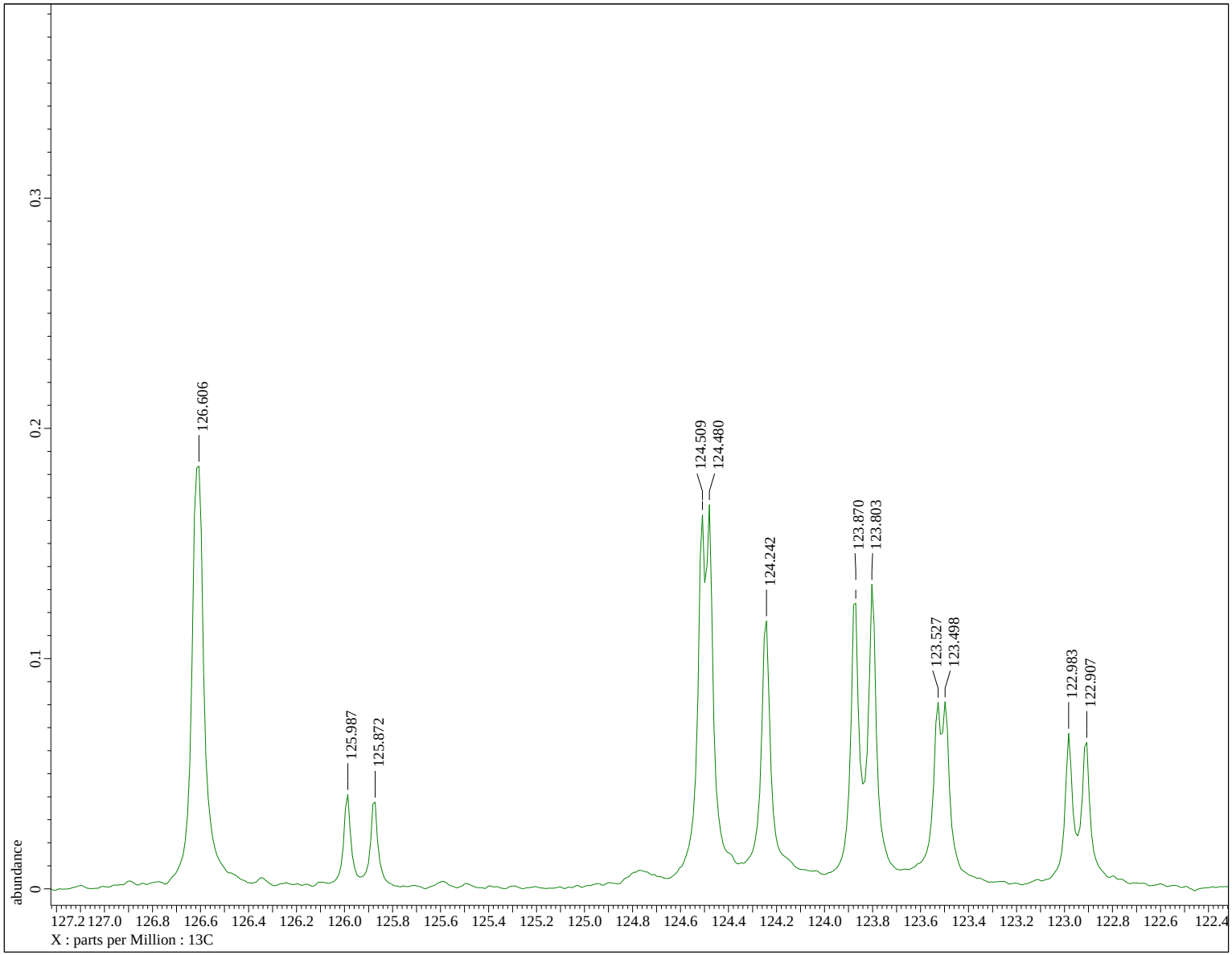

Fig. S128 ^{13}C NMR (100.5 MHz, $CDCl_3$) spectrum of **20** at 1.27×10^{-1} M concentration in the indicated region

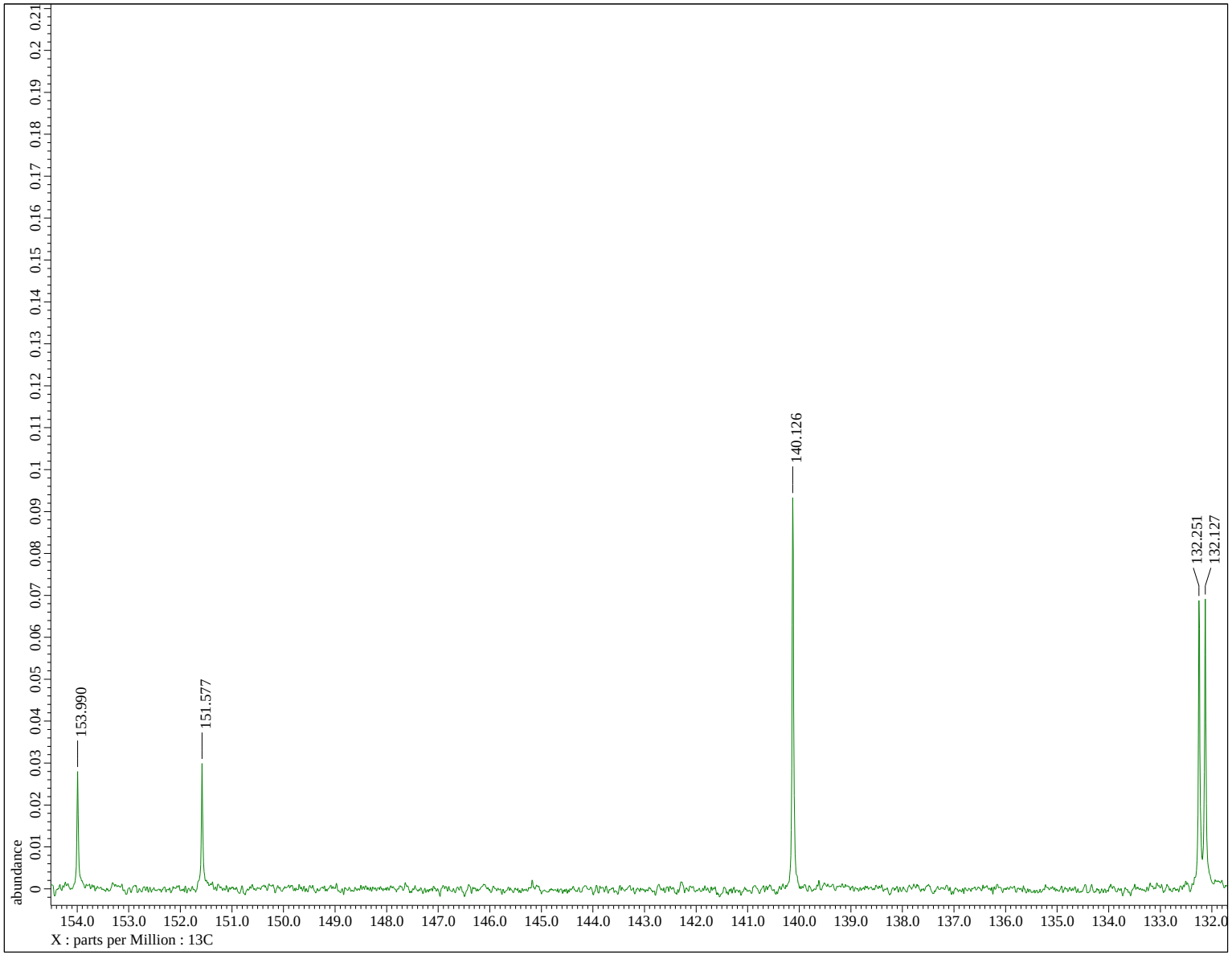

Fig. S129 ^{13}C NMR (100.5 MHz, $CDCl_3$) spectrum of **20** at 1.27×10^{-1} M concentration in the indicated region

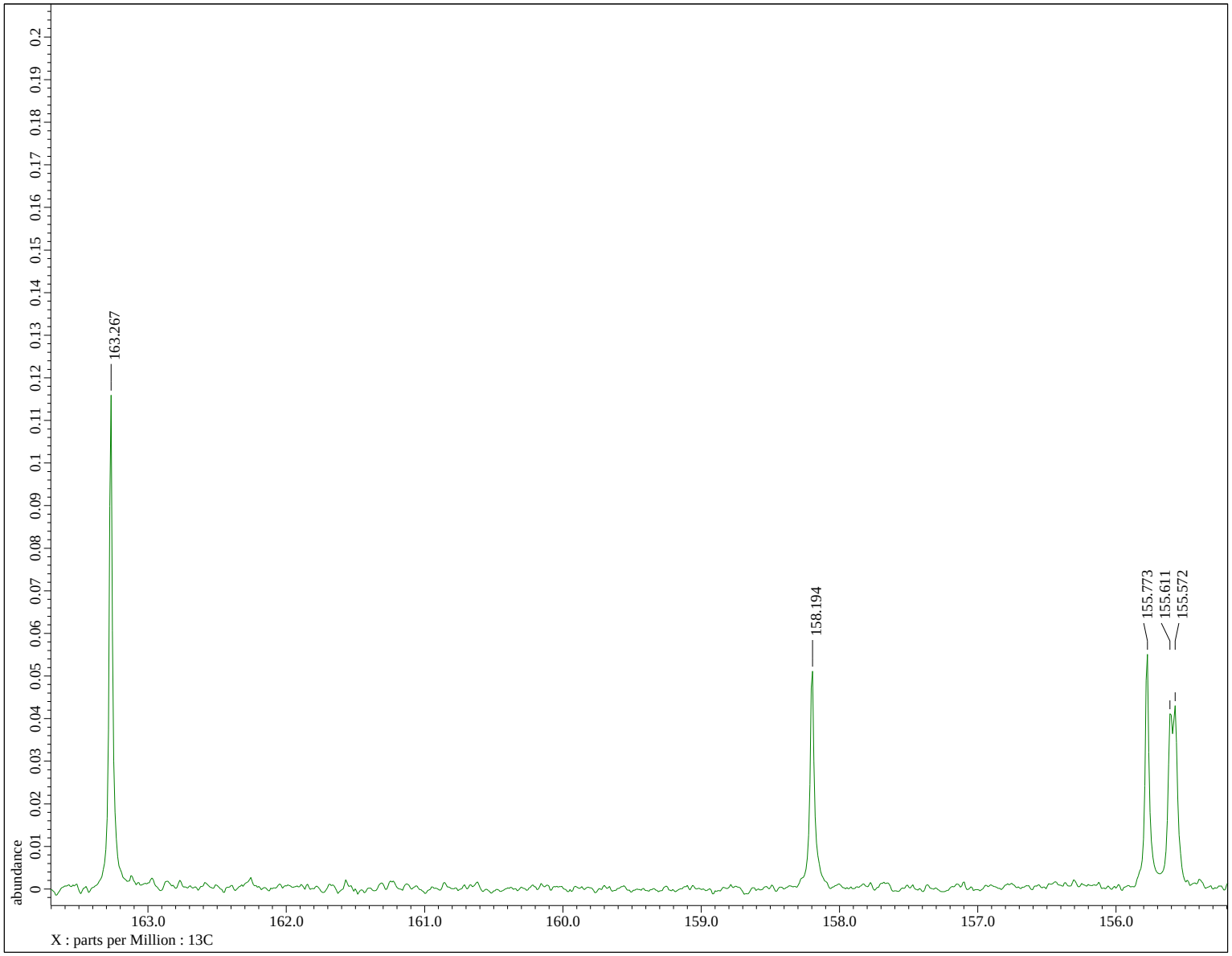

Fig. S130 ^{13}C NMR (100.5 MHz, $CDCl_3$) spectrum of **20** at 1.27×10^{-1} M concentration in the indicated region

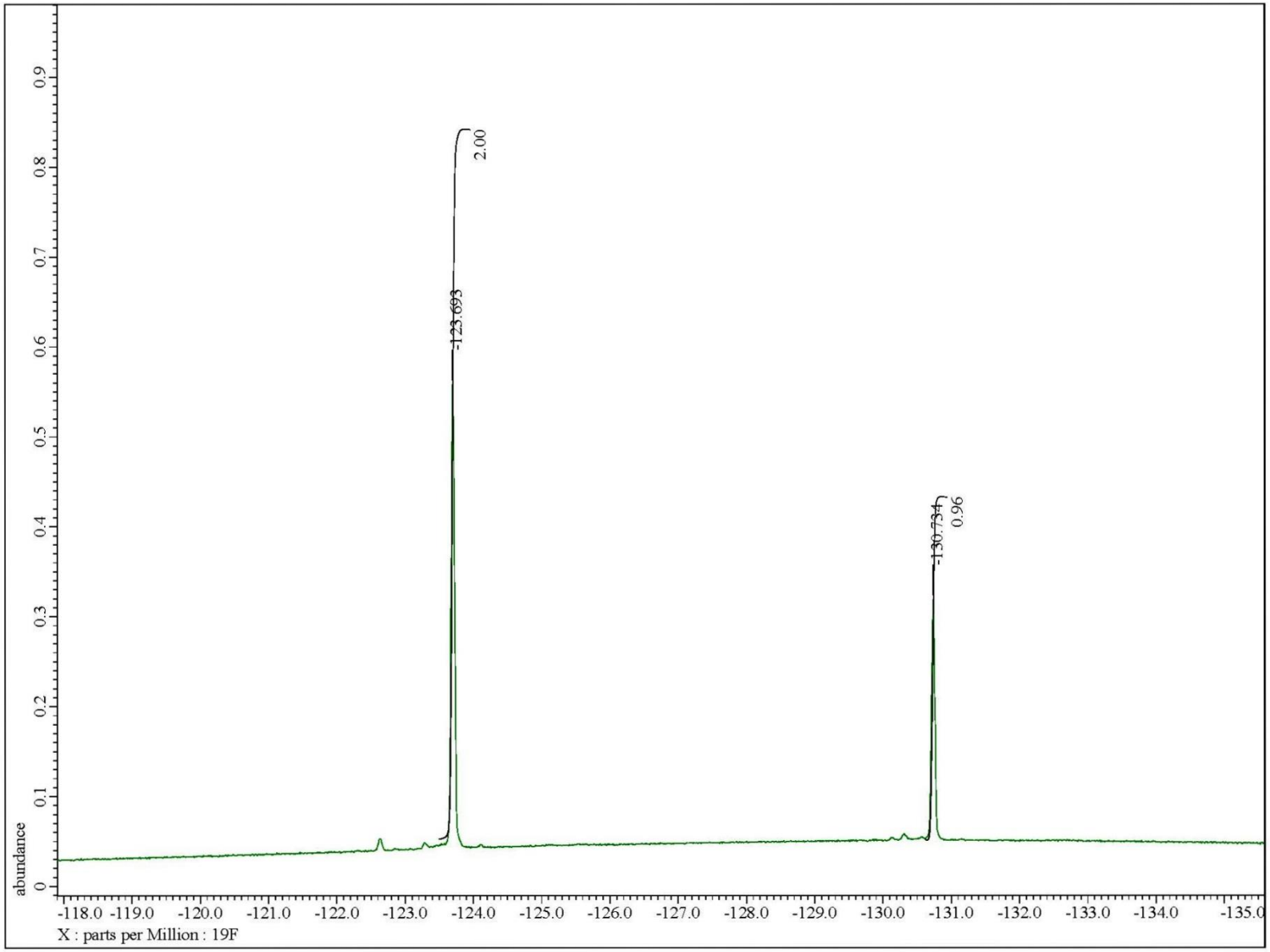

Fig. S131 ^{19}F NMR (376.5 MHz, $CDCl_3$) spectrum of **20** at 1.27×10^{-1} M concentration

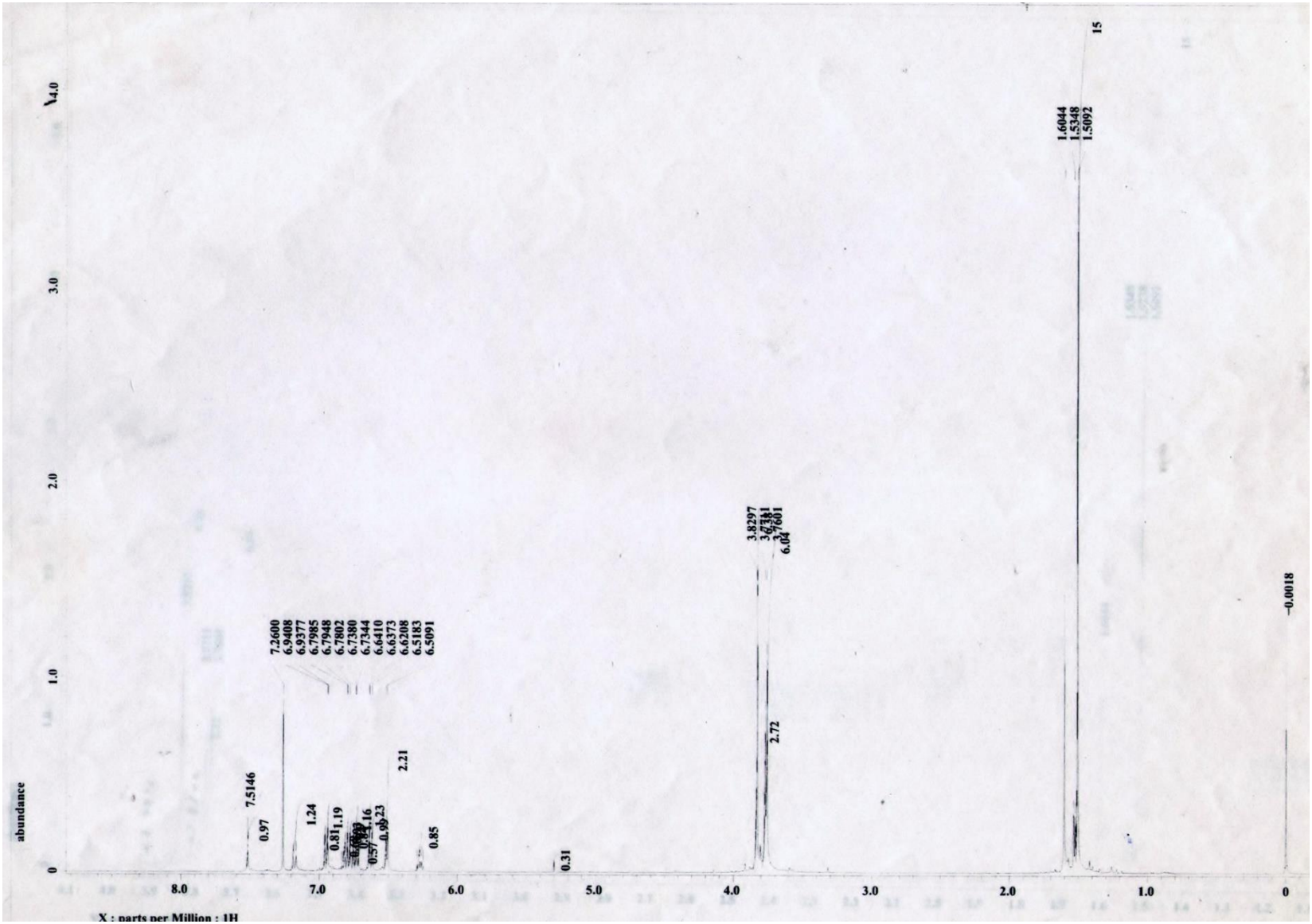

Fig. S132 ^{1}H NMR (400 MHz, $CDCl_3$) spectrum of **21**

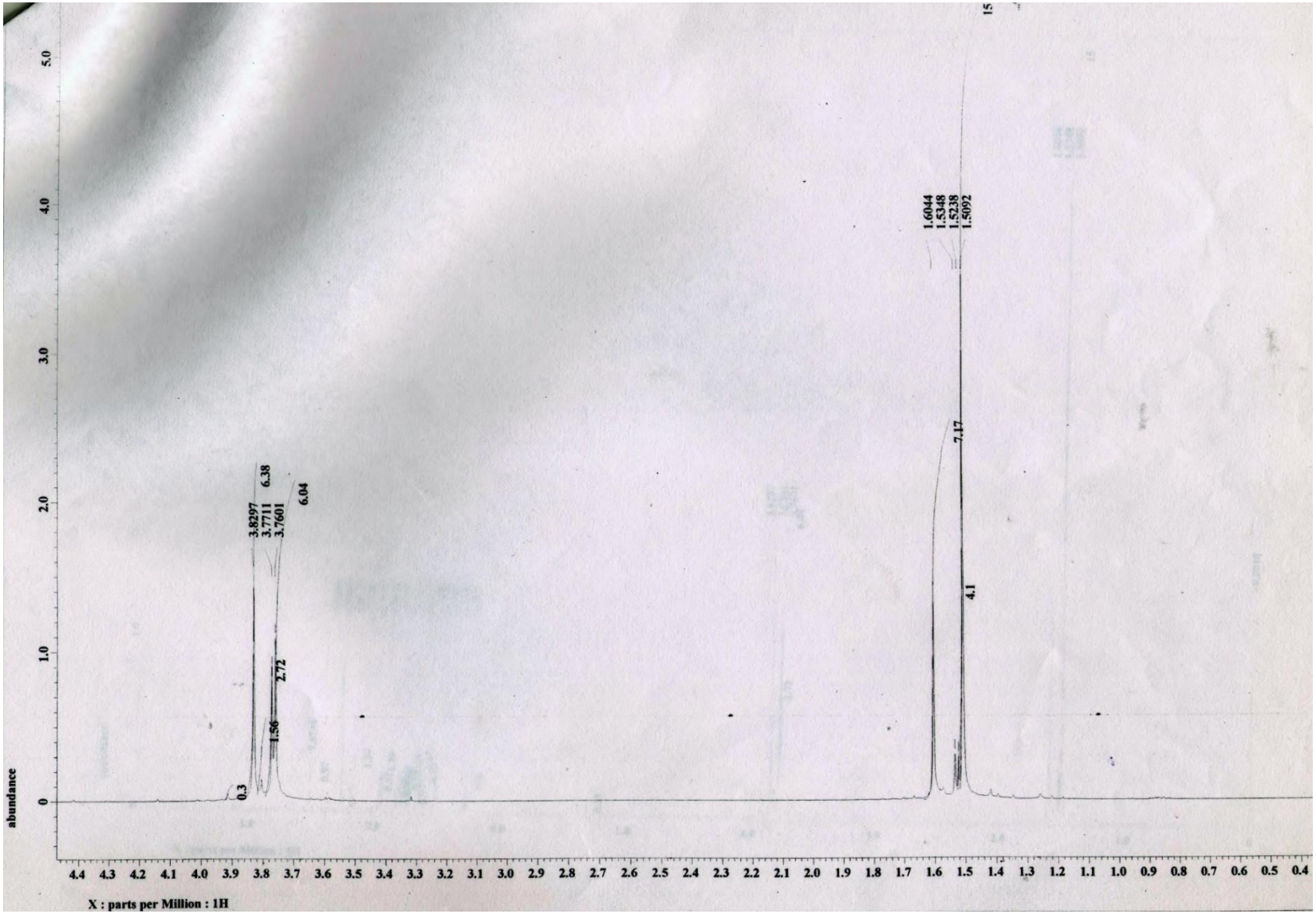

Fig. S133 ^{1}H NMR (400 MHz, $CDCl_3$) spectrum of **21** in the indicated region

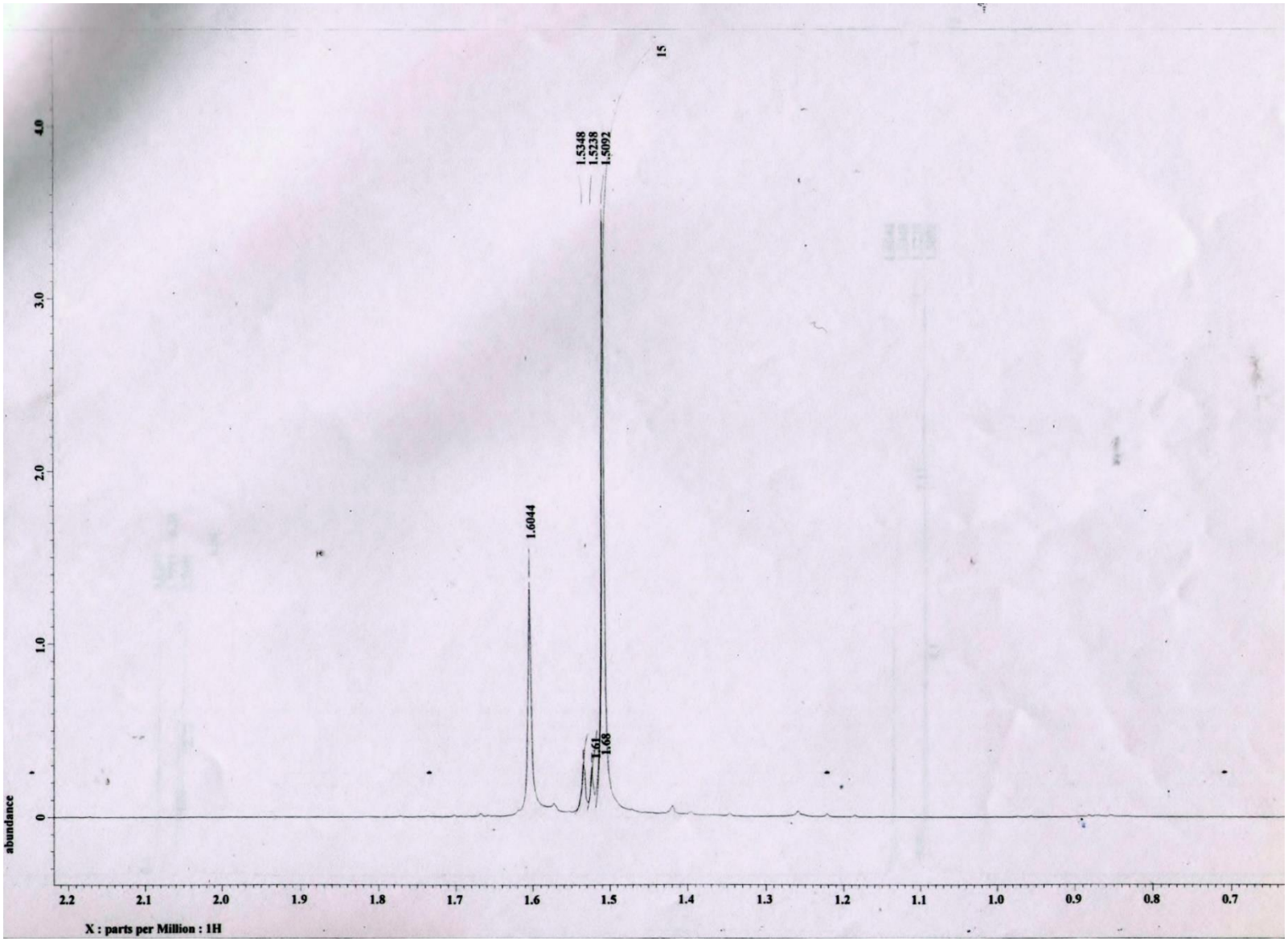

Fig. S134 ^{1}H NMR (400 MHz, $CDCl_3$) spectrum of **21** in the indicated region. The peak at 1.60 ppm refers to traces of water in $CDCl_3$.

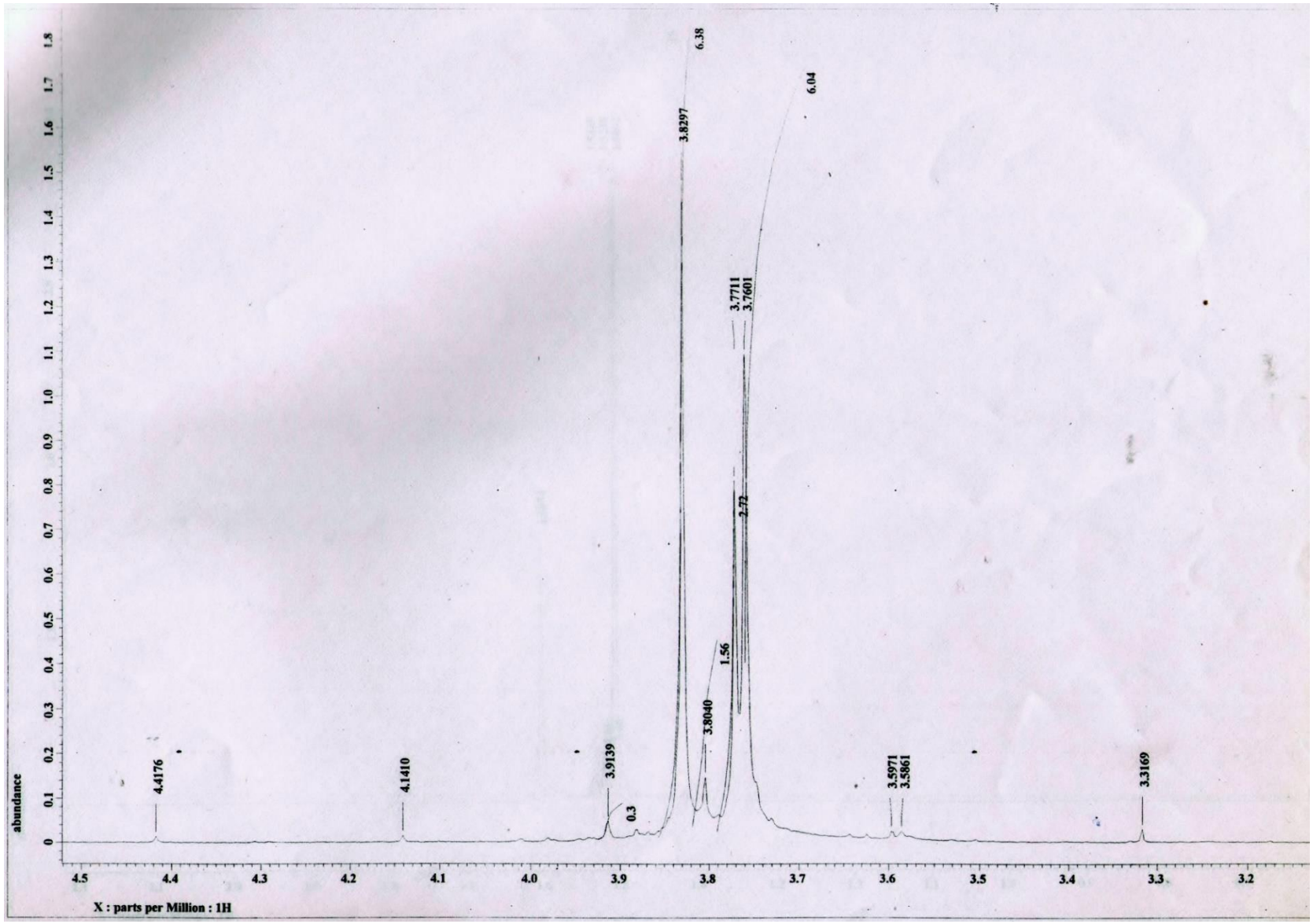

Fig. S135 ^{1}H NMR (400 MHz, $CDCl_3$) spectrum of **18** in the indicated region

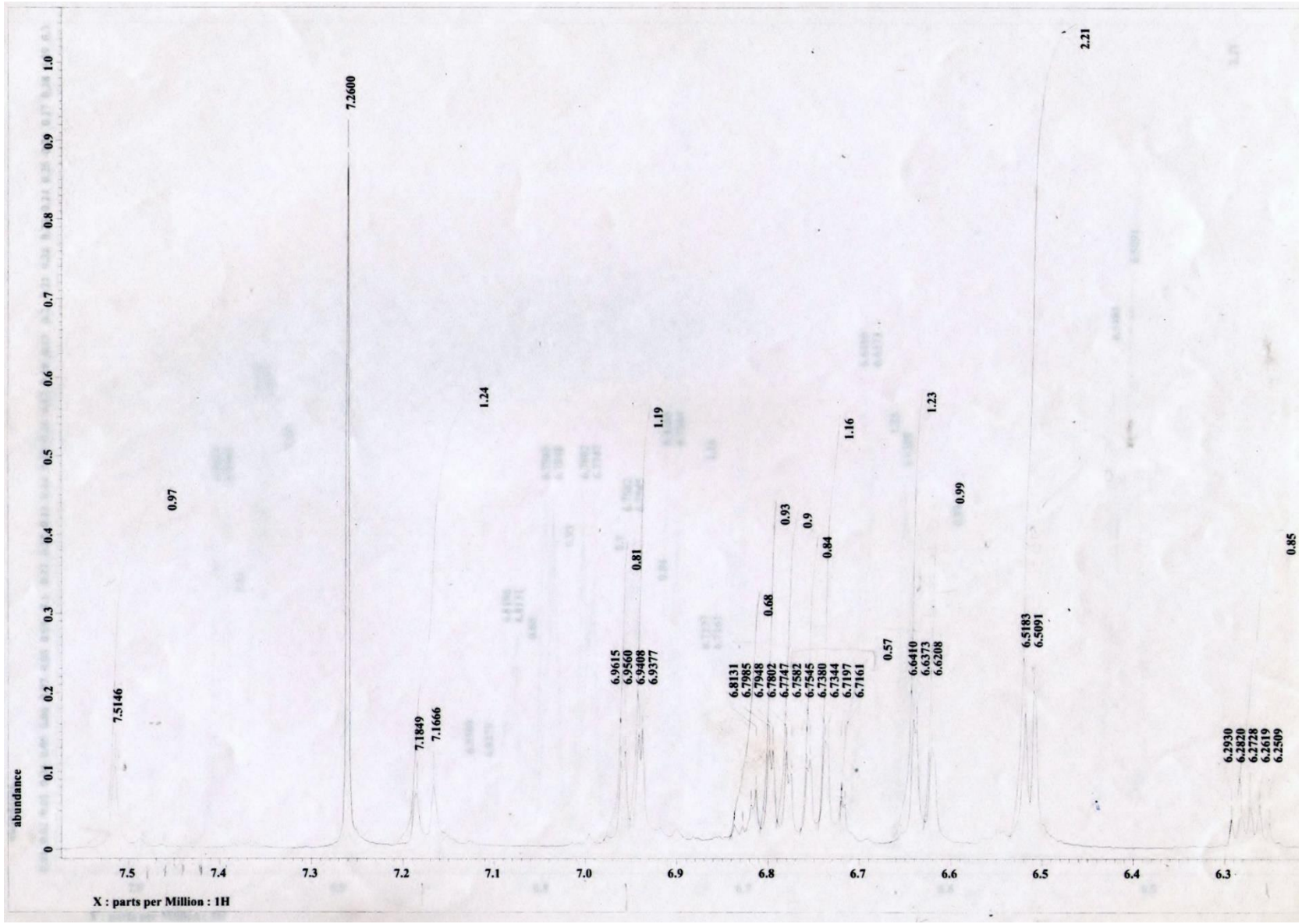

Fig. S136 ^{1}H NMR (400 MHz, $CDCl_3$) spectrum of **21** in the indicated region

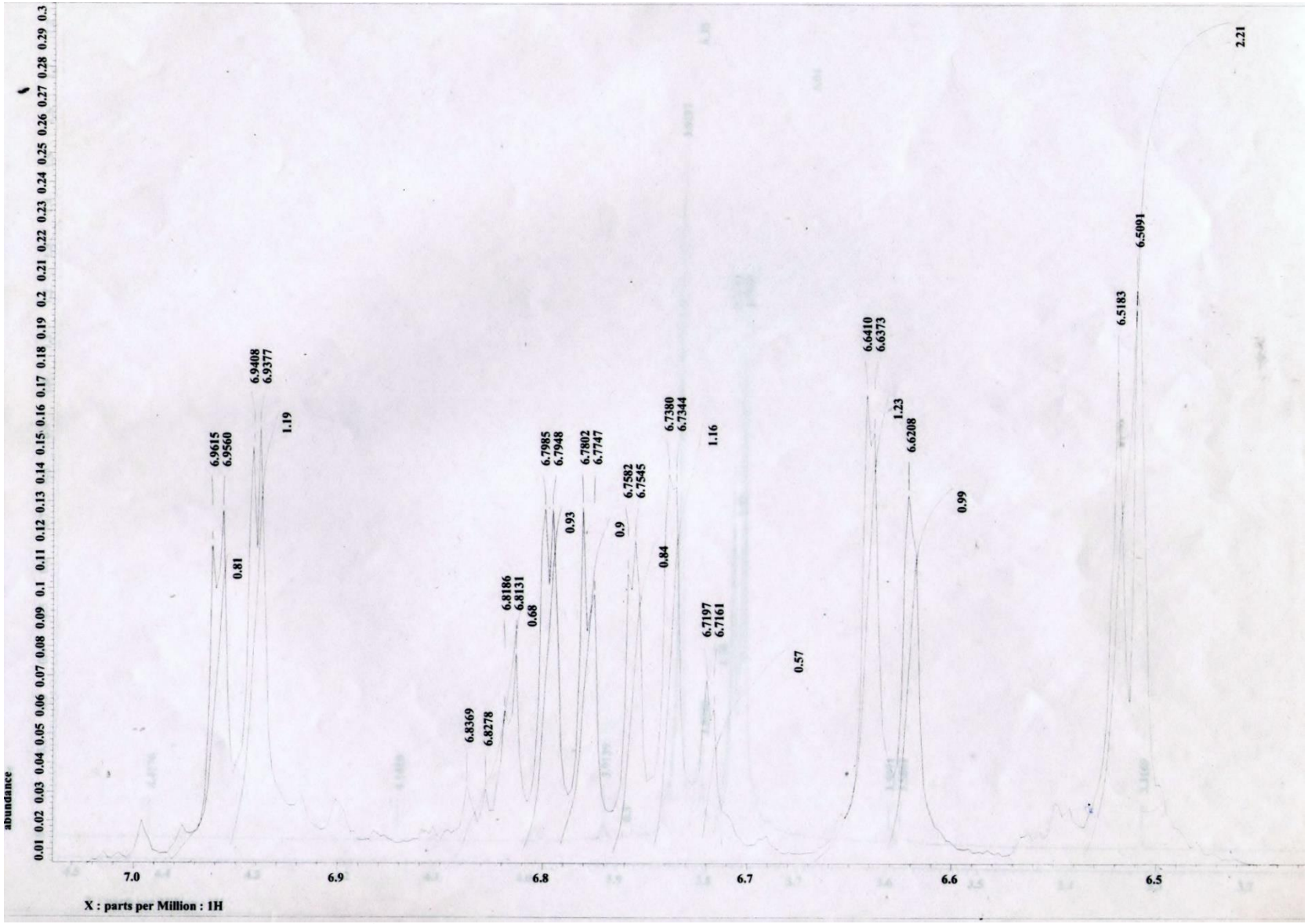

Fig. S137 ^{1}H NMR (400 MHz, $CDCl_3$) spectrum of **21** in the indicated region

Cartesian coordinates of the optimized *syn-syn* conformer of 14

Rh	-1.69579400	-0.42660400	0.33707700
Cl	-1.02263000	3.28058500	-2.24758400
Cl	4.51911600	1.95732700	-1.28960700
N	0.38770700	-0.81371500	0.13817200
N	-0.34492500	1.26158200	-0.08098000
N	2.00874600	0.98329900	0.01746300
H	2.09807800	1.89056600	-0.42304000
N	-1.36902700	-0.06085600	2.40958700
N	-0.57376500	-0.76975700	2.98546500
N	0.17609200	-1.41394300	3.59583000
C	0.72792800	0.47282900	0.02365300
C	-0.35280500	2.60323600	0.33563900
C	-0.69528200	3.64069500	-0.55412400
C	-0.75960500	4.97207000	-0.14296400
H	-1.02248600	5.73936500	-0.86355200
C	-0.47597200	5.30029200	1.18182400
H	-0.52521800	6.33732100	1.50118800
C	-0.13054000	4.29315000	2.08622400
H	0.08746900	4.53884700	3.12175200
C	-0.07418100	2.96678000	1.66852200
H	0.15454900	2.17384900	2.37147200
C	1.10224600	-1.94556900	-0.26498100
C	1.65003800	-2.11535800	-1.55543800
C	2.31426900	-3.28811800	-1.91780700
H	2.72974100	-3.37174200	-2.91672400
C	2.42014400	-4.33973300	-1.00977700
H	2.93416600	-5.25168300	-1.29919200
C	1.85718000	-4.21056600	0.26243300
H	1.93206800	-5.02317700	0.97968100
C	1.21390800	-3.03180600	0.62663100
C	3.18030900	0.45280100	0.58039200
C	4.43437700	0.83751100	0.06999200
C	5.62247300	0.37129500	0.62707000
H	6.56756300	0.69417200	0.20337300
C	5.58073500	-0.50394000	1.71125200
H	6.50627400	-0.87460100	2.14141800
C	4.34593100	-0.88449000	2.23956700
H	4.29738600	-1.54809300	3.09783400
C	3.15925600	-0.40416000	1.69282000
H	2.21030200	-0.67825000	2.14027400
C	-3.20410800	-2.02527100	0.40471900
C	-3.88654500	-0.77121600	0.65786400

C	-3.71635600	0.06162400	-0.48902600
C	-2.97475300	-0.68805900	-1.49417600
C	-2.68944200	-1.97828000	-0.94451900
C	-3.19530100	-3.21416500	1.31986100
H	-3.19318400	-2.90606300	2.36915600
H	-2.31385700	-3.84023100	1.15433800
H	-4.08403400	-3.84007300	1.15636800
C	-4.60419900	-0.43280000	1.92886400
H	-3.93142600	-0.52779200	2.78789900
H	-5.45594700	-1.10850900	2.07829600
H	-4.98505200	0.59119700	1.91573600
C	-4.26077300	1.44652300	-0.67377400
H	-3.59976300	2.05391600	-1.29707800
H	-4.38361300	1.96039700	0.28305100
H	-5.24316700	1.40879300	-1.16462800
C	-2.67024100	-0.22287400	-2.88666200
H	-2.49282600	0.85462900	-2.91329600
H	-3.50756200	-0.44658000	-3.56272300
H	-1.77605500	-0.71065000	-3.28354900
C	-1.98887200	-3.10302400	-1.64246700
H	-1.35937700	-3.67596900	-0.95570600
H	-1.35441600	-2.74135700	-2.45491200
H	-2.72712200	-3.79348800	-2.07290200
Cl	1.46667100	-0.86502400	-2.78018900
H	0.80183100	-2.90925400	1.62404900

Cartesian coordinates of the optimized *syn-anti* conformer of 14

Rh	-1.81872700	-0.22622300	0.23262200
Cl	4.48814600	1.23108900	-1.93089500
N	0.24855500	-0.78196000	0.21906200
N	-0.31746000	1.27121300	-0.34964100
N	2.00634500	0.80281300	-0.31469200
H	2.13790700	1.61966900	-0.89840700
N	-1.64399300	0.34078700	2.25898600
N	-0.70478700	-0.05300100	2.91224000
N	0.16672200	-0.39973400	3.59564800
C	0.69306500	0.42910600	-0.14016200
C	-0.22666500	2.66761500	-0.41254400
C	-0.70903900	3.30754300	-1.57229800
C	-0.71554400	4.69301200	-1.70584400
H	-1.09167400	5.14650100	-2.61867700
C	-0.22764900	5.49106500	-0.66976900
H	-0.22364100	6.57352400	-0.75862600
C	0.26124200	4.89105400	0.48959200
H	0.64322000	5.49450900	1.30650800

C	0.25945600	3.50114800	0.62227700
C	0.86213200	-2.02230800	0.03169100
C	1.37498600	-2.48504000	-1.20015500
C	1.93632900	-3.75634300	-1.32823600
H	2.32859700	-4.06569000	-2.29151000
C	1.96955600	-4.61762400	-0.23346500
H	2.40309400	-5.60773100	-0.34006600
C	1.43714800	-4.19902500	0.98901900
H	1.45608300	-4.86155600	1.84988300
C	0.89721000	-2.92351200	1.11601100
C	3.16468100	0.27873100	0.28154800
C	4.40495200	0.41671600	-0.36798700
C	5.58384700	-0.05392800	0.20449500
H	6.51984600	0.07422900	-0.32885900
C	5.54275400	-0.68587700	1.44642300
H	6.45983700	-1.06076300	1.89097200
C	4.32251600	-0.81623600	2.11237700
H	4.28031600	-1.28321800	3.09193700
C	3.14745000	-0.32844700	1.54735000
H	2.21304700	-0.38843000	2.09478800
C	-3.40611500	-1.73832800	0.38062300
C	-4.04396000	-0.44403600	0.49703500
C	-3.78546900	0.28145000	-0.70421500
C	-3.05646700	-0.59115600	-1.61855300
C	-2.85094100	-1.83669800	-0.95358600
C	-3.48264900	-2.83804400	1.39772600
H	-3.49352600	-2.43086800	2.41258600
H	-2.62857000	-3.51702200	1.31908900
H	-4.39603600	-3.43491400	1.26364800
C	-4.77707200	0.03387900	1.71260800
H	-4.08817400	0.11703200	2.56184700
H	-5.57452300	-0.67035700	1.97880000
H	-5.23288700	1.01382700	1.55140300
C	-4.24805400	1.67052000	-1.02915900
H	-3.46017100	2.25194200	-1.51758800
H	-4.54431300	2.21419100	-0.12904300
H	-5.11111000	1.64087300	-1.70814400
C	-2.69286700	-0.25945500	-3.03506000
H	-2.50954800	0.81195700	-3.15576600
H	-3.50598700	-0.53410500	-3.72160200
H	-1.79034200	-0.78849100	-3.35218900
C	-2.19515500	-3.05705700	-1.52271900
H	-1.56930900	-3.55990700	-0.77963300
H	-1.56491400	-2.81538700	-2.38124400
H	-2.95952700	-3.77354400	-1.85337000
Cl	1.27519000	-1.48789300	-2.64954900

H	0.51009100	-2.57337500	2.06846700
Cl	0.87043400	2.82162400	2.11534400
H	-1.06489700	2.67204400	-2.37784100

Cartesian coordinates of the optimized *anti-syn* conformer of 14

Rh	-1.62016700	-0.21081000	0.10562500
Cl	0.15905000	-3.43388900	1.21820100
Cl	-0.42562000	3.60851600	-2.22528300
Cl	4.89657600	1.75561900	-1.07317300
N	0.43501200	-0.76743600	-0.21046800
N	-0.11743200	1.38127400	-0.18711200
N	2.20392100	0.87472700	-0.12347000
H	2.38029700	1.83887200	-0.37821200
N	-1.04400000	-0.01156200	2.15066300
N	-1.56477400	-0.76077000	2.94464300
N	-2.04040900	-1.44563700	3.75498300
C	0.87553400	0.49250700	-0.17174400
C	0.00895600	2.68159600	0.33129000
C	-0.15408100	3.81157000	-0.49428200
C	-0.07906100	5.10929200	0.01128700
H	-0.20404100	5.95166900	-0.66092800
C	0.16488900	5.30583700	1.36991500
H	0.22395900	6.31636200	1.76397000
C	0.33222400	4.20358500	2.21178500
H	0.51859600	4.34967500	3.27209100
C	0.25398400	2.91110900	1.70005600
H	0.34176700	2.04420800	2.34565500
C	1.08331400	-1.83777700	-0.82145500
C	1.79531500	-1.67904500	-2.03021900
H	1.86123200	-0.68470900	-2.46086600
C	2.40979100	-2.75566900	-2.66161900
H	2.95608600	-2.59222900	-3.58651800
C	2.31436000	-4.03875600	-2.11771100
H	2.78558400	-4.88557400	-2.60777300
C	1.60742400	-4.22871200	-0.93147000
H	1.52559700	-5.21430600	-0.48476500
C	1.00801400	-3.14389800	-0.29212100
C	3.26880500	0.19879500	0.49670200
C	4.59306400	0.52242100	0.15123000
C	5.67886900	-0.09726100	0.76464900
H	6.68470800	0.18433900	0.47145100
C	5.45843700	-1.07189000	1.73674300
H	6.30366500	-1.56280500	2.20951000
C	4.15016400	-1.40084700	2.09721800

H	3.96488200	-2.14747200	2.86378700
C	3.06647800	-0.76742800	1.49551300
H	2.05269200	-1.00353100	1.79959300
C	-3.35872300	-1.59160800	0.09026700
C	-3.82600900	-0.25341000	0.40190700
C	-3.52115100	0.59207500	-0.71060200
C	-2.88350600	-0.21494100	-1.73759900
C	-2.80526500	-1.55780800	-1.24198700
C	-3.57587000	-2.79979200	0.94883400
H	-3.30597800	-2.60663200	1.99291300
H	-2.98202700	-3.64959800	0.60528700
H	-4.63414300	-3.09508200	0.92779500
C	-4.54283000	0.13595000	1.65928400
H	-4.16252900	-0.41348500	2.52546000
H	-5.61442900	-0.08917400	1.56693900
H	-4.44245200	1.20457400	1.86575500
C	-3.85602500	2.04770200	-0.83533700
H	-3.09968200	2.58545000	-1.41246300
H	-3.93636200	2.52612600	0.14420600
H	-4.82024100	2.17023000	-1.34787100
C	-2.49343100	0.25292600	-3.10768000
H	-2.14379900	1.28801100	-3.08973200
H	-3.34803600	0.19600800	-3.79648100
H	-1.69072600	-0.36182100	-3.52481300
C	-2.26293100	-2.73328500	-1.99609300
H	-1.92350000	-3.52348300	-1.32296400
H	-1.41967100	-2.45188700	-2.63248100
H	-3.04470500	-3.15505500	-2.64258200

Cartesian coordinates of the optimized *anti-anti* conformer of 14

Rh	1.55704400	-0.33776100	0.00743100
Cl	-0.41515000	-3.41365800	-1.24345600
Cl	-4.81494100	2.17379600	0.92506600
N	-0.58016500	-0.70721700	0.11462200
N	0.18067000	1.37006300	0.01416100
N	-2.19031300	1.09035800	0.02179400
H	-2.26198300	2.09072200	0.16681000
N	1.22889300	-0.34850500	-2.08481100
N	1.76803000	-1.23070800	-2.71069300
N	2.26505600	-2.04779800	-3.37454500
C	-0.89941000	0.59266400	0.06392400
C	0.20280100	2.75223200	0.16919200
C	-0.45855400	3.37119600	1.25609800
C	-0.41718300	4.74874200	1.45754200

H	-0.94610800	5.18311200	2.30131900
C	0.31712800	5.55896300	0.59084600
H	0.36375800	6.63339300	0.74092200
C	1.00032400	4.97665600	-0.47685300
H	1.57460300	5.58771900	-1.16567200
C	0.94265400	3.59899600	-0.68834300
C	-1.35555500	-1.70694800	0.69523800
C	-2.13621700	-1.47465100	1.85004300
H	-2.16420600	-0.46982900	2.25936000
C	-2.86972800	-2.48970400	2.45515500
H	-3.46443300	-2.26653700	3.33681400
C	-2.83297500	-3.78774700	1.94054300
H	-3.39829500	-4.58752100	2.40967500
C	-2.06212100	-4.05218500	0.80980300
H	-2.02264500	-5.05012100	0.38524100
C	-1.34124500	-3.02805700	0.19503400
C	-3.29320700	0.50439400	-0.63442800
C	-4.59169700	0.93321600	-0.30924300
C	-5.71347500	0.41506800	-0.95136300
H	-6.69812700	0.77667700	-0.67460500
C	-5.55413800	-0.56275200	-1.93223900
H	-6.42746800	-0.97511800	-2.42847300
C	-4.27130400	-0.99656100	-2.27205800
H	-4.13424800	-1.74619500	-3.04567200
C	-3.15053800	-0.46323200	-1.64103600
H	-2.15401300	-0.78137900	-1.92793800
C	3.09085600	-1.88211600	0.41179800
C	3.76642500	-0.67132300	-0.00890000
C	3.45127400	0.35869300	0.93125800
C	2.61672300	-0.21376900	1.97736700
C	2.41250900	-1.59168200	1.65759900
C	3.23791400	-3.22410100	-0.23850900
H	3.17661200	-3.15226100	-1.32969900
H	2.45973000	-3.91659900	0.09056200
H	4.21291400	-3.66414700	0.01380900
C	4.66220800	-0.55452000	-1.20396200
H	4.29935400	-1.15904000	-2.04051900
H	5.67078500	-0.90948600	-0.95028600
H	4.74642600	0.48018900	-1.54508400
C	3.96059200	1.76831500	0.91706000
H	3.20171100	2.47443800	1.26698400
H	4.26547200	2.07760500	-0.08490000
H	4.83158800	1.86068000	1.58075100
C	2.15478800	0.50705100	3.20899500
H	1.88123500	1.54296300	2.98692400
H	2.94779900	0.52981900	3.96934400

H	1.28365500	0.01993800	3.65593500
C	1.64781200	-2.58384800	2.47918400
H	1.17060500	-3.34240900	1.85413900
H	0.86560100	-2.10358400	3.07254900
H	2.32768600	-3.09968300	3.17097600
Cl	1.78966400	2.92961400	-2.06316800
H	-0.99292300	2.73883300	1.96066900